UNIL | Université de Lausanne

Unicentre
CH-1015 Lausanne
http://serval.unil.ch

Year : 2013

THE ADULA NAPPE: STRATIGRAPHY, STRUCTURE AND KINEMATICS OF AN EXHUMED HIGH-PRESSURE NAPPE

Cavargna-Sani Mattia

Cavargna-Sani Mattia, 2013, THE ADULA NAPPE: STRATIGRAPHY, STRUCTURE AND KINEMATICS OF AN EXHUMED HIGH-PRESSURE NAPPE

Originally published at : Thesis, University of Lausanne

Posted at the University of Lausanne Open Archive.
http://serval.unil.ch

Droits d'auteur
L'Université de Lausanne attire expressément l'attention des utilisateurs sur le fait que tous les documents publiés dans l'Archive SERVAL sont protégés par le droit d'auteur, conformément à la loi fédérale sur le droit d'auteur et les droits voisins (LDA). A ce titre, il est indispensable d'obtenir le consentement préalable de l'auteur et/ou de l'éditeur avant toute utilisation d'une oeuvre ou d'une partie d'une oeuvre ne relevant pas d'une utilisation à des fins personnelles au sens de la LDA (art. 19, al. 1 lettre a). A défaut, tout contrevenant s'expose aux sanctions prévues par cette loi. Nous déclinons toute responsabilité en la matière.

Copyright
The University of Lausanne expressly draws the attention of users to the fact that all documents published in the SERVAL Archive are protected by copyright in accordance with federal law on copyright and similar rights (LDA). Accordingly it is indispensable to obtain prior consent from the author and/or publisher before any use of a work or part of a work for purposes other than personal use within the meaning of LDA (art. 19, para. 1 letter a). Failure to do so will expose offenders to the sanctions laid down by this law. We accept no liability in this respect.

UNIL | Université de Lausanne

FACULTÉ DES GÉOSCIENCES ET DE L'ENVIRONNEMENT
INSTITUT DES SCIENCES DE LA TERRE

THE ADULA NAPPE: STRATIGRAPHY, STRUCTURE AND KINEMATICS OF AN EXHUMED HIGH-PRESSURE NAPPE

THÈSE DE DOCTORAT

présentée à la Faculté des géosciences et de l'environnement de l'Université de Lausanne

pour l'obtention du grade de Docteur en Sciences de l'environnement

par

Mattia Cavargna-Sani

Master of science (MSc) in Geology, Université de Lausanne

Jury

Prof. Eric Verrecchia (Président du jury)

Prof. Jean-Luc Epard (Directeur de thèse)

Prof. Lukas Baumgartner (Expert interne)

Prof. François Bussy (Expert interne)

Prof. Neil Mancktelow (Expert externe)

Dr Thorsten Nagel (Expert externe)

LAUSANNE 2013

UNIL | Université de Lausanne

FACULTÉ DES GÉOSCIENCES ET DE L'ENVIRONNEMENT
INSTITUT DES SCIENCES DE LA TERRE

THE ADULA NAPPE: STRATIGRAPHY, STRUCTURE AND KINEMATICS OF AN EXHUMED HIGH-PRESSURE NAPPE

THÈSE DE DOCTORAT

présentée à la Faculté des géosciences et de l'environnement de l'Université de Lausanne

pour l'obtention du grade de Docteur en Sciences de l'environnement

par

Mattia Cavargna-Sani

Master of science (MSc) in Geology, Université de Lausanne

Jury

Prof. Eric Verrecchia (Président du jury)

Prof. Jean-Luc Epard (Directeur de thèse)

Prof. Lukas Baumgartner (Expert interne)

Prof. François Bussy (Expert interne)

Prof. Neil Mancktelow (Expert externe)

Dr Thorsten Nagel (Expert externe)

LAUSANNE 2013

UNIL | Université de Lausanne
Décanat Géosciences et de l'Environnement
bâtiment Géopolis
CH-1015 Lausanne

IMPRIMATUR

Vu le rapport présenté par le jury d'examen, composé de

Président de la séance publique :	M. le Professeur Eric Verrecchia
Président du colloque :	M. le Professeur Eric Verrecchia
Directeur de thèse :	M. le Professeur Jean-Luc Epard
Expert interne :	M. le Professeur François Bussy
Expert interne :	M. le Professeur Lukas Baumgartner
Expert externe :	M. le Professeur Neil Mancktelow
Expert externe :	M. le Docteur Thorsten Nagel

Le Doyen de la Faculté des géosciences et de l'environnement autorise l'impression de la thèse de

Monsieur Mattia CAVARGNA-SANI

Titulaire d'une
Maîtrise universitaire ès Sciences en géologie
Université de Lausanne

intitulée

THE ADULA NAPPE : STRATIGRAPHY, STRUCTURE AND KINEMATICS OF AN EXHUMED HP NAPPE

Lausanne, le 20 septembre 2013

Pour le Doyen de la Faculté des géosciences et de l'environnement

Professeur Eric Verrecchia, Vice-Doyen

MATTIA CAVARGNA-SANI

THE ADULA NAPPE: STRATIGRAPHY, STRUCTURE AND KINEMATICS OF AN EXHUMED HIGH-PRESSURE NAPPE

Abstract

This study analyses the stratigraphy, structure and kinematics of the northern part of the Adula nappe of the Central Alps. The Adula nappe is one of the highest basement nappes in the Lower Penninic nappe stack of the Lepontine Dome. This structural position makes possible the investigation of the transition between the Helvetic and North Penninic paleogeographic domains.

The Adula nappe is principally composed of crystalline basement rocks. The investigation of the pre-Triassic basement shows that it contains several Palaeozoic detrital metasedimentary formations dated from the Cambrian to the Ordovician. These formations contain also some volcanic or intrusive magmatic rocks. Ordovician metagranites dated at ~450 Ma are also a common rock-type of the Adula basement. These formations underwent Alpine and Variscan deformation and metamorphism. Permian granites (Zervreila orthogneiss, dated at ~290 Ma) have intruded this pre-structured basement in a post-orogenic geodynamic context. Due to their age, the Zervreila orthogneiss are good markers for lpine deformation.

The stratigraphy of the Mesozoic and Paleogene sedimentary cover of the Adula nappe is essential to unraveling its pre-orogenic history. The autochthonous cover is assigned to a North Penninic Triassic series that testifies for a transition between the Helvetic and Briançonnais Triassic domains. The Adula domain goes through an emersion during the Middle Jurassic, and is part of a topographic high during the first phase of the Alpine rift. The sediments of the late Middle Jurassic show a drowning phase associated with a tectonic activity and a breccia formation. In the neighbouring domains, coeval with the drowning phase in the Adula domain, a strong extensional crustal delamination and a scattered magmatic activity is associated with the main opening of the North Penninic domain. The Upper Jurassic of the Adula nappe is characterized by a carbonate formation comparable with those in the Helvetic or Subbriaçonnais domains. Flysch s.l. deposition starts probably at the end of the Cretaceous. These sediments are deposited on a large unconformity testifying for a Cretaceous sedimentary gap.

The Adula nappe exhibits a very complex structure. This structure is formed by several deformation phases. Two ductile deformations are responsible for the nappe emplacement. The first deformation phase is associated with a folding compatible with a top-to-south movement at the top of the nappe. The second phase is dominant and pervasive throughout the whole nappe. It goes with a strong north vergent folding and the main nappe emplacement. These two phases cause the exhumation and emplacement of a coherent, although pre-structured, piece of continental crust. Two further deformation phases postdate the nappe emplacement.

MATTIA CAVARGNA-SANI

LA NAPPE DE L'ADULA: STRATIGRAPHIE, STRUCTURE ET CINÉMATIQUE D'UNE NAPPE DE HAUTE-PRESSION

Résumé

Ce travail concerne l'étude géologique de la partie nord de la nappe de l'Adula dans les Alpes centrales. La nappe de l'Adula est l'une des nappes cristallines la plus élevée dans la pile des nappes du Pennique inférieur des Alpes lepontines. Cette position particulière permet d'étudier la transition entre les nappes des domaines helvétique et pennique inférieur.

La nappe de l'Adula est principalement composée de socle cristallin : l'étude de l'histoire géologique du socle est donc un des thèmes de cette recherche. Ce socle contient plusieurs formations métasédimentaires paléozoïques du Cambrien à l'Ordovicien. Ces métasédiments sont issus de formations clastiques comprenant souvent des roches magmatiques volcaniques et intrusives. Ces métasédiments ont subi les cycles orogéniques varisque et alpin. La nappe de l'Adula contient plusieurs corps magmatiques granitiques métamorphisés. Les premiers métagranites sont Ordovicien et témoignent d'un environnement de marge active. Ces granites sont aussi polymétamorphiques. Les deuxièmes métagranites sont représentés par les orthogneiss de type Zervreila. Ce métagranite est d'âge permien (~290 Ma). Il est mis en place dans un contexte tectonique post-orogénique. Ce granite est un maqueur de la déformation alpine car il n'est pas affecté par les orogenèses précédentes.

Le contenu stratigraphique des roches mésozoïques et cénozoiques de la couverture sédimentaire de la nappe de l'Adula est important pour en étudier son histoire pré-alpine. La couverture autochtone est composée d'une série d'âge triasique d'affinité nord-pennique, un faciès qui marque la transition entre les domaines helvétiques et briançonnais au Trias. Le domaine paléogéographique représenté dans la nappe de l'Adula connaît une émersion pendant le Jurassique moyen. Cette émersion marque le commencement du rift dans le domaine alpin. La sédimentation de la fin du Jurassique moyen est marquée par une transgression marine accompagnée par des mouvements tectoniques et la formation d'une brèche. Cette transgression est contemporaine des importants mouvements tectoniques et des manifestations magmatiques dans les unités voisines qui marquent la phase principale d'ouverture du bassin nord-pennique. Le Jurassique supérieur est caractérisé par l'instauration d'une sédimentation carbonatée comparable à celle du domaine helvétique ou subbriançonnais. Une sédimentation flyschoïde, probablement du Crétacé à Tertiaire, est déposée sur une importante discordance qui témoigne d'une lacune au Crétacé.

La structure complexe de la nappe de l'Adula témoigne de nombreuses phases de déformation. Ces phases de déformation sont en partie issues de la mise en place de la nappe et de déformations plus tardives. La mise en place de la nappe produit deux phases de déformation ductile : la première produit un plissement compatible avec un cisaillement top-vers-le sud dans la partie supérieure de la nappe; la deuxième produit un intense plissement qui accompagne la mise en place de la nappe vers le nord. Ces deux phases de déformation témoignent d'un mécanisme d'exhumation par déformation ductile d'un bloc cohérent.

REMERCIEMENTS

Cette thèse a éte financée par le Fonds national suisse de la recherche scientifique (FNS), fond no 200021_132460 et par la Société Académique Vaudoise.

Comme ces quatre années, heureusement, je ne les ai pas passées tout seul sur cette thèse, je tiens à remercier les personnes qui m'ont permis d'aboutir ce travail.

Je tiens à remercier d'abord mon directeur de thèse Jean-Luc Epard pour ses cafés, les discussions, l'Himalaya et d'avoir permis cette thèse. Merci également aux membres du jury de thèse Lukas Baumgartner, François Bussy, Neil Mancktelow et Thorsten Nagel pour les corrections, les critiques et les collaborations.

Une thèse ne serait pas possible sans les personnes qui s'occupent de l'institut et des laboratoires : merci à Anne-Marie (toujours avec le sourire), Laurent (pour la cuisine et les lames), Jean-Claude, Pierre, Alex, Nadia, Krystel, Benita et sûrement d'autres.

Pour les nombreuses discussions et les journées de terrain je veux remercier Henri Masson et Albrecht Steck : des sources incontournables de géologie alpine.

Pour les discussions, corrections suggestions et autres j'aimerais remercier Stefan Schmallholz, Sébastien Pilet et mes collègues Battista, Federico, Florian, Marc, Mathias, Anne-Cecile et Eveline.

Merci aux amis qui m'ont accompagné des journées sur le terrain : Dumeng, Adrien et Thierry.

Merci à tous les amis tessinois, vaudois, valaisans, grisons, néozélandais et du reste du globe avec qui j'ai passé les moments hors uni et aux collègues de l'institut et de la faculté pour les pauses café ou bière.

Je veux remercier particulièrement mes parents qui m'ont beaucoup soutenu, surtout pendant mes nombreuses années d'études de géologie et aussi toute ma famille.

Un merci particulier va à Claire.

TABLE OF CONTENT

1. General introduction 19

1.1. The Lower Penninic enigma and the Adula nappe 19

1.2. Regional setting 22

1.3. The Adula nappe 22

1.4. Aim of the thesis 23

2. Basement lithostratigraphy of the Adula nappe: implications for Palaeozoic evolution and Alpine kinematics 25

2.1. Introduction 27

2.2. Lithology of the northern Adula nappe 29

2.2.1. Introduction 29

2.2.2. Salahorn Formation 29

2.2.3. Trescolmen Formation 32

2.2.4. Heinisch Stafel Formation 33

2.2.5. Garenstock Augengneiss 34

2.2.6. Rossa Orthogneiss 35

2.2.7. Zervreila orthogneiss 35

2.2.8. Adula nappe cover 38

2.3. Zircon geochronology 39

2.3.1. Method 39

2.3.2. Salahorn Formation 39

2.3.3. Trescolmen Formation 43

2.3.4. Garenstock Augengneiss 43

2.3.5. Rossa orthogneiss 43

2.3.6. Heinisch Stafel Formation 47

2.3.7. Zervreila orthogneiss 48

2.4. Discussion 48

2.4.1. Cambrian sedimentation and magmatism 48

2.4.2. Trescolmen Formation: age and sedimentation environment 50

2.4.3. Ordovician evolution 51

2.4.4. Variscan metamorphism 52

2.4.5. Late Variscan granites emplacement 52

2.4.6. Triassic transgression and Mesozoic stratigraphy 53

2.4.7. Implications for Alpine tectono-metamorphic evolution 54

2.5. Conclusions 55

3. Structure, geometry and kinematics of the northern Adula nappe (Central Alps) and its emplacement in the Lower Penninic nappe stack. 57

3.1. Introduction 59

3.2. Geological setting 59

3.3. Structures of the northern Adula nappe 62

3.3.1. Introduction 62

3.3.2. Zapport Valley 67

3.3.3. Hennasädel 69
3.3.4. Plattenberg 71
3.3.5. Nappe-scale geometry and structure 72
3.4. Discussion 77
3.4.1. The pre-Alpine Adula 77
3.4.2. The Ursprung phase – nappe exhumation 77
3.4.3. The Zapport phases – nappe placement 81
3.4.4. Leis and Carassino – nappe front and post-nappe emplacement deformation 82
3.4.5. The Internal Mesozoic 83
3.4.6. The structures of the Adula nappe in a regional context 83
3.4.7. Subduction of the Adula nappe 84
3.5. Conclusions 86

4. Stratigraphy of the Mesozoic sedimentary cover of the northern Adula nappe, Central Alps 89

4.1. Introduction 91
4.2. Regional setting 91
4.3. Sedimentary cover outcrops of the northern Adula nappe 95
4.3.1. Introduction 95
4.3.2. Plattenberg 95
4.3.3. Hennasädel 96
4.3.4. Usser Rossbodma 98
4.3.5. Hohbüel 99
4.3.6. Inder Rossbodma 99
4.3.7. Scattered outcrops 100
4.4. Stratigraphic correlation 100
4.4.1. Correlation base 100
4.4.2. Pre-Triassic 101
4.4.3. The Triassic sedimentary cycle 101
4.4.4. The Lower and Middle Jurassic 101
4.4.5. The Jurassic transgression and onset of carbonate sedimentation 102
4.4.6. Flyschoid sediments group 103
4.4.7. Chloritoid-rich quartzite of the Hennasädel 103
4.5. Discussion 104
4.5.1. Significance of the Triassic stratigraphy of the Adula nappe 104
4.5.2. The role of the Adula block in Alpine rifting 104
4.5.3. The Adula domain during the Cretaceous and Tertiary 106
4.5.4. Variation in time of the limits of the paleogeographic domains 107
4.5.5. Orogenic connotation of the Adula nappe cover 107
4.6. Conclusions 108

5. New stratigraphic data from the Lower Penninic between the Adula nappe and the Gotthard massif and consequences for the tectonics and the paleogeography of the Central Alps 109

5.1. Introduction 111
5.2. Geological setting and background 112
5.3. Stratigraphic data 115
5.3.1. The Simano nappe 116
5.3.2. Soja unit s.str. 116
5.3.3. Adula nappe 116
5.3.4. Valser slices 116
5.3.5. The Piz Terri-Lunschania zone and its tectonic substratum 119

5.4. Stratigraphic correlations 120
5.4.1. Permian and lower Triassic 120
5.4.2. Middle-Upper Triassic 122
5.4.3. Rethian 125
5.4.4. Hettangian-Sinemurian 125
5.4.5. Pliensbachien-Toarcian 125
5.4.6. Aalenian 126
5.4.7. Middle Jurassic 126
5.4.8. Upper Jurassic 126
5.5. The Stratigraphic signature in the local context 126
5.5.1. The Garzott slices 127
5.5.2. The Guda-Alpettas zone 127
5.5.3. The Adula nappe 127
5.6. Discussion on the Preorogenic history 128
5.6.1. The North Penninic Triassic: The missing link between the Briançonnais and the Helvetic? 128
5.6.2. The Jurassic rifting and the associated subsidence: when and where? 129
5.6.3. The rising area between the Helvetic distal margin and the Briançonnais 131
5.6.4. The Plattenberg and Garzott breccias: a second rifting or a protracted history? 132
5.7. Discussion on the orogenic history 134
5.7.1. The Piz Terri-Lunschania zone: an internal klippen-belt 134
5.7.2. The Garzott fault: the escape from deep subduction 135
5.8. Conclusion 135
6. General conclusions 137

PREAMBLE

„ Das „Tessinermassiv“ steht nach Form und Ausdehnung in keinem Verhältnisse zu den andern Centralmassiven. Es erscheint zunächst wie ein ungeheures ungegliedertes Gneissgebiet. Allein an manchen Stellen seines Randes streichen Mulden jüngerer Gesteine in dasselbe ein Stück weit hinein und gehen dann wieder aus. Gewiss sind damit Synclinalzonen weit in das Massiv hineingreifend – oft vielleicht durchgreifend – verbunden, allein Gneiss an Gneiss und abermals Gneiss anschlissend – Gneiss das jüngste und Gneiss das älteste Glied des gefaltetem Systemes – wie wollen wir da die Gliderung vervolgen? “

Heim (1981), in the chapter: *Der nördliche Theil des Adulamassives*

1. General introduction

1.1. The Lower Penninic enigma and the Adula nappe

The Lower Penninic nappes (Fig. 1) represent almost certainly the most enigmatic segment of the Alps. They are structurally comprised between the Helvetic domain and the Middle and Upper Penninic domains (Escher et al. 1993; Schmid et al. 1996). The paleogeographic origin of the Lower Penninic nappes is the North Penninic domain (that includes the Valais domain) between the European continental margin and the Briançonnais mid-Jurassic rise (Trümpy 1955). The enigmatic nature is principally a consequence of the more doubtful chronostratigraphic correlation and tectonic significance of the Lower Penninic sediments together with the structural complexity of these units. Most of the recent controversies of Alpine geology are related to the evolution of this domain. In particular these controversies are:

- The geologic significance of the North Penninic basin is a matter of controversial interpretation. The first theory suggests the North Penninic opening as a link with the North Atlantic oceanic opening and the westwards subduction of the Austroalpine (Frisch 1979; Stampfli 1993). The second suggests the relation of this opening with a complex Alpine rift mechanism (Manatschal et al. 2006; Masson et al. 2008) and related directly to the Piemont-Ligurian Ocean opening.

- The age of the opening of the North Penninic domain is based more on working hypothesis than on geological facts. The

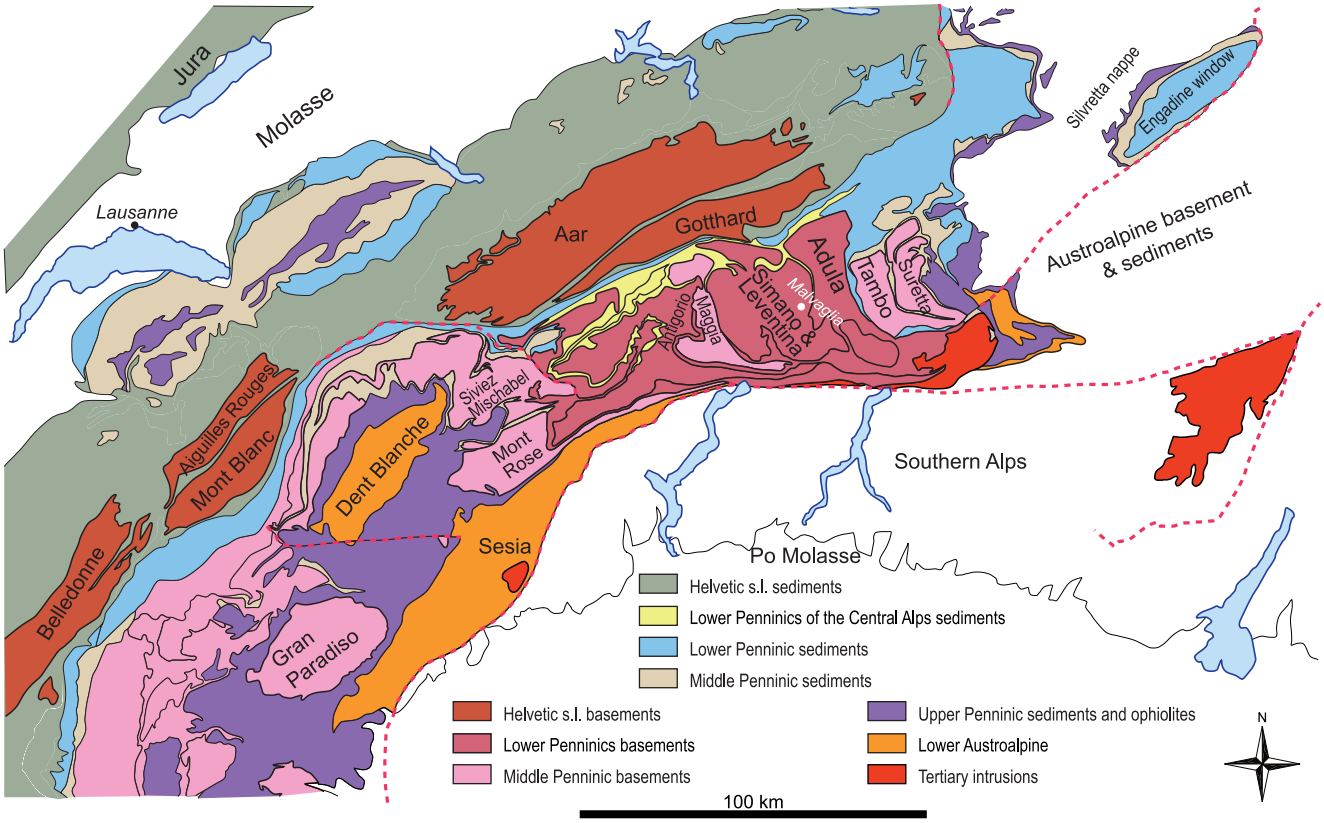

Fig. 1 *Tectonic map of the Central and Western Alps. Modified after Spicher (1980), Schmid et al (2004).*

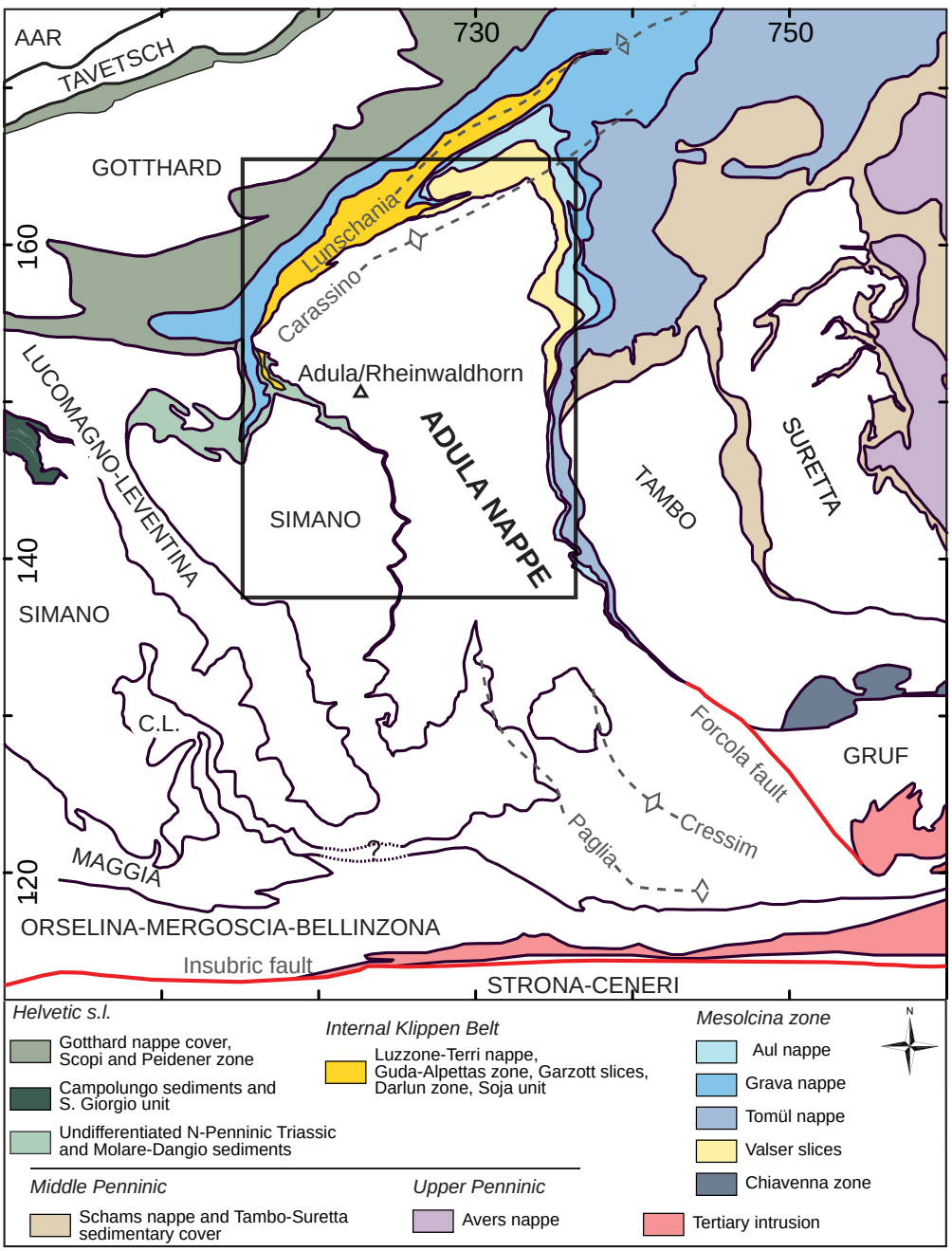

Fig. 2 *Tectonic map of the Eastern Lepontine Alps. Basement nappes are shown in white; sediments are shown in color. Modified after Spicher (1980), Berger & Mercolli (2006), Steck (2008) and Galster et al. (2012) and updated. The rectangle indicates the limit of field area. The coordinate system is the kilometric Swiss grid (CH 1903).*

stratigraphy of the North Penninic sediments provides only scattered information about the age of the domain opening. The discover of Lower Cretaceous sediments deposited on an exhumed mantle (Florineth and Froitzheim 1994) is the main argument for a Cretaceous opening of this basin. It supports the original idea of Frisch (1979) of an Albian-Aptian opening. However more recent radiometric dating suggests a late Middle Jurassic opening (Liati et al. 2005; Manatschal et al. 2006, Hauser and Müntener 2011).

- The existence of a true North Penninic ophiolitic sequence was never confirmed. The existence of serpentinized exhumed mantle is not questioned in the Tasna nappe (Florineth and Froitzheim 1994). Mafic intrusive and volcanics in the Mesolcina zone confirms also an “oceanic” origin (Steinmann and Stille 1999). However in the western part of the North Penninic domain the extension of the exhumed mantle is more doubtful. The Versoyen “ophiolite”, type locality

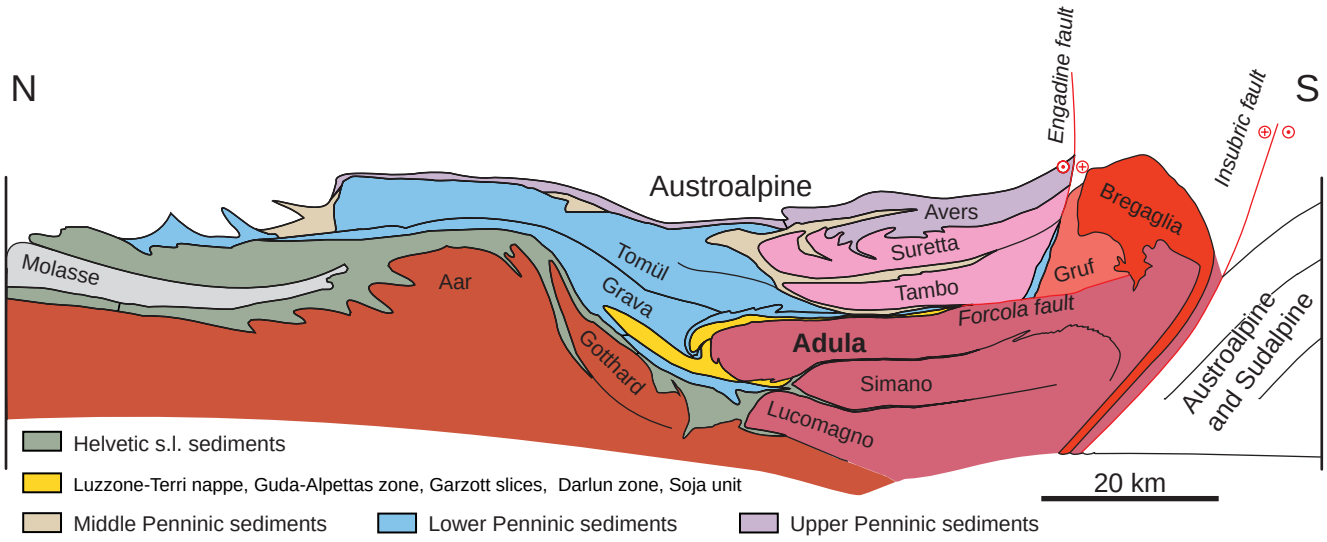

Fig 3. *Cross-section of the Eastern Lepontine Alps. Modified after Schmid et al. 1996, Nagel et al. 2002a, Berger et al. 2005, Galli et al. 2012 and Galster et al. 2012.*

for the classical "Valais Ocean" ophiolite is now dated at Lower Carboniferous (Masson et al. 2008). Many authors (e.g. Masson 2002; Manatschal et al. 2006; Masson et al. 2008; Mohn et al. 2011; Beltrando et al. 2012) suggest an oceanisation in the east and a closure to the west of the North Penninic domain.

- The high-pressure, subduction-related, metamorphic rocks are principally found in two structural positions in the Central and Western Alps: 1) in the Upper Penninic nappes (e.g. Zermatt-Saas, Lanzo); 2) in the Lower Penninic nappes (e.g. Adula-Cima Lunga nappe, Versoyen zone). The geodynamic signification of the high-pressure subduction related metamorphism in the Lower Penninic nappes is not completely elucidated. Some authors postulate the presence of two subduction zones, one in the North Penninic domain and one related to the Liguro-Piemont Ocean (Frisch 1979;Frisch 1981;Froitzheim et al. 2003;Berger and Bousquet 2008; Mohn 2010). The classic kinematic reconstruction proposed in the NFP-20-East cross-section (Schmid et al. 1996) and in numerous recent publications (e.g., Handy et al. 2010) postulate one single subduction zone.

- The exhumation of the high-pressure units of the Lower Penninic lead to models of "lithospheric mélange" (Engi et al. 2001;Bousquet 2008). The validity of these models is currently disputed (see Herwartz et al. 2011).

The last two controversial points concerns directly the Adula nappe as it is established that it contains Alpine high-pressure metamorphic rocks.

To unravel these controversies, a better geological understanding of the Lower Penninics to Helvetics transition is one possible starting point. This transition is exposed in the Lepontine Dome (Fig. 1). These nappes are the deepest units exposed in the Alps. Consequently they are characterized by a considerable structural complexity and a high metamorphic grade. The nappes of the Lepontine Dome are mainly gneiss nappes with a Helvetic s.l. origin. Some of these nappes and other tectonic units contain a Mesozoic cover series.

The Adula nappe is the highest of the Lower Penninic basement nappes (Fig. 1 and 2) that belongs to the eastern border of the Lepontine Dome. It is therefore located in a convenient situation to study the structures of the Helvetics – Lower Penninics transition and to unravel the paleogeography of this specific domain using its stratigraphic record.

1.2. Regional setting

The Adula nappe is situated on top of the Simano nappe (Fig. 2). The Adula and Simano nappes and are separated by a thin band of Mesozoic rocks.

Between the Adula nappe and the Gotthard Crystalline basement, there are several nappes and tectonic slices zones of mainly Mesozoic sedimentary rocks (Fig. 2 and 3). Some of these sediments are of Helvetic type (Baumer et al. 1961) others are Bündnerschiefer (Probst 1980) found in different units.

At the top, the Adula nappe is separated from the Middle Penninic nappes by the Mesolcina (Misox) zone. Several nappes and slices of metasedimentary clastic rocks form this zone and are described below (Fig. 2). the Lower and Upper Valser slices are directly on top of the Adula nappe, at the base of the Mesolcina zone. These two units are composed of slices of various rock types such as gneiss, greenstone and marble. Calcschists are observed only in the Upper Valser slices (Steinmann 1994; Wyss and Isler 2007). The Aul, Tomül and Grava nappes are formed by Jurassic to Cretaceous calcschist sediments (Bündnerschiefer) that were deposited in the North Penninic basin (Steinmann 1994). These nappes are composed in part by coherent sedimentary sequences associated with slice zones. The cover of the Middle Penninic Tambo and Suretta nappes and of the Schams nappe has a classical Briançonnais stratigraphy (Baudin et al. 1995; Rück 1995).

In the southern part, the Forcola normal fault separates the Adula and the Tambo nappes (Meyre et al. 1998).

The units surrounding the Adula nappe experienced a subduction-related metamorphism of lower grade (blueschist) in comparison with the Adula nappe (Bousquet et al. 2002, Wiederkehr et al. 2008). The Mesolcina (Misox) zone between the Adula and Tambo nappes experienced a high-pressure metamorphic event of upper blueschist to eclogitic grade as indicated by the presence of eclogite preserved within the basic rocks (e.g., “Neu Wahli” outcrop) (Gansser 1937; Santini 1992). The Tambo nappe experienced peak pressure conditions of ~1.0-1.3 GPa and temperatures ranging from approximately 400°C in the N to 550°C in the central part of the nappe (Baudin and Marquer 1993). The Simano nappe retains peak pressures of approximately 1.0-1.2 GPa (Rütti 2003).

The green-schist – amphibolite facies isograds of the subsequent Barrovian metamorphism crosscut the nappe boundaries (Todd and Engi 1997; Nagel 2008; Wiederkehr et al. 2011).

1.3. The Adula nappe

The Adula nappe is classically considered to be connected to the Gruf (Fig. 2). Recently Galli et al. (2011) demonstrated that they are two independent tectonic units. The (ultra-) high-pressure bearing Cima Lunga unit (Fig. 2) is interpreted as being part of the Adula nappe, owing their lithological similarity and structural position. Nevertheless Quaternary sediments filling the large Ticino Valley mask the connection between these two units.

The sedimentary cover of the Adula nappe is a largely unknown topic. The existence of the “Internal Mesozoic” (sedimentary cover occurring within the basement) was already reported by Heim (1891). Stratigraphic series were proposed for the Plattenberg, Wissgrätli and Hennasädel Internal Mesozoic localities by Jenny et al. (1923); Van der Plas (1959); Egli (1966). However these propositions were not sufficient for a further understanding on the pre-orogenic position of the Adula nappe.

Remarkably fresh eclogites and eclogitic facies metapelites have been described in several localities of the Adula nappe. This feature continues to maintain the interest of many metamorphic petrologists for the Adula nappe. Van der Plas (1959) was

already interested at the occurrence of blue amphiboles in the Adula nappe. Petrology of eclogitic facies rocks was studied mostly in the polymetamorphic basements (e.g. Heinrich 1983; Meyre et al. 1999; Dale and Holland 2003), even if it is now established by data from eclogites (Liati et al. 2009; Herwartz et al. 2011) that the basement of the Adula nappe was subject to high-pressure metamorphic conditions during the Carboniferous and during the Alpine orogeny. Alpine decompression and a general Barrovian metamorphism in the Lepontine dome is expressed as amphibolite facies conditions in the south and greenschist facies conditions in the northern part of the Adula nappe (Nagel et al. 2002b). Eclogites and eclogitic metapelites occur in scattered outcrops throughout the nappe but are rare. They are more abundant in the eastern part of the Northern Adula nappe.

The overall structure of the Adula nappe appears as a classic recumbent north-vergent fold-nappe. The nappe is rooted in the south between the zone of Orselina-Mergoscia-Bellinzona and the Simano nappe (Fig. 3; Jenny et al. 1923; Schmid et al. 1996). The Adula nappe is folded by S-verging post-nappe folds in the southern region (Nagel et al. 2002a). The internal structure of the nappe is very complicated with several deformation phases (Löw 1987). The presence of Mesozoic rocks refolded within the Paleozoic basement, known as the Internal Mesozoic, is a distinctive feature of the internal structure of the Adula nappe.

The Adula nappe experienced higher subduction-related high-pressure metamorphism than the surrounding nappes, and this raises the question of its exhumation. Most kinematic models (e.g. Schmid et al. 1996) propose the subduction and subsequent exhumation of the Adula as a single coherent entity. However these models do not take into account or explain the complex internal deformation of the Adula nappe. The limited occurrence of eclogite relicts in a few formations and the strong internal deformation are the main arguments that led several authors to introduce a “lithospheric mélange” concept to explain the geometry and kinematics of the Adula nappe (Trommsdorff 1990; Berger et al. 2005). Already Heydweiler (1918) used the term « Teildecken » to explain the constitution of the Adula nappe by the juxtaposition of several pieces. However, the concept of “lithospheric mélange” to explain the complex internal structure of the Adula nappe is still controversial.

1.4. Aim of the thesis

The principal purpose of this thesis is to contribute to the geological knowledge of the Alpine geology, in particular to clarify the geology of the Lower Penninics. The structural position of the Adula nappe at the top of the Lower Penninic basement nappe stack makes it a key area to understand the Helvetic – North Penninic transition. Thus this thesis is principally the result of a regional study of the northern Adula nappe. The research is mainly focused on the northern part of the nappe because its strain and metamorphic grade are lower in that area. The interferences between successive deformation phases are also much easier to decipher in the frontal part of the nappe.

This study has also larger-scale implications. The Adula nappe is well known for its eclogitic rocks. The geological evolution, from high-pressure metamorphism to nappe emplacement is nowadays a strongly debated theme. To be able to precisely describe the geologic context of the high-pressure nappes is essential to unravel their subduction and exhumation process.

The main scientific issues that underlie this thesis are:

- *What is the pre-Triassic evolution of the Adula basement, the age of the magmatic rocks and is it possible to define and date formations in the basement?* To unravel the Alpine evolution, it is necessary to better know its pre-Alpine geological history. This investigation is also essential to define key markers within the basement for a detailed mapping.

- The Adula nappe contains frequently bodies of sedimentary cover deeply infolded within the basement; some of them consist of a larger sedimentary series. *Is it possible to decipher their stratigraphic content and to propose a Mesozoic – Tertiary stratigraphic evolution? What is the pre-orogenic significance of the Adula nappe in the regional tectono-sedimentary context?*

- *What is the internal geometry of the northern Adula nappe, and what is the kinematics necessary to produce it?* The deformation of the Adula nappe is probably principally produced during the nappe exhumation and emplacement. This emplacement kinematics is crucial to a better understanding of the specific role of the Adula nappe within the Lower Penninic nappe stack. A special attention is also needed to understand the geometry and the significance of the sedimentary cover within the basement.

2. Basement lithostratigraphy of the Adula nappe: implications for Palaeozoic evolution and Alpine kinematics

Mattia Cavargna-Sani, Jean-Luc Epard, François Bussy, Alex Ulianov

Published in: International Journal of Earth Science (In Press), doi:10.1007/s00531-013-0941-1

ABSTRACT

The Adula nappe belongs to the Lower Penninic domain of the Central Swiss Alps. It consists mostly of pre-Triassic basement lithologies occurring as strongly folded and sheared gneisses of various types with mafic boudins. We propose a new lithostratigraphy for the northern Adula nappe basement that is supported by detailed field investigations, U-Pb zircon geochronology, and whole-rock geochemistry. The following units have been identified:

- Cambrian clastic metasediments with abundant carbonate lenses and minor bimodal magmatism (Salahorn Formation);
- Ordovician metapelites associated with amphibolite boudins with abundant eclogite relicts representing oceanic metabasalts (Trescolmen Formation);
- Ordovician peraluminous metagranites of calc-alkaline affinity ascribed to subduction-related magmatism (Garenstock augengneiss);
- Ordovician metamorphic volcanic-sedimentary deposits (Heinisch Stafel Formation);
- Early Permian post-collisional granites recording only Alpine orogenic events (Zervreila Orthogneiss).

All basement lithologies except the Permian granites record a Variscan+Alpine polyorogenic metamorphic history. They document a complex Paleozoic geotectonic evolution consistent with the broader picture given by the pre-Mesozoic basement framework in the Alps. The internal consistency of the Adula basement lithologies and the stratigraphic coherence of the overlying Triassic sediments suggest that most tectonic contacts within the Adula nappe are pre-Alpine in age. Consequently, mélange models for the Tertiary emplacement of the Adula nappe are not consistent and must be rejected. The present-day structural complexity of the Adula nappe is the result of the intense Alpine ductile deformation of a pre-structured entity.

2.1. Introduction

Palaeozoic basement rocks in the Alpine realm experienced a complex pre-Mesozoic geological evolution, which has generated major lithostratigraphic unconformities. These structures are relatively easy to distinguish from those resulting from the Alpine orogeny in the external parts of the Alpine belt because pre-Mesozoic structures were mostly formed under high-grade metamorphic conditions, whereas Alpine structures developed under low-grade metamorphic conditions. The situation is much more confusing in the internal parts of the Alpine belt because both pre- and post-Mesozoic tectonic structures formed under high-grade conditions. There is thus a potential risk in ascribing pre-Mesozoic features to Alpine events, which may lead to erroneous tectonic interpretations. The best way to avoid such cases is to identify internally consistent lithologic formations within the Alpine basement, which will document its Paleozoic geodynamic evolution.

The Alpine domain is composed in part by nappes made of Palaeozoic basement. Nappes of this type occur in the Lepontine dome. The nappes of the Lepontine dome are mainly assigned to Lower Penninic structural domain. Their Paleogeographic position prior to the Alpine orogenesis is the distal European margin. The Lepontine dome represents a structural and metamorphic dome and includes the deepest nappes of the Alpine edifice. Consequently these nappes are mainly formed by Palaeozoic basement rocks affected by a strong Alpine metamorphism and deformation.

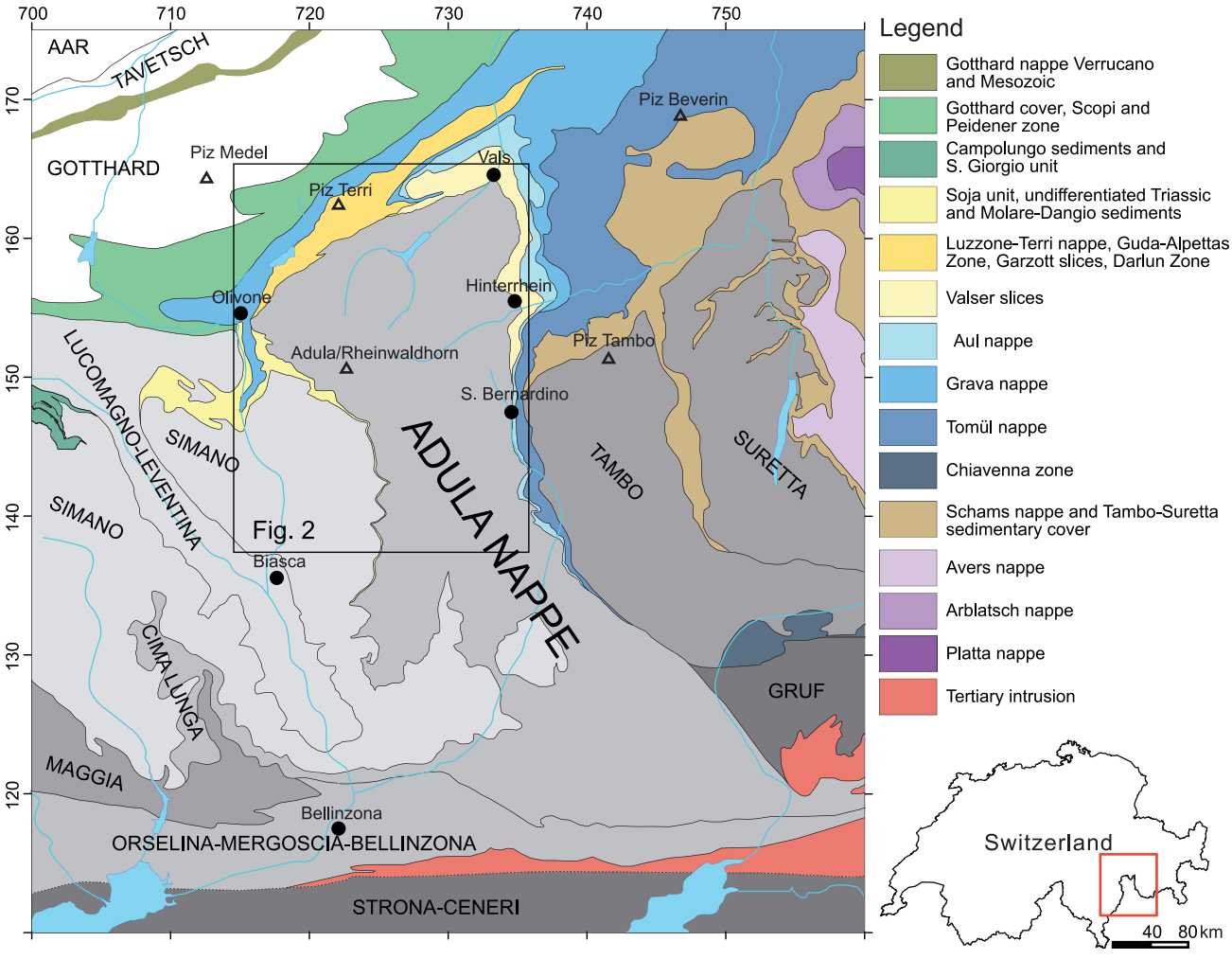

Fig. 1 *Tectonic map of the eastern Lepontine Alps. Grey and white tones are basement nappes, and sediments are illustrated with colours. Modified based on the work of Speichert (1980), Berger & Mercolli (2006), Steck (2008), and Galster et al. (2012). The square indicates the emplacement of Fig. 2 and the study area. The coordinates represent the kilometric Swiss grid (CH 1903).*

The Adula nappe, in the Central Alps, is a good example of a complexly structured polyorogenic unit and is a key tectonic unit located at the transition between the Helvetic and Briançonnais domains. It is mostly composed of Paleozoic basement rocks and has been strongly deformed by Alpine orogenic events. Various interpretations have led to contrasting kinematic models of its Alpine evolution in the literature.

The Adula nappe is located on the border of the Swiss-Italian Alps on the eastern Lepontine dome and is one of the highest units of the Lower Penninic basement nappe stack (Fig. 1). It is overthrust by the Bündnerschiefer (Gansser 1937; Schmid et al. 1996), a sedimentary series deposited in the North Penninic basin (Steinmann 1994) and followed upward by the easternmost Middle Penninic Tambo and Suretta basement nappes with their associated sediments of Briançonnais affinity. The Adula nappe has been the subject of numerous recent publications and a recent review paper by Nagel (2008); it can be considered one of the best-studied nappes of the Central Alps. The overall structure of the Adula nappe is a north-facing recumbent fold, but its internal structure, which records several deformation phases, is much more complex than that of a simple fold-nappe and contains several slices of Mesozoic rocks folded within the basement (Jenny et al. 1923; Nagel et al. 2002a). The oldest Alpine deformation phases are only locally observable. The dominant Alpine structure in the northern part of the nappe is called the Zapport phase (Löw 1987; Nagel et al. 2002a); it is also the oldest recorded pervasive phase. This phase is associated with the regional foliation, isoclinal folding with approximately N-S fold axes, and a well-marked N-S stretching lineation associated with a top-to-the-North sense of shear. The Leis and Carassino deformation phases (Löw 1987) are younger and more pronounced in the western part of the northern Adula nappe. The Leis phase is principally expressed by folds, which are locally associated with a cleavage. Large open folds are ascribed to the Carassino phase.

Eclogites and eclogitic facies metapelites are well known in numerous areas of the Adula nappe (Heinrich 1983; Meyre et al. 1999; Dale and Holland 2003; Zulbati 2010). They have been studied mostly in the polymetamorphic basements. The Adula nappe was subject to high-pressure metamorphic conditions during the Alpine orogeny as demonstrated by the metamorphic overprint observed in Mesozoic cover rocks (Zulbati 2008) and the dating of two metamorphic events (the last one being of Alpine age) in eclogites (Herwartz et al. 2011). Alpine decompression and a general Barrovian metamorphism in the Lepontine dome resulted in amphibolite facies conditions in the south and greenschist facies conditions in the northern part of the Adula nappe (Nagel et al. 2002b). Eclogite facies assemblages are restricted to eclogites, garnet-phengite-metapelite and garnet peridotite (only in the southern part). They are more abundant in the eastern part of the northern Adula nappe.

The pre-Alpine paleogeographic position of the Adula nappe is at the limit of the distal Helvetic margin (Steinmann 1994; Galster et al. 2012), close to the North Penninic basin. The Triassic and Jurassic stratigraphy of the Adula nappe and its surrounding nappes show a transition between the Briançonnais domain and the Helvetic domain (Galster et al. 2012). The limited occurrence of eclogite relicts in a few formations and the strong internal deformation are the main arguments that led several authors to introduce a “lithospheric mélange” model to explain the geometry and kinematics of the Adula nappe (Trommsdorff 1990; Berger et al. 2005). This hypothesis implies that the Adula nappe is a mélange representing the suture between Lower and Middle Penninic (Engi et al. 2001; Berger et al. 2005). This hypothesis remains controversial (see discussion in Herwartz et al. 2011).

The petrographic subdivisions of the Adula nappe were defined in a few classical papers (i.e. Jenny et al. 1923; Kündig 1926; Van der Plas 1959; Egli 1966). A clear lithostratigraphic sequence, however, was never established, and the granitic rocks are still undated. Hence, a consistent picture of the Adula basement architecture, also essential to unravel the Alpine structures, was never proposed.

This work thus aims to:

- determine the protolith of the northern Adula basement rocks;
- date the magmatic protoliths of the northern Adula nappe;
- propose a lithostratigraphy for the Alpine basement rocks;
- suggest a paleogeographic scenario for the protolith formation;
- identify information regarding the pre-Alpine orogenic cycles;
- discuss the implications of the pre-Alpine unconformities for the Alpine kinematics.

Obtaining an accurate lithostratigraphy is essential for constructing a reliable geological and structural map and is of primary importance for the understanding of the nappe kinematics and its metamorphic evolution. This work combines analytical and precise field investigations to constrain the nature of the protoliths of the northern Adula nappe rocks and to propose a complete basement lithostratigraphy. Magmatic ages were determined through U-Pb LA-ICPMS dating of zircon. The geodynamic interpretation is supported by whole-rock geochemistry. The proposed new geological map of the northern Adula (Fig. 2) is a combination of the new results from this study and existing geological data. This work is restricted to the northern part of the nappe because it is less metamorphosed and deformed.

2.2. Lithology of the northern Adula nappe

2.2.1. Introduction

The names used for the metasedimentary formations and magmatic bodies are as consistent as possible with those used in the literature. The term “Formation” is used to define a lithologically homogeneous body of rock that can be mapped at the 1:25’000 scale. The local names for new Formations are chosen from a well outcropping area and are shown on the geologic map (Fig. 2).

The rocks described in the following sections underwent one or more metamorphic events and are highly strained. From a geochemical point of view, their content of mobile elements has most likely been modified. For example, some samples of the Garenstock Augengneiss (MC 219, MC 227, MC 272, and MC 302; Table 2) show clear evidence of weathering, which is marked by anomalous values of K_2O, Na_2O, CaO, Sr, Ba, and Pb content. This alteration is most likely due to surface weathering during the pre-Triassic emersion, as suggested by the presence of calcrete and dolocrete underTriassic quartzites (Chapter 3.2.8). The classification of Pearce (1996; modified after Winchester and Floyd 1977) was chosen to classify mafic rocks because it is based on the distribution of trace elements that are considered as immobile under metamorphic conditions.

2.2.2. Salahorn Formation

The Salahorn Formation is the largest paragneiss formation of the northern Adula basement. The highest peak, Adula (or Rheinwaldhorn, 3402 m), is composed of these rocks. The type locality is located near the Salahorn peak in the Zapport valley (Fig. 2), where this formation is completely exposed. The Salahorn Formation is principally composed of metamorphosed clastic sediments (Fig. 3b) varying from quartzitic arkose to metapelites. The transitional contacts between these different clastic rocks are clear in the field, leading to the conclusion that they have to be included in the same formation. The Salahorn

Formation is rich in carbonates. Carbonates are generally present as centimetric lenses (Fig. 3b) of brown calcitic, ankeritic, or dolomitic marble. Metric lenses of these carbonates can be found locally (Fig. 3c). The Palaeozoic carbonates of the Salahorn Fm. are not to be confused with the abundant boudins of Mesozoic sediments folded into the Adula basement. In the Salahorn Fm., there is a close association of meta-igneous greenstone and gneiss with the felsic paragneisses. The meta-igneous bodies are observable as decimetric to decametric lenses or boudins. Contacts with the clastic country rocks are generally sharp. A transitional contact is sometimes observed.

The appearance and mineralogy of the meta-igneous rocks of the Salahorn Fm. are quite variable. They can be divided into two types: a) mafic rocks varying from prasinites to eclogites and b) amphibole plagioclase gneiss. The mafic rocks of type (a) are very common. They generally have a fine-grained texture, often with symplectites, and they are dark green in colour. Amphibole plagioclase gneiss of type (b) is less mafic and crops out only locally. The texture is medium- to coarse-grained, dominated by hornblende and plagioclases. Two samples were dated at 517-518 Ma (Chapter 3.2). Magmatic contacts are observed between types (a) and (b) (Fig. 3a). Their relative ages seem to be identical based on field relationships. The Salahorn Formation also encloses large ultramafic bodies. The two largest bodies are reported on the map (Fig. 2), one located at Monte Amianto (720200/153000) and the other located at Cima di Sgiu (718000/153500). The Cima di Sgiu rocks are serpentinites and rodingites, which were described by Deutsch (1979). These bodies are in close association with mafic rocks. The Salahorn Formation includes partly what was mapped as "Paragneise und Glimmerschifer" by Jenny and Frischkecht (in Jenny et al. 1923) and "Glimmerschifer und Paragneise" by Egli (1966).

The whole-rock chemical composition of the magmatic rock types of the Salahorn Fm. was analysed (Table 1). Mafic rocks (a) varying from prasinites to eclogites were interpreted as volcanic rocks based on their texture and the relationships with the nearby paragneiss. Amphibole plagioclase gneiss (b) was interpreted as plutonic. To facilitate comparison of the rocks, both rock types were plotted in classification diagrams of volcanic rocks. Mafic rocks (a) are attributed to basalt (Fig. 6) in the classification of Pearce (1996, modified after Winchester and Floyd 1977). The five samples analysed (Table 1) display a rather large compositional spread from 47-53 wt.% SiO_2, which does not correlate with the corresponding mg# (63-72), in contrast to what would be expected for a differentiation series. This discrepancy is interpreted as resulting from the contamination of magmas by country-rock at the time of emplacement and/or by metamorphic remobilisation. The relatively high Fe_2O_3 contents (12-16 wt.%) and low mg# point to some degree of differentiation of these mafic magmas. They lie in the range of tholeiitic basalts in classification diagrams (Fig. 7). The REE-normalised patterns (Fig. 8a) of the five samples also display a large range of LREE values, with La_N ranging from 30 to 100. Nevertheless, three samples display a coherent set of weakly fractionated REE patterns with La/Lu_N = ~1.6, whereas the two other samples are more enriched in LREE. The absence of an Eu anomaly suggests that no significant plagioclase fractionation occurred during differentiation. The three coherent samples point to a typical pattern of tholeiitic basalts. They also show significant negative anomalies in Ta, Nb, and, to a lesser extent, Ti, coupled with a positive anomaly in Pb in the spider diagrams (Fig. 8b). This distribution of incompatible elements is usually indicative of subduction-related magmas. These anomalies are not expressed at all in the two samples enriched in LREE. Considering the rather large variability and the limited number of analyses, it is not possible to provide an unequivocal interpretation of the geochemical signature of these mafic rocks. Relying on the least REE-enriched samples, we would consider these mafic rocks to be tholeiitic basalts with a calc-alkaline signature, which may

Fig. 2 *Geologic map of the northern Adula nappe. Compilation after Jenny et al. (1923), Künding (1926), Van der Plas (1959), Egli (1966), Frey (1967), Pleuger et al. (2003), Berger and Mercolli (2006), Arnold et al. (2007), Cavargna-Sani (2008), Galster (2010), and Swisstopo (2012), and newly mapped area by Cavargna-Sani et al. (submitted; left side of the upper Calanca Valley, Zapport Valley, Plattenberg area, and Hennasädel-Heinisch Stafel area). Geologic limits of the newly defined formations are well identified in the new mapped areas; these limits are not newly mapped in other areas. The coordinates represent the kilometric Swiss grid (CH 1903).* ▶

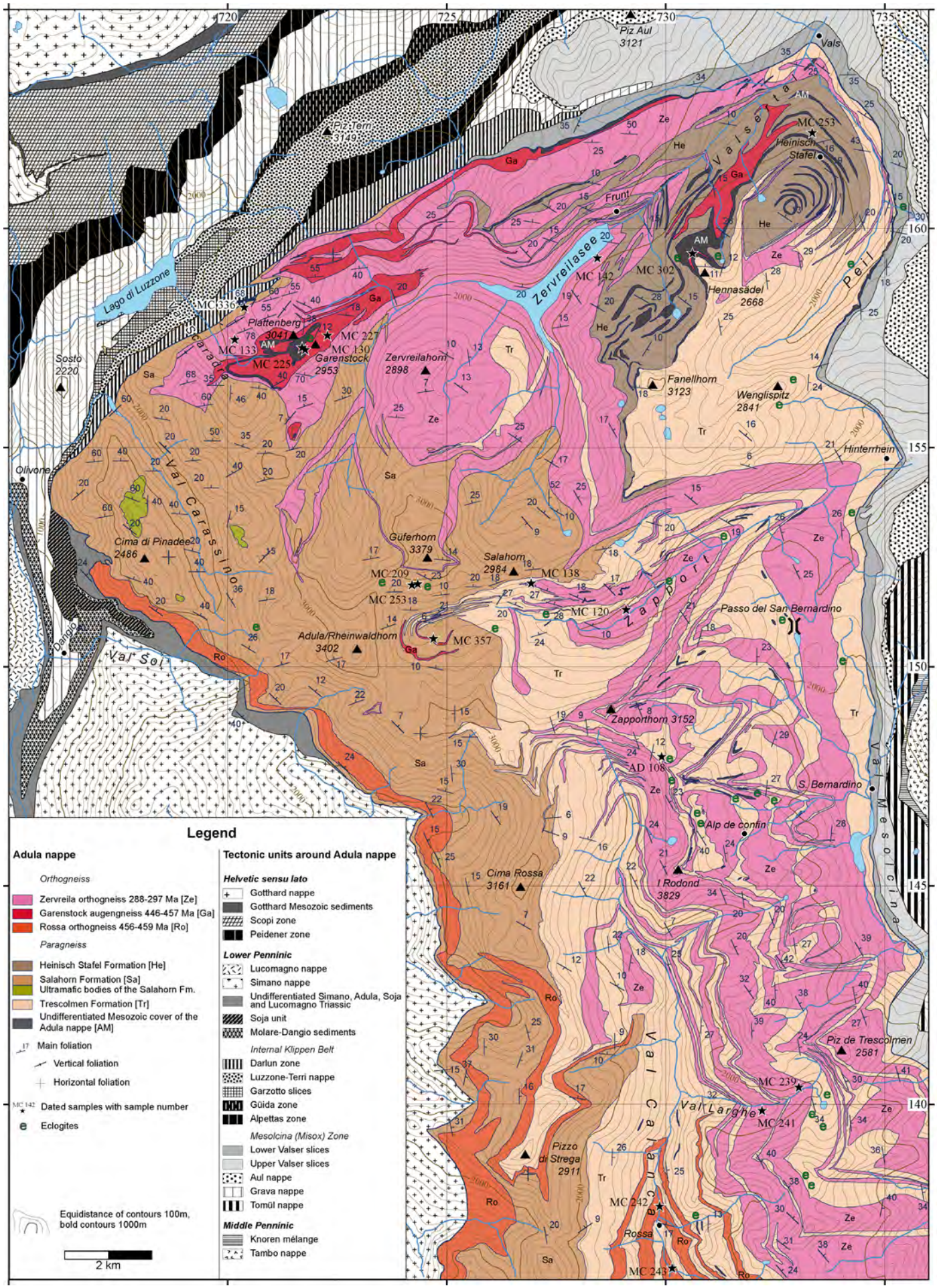
Legend
Adula nappe
Orthogneiss
Zervreila orthogneiss 288-297 Ma [Ze]
Garenstock augengneiss 446-457 Ma [Ga]
Rossa orthogneiss 456-459 Ma [Ro]
Paragneiss
Heinisch Stafel Formation [He]
Salahorn Formation [Sa]
Ultramafic bodies of the Salahorn Fm.
Trescolmen Formation [Tr]
Undifferentiated Mesozoic cover of the Adula nappe [AM]
Main foliation
Vertical foliation
Horizontal foliation
Dated samples with sample number
Eclogites
Equidistance of contours 100m, bold contours 1000m
2 km
Tectonic units around Adula nappe
Helvetic sensu lato
Gotthard nappe
Gotthard Mesozoic sediments
Scopi zone
Peidener zone
Lower Penninic
Lucomagno nappe
Simano nappe
Undifferentiated Simano, Adula, Soja and Lucomagno Triassic
Soja unit
Molare-Dangio sediments
Internal Klippen Belt
Darlun zone
Luzzone-Terri nappe
Garzotto slices
Güida zone
Alpettas zone
Mesolcina (Misox) Zone
Lower Valser slices
Upper Valser slices
Aul nappe
Grava nappe
Tomül nappe
Middle Penninic
Knoren mélange
Tambo nappe
Piz Aul 3121
Vals
Piz Terri 3149
Lago di Luzzone
Plattenberg 3041
Garenstock 2953
Zervreilahorn 2898
Zervreilasee
Frunt
Heinisch Stafel
Hennasadel 2668
Fanellhorn 3123
Wenglispitz 2841
Hinterrhein
Sosto 2220
Olivone
Cima di Pinadee 2486
Güferhorn 3379
Salahorn 2984
Adula/Rheinwaldhorn 3402
Passo del San Bernardino
Zapporthorn 3152
AD 108
S. Bernardino
Alp de confin
I Rodond 3829
Cima Rossa 3161
Piz de Trescolmen 2581
Pizzo di Strega 2911
Rossa
Val Carassino
Val Soi
Val Zapport
Val Mesolcina
Val Calanca
Val Larghe
Peil
MC 133
MC 225
MC 227
MC 130
MC 336
MC 142
MC 302
MC 253
MC 209
MC 138
MC 120
MC 357
MC 239
MC 241
MC 242
MC 243
AD 108

Fig. 3 *Lithologies of the Salahorn Formation.* ***a.*** *Magmatic rocks of the Salahorn Formation, magmatic contact between the amphibole-plagioclase gneiss and the dark mafic rock. Zapport Valley (724340/151890).* ***b.*** *Albitic meta-arkose containing abundant carbonates in the matrix. Zapport valley.* ***c.*** *Carbonates in the micaschists. Zapport Valley (724160/151800).*

correspond to continental or back-arc tholeiites.

The two analyses of amphibole plagioclase gneisses (Table 1) are quite contrasting in their SiO_2 contents (53 and 64 wt.%, mg# (79 and 64), and REE concentrations (e.g., La = 7 and 16 ppm, respectively). We attribute this difference to distinct degrees of magma differentiation. Both analyses show striking features, such as very high Sr concentrations (>600 ppm), positive Eu anomalies, and strongly fractionated normalised REE patterns (Fig. 8a; La/Lu_N = 7-10) with low HREE contents (spoon-like patterns). Ta and Nb are also very low-generating, strongly negative anomalies in a primitive mantle-normalised diagram (Fig. 8b). The spoon-like REE patterns are typical of differentiated melts from which large amounts of amphibole have been subtracted (Davidson et al. 2007; Alonso-Perez et al. 2009). The positive Eu anomaly coupled with high concentrations of Sr points either to plagioclase accumulation in the rock or to the retarded crystallisation of this mineral in the melt. Altogether, we interpret these chemical characteristics as resulting from the early fractionation of amphibole at relatively high pressures (e.g., at the base of the continental crust) from a hydrated basaltic magma (Alonso-Perez et al. 2009). The high water content and high pressure prevented plagioclase crystallisation, thus enriching the differentiating melt in Sr, Eu, and Al (e.g., Barboni et al. 2011). The formation of the amphibole-plagioclase gneisses would thus require magma differentiation at deep levels in a wet environment in a tectonic context, such as a continental active margin or a back-arc environment (Pearce and Stern, 2006).

Given that the Salahorn mafic rocks are tholeiitic with a calc-alkaline signature and are contemporaneous with the amphibole-plagioclase gneisses, we suggest a back-arc geotectonic context for the Salahorn magmatic activity.

2.2.3. Trescolmen Formation

The Trescolmen Formation outcrops in the eastern part of the northern Adula nappe. This formation is composed of metapelites (Fig. 4a) that contain basic boudins. The metapelites are rather homogeneous and show characteristic brown

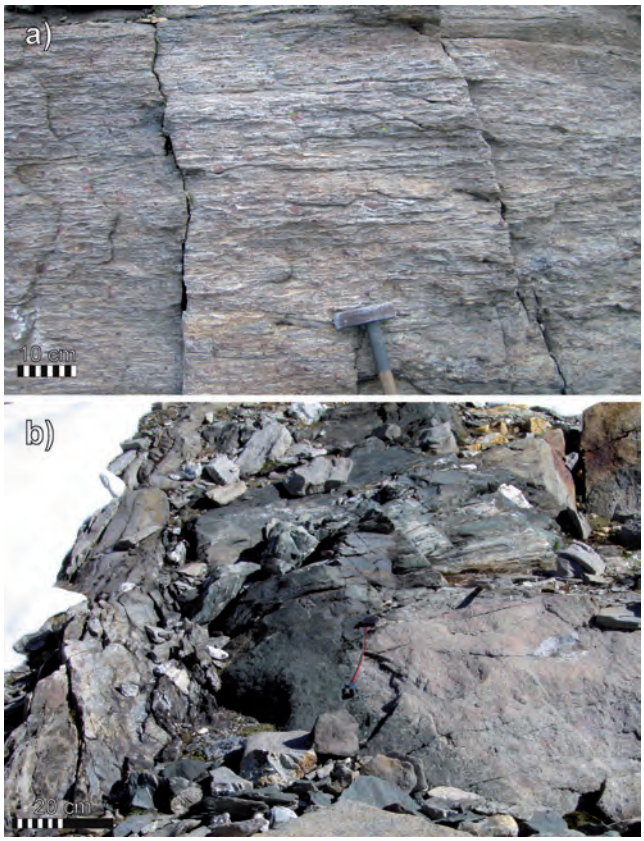

Fig. 4 *Lithologies of the Trescolmen Formation.* ***a.*** *Garnet metapelites. Alp de Ganan (733000/137900).* ***b.*** *Eclogic mafic boudins with a retrogressed rim in the metapelitic matrix. Alp de Ganan (733100/137780)*

alteration. They are tightly foliated and contain abundant quartz segregations. Phengite and quartz are the dominant minerals. The rock also contains a variable amount of metamorphic minerals, such as garnet, kyanite, staurolite, chloritoid, biotite, paragonite, and albite. The distinctive feature of the rock is the absence of carbonates. The whole-rock chemical composition of the metapelites is rather constant (Cavargna-Sani 2008).

Mafic boudins in the Trescolmen Formation vary from eclogites (Fig. 4b) to prasinites. The contacts between the metapelites and the mafic boudins are always sharp. Spectacular eclogites (Fig. 4b) are preserved in many localities (Hennasädel, Zapport Tal, Alp da Confin, Alp de Trescolmen, Alp de Ganan; see Fig. 2). A few ultramafic boudins are also located in the metapelites of the Trescolmen Formation (Pfeifer et al. 1993).

The geochemical whole-rock composition of the mafic rocks of the Trescolmen Formation was extensively analysed by Santini (1992), yielding the conclusion that the basic rocks have an oceanic origin with a tholeiitic affinity, often with a MORB signature.

Metamorphic conditions recorded by the rocks of the Trescolmen Formation are well studied. The metapelites have suffered a pressure of 25 kbar in the Central Adula Nappe (Meyre et al. 1999; Cavargna-Sani 2008). The metamorphic mineral assemblages in mafic rocks indicate high-pressure peak conditions increasing from north to south (Heinrich 1986; Dale and Holland 2003). The polymetamorphic history of the Trescolmen Formation is well recorded in garnets (Koch 1982; Zulbati 2010; Herwartz et al. 2011). However, only the recent radiogenic ages (Liati et al. 2009; Herwartz et al. 2011) clearly distinguish the two episodes in these rocks.

2.2.4. Heinisch Stafel Formation

The Heinisch Stafel Formation outcrops in the north-eastern part of the Adula nappe (Fig. 2). This formation is mainly composed of metamorphosed clastic sediments, which range from micaschists to meta-arkose (Fig. 5b). White mica and chlorite are very abundant; quartz and feldspar occur in more variable amounts. The general colour of this paragneiss is grey to green-grey. In this formation, a clear transition between micaschist and greenstone can be observed (Fig. 5c). This transition is marked by enrichment in chlorite, amphibole, and plagioclase of the micaschist and is very typical and specific to this formation. Considering the traits described above, the protolith of the greenstone layers is interpreted as meta-tuff. Greenstones can vary from eclogites to prasinites with the presence of layered amphibolites (Fig. 5a), which are dated as Ordovician (Chapter 3.6). Ankeritic nodules that are smaller than 1 cm are very frequent in this formation, and they occur in both the clastic metasediments and the greenstones.

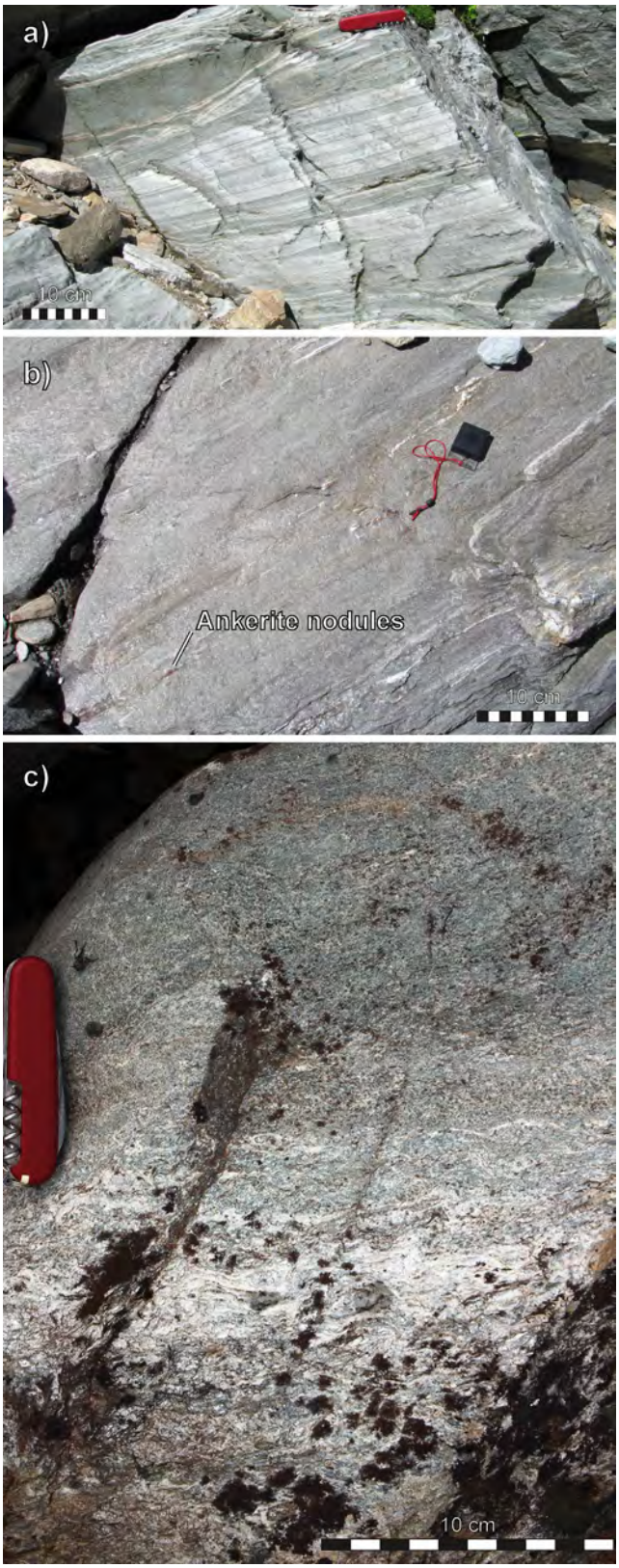

Fig. 5 *Lithologies of the Heinisch Stafel Formation.* ***a.*** *Banded amphibolite, outcrop of sample MC 253. Heinisch Stafel Alp (733500/161800).* ***b.*** *Micaschist with ankeritic spots. Heinisch Stafel Alp (733500/161800).* ***c.*** *Transition between micaschist and greenstone, Heinisch Stafel Alp (733500/161800).*

2.2.5. Garenstock Augengneiss

The Garenstock Augengneiss (Fig. 9a) is an Ordovician (Chapter 3.4) granitoid that is characterised by a prominent augen texture of K-feldspar in a mica-rich matrix occurs in the northern part of the Adula nappe. The augen texture is not present everywhere, and a transition to an augen-free gneiss can be observed locally. The gneiss composition is quartz, K-feldspar, plagioclase, white mica, biotite, garnet, epidote, zircon, apatite, and ilmenite. Metric to decimetric mafic boudins and lenses (Garenstock mafic rocks, Fig. 9b) are locally abundant within the augengneiss (Fig. 9b). Eclogite relicts are sometimes present in these boudins. A lithologic description of the Garenstock Augengneiss can be found in Kopp (in Jenny et al. 1923) and Egli (1966).

Garenstock Augengneiss samples (Table 2) are located in the granite field of the R1-R2 classification diagram (Fig. 10a). They are SiO_2-rich (69-77 wt.%) and strongly peraluminous (A/CNK = 1.2 - 1.5) (Fig. 10b). Many samples show abnormally low Na2O concentrations below 2 wt.% and as low as 0.07 wt.%, with a K_2O/Na_2O ratio between 1.5 and 3.7 and extreme values above 25. Ba concentrations are high to very high (400 to 1500 ppm). As mentioned in the introduction, the low-Na samples are interpreted as weathered rocks in relation to a pre-Triassic emersion of the basement (see Chapter 4.6). It is difficult to assess whether all analysed samples have been modified by this alteration event. The zircon morphology is mostly of type S_{13}, S_8, and S_3, which is a distinguishing characteristic of aluminous granitoids (Pupin 1980). In other words, the peraluminous character of the Garenstock granite is partly an original feature of the rock. The REE concentrations (Fig. 11a) are presumably unmodified by alteration processes. Their normalised patterns are consistent with the classic patterns of calc-alkaline granitoids; they show a significant negative Eu anomaly (Eu/Eu* = 0.4-0.7), a fractionated LREE segment (La/Sm_N = 3.1-3.7), and a relatively flat HREE (Gd/Lu_N = 1.2-2.0). The primitive mantle-normalised spider diagram (Fig. 11b) shows strong negative anomalies in Ta, Nb, Sr, and Ti. Altogether and considering the many contemporaneous mafic lenses hosted by the granite, we tentatively interpret this rock as differentiated K-feldspar-rich calc-alkaline granite.

Its peraluminous character is most likely a consequence of protracted amphibole fractionation from a wet calc-alkaline melt at deep crustal levels (Alonso-Perez et al. 2009) rather than the result of crustal anatexis, which is also suggested by the lack of inherited zircon cores.

Two samples of Garenstock mafic rocks hosted by the augengneiss were analysed (Table 1). One of them was also dated and yielded an age equivalent to that of the augengneiss (ca. 445 Ma, Chapter 3.4). Garenstock mafic rocks are considered as former microgranular enclaves or dismembered crosscutting synplutonic dykes of basaltic composition (Fig. 6), and they plot in the calc-alkaline field of the AFM diagram (Fig. 7). Their REE-normalised patterns (Fig. 8a) show a moderately fractionated LREE segment (La/Sm_N = ~2) and a relatively flat HREE segment (Gd/Lu_N = ~1.3) without an Eu anomaly. The primitive mantle-normalised spider diagrams (Fig. 8b) exhibit strong negative anomalies for Ta, Nb, and, to a lesser extent, Ti, as well as coupled positive anomalies in K and Pb. All of these geochemical features are characteristic for calc-alkaline basalts related to subduction environments (e.g., Leuthold et al. 2013).

2.2.6. Rossa Orthogneiss

The Rossa Orthogneiss and the Garenstock Augengneiss are considered separately because they are not connected in outcrop. They both have the same Ordovician age (Chapter 3.5). The Rossa Orthogneiss texture is usually fine-grained and does not exhibit the characteristic augengneiss texture typical of the Garenstock gneiss. However, some K-feldspar phenocrysts can be locally observed. Mafic boudins are rarely present, and eclogites were not found. Descriptions of this formation can be found in Frischknecht (in Jenny et al. 1923) and Kündig (1926). Frischknecht proposes a distinction between orthogneisses based on biotite content. However, the biotite content is strongly related to metamorphic grade (Spear 1995) and therefore cannot be used in the formation definition.

The Rossa orthogneiss analyses (Table 2) plot in the fields of granodiorites in the R1-R2 classification diagram (Fig. 10a) and are peraluminous (Fig. 10b) and SiO_2-rich (~69 wt.%). The REE-normalised pattern (Fig. 11a) shows a significant Eu anomaly (Eu/Eu* = ~ 0.6), a fractionated LREE segment (La/Sm_N = 3.4-3.7), and a relatively flat HREE (Gd/Lu_N = 1.5-1.9). The primitive mantle-normalised spider diagram (Fig. 11b) shows strong negative anomalies in Ta, Nb, Sr, and Ti. The two Ordovician granites, Garenstock Augengneiss and Rossa Orthogneiss, exhibit very similar geochemical characteristics. The small number of analysed samples does not allow us to compare the magmatic evolution of the two Ordovician granites, but the Rossa orthogneiss seems slightly more depleted in HREE than the Garenstock augengneiss. Both granites are interpreted as calc-alkaline.

2.2.7. Zervreila orthogneiss

The Early Permian (Chapter 3.7) Zervreila orthogneiss (Fig. 12) is one of the most widespread rock types of the northern part of the Adula nappe. It outcrops at several structural levels (base to top) of the nappe (Fig. 2). The Zervreila orthogneiss is a leucocratic granitic rock, mainly fine-grained, sometimes with an augengneiss texture formed by K-feldspar (Fig. 12). The main minerals are quartz, K-feldspar, plagioclase, and phengite. Phengite gives a typical greenish colour to the rock and is the reason why this formation is also classically called “Phengitgneise” (Jenny et al. 1923; Van der Plas 1959; Egli 1966). Biotite becomes more abundant to the south with increasing Barrovian metamorphic conditions. The accessory minerals are epidote, zircon, apatite, and garnet. The Zervreila orthogneiss is completely devoid of mafic boudins and other associated rocks. Rare biotite-rich schlieren were most likely enclaves at the origin. Zervreila Orthogneiss are muscovite-bearing peraluminous granitoids according to the classification of Barbarin (1999). A good petrographic description can be found in Jenny et al. (1923) and Egli (1966). The intrusive contacts in to the surrounding paragneiss were also described (Egli 1966;

Sample		MC 215	MC 225	MC 205	MC 210	MC 333	MC 335	MC 354	MC 209	MC 336
Formation		Garenstock	Garenstock	Salahorn	Salahorn	Salahorn	Salahorn	Salahorn	Salahorn	Salahorn
Lithology		Greenstone	Greenstone	Greenstone	Greenstone	Greenstone	Greenstone	Greenstone	Am Pl gneiss	Am Pl gneiss
SiO2	wt-%	51.04	51.80	50.68	53.01	47.93	52.80	46.64	63.81	53.14
TiO2	wt-%	1.41	1.13	1.72	1.34	1.99	1.30	2.84	0.64	0.64
Al2O3	wt-%	15.39	15.60	13.32	14.82	15.50	14.94	14.87	16.88	18.60
Fe2O3	wt-%	10.85	8.63	12.89	12.15	11.57	11.58	15.75	4.43	6.65
MnO	wt-%	0.20	0.16	0.19	0.21	0.19	0.21	0.27	0.07	0.13
MgO	wt-%	7.11	7.74	7.07	5.32	7.47	5.47	7.08	2.03	6.27
CaO	wt-%	8.61	8.00	9.42	8.86	9.94	8.19	7.91	4.42	7.78
Na2O	wt-%	2.48	3.23	3.03	3.21	3.20	2.88	2.70	4.04	3.06
K2O	wt-%	1.40	1.24	0.77	0.56	0.48	0.59	0.55	1.95	1.49
P2O5	wt-%	0.18	0.14	0.19	0.15	0.41	0.14	0.36	0.16	0.12
LOI	wt-%	1.21	2.18	0.51	0.44	1.10	1.84	0.91	1.17	2.17
Total		99.89	99.85	99.80	100.05	99.78	99.93	99.87	99.59	100.05
mg#		72	78	68	63	72	65	64	64	79
Cr	ppm	116.13	419.51	236.49	67.36	322.85	50.21	114.74	91.39	179.56
Ni	ppm	17.95	77.29	76.84	19.61	97.89	10.81	61.87	25.56	96.90
Ga	ppm	16.85	15.43	16.14	18.15	18.64	17.65	20.80	18.81	17.18
V	ppm	266.01	226.53	351.53	286.19	290.33	279.88	421.12	87.31	110.37
Rb	ppm	40.67	41.01	14.97	9.99	11.10	12.20	16.94	46.18	61.12
Ba	ppm	312.55	320.45	295.42	168.09	78.23	160.25	57.36	637.41	323.37
Sr	ppm	155.31	365.60	127.17	190.19	238.81	240.43	176.87	616.68	628.36
Ta	ppm	0.51	0.38	0.31	0.17	0.74	0.19	1.16	0.24	0.09
Nb	ppm	10.15	8.43	5.55	2.62	12.86	2.65	20.74	3.10	1.69
Hf	ppm	3.32	2.34	2.73	2.94	3.74	2.90	4.55	3.00	1.63
Zr	ppm	131.61	90.85	107.98	105.20	150.98	103.01	194.84	117.89	67.81
Y	ppm	31.62	26.24	31.49	32.07	32.71	31.59	41.78	12.07	8.98
Pb	ppm	11.05	23.33	2.97	4.82	10.91	3.93	8.57	6.90	4.04
Th	ppm	3.17	2.63	0.61	1.51	1.13	1.46	2.62	2.65	0.58
U	ppm	0.49	0.53	0.41	0.82	0.48	0.87	0.56	1.74	0.59
La	ppm	17.96	13.62	7.02	8.17	11.75	8.07	22.61	16.06	7.00
Ce	ppm	36.84	27.79	17.31	19.09	26.49	17.98	44.68	32.36	14.56
Pr	ppm	4.37	3.48	2.43	2.59	3.50	2.60	5.55	3.72	1.88
Nd	ppm	19.14	14.67	13.00	12.36	17.55	13.00	26.30	16.61	8.78
Sm	ppm	4.98	4.39	3.86	4.05	4.75	3.70	6.04	3.17	2.01
Eu	ppm	1.72	1.32	1.46	1.35	1.59	1.31	2.16	1.07	0.81
Gd	ppm	5.06	3.91	4.50	4.60	5.40	4.59	6.65	2.61	1.99
Tb	ppm	0.84	0.75	0.80	0.85	0.88	0.83	1.18	0.39	0.30
Dy	ppm	5.52	4.62	5.46	5.65	6.10	5.53	7.42	2.16	1.48
Ho	ppm	1.16	0.96	1.17	1.24	1.28	1.19	1.61	0.44	0.35
Er	ppm	3.44	2.74	3.18	3.34	3.37	3.29	4.47	1.22	0.86
Tm	ppm	0.47	0.38	0.43	0.50	0.51	0.51	0.62	0.17	0.14
Yb	ppm	3.53	2.61	3.29	3.33	3.40	3.66	4.31	1.13	0.97
Lu	ppm	0.49	0.38	0.47	0.50	0.50	0.50	0.61	0.16	0.12

Table 1 *Chemical analysis of the mafic rocks of the northern Adula nappe. Major elements (wt.%) were measured by XRF (Philips PW2400 spectrometer, Université de Lausanne). Trace elements (ppm) were measured by LA-ICP-MS on glass discs (quadrupole spectrometer Elan 6100 DRC interfaced with a GeoLas 200M ArF excimer ablation system, Université de Lausanne).*

Löw 1987). The precise metamorphic conditions recorded by the Zervreila orthogneiss are unknown.

The Zervreila orthogneiss samples (Table 2) plot in the granite and granodiorite fields of the R1-R2 classification diagram (Fig. 10a). They are rich in silica (66-77wt.% SiO2), peraluminous (Fig. 10b), and alkali-calcic according to the classification of Peacock (1931). The REE-normalised patterns are typical of granitoids (Fig. 11a), with a significant negative Eu anomaly (Eu/Eu* = 0.3-0.8), a fractionated LREE segment (La/Sm_N = 2.8-4.1), and a relatively flat HREE segment (Gd/Lu_N = 0.9-

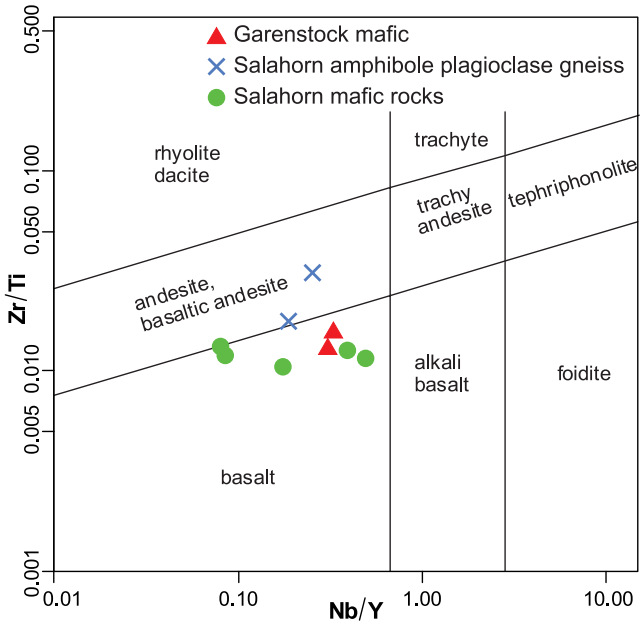

Fig. 6 a. *Mafic magmatic rocks of the northern Adula nappe plotted in the classification diagram of volcanic rocks (Pearce 1996, modified from Winchester & Floyd, 1977).*

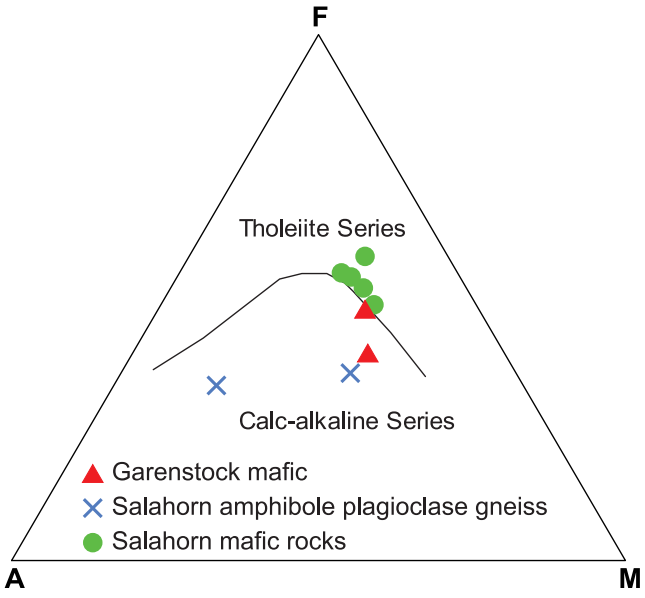

Fig. 7 *AFM discrimination diagram of the mafic rocks of the northern (after Irvine and Bargar, 1971).*

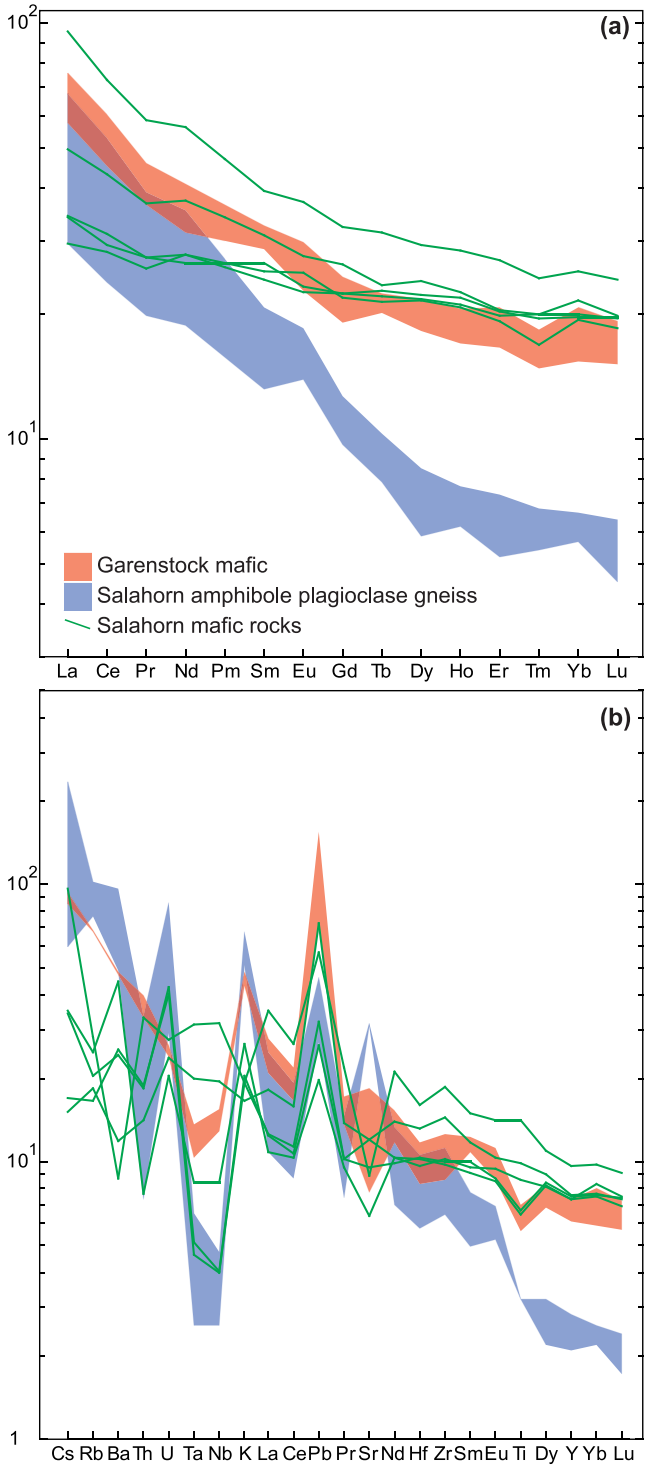

Fig. 8 *Variation diagrams of the northern Adula mafic rocks. The areas used for Garenstock mafics and amphibole-plagioclase gneiss represent only two samples.* ***a.*** *Chondrite-normalised REE diagram (after Sun and McDonough, 1989).* ***b.*** *Primitive mantle-normalised spider diagram (after McDonough and Sun, 1995).*

2.2). The primitive mantle-normalised spider diagram (Fig. 11b) shows strong negative anomalies in Ta, Nb, Sr, and Ti. Zircon morphology is restricted to P-types (Pupin 1980), i.e., the {211} pyramid is absent, a feature typical of "subalkaline" (i.e., alkali-calcic) and alkaline granites according to Pupin (1980). Nevertheless, the Zervreila orthogneiss analyses plot outside the A-type granite field in the discrimination diagrams of Whalen et al. (1987).

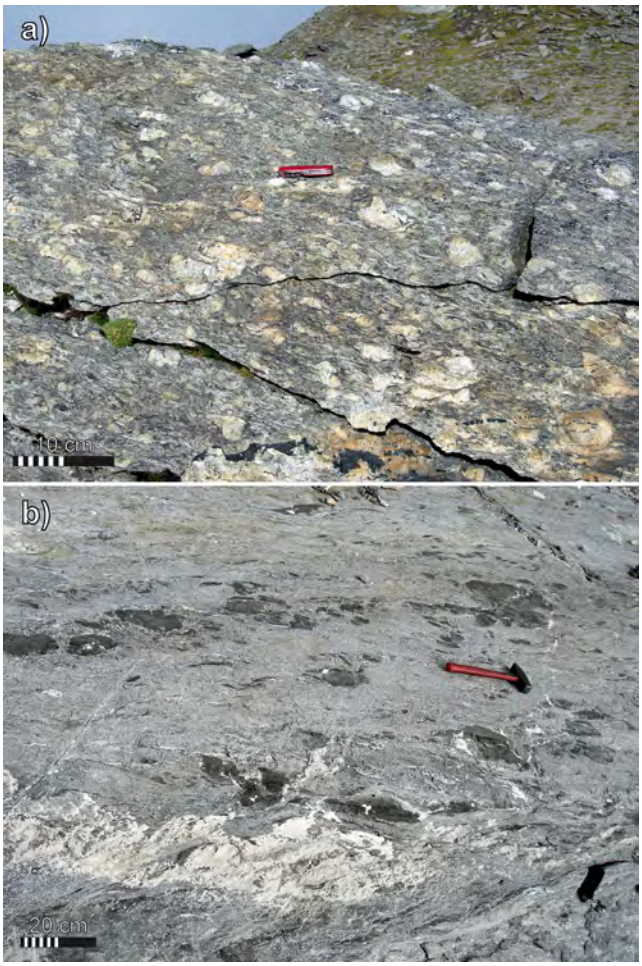

Fig. 9 *Ordovician Garenstock Augengneiss, of the northern Adula nappe.* ***a.*** *Granitic augengneiss. Garenstock (721870/157300).* ***b.*** *Garenstock mafic rock associated with the granite. Garenstock (721870/157300).*

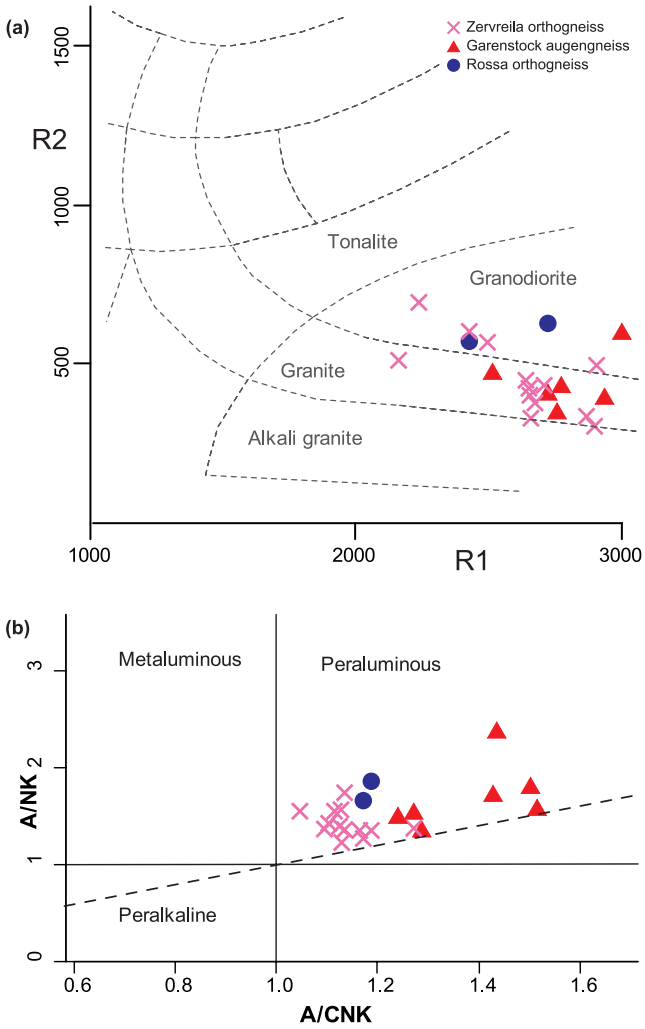

Fig. 10 *Classification of the granitoid rocks of the northern Adula.* ***a.*** *R_1-R_2 diagram (Roche et al, 1980); R1=4Si-11(Na+K)-2(Fe+Ti); R2=Al+2Mg+6Ca.* ***b.*** *Discrimination diagram for granites derived from Maniar and Piccoli (1989).*

The mineralogical and chemical characteristics of the Zervreila orthogneiss, including zircon morphology, are typical of differentiated K-feldspar-rich alkali-calcic granites, such as the Mont-Blanc granite in the western Alps (Bussy et al. 2000). Alkali-calcic granites usually occur in the late-stages of orogenic cycles or even during the initiation of subsequent extensional tectonics (Bonin et al. 1998; Barbarin 1999). We suggest that the peraluminous signature of these leucogranites is constrained by crystal fractionation at high pressure (Alonso-Perez et al. 2009) and therefore does not represent simple crustal melts because restitic enclaves are nearly absent and zircon cores are not abundant.

2.2.8. Adula nappe cover

Mesozoic (or younger?) cover rock outcrops in several places in the northern Adula nappe. In most cases, only slices or boudins of dolomitic and calcitic marble can be observed. The thickness of the slices and boudins vary from a few centimetres to several meters. A few outcrops show a more complete autochthonous stratigraphic series (Cavargna-Sani et al. 2010; Galster et al. 2012) that displays a stratigraphic contact with the basement and a characteristic North Penninic Triassic (Galster et al. 2012) sequence at its base. Basement rocks show evidence of surface alteration prior to the Mesozoic sedimentation. Dolocrete and calcrete nodules and lenses (Fig. 13) at the base of the Mesozoic sequence can locally be

observed. These formations are equivalent to the well-known pre-Triassic paleosols in less metamorphic domains: Aiguilles rouges (Demathieu and Weidmann 1982); Mont Blanc (Epard 1989); Aar (Gisler et al. 2007). Clear stratigraphic contacts of the Adula nappe cover are found on the Garenstock Augengneiss, the Salahorn Formation, the Trescolmen Formation, and the Heinisch Stafel Formation. Carboniferous or Permian clastic sediments of Verrucano type were not found on the older basement.

2.3. Zircon geochronology

2.3.1. Method

Rock samples of several kilograms in mass were crushed and ground to a powder using an oscillatory tungsten carbide disc. Zircons were extracted with manual panning and the use of heavy liquid if necessary. Magnetic separation was used to separate the zircons from magnetic minerals and to select non-metamict zircons. Transparent, "gem"-quality zircons were selected by hand picking. The morphology of the selected zircon grains was studied using secondary electron (SE) imaging with a SEM (Tescan Mira LMU, University of Lausanne). Zircons used for dating were chemically abraded following a modified procedure described by Mattinson (2005). The zircons were thermally annealed at 800°C for 10 h and then leached in a mixture of concentrated HF and HNO_3 at 110°C for 12 h. They were then carefully rinsed with distilled water, mounted in epoxy resin, abraded to the (approximately) equatorial plane, and polished. The textures of each single zircon were investigated through cathodoluminescence (CL) imaging by SEM (CamScan MV2300, University of Lausanne).

The analyses of the zircons were performed using a mono-collector Element XR sector-field instrument interfaced with an UP-193 excimer ablation system (University of Lausanne). The analytical approach applied is outlined by Ulianov et al. (2012). The operation conditions included a 35-25-µm spot size, an on-sample energy density of 2.1-2.3 J/cm^2, and a repetition rate of 5 Hz. A GJ-1 standard zircon (Pb^{206}-U^{238} age of 600.5 ± 0.4 Ma; Schaltegger et al. unpublished) was used as an external standard. The 91500 standard (Wiedenbeck et al. 1995) was measured on each run to monitor the accuracy. The ratio-of-the-mean intensity method was used for the data treatment using LAMTRACE software (Jackson 2008). No correction for common lead was applied because of the presence of mercury in the system and low $(Hg+Pb)^{204}$ intensities. Instead, a qualitative control for the presence of anomalously high $(Hg+Pb)^{204}$ net intensity values was utilised and indicated low to negligible common Pb contents. The CL image and the intensity vs. ablation time plots were accurately controlled to avoid the analysis of domains potentially enriched in common lead and/or lead losses in each measurement. Only concordant or sub-concordant zircon ages were considered.

2.3.2. Salahorn Formation

Zircons were found in one sample of the metaclastic sediments (MC 353) and in two samples of the magmatic amphibole plagioclase gneiss (MC 209, MC 336). This gneiss corresponds to group (b) of the mafic rocks described in Chapter 2.2. In mafic rocks of group (a), zircons were observed by BSE in thin sections but were very small (< 20 µm), usually interstitial, and rich in amphibole inclusions. Their internal texture is homogeneous, and they are most likely of metamorphic origin. No zircon grains were obtained from samples of mafic rocks of type (a).

The paragneiss sample MC 353 is composed mainly of quartz, albite, white mica, and chlorite and contains a few ankerite grains. The sampled outcrop shows a transition to micaceous garnet gneiss. Zircons in this sample have a size of approximately 50-250 µm and are of pale pink colour. Morphologically, these zircons form a homogeneous population. They present

Sample		MC 084	MC 120	MC 130	MC 132	MC 133	MC 138	MC 142	MC 152	MC 212	MC 239	MC 240	MC 241	MC 247
Formation		Zervreila	Zervreila	Zervreila	Zervreila	Zervreila	Zervreila	Zervreila	Zervreila	Zervreila	Zervreila	Zervreila	Zervreila	Zervreila
Lithology		Orthogneiss	Orthogneiss	Orthogneiss	Orthogneiss	Orthogneiss	Orthogneiss	Orthogneiss	Orthogneiss	Orthogneiss	Orthogneiss	Orthogneiss	Orthogneiss	Orthogneiss
SiO2	wt-%	73.35	76.49	68.29	73.14	73.59	74.98	73.54	75.09	73.94	69.71	70.45	66.21	73.36
TiO2	wt-%	0.21	0.07	0.48	0.24	0.20	0.10	0.19	0.11	0.20	0.43	0.36	0.61	0.31
Al2O3	wt-%	13.83	12.57	14.94	13.45	13.61	13.15	13.54	13.07	13.71	15.04	14.99	16.46	13.66
Fe2O3	wt-%	1.92	1.28	2.99	2.13	1.92	1.69	1.77	1.17	1.70	3.40	2.90	4.29	2.60
MnO	wt-%	0.04	0.02	0.05	0.06	0.06	0.03	0.05	0.03	0.05	0.08	0.06	0.07	0.07
MgO	wt-%	0.53	0.22	0.89	0.79	0.55	0.59	0.71	0.40	0.61	0.75	1.08	1.41	0.64
CaO	wt-%	1.37	0.40	1.59	1.03	1.22	0.40	0.81	0.48	0.73	2.51	2.01	2.76	1.84
Na2O	wt-%	3.31	3.03	3.05	3.40	3.55	3.32	3.15	3.29	3.17	3.59	3.40	3.49	3.11
K2O	wt-%	4.33	4.63	5.18	4.05	3.74	3.82	4.58	4.89	4.61	3.58	3.85	3.45	3.41
P2O5	wt-%	0.08	0.02	0.21	0.08	0.08	0.03	0.07	0.02	0.07	0.16	0.13	0.21	0.13
LOI	wt-%	0.66	0.48	1.51	0.73	0.77	0.91	0.76	0.63	0.99	0.42	0.51	0.62	0.73
Total		99.62	99.20	99.17	99.11	99.30	99.02	99.17	99.17	99.79	99.66	99.74	99.57	99.85
mg#		52	40	54	60	53	58	62	57	59	47	60	57	49
Cr	ppm	41.25	91.93	73.75	246.74	187.66	187.60	250.03	135.32	37.27	52.31	54.28	65.41	74.54
Ni	ppm	21.11	0.00	14.05	5.52	78.60	8.96	20.37	10.12	21.79	17.71	20.22	27.31	21.93
Ga	ppm	16.09	13.26	18.91	15.53	16.09	13.92	13.19	13.47	14.60	19.89	19.30	21.14	17.74
V	ppm	26.13	13.09	44.43	30.53	28.83	12.15	26.12	14.52	22.30	46.41	41.73	54.20	38.66
Rb	ppm	121.28	122.91	110.00	176.15	184.96	82.21	163.96	160.24	174.17	151.99	139.77	126.62	167.74
Ba	ppm	464.58	240.00	1213.47	259.82	297.37	258.56	290.46	122.44	265.77	560.95	443.25	650.22	250.72
Sr	ppm	125.89	26.21	172.32	114.09	97.07	38.07	85.96	47.28	76.14	153.18	240.44	309.23	154.27
Ta	ppm	0.79	0.78	0.77	2.66	2.80	0.40	1.78	1.69	1.55	1.04	1.13	0.79	2.08
Nb	ppm	10.53	9.10	13.06	17.80	17.05	10.27	12.92	11.66	13.09	14.50	10.76	12.52	14.67
Hf	ppm	3.25	2.86	6.60	3.52	3.23	4.56	2.85	3.07	3.03	5.72	3.51	4.71	3.65
Zr	ppm	111.72	88.98	250.34	110.67	101.52	146.33	90.58	79.00	97.20	220.61	123.46	189.59	128.52
Y	ppm	29.59	16.12	47.56	32.92	36.35	18.60	23.63	19.15	28.55	28.66	23.75	19.33	25.79
Pb	ppm	19.83	19.57	22.78	45.41	15.88	8.66	16.78	17.13	18.24	12.80	19.88	14.98	20.82
Th	ppm	15.71	7.00	21.58	19.87	14.64	10.26	13.53	25.24	13.33	13.37	12.24	9.29	15.19
U	ppm	4.44	2.35	2.12	9.56	11.26	1.83	6.92	7.17	5.22	5.08	6.04	3.81	6.28
La	ppm	34.92	14.15	54.22	27.49	23.81	33.28	18.87	16.52	19.36	44.71	31.85	33.29	29.77
Ce	ppm	68.15	30.71	109.07	56.43	47.93	73.31	38.57	36.58	38.00	84.66	60.90	62.54	56.44
Pr	ppm	7.65	3.58	12.30	6.29	5.26	8.54	4.07	4.39	4.22	9.43	6.87	6.60	6.30
Nd	ppm	28.96	14.52	46.91	22.42	19.89	34.32	15.22	15.70	16.23	35.59	25.47	26.62	24.04
Sm	ppm	6.22	3.20	9.52	4.99	4.80	7.55	3.55	3.72	3.82	6.86	5.50	5.09	4.79
Eu	ppm	0.88	0.34	1.38	0.58	0.48	0.62	0.45	0.32	0.51	1.23	0.92	1.30	0.65
Gd	ppm	5.39	2.82	8.69	4.88	4.38	6.00	3.37	3.14	3.48	5.44	4.12	4.47	4.41
Tb	ppm	0.91	0.43	1.25	0.83	0.82	0.82	0.54	0.49	0.64	0.85	0.71	0.60	0.71
Dy	ppm	5.02	2.81	8.51	5.19	5.34	4.40	3.74	3.02	4.27	4.92	4.10	3.49	4.04
Ho	ppm	1.03	0.57	1.64	1.04	1.18	0.80	0.77	0.63	0.92	1.00	0.82	0.64	0.90
Er	ppm	2.71	1.63	4.89	3.20	3.48	1.93	2.39	1.83	2.72	2.67	2.12	1.65	2.28
Tm	ppm	0.41	0.23	0.74	0.51	0.53	0.27	0.38	0.31	0.46	0.40	0.33	0.25	0.38
Yb	ppm	2.64	1.50	4.89	3.64	4.34	1.70	2.72	2.32	3.10	2.82	2.25	1.65	2.65
Lu	ppm	0.38	0.23	0.68	0.54	0.61	0.25	0.40	0.37	0.49	0.39	0.30	0.25	0.40

Table 2 *Chemical analysis of the granitoid rocks of the northern Adula nappe. Major elements (wt.%) were measured by XRF (Philips PW2400 spectrometer, Université de Lausanne). Trace elements (ppm) were measured by LA-ICP-MS on glass discs (quadrupole spectrometer Elan 6100 DRC interfaced with a GeoLas 200M ArF excimer ablation system, Université de Lausanne).*

Sample			MC 184	MC 213	MC 219	MC 227	MC 272	MC 302	MC 357	MC 243	MC 242
Formation			Garenstock	Garenstock	Garenstock	Garenstock	Garenstock	Garenstock	Garenstock	Rossa	Rossa
Lithology			Orthogneiss	Orthogneiss	Orthogneiss	Orthogneiss	Orthogneiss	Orthogneiss	Orthogneiss	Orthogneiss	Orthogneiss
SiO2	wt-%		70.98	69.17	71.72	67.49	77.38	73.25	73.18	69.03	69.45
TiO2	wt-%		0.51	0.40	0.41	0.59	0.14	0.44	0.22	0.53	0.32
Al2O3	wt-%		14.51	16.52	14.18	15.33	12.26	13.05	14.21	14.95	16.14
Fe2O3	wt-%		3.55	2.58	2.65	3.12	0.83	3.22	1.97	4.21	2.21
MnO	wt-%		0.05	0.04	0.03	0.06	0.02	0.04	0.03	0.07	0.03
MgO	wt-%		0.94	1.12	0.87	1.01	0.32	0.56	0.40	1.46	0.52
CaO	wt-%		0.85	0.90	0.21	2.32	0.20	0.98	0.97	2.47	2.13
Na2O	wt-%		2.57	2.85	0.07	0.21	1.63	1.86	2.59	2.72	3.14
K2O	wt-%		4.04	4.30	8.20	5.63	6.07	5.07	4.99	3.33	4.36
P2O5	wt-%		0.23	0.23	0.09	0.22	0.12	0.24	0.19	0.17	0.20
LOI	wt-%		1.70	1.87	1.61	3.84	0.78	1.11	1.18	0.58	0.64
Total			99.93	99.98	100.04	99.82	99.75	99.82	99.93	99.52	99.12
mg#			51	63	57	56	61	41	45	58	48
Cr		ppm	52.69	42.39	26.53	39.88	21.67	22.27	23.91	92.42	67.21
Ni		ppm	10.88	10.87	0.00	9.23	6.88	6.96	6.20	32.80	26.30
Ga		ppm	18.80	18.35	14.67	18.79	9.96	19.83	17.76	18.58	19.32
V		ppm	43.52	40.72	35.31	53.59	15.32	42.19	26.89	70.07	29.71
Rb		ppm	98.50	101.74	138.89	166.14	103.62	254.32	174.96	107.34	104.03
Ba		ppm	745.30	1492.77	848.50	1370.55	629.83	395.85	508.55	680.32	1152.54
Sr		ppm	113.97	192.18	33.86	80.80	45.95	55.12	98.39	205.59	255.90
Ta		ppm	0.62	0.44	0.59	0.60	0.19	1.63	0.79	0.73	1.38
Nb		ppm	12.15	8.83	9.69	13.03	3.14	18.52	9.89	11.38	9.60
Hf		ppm	7.25	5.43	4.99	7.46	2.46	5.53	3.78	5.31	3.98
Zr		ppm	281.20	210.76	188.54	290.71	82.72	202.92	121.61	211.11	150.35
Y		ppm	58.30	32.68	43.77	47.95	31.23	41.22	35.28	33.15	36.09
Pb		ppm	9.82	21.83	9.17	18.40	9.55	10.23	18.04	15.37	22.80
Th		ppm	22.69	15.96	16.78	21.12	7.72	16.76	10.75	11.18	13.75
U		ppm	1.92	2.06	1.89	1.62	0.97	1.85	4.36	2.72	2.01
La		ppm	52.98	47.68	37.02	56.67	12.14	32.29	20.88	33.66	38.71
Ce		ppm	102.76	90.31	71.55	108.67	24.93	62.81	40.40	63.59	73.37
Pr		ppm	11.63	10.07	8.01	12.25	2.82	7.14	4.61	7.12	8.28
Nd		ppm	44.24	39.23	31.19	47.69	10.76	27.90	18.71	28.10	31.52
Sm		ppm	8.91	8.08	7.03	9.89	3.14	6.08	4.26	6.16	6.45
Eu		ppm	1.05	1.65	0.96	1.30	0.44	0.77	0.66	1.10	1.31
Gd		ppm	8.42	6.52	6.68	8.40	3.40	6.34	4.40	5.45	6.15
Tb		ppm	1.46	1.08	1.08	1.34	0.73	1.20	0.88	0.90	1.03
Dy		ppm	9.21	6.02	7.12	8.07	5.20	7.38	5.52	5.51	6.23
Ho		ppm	2.10	1.19	1.57	1.77	1.11	1.47	1.25	1.18	1.24
Er		ppm	6.01	3.01	4.61	4.86	2.80	3.77	3.41	3.22	3.40
Tm		ppm	0.82	0.45	0.68	0.71	0.41	0.56	0.45	0.44	0.44
Yb		ppm	5.74	2.90	4.69	4.53	2.43	3.47	3.31	2.96	3.02
Lu		ppm	0.75	0.41	0.66	0.66	0.33	0.48	0.45	0.46	0.41

Table 2 *Continued*

a clear crystalline shape with well-developed prisms and pyramids usually found in plutonic rocks (Fig. 14 i). Distinct oscillatory zoning is ubiquitous. Xenocrystic cores or metamorphic overgrowths were not found. The analysed zircons form a surprisingly homogeneous age population for a paragneiss (Table 3). Even with the sedimentary origin of the sample, we chose to calculate the median age using the TuffZirc algorithm (Ludwig and Mundil 2002) and did not retain only the youngest age; the age distribution is unimodal and the possibility of radiogenic lead loss during metamorphism cannot be ruled out. The calculated median age is 518.3 + 4.0 - 3.5 Ma (Fig. 15b). We interpret that this age is close to the sedimentation age of this formation (see the discussion in chapter 4.1).

Zircons in the amphibolite gneiss (MC 209, MC 336) are very abundant. Their sizes range from approximately 30-500 μm, and they are pink-coloured. The crystal habit is essentially defined by elongated prisms, and the pyramids are lacking (Fig. 14h). The texture of the amphibolite gneiss zircons is homogeneous or broadly zoned (Fig. 14h). Xenocrystic cores or

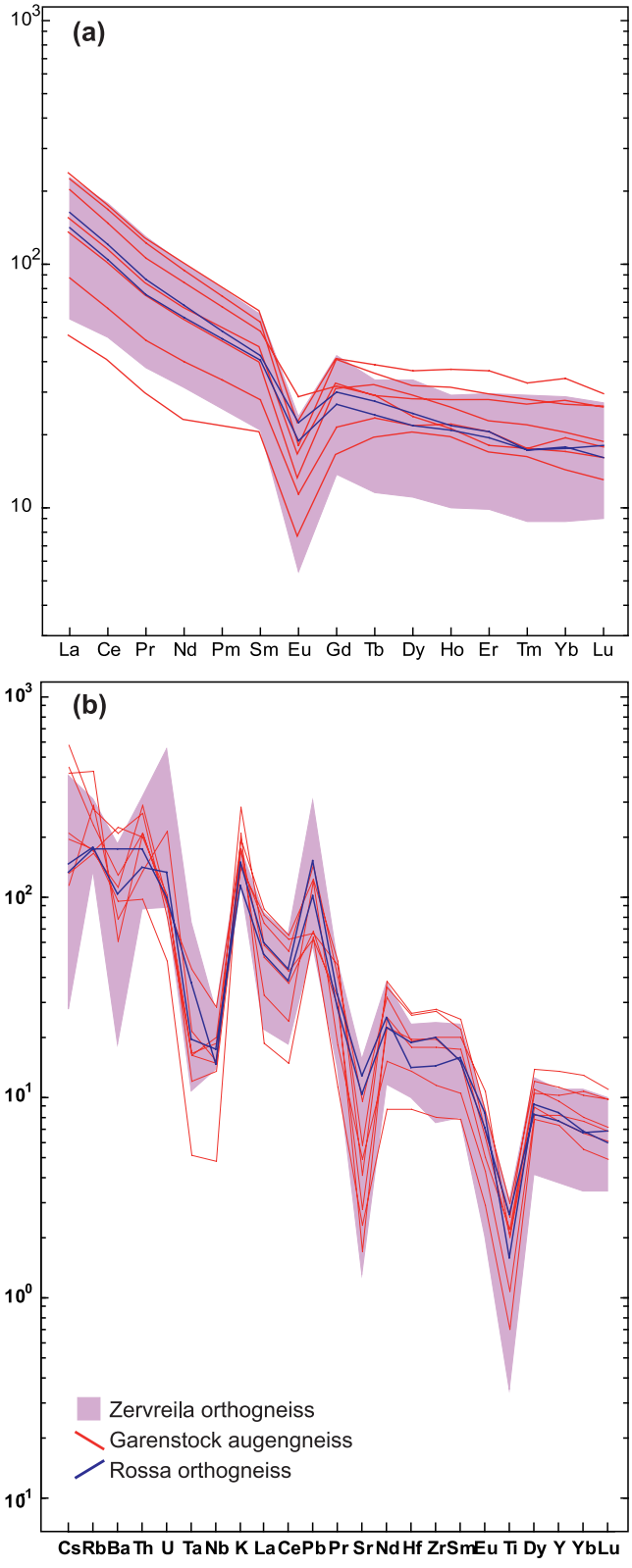

Fig. 12 *Zervreila orthogneiss. Val Scaradra (719950/157250).*

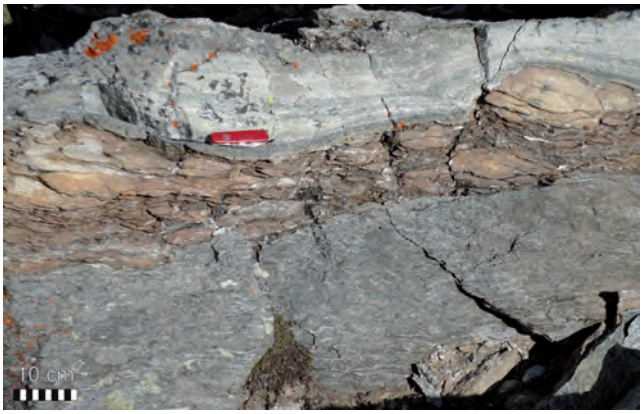

Fig. 13 *Dolocrete on the Garenstock Augengneiss and below Triassic quartzite interpreted as pre-Triassic paleosol (see text). Plattenberg area (721600/157250).*

◀ ***Fig. 11*** *Variation diagrams of the northern Adula granitoid rocks.* ***a.*** *Chondrite-normalised REE diagram (derived from Sun and McDonough, 1989).* ***b.*** *Primitive mantle-normalised spider diagram (after McDonough and Sun, 1995).*

metamorphic overgrowths were not found. The calculated median TuffZirc ages (Table 3) of these two samples are similar at 514.7 +2.6 -2.2 and 517.1 +2.0 -3.7 Ma (Fig. 15b). These ages are interpreted as a magmatic age because of the lack of metamorphic overgrowths and the oscillatory zoning of the analysed domains.

2.3.3. Trescolmen Formation

A few zircons of a kyanite eclogite (AD 108; extracted by Lucia Santini) were analysed. Five multigrain zircon fractions were previously analysed by Santini (1992) using ID-TIMS. Concordant or nearly concordant ages ranging between 520 and 540 Ma were obtained by this author.

The zircons analysed in our study are small, elongated grains with a broad oscillatory zoning. The measured age (Table 3; Fig. 15c) is 521.1 +4.0 -5.3 Ma. This age is interpreted as magmatic and confirms the previous results obtained by Santini (1992).

2.3.4. Garenstock Augengneiss

Four samples of the Garenstock Augengneiss (MC 130, MC 227, MC 302, and MC 357) and one sample of an amphibolite boudin (MC 225) were analysed. The Garenstock Augengneiss is very rich in zircon. Their size ranges between 50 and 500 µm, and their colour is generally white, grey, or colourless. The crystal edges are generally slightly smoothed, but the crystalline form is still well identifiable. Textures of the zircon show good magmatic oscillatory zoning (Fig. 14f) with a locally thin (< 5 µm) metamorphic overgrowth. A few xenocrystic cores were observed and analysed. The CL images of several zircons show some patches, most likely indicating late lead losses. The calculated median ages of the four Garenstock Augengneiss samples are 457.8 +3.4 -3.2, 446.4 +2.0 -4.9, 451.4 +1.7 -2.7, and 451.5 +2.1 -3.4 (Table 3; Fig. 15d). The magmatic origin of these ages is supported by the CL features of the analysed domains and by the reproducibility of the age. The xenocrystic cores yielded ages of 518.9 ± 6.1, 572.1 ± 5.9, and 579.4 ± 7.3 Ma (Table 3). It was not possible to analyse the metamorphic rim.

The amphibolite sample (MC 225) provided a reasonable amount of zircon with variable morphology and texture. Many crystals are lacking the pyramids, presenting only prisms; some grains with pyramids are similar to the zircons of the augengneiss but slightly rounded (Fig. 14e). Only a few grains show a clear oscillatory zoning. More frequently, the zircons are unzoned or present a broadly patchy zoning (Fig. 14e). Xenocrystic cores are relatively abundant. The ages of the analysed zircons were coherently distributed (Table 3; Fig. 15d), and the median calculated age was 444.5 +2.7 -2.0 Ma. This age is interpreted as magmatic due to the coherency of the analysed spot and the reproducibility of the data. Xenocrystic cores have ages of 540.9 ± 5.7, 555.2 ± 5.4, and 901.9 ± 7.6 Ma.

The age obtained from the amphibolite is identical, within the uncertainties, to the orthogneiss ages, which suggests a contemporaneous emplacement of both magmatic rocks that is also confirmed by the narrow association of these two magmatic rocks in the field.

2.3.5. Rossa orthogneiss

Two samples (MC 242 and MC 243) were analysed. The size of the extracted zircons ranges from 50-300 µm, and the zircons are white, grey, or pale pink. The morphology of the Rossa orthogneiss and the Garenstock Augengneiss zircons is almost identical. They are categorised as S-type according to the Pupin classification (1980). The zircons are oscillatory-zoned (Fig. 14d) locally with a thin (< 5 µm) overgrowth. A few xenocrystic cores were found. The two samples yielded nearly equal calculated ages of 459.3 +3.4 -1.7 and 455.7 +2.6 -2.7 Ma (Table 3; Fig. 15e), which are interpreted as magmatic ages. One concordant xenocryst age was 533 ± 10.8 Ma.

Sample	Zircon domain	207Pb/235U Ratio	1s %	206Pb/238U Ratio	1s %	Rho	206Pb/238U AGE (Ma)	+/- 2 S.D.	207Pb/235U AGE (Ma)	+/- 2 S.D.
MC 120 Zervreila orthogneiss (728701/151039/1910)										
MC 120	osc	0.3237	0.8	0.0457	0.41	0.26	287.9	2.3	284.7	4.2
MC 120	osc	0.3312	1.1	0.0459	0.48	0.22	289.4	2.7	290.5	5.7
MC 120	osc	0.332	1	0.0463	0.59	0.30	291.9	3.4	291.1	5.1
MC 120	osc	0.3386	1.5	0.0461	0.4	0.13	290.6	2.3	296.1	7.7
MC 120	osc	0.3425	1.8	0.0455	0.51	0.14	286.9	2.9	299.1	9.2
MC 133 Zervreila orthogneiss (720035/157255/2090)										
MC 133	homog	0.3399	1.5	0.0477	1.37	0.46	300.6	8.1	297.1	7.9
MC 133	osc	0.341	1.1	0.0467	0.69	0.31	294.5	4	298	5.9
MC 133	osc	0.342	1.5	0.0466	1.2	0.40	293.4	6.9	298.7	7.5
MC 133	osc	0.3423	1.1	0.0472	1.22	0.55	297.6	7.1	298.9	5.8
MC 133	osc	0.3433	1.3	0.0471	0.65	0.25	297	3.8	299.7	7
MC 133	osc	0.3436	1.1	0.047	0.54	0.25	296.1	3.1	299.9	5.5
MC 133	osc	0.3437	0.8	0.0465	0.53	0.33	292.9	3.1	300	3.9
MC 133	osc	0.3442	1	0.0467	0.41	0.21	294.4	2.4	300.3	5
MC 133	osc	0.3453	1.1	0.047	0.44	0.20	296.1	2.6	301.2	5.9
MC 133	osc	0.3454	1.8	0.0467	1.26	0.35	294.3	7.3	301.3	9.4
MC 133	osc	0.3484	1.4	0.0475	0.9	0.32	299	5.2	303.5	7.1
MC 133	homog	0.3504	1.1	0.0472	0.51	0.23	297.1	3	305	5.6
MC 133	osc	0.3513	1	0.0477	0.51	0.26	300.5	3	305.7	5.4
MC 133	osc	0.3526	1.5	0.0477	0.68	0.23	300.6	4	306.7	8
MC 138 Zervreila orthogneiss (726913/151803/2582)										
MC 138	osc	0.331	1.2	0.0463	1.03	0.43	291.6	5.7	293.1	6.6
MC 138	osc	0.332	0.7	0.0465	0.32	0.23	292.8	1.8	291.1	3.6
MC 138	osc	0.3341	1	0.0464	0.47	0.24	292.7	2.7	292.7	5.2
MC 138	osc	0.3342	1.4	0.0462	0.68	0.24	288.7	3.9	293.5	7.2
MC 138	osc	0.3382	1.1	0.0462	0.41	0.19	291.4	2.3	295.8	5.9
MC 138	osc	0.3389	1.3	0.0464	0.43	0.17	292.7	2.4	296.4	6.5
MC 138	osc	0.3482	2.1	0.0471	0.78	0.19	295.8	4.5	307	12
MC 138	core	0.5328	1.1	0.0678	0.78	0.35	423.1	6.4	434	8.1
MC 142 Zervreila orthogneiss (728434/159328/1971)										
MC 142	osc	0.3291	1.2	0.0465	0.53	0.22	293.2	3	288.9	5.8
MC 142	osc	0.3295	0.9	0.046	0.46	0.26	289.6	2.6	289.1	4.7
MC 142	osc	0.3298	1	0.0459	0.43	0.22	289.5	2.4	289.4	5.1
MC 142	osc	0.3309	1	0.0462	0.48	0.24	291.2	2.7	290.2	5
MC 142	osc	0.3321	1.3	0.0463	0.92	0.35	292.1	5.3	291.2	6.8
MC 142	osc	0.3322	1.1	0.046	0.58	0.26	290.2	3.3	291.3	5.5
MC 142	patchy	0.339	1.2	0.0457	0.73	0.30	288.2	4.1	296.4	6.1
MC 142	osc	0.3531	1.3	0.0462	0.47	0.18	291.5	2.7	307	6.7
MC 239 Zervreila orthogneiss (733211/140387/1886)										
MC 239	osc	0.3261	1.7	0.0465	0.5	0.15	292.9	2.9	286.6	8.4
MC 239	osc	0.3284	1.1	0.0462	1.03	0.47	291.3	5.9	288.3	5.7
MC 239	osc	0.3298	1.2	0.0462	0.47	0.20	290.9	2.7	289.5	5.8
MC 239	osc	0.3361	2	0.0463	0.96	0.24	291.8	5.5	294.2	10.3
MC 239	osc	0.3384	1.2	0.0459	0.44	0.18	289.3	2.5	295.9	6.2
MC 239	osc	0.3415	2.6	0.046	0.89	0.17	289.8	5	298.3	13.3
MC 239	osc	0.3435	2	0.0458	0.76	0.19	288.6	4.3	299.8	10.3
MC 239	osc	0.3483	2.1	0.0455	1.48	0.35	287	8.3	303.5	10.9
MC 239	osc	0.35	2	0.0461	1.7	0.43	290.6	9.6	304.7	10.3
MC 239	osc	0.3525	1.2	0.0466	1.23	0.51	293.3	7	306.6	6.4
MC 239	homog	0.3526	1.2	0.0458	0.8	0.33	288.8	4.5	306.6	6.5
MC 239	patchy	0.3613	2.3	0.0458	0.78	0.17	288.7	4.4	313.2	12.4
MC 239	core	0.5571	1.6	0.0726	0.78	0.24	451.9	6.8	449.6	11.3
MC 239	core	0.7052	2.3	0.0842	1.4	0.30	521.4	14	541.9	19.7
MC 241 Zervreila orthogneiss (732191/139867/1656)										
MC 241	osc	0.3222	1.1	0.0462	0.93	0.42	291.2	5.3	283.6	5.2
MC 241	osc	0.3269	1.5	0.0456	0.88	0.29	287.2	5	287.2	7.4
MC 241	osc	0.3276	1.5	0.0453	0.71	0.24	285.6	4	287.8	7.4
MC 241	osc	0.3278	1.4	0.0456	0.97	0.35	287.7	5.5	287.9	6.9
MC 241	osc	0.3295	1.7	0.0454	1.14	0.34	286.3	6.4	289.2	8.3
MC 241	homog	0.3305	2.2	0.0447	1	0.23	282	5.5	290	11.3
MC 241	osc	0.3314	1.5	0.0442	1.4	0.47	278.6	7.6	290.7	7.8
MC 241	osc	0.3323	1.4	0.0466	1.27	0.45	293.4	7.3	291.3	7.3
MC 241	osc	0.3358	1.5	0.0457	0.85	0.28	288	4.8	293.9	7.5
MC 241	osc	0.3361	1.4	0.0464	1.43	0.51	292.5	8.2	294.2	7.3
MC 241	osc	0.3383	1.4	0.0461	0.81	0.29	290.6	4.6	295.9	7.1
MC 241	core	1.625	1.2	0.1632	1.02	0.43	974.3	18.5	979.9	15.6
MC 130 Garenstock augengneiss (721891/157321/2943)										
MC 130	osc	0.6004	1.4	0.073	0.5	0.18	454.2	4.4	477.8	10.6
MC 130	osc	0.5708	1.5	0.0742	0.48	0.16	461.2	4.3	458.8	11.4
MC 130	osc	0.5729	1.3	0.0734	0.49	0.19	456.9	4.3	460.1	9.9
MC 130	homog	0.5781	1	0.0741	0.49	0.25	460.7	4.4	462.5	6.7
MC 130	homog	0.5863	1.7	0.0731	0.67	0.20	454.6	5.9	468.7	13.1
MC 130	osc	0.5983	1.4	0.0734	0.61	0.22	456.6	5.4	476.3	10.8
MC 130	patchy	0.58	1.6	0.0736	0.62	0.19	457.8	5.5	464.5	11.6
MC 130	osc	0.5593	1.7	0.0734	0.57	0.17	456.4	5	451.1	12.1
MC 130	osc	0.5772	1.7	0.0737	1.24	0.36	458.5	11	462.7	12.8
MC 130	patchy	0.574	1.5	0.0728	0.55	0.18	452.9	4.8	460.6	10.9

Table 3 *U-Pb isotopic data on zircons from the northern Adula basement.*

Sample	Zircon domain	207Pb/235U Ratio	1s %	206Pb/238U Ratio	1s %	Rho	206Pb/238U AGE (Ma)	+/- 2 S.D.	207Pb/235U AGE (Ma)	+/- 2 S.D.
MC 130	osc	0.592	1.6	0.0741	0.69	0.22	460.8	6.1	472.2	12.1
MC 130	osc	0.5846	1.6	0.0742	0.62	0.19	461.7	5.5	467.4	11.9
MC 130	osc	0.6031	1.5	0.0747	0.65	0.22	464.4	5.8	479.2	11.4
MC 227 Garenstock augengneiss (721694/157281/2972)										
MC 227	osc	0.5649	1.3	0.0721	0.54	0.21	448.8	4.7	454.7	9.5
MC 227	osc	0.5678	1.8	0.0717	0.63	0.18	446.7	5.5	456.6	13.1
MC 227	homog	0.5484	1	0.0717	0.52	0.26	446.4	4.5	444	7.4
MC 227	osc	0.5599	1.4	0.0709	0.64	0.23	441.5	5.4	451.4	9.8
MC 227	osc	0.5548	1	0.072	0.45	0.23	448.4	3.9	448.1	7.5
MC 227	homog	0.5514	1.9	0.0714	0.61	0.16	444.3	5.2	445.9	13.9
MC 227	osc	0.5632	1.9	0.0708	0.66	0.17	440.7	5.6	453.6	13.8
MC 227	osc	0.5688	1.2	0.0707	0.66	0.28	440.6	5.6	457.2	8.6
MC 227	osc	0.5529	1.1	0.0713	0.65	0.30	444	5.6	446.9	7.8
MC 227	osc	0.5638	2	0.0716	0.55	0.14	445.9	4.7	454	14.6
MC 227	osc	0.5583	2	0.0709	0.57	0.14	441.3	4.9	450.4	14.7
MC 227	core	0.7768	1.3	0.0928	0.54	0.21	572.1	5.9	583.7	11.9
MC 227	osc	0.56	1.9	0.0725	0.95	0.25	451	8.3	451.5	13.9
MC 227	osc	0.5598	2.2	0.0718	0.98	0.22	447	8.5	451.4	16.2
MC 227	osc	0.5674	2.2	0.0727	0.83	0.19	452.5	7.2	456.3	16.3
MC 227	osc	0.5456	1.5	0.072	1.33	0.44	448.3	11.5	442.1	10.9
MC 302 Garenstock augengneiss (730609/159303/2532)										
MC 302	osc	0.5557	1.3	0.0727	1.21	0.47	452.6	10.6	448.7	9.2
MC 302	osc	0.5538	1.1	0.0721	0.82	0.37	448.9	7.1	447.5	7.7
MC 302	osc	0.5668	1.4	0.072	1.08	0.39	448.3	9.4	455.9	10.5
MC 302	osc	0.5507	0.9	0.0721	0.69	0.38	448.7	6	445.5	6.3
MC 302	homog	0.561	1.1	0.0718	0.57	0.26	447	4.9	452.2	8.1
MC 302	patchy	0.5569	1.2	0.0725	0.63	0.26	451.5	5.5	449.5	8.5
MC 302	osc	0.565	1	0.0723	0.55	0.28	449.9	4.8	454.8	7.2
MC 302	osc	0.5762	1.4	0.0738	0.83	0.30	458.8	7.4	462	10.2
MC 302	osc	0.5646	1	0.0726	0.58	0.29	451.9	5.1	454.5	7.1
MC 302	osc	0.5755	1.1	0.0728	0.67	0.30	453	5.9	461.5	8.5
MC 302	osc	0.5552	1.5	0.0732	0.77	0.26	455.2	6.7	448.4	11
MC 302	osc	0.5679	1	0.073	0.47	0.24	454.4	4.1	456.7	7.1
MC 302	osc	0.5746	1.2	0.0725	0.66	0.28	451.2	5.8	461	9.1
MC 302	osc	0.5443	1	0.0713	0.59	0.30	444	5.1	441.3	7.4
MC 357 Garenstock augengneiss (724753/150514/2508)										
MC 357	osc	0.5496	1.4	0.0729	0.69	0.25	453.8	6.1	444.8	10.3
MC 357	osc	0.5657	1.5	0.072	0.55	0.18	448.1	4.8	455.3	11.1
MC 357	osc	0.5597	1	0.073	0.46	0.23	453.9	4	451.3	7.6
MC 357	osc	0.5631	1.3	0.0728	0.53	0.20	453.2	4.6	453.5	9.2
MC 357	osc	0.5657	1.2	0.0726	0.48	0.20	451.8	4.2	455.2	8.6
MC 357	osc	0.5618	0.8	0.0725	0.54	0.34	451.5	4.7	452.7	5.6
MC 357	osc	0.5686	0.9	0.0729	0.36	0.20	453.6	3.1	457.1	6.5
MC 357	osc	0.5723	1.3	0.0723	0.69	0.27	449.8	6	459.5	9.9
MC 357	osc	0.563	1.3	0.0727	0.51	0.20	452.2	4.5	453.5	9.5
MC 357	osc	0.5636	0.9	0.0732	0.53	0.29	455.7	4.7	453.8	6.3
MC 357	osc	0.5706	1.1	0.0724	0.63	0.29	450.9	5.5	458.4	8.4
MC 357	osc	0.5726	1.2	0.0717	0.67	0.28	446.1	5.8	459.7	8.8
MC 357	osc	0.5775	1.6	0.072	0.59	0.18	448.3	5.2	462.9	11.7
mc 357	core	0.6701	1	0.0838	0.61	0.31	518.9	6.1	520.8	8.6
MC 357	osc	0.5504	1.2	0.0718	0.62	0.26	446.7	5.4	445.2	8.6
MC 357	osc	0.5659	1	0.0718	0.47	0.24	447.3	4.1	455.4	7.2
MC 242 Rossa orthogneiss (729914/137278/1165)										
MC 242	homog	0.5447	1.9	0.0738	0.94	0.25	459.2	8.4	441.5	13.3
MC 242	osc	0.5881	1.7	0.0749	1.54	0.45	465.3	13.9	469.7	13.1
MC 242	osc	0.5627	1.4	0.0736	1.6	0.57	457.6	14.1	453.3	10.1
MC 242	osc	0.589	1.6	0.0756	1.69	0.53	469.8	15.3	470.2	12.4
MC 242	osc	0.5861	1.7	0.075	1.79	0.53	466.5	16.1	468.4	12.6
MC 242	osc	0.5597	1.3	0.0741	1.32	0.51	461.1	11.7	451.3	9.2
MC 242	homog	0.5662	1.2	0.0735	1.06	0.44	457.3	9.4	455.5	9
MC 242	osc	0.5734	1.9	0.0729	1.69	0.44	453.8	14.8	460.2	13.7
MC 242	osc	0.5721	1.7	0.0754	1.66	0.49	468.6	15	459.3	12.6
MC 242	osc	0.5701	1.7	0.073	1.33	0.39	454	11.6	458.1	12.7
MC 242	osc	0.5511	1.4	0.0736	2.05	0.73	457.9	18.1	445.7	9.9
MC 242	osc	0.5617	1.5	0.0733	1.43	0.48	455.9	12.6	452.6	11.1
MC 242	osc	0.5764	2.4	0.0755	1.69	0.35	469.1	15.3	462.1	17.8
MC 242	osc	0.577	1.7	0.0746	2.08	0.61	464.1	18.6	462.6	12.8
MC 242	osc	0.5705	1.5	0.0735	1.92	0.64	457.2	16.9	458.3	11.4
MC 242	osc	0.5569	1.9	0.0756	2.55	0.67	469.9	23.1	449.5	13.6
MC 242	osc	0.5653	1.8	0.0729	1.42	0.39	453.8	12.4	455	13.5
MC 242	osc	0.5702	2.2	0.0736	1.39	0.32	457.6	12.3	458.1	16
MC 242	osc	0.5603	1.5	0.0748	1.51	0.50	464.9	13.6	451.7	11.3
MC 242	osc	0.5597	2.8	0.0723	3.55	0.63	449.8	30.8	451.3	20.4
MC 242	osc	0.5772	1.8	0.0744	1.43	0.40	462.7	12.8	462.7	13.6
MC 242	osc	0.5617	1.8	0.0742	1.22	0.34	461.2	10.9	452.6	13.1
MC 242	homog	0.5591	2.7	0.0739	1.34	0.25	459.4	11.9	450.9	19.4
MC 242	osc	0.5789	1.7	0.074	1.25	0.37	460.2	11.1	463.7	12.4
MC 242	osc	0.5586	2	0.0738	2.07	0.52	459	18.4	450.6	14.5

Table 3 *Continued*

Sample	Zircon domain	207Pb/235U Ratio	1s %	206Pb/238U Ratio	1s %	Rho	206Pb/238U AGE (Ma)	+/- 2 S.D.	207Pb/235U AGE (Ma)	+/- 2 S.D.
MC 242	osc	0.5903	2.2	0.0735	1.77	0.40	457.3	15.7	471	16.5
MC 243 Rossa orthogneiss (730094/136062/1050)										
MC 243	osc	0.5683	1.4	0.0726	1.24	0.44	451.7	10.8	456.9	10.3
MC 243	osc	0.55	1.1	0.0719	1.07	0.49	447.6	9.3	445	8.2
MC 243	osc	0.548	1.7	0.0724	1.2	0.35	450.5	10.4	443.7	12.4
MC 243	osc	0.5709	1.5	0.0731	1.16	0.39	454.7	10.2	458.6	11.2
MC 243	osc	0.5523	1.5	0.0728	1.18	0.39	452.9	10.3	446.5	10.6
MC 243	osc	0.5738	1.6	0.0724	1.34	0.42	450.8	11.7	460.5	12.1
MC 243	osc	0.5633	1.8	0.0743	1.21	0.34	462.1	10.8	453.7	13.1
MC 243	osc	0.5694	1.4	0.0745	1.12	0.40	463.3	10	457.6	10.5
MC 243	osc	0.5715	2	0.0727	1.36	0.34	452.7	11.9	459	14.5
MC 243	osc	0.5853	2.1	0.0744	0.95	0.23	462.6	8.4	467.9	15.9
MC 243	osc	0.5647	1.5	0.0731	1.14	0.38	454.9	10	454.6	11.3
MC 243	osc	0.5574	1.7	0.0728	1.26	0.37	453	11	449.8	12.1
MC 243	osc	0.5684	1.7	0.0735	1.06	0.31	457.1	9.4	457	12.3
MC 243	osc	0.5586	1.9	0.0734	1.18	0.31	456.5	10.4	450.6	13.5
MC 243	osc	0.5724	2.1	0.0735	1.09	0.26	457.2	9.6	459.6	15.6
MC 243	osc	0.5676	2.1	0.0739	0.96	0.23	459.9	8.5	456.4	15.2
MC 243	osc	0.5688	1.5	0.0736	0.93	0.31	457.6	8.2	457.2	11.1
MC 243	osc	0.5698	1.4	0.0741	1.44	0.51	460.8	12.8	457.9	10.5
MC 243	osc	0.5629	2.1	0.0737	0.88	0.21	458.6	7.8	453.4	15.3
MC 243	osc	0.5504	1.3	0.0729	0.93	0.36	453.4	8.1	445.3	9.4
MC 243	osc	0.5715	2	0.0728	0.82	0.21	452.9	7.2	459	15
MC 243	core	0.6963	1.3	0.0862	1.05	0.40	533	10.8	536.6	11.2
MC 243	osc	0.5629	1.2	0.0728	1.02	0.43	453.1	8.9	453.4	9.1
MC 243	osc	0.5525	1.2	0.0726	0.81	0.34	451.9	7	446.7	8.5
MC 243	osc	0.5907	1.4	0.074	0.86	0.31	460.2	7.7	471.3	10.3
MC 243	osc	0.5909	1.6	0.0737	0.74	0.23	458.3	6.5	471.4	12.1
MC 243	homog	0.5855	1.4	0.0746	0.74	0.26	464	6.6	468	10.2
MC 243	osc	0.5652	1.1	0.072	0.61	0.28	448.3	5.3	454.9	8.4
MC 243	osc	0.5669	1.1	0.0731	0.71	0.32	454.5	6.2	456	8.4
MC 243	osc	0.5756	2.1	0.0737	0.78	0.19	458.2	6.9	461.7	15.5
MC 243	osc	0.5809	2.1	0.0737	0.58	0.14	458.6	5.2	465	15.6
MC 225 Garenstock, amphibolite boudin (721759/157231/2956)										
MC 225	homog	0.5461	1.7	0.072	0.67	0.20	447.9	5.8	442.5	12.3
MC 225	osc	0.5643	1.3	0.072	0.8	0.31	448.1	6.9	454.3	9.4
MC 225	core	0.7267	1	0.0875	0.55	0.28	540.9	5.7	554.6	8.7
MC 225	core	0.7639	1.1	0.0899	0.51	0.23	555.2	5.4	576.3	9.6
MC 225	patchy	0.5504	1.7	0.0713	0.58	0.17	444.1	5	445.3	11.9
MC 225	osc	0.573	1.6	0.0714	0.56	0.18	444.7	4.8	459.9	11.6
MC 225	patchy	0.5551	1.3	0.0724	0.79	0.30	450.4	6.9	448.3	9.4
MC 225	core	1.4859	1.2	0.1502	0.45	0.19	901.9	7.6	924.7	15.1
MC 225	osc	0.5479	1.9	0.0718	0.55	0.14	447	4.8	443.7	13.3
MC 225	homog	0.556	1.2	0.0723	0.44	0.18	450.1	3.9	448.9	9.1
MC 225	homog	0.5431	1.7	0.0718	1.34	0.39	447.2	11.6	440.5	12.4
MC 225	osc	0.5537	1.7	0.071	1.25	0.37	442.4	10.7	447.4	12.4
MC 225	homog	0.5527	1.8	0.0724	0.87	0.24	450.5	7.6	446.8	13.3
MC 225	patchy	0.5629	1.3	0.0717	0.72	0.28	446.4	6.2	453.4	9.4
MC 225	osc	0.5547	1.6	0.0708	0.62	0.19	440.9	5.3	448.1	11.9
MC 225	homog	0.5569	2.3	0.0706	0.73	0.16	439.8	6.2	449.5	16.9
MC 225	osc	0.5418	1.1	0.0709	0.92	0.42	441.7	7.9	439.6	7.8
MC 225	osc	0.558	2.1	0.0722	1.04	0.25	449.2	9	450.2	15.5
MC 225	osc	0.5608	1.5	0.0714	1.38	0.46	444.3	11.9	452	10.9
MC 225	patchy	0.5693	1.5	0.0711	1.44	0.48	443.1	12.3	457.5	10.7
MC 225	osc	0.5655	1.3	0.0709	0.47	0.18	441.5	4	455.1	9.8
MC 225	osc	0.5546	1.1	0.0709	0.39	0.18	441.7	3.3	448	7.9
MC 225	osc	0.5593	1.3	0.0708	0.49	0.19	441	4.2	451.1	9.8
MC 225	patchy	0.5458	1.8	0.0715	0.53	0.15	445.2	4.6	442.3	12.8
MC 225	osc	0.5719	1.9	0.0724	0.67	0.18	450.7	5.9	459.3	14
MC 225	osc	0.5518	1.6	0.0712	0.48	0.15	443.4	4.1	446.2	11.4
MC 225	osc	0.5617	1.8	0.0723	0.68	0.19	450.1	5.9	452.6	13.2
MC 225	osc	0.564	1	0.0708	0.46	0.23	441	3.9	454.1	7.6
MC 225	patchy	0.5667	1.3	0.0711	0.43	0.17	442.5	3.7	455.9	9.8
MC 253 Heinisch Stafel, meta-volcanic rock (733417/161950/1857)										
MC 253	osc	0.584	2.9	0.0714	1.09	0.19	444.7	9.4	467	21.9
MC 253	osc	0.6209	2	0.0739	0.76	0.19	459.7	6.7	490.4	15.7
MC 253	homog	0.6054	1.4	0.0724	0.85	0.30	450.5	7.4	480.7	10.4
MC 253	osc	0.5741	2.6	0.072	0.87	0.17	448.5	7.5	460.6	19.3
MC 253	homog	0.5913	1.4	0.0733	0.82	0.29	455.9	7.2	471.7	10.2
MC 253	osc	0.5794	1.1	0.0728	0.84	0.38	453.3	7.3	464.1	8.5
MC 253	osc	0.5639	2.2	0.073	0.74	0.17	454.4	6.5	454	15.8
MC 253	osc	0.5846	1.5	0.0721	0.78	0.26	448.6	6.8	467.4	11.5
MC 253	homog	0.5855	2.2	0.0725	0.93	0.21	450.9	8.1	468	16.3
MC 253	homog	0.5657	2	0.0725	1.12	0.28	451.2	9.7	455.2	14.9
AD 108 Trescolmen Fm. kyanite eclogite (7299007147950/2430)										
AD 108	homog	0.6446	4	0.0816	1	0.13	505.5	9.7	505.2	31.8
AD 108	osc	0.6984	4.5	0.0833	1.31	0.15	515.8	13	537.8	37.4
AD 108	osc	0.7149	3.1	0.0839	0.79	0.13	519.5	7.9	547.7	26.3

Table 3 *Continued*

Sample	Zircon domain	207Pb/235U Ratio	1s %	206Pb/238U Ratio	1s %	Rho	206Pb/238U AGE (Ma)	+/- 2 S.D.	207Pb/235U AGE (Ma)	+/- 2 S.D.
AD 108	homog	0.6603	2.5	0.0842	2.02	0.40	521.1	20.2	514.8	19.9
AD 108	homog	0.6821	4.6	0.0842	1.18	0.13	521.1	11.8	528	37.8
AD 108	homog	0.6764	2.7	0.0849	2.08	0.39	525.1	21	524.6	22.4
AD 108	osc	0.6774	3.1	0.0849	1.38	0.22	525.1	13.9	525.2	25.1
AD 108	osc	0.6752	3.4	0.0852	1.43	0.21	527.3	14.4	523.9	28.1
MC 209 Salahorn Fm. plagioclase-amphibole gneiss (724335/151886/2900)										
MC 209	homog	0.6653	1.2	0.0825	0.89	0.37	510.8	8.8	517.9	9.7
MC 209	homog	0.6611	0.7	0.0825	0.44	0.31	510.9	4.3	515.3	5.9
MC 209	homog	0.664	0.7	0.0825	0.45	0.32	511	4.5	517.1	6
MC 209	homog	0.6568	1	0.0825	0.44	0.22	511.3	4.3	512.6	8.1
MC 209	homog	0.6536	0.8	0.0825	0.42	0.26	511.3	4.1	510.7	6.2
MC 209	homog	0.6678	0.8	0.0827	0.4	0.25	512	3.9	519.4	6.4
MC 209	homog	0.6618	1	0.0827	0.41	0.21	512.4	4	515.7	7.8
MC 209	homog	0.6699	0.9	0.0828	0.62	0.34	512.6	6.1	520.6	7.4
MC 209	homog	0.6652	0.9	0.0829	0.49	0.27	513.4	4.9	517.8	7
MC 209	homog	0.6617	1	0.083	0.96	0.48	514	9.5	515.7	7.9
MC 209	homog	0.6645	0.8	0.083	0.39	0.24	514.1	3.9	517.4	6.3
MC 209	homog	0.6694	0.7	0.0831	0.41	0.29	514.4	4	520.4	5.7
MC 209	homog	0.6768	0.9	0.0831	0.42	0.23	514.9	4.1	524.9	7.2
MC 209	homog	0.6654	1.2	0.0831	0.76	0.32	514.9	7.5	517.9	9.6
MC 209	homog	0.6716	1.3	0.0833	1.13	0.43	515.7	11.2	521.7	10.4
MC 209	homog	0.6608	1	0.0834	0.45	0.23	516.3	4.4	515.1	7.7
MC 209	homog	0.6688	0.8	0.0835	0.52	0.33	517	5.2	520	6.8
MC 209	homog	0.6732	1.2	0.0835	0.81	0.34	517.2	8.1	522.7	9.5
MC 209	osc	0.6685	1.1	0.0835	0.45	0.20	517.3	4.5	519.8	8.7
MC 209	homog	0.6675	1.2	0.0836	0.49	0.20	517.6	4.8	519.2	9.4
MC 209	homog	0.6553	1.1	0.0837	0.76	0.35	518.1	7.5	511.7	8.6
MC 209	homog	0.6721	0.7	0.0837	0.39	0.28	518.3	3.9	522	5.6
MC 209	homog	0.6877	1.2	0.0841	0.56	0.23	520.6	5.6	531.4	10.2
MC 209	homog	0.6748	0.8	0.0842	0.46	0.29	521	4.6	523.6	6.4
MC 336 Salahorn Fm. plagioclase-amphibole gneiss (720504/158227/2503)										
MC 336	homog	0.6618	1.2	0.0824	0.48	0.20	510.7	4.7	515.7	9.4
MC 336	homog	0.6631	1.3	0.0829	0.47	0.18	513.2	4.6	516.5	10.2
MC 336	homog	0.6548	0.9	0.0829	0.49	0.27	513.4	4.8	511.4	7.1
MC 336	homog	0.6613	1	0.0831	0.31	0.16	514.5	3	515.4	7.8
MC 336	homog	0.6626	1.1	0.0832	0.38	0.17	515.1	3.8	516.2	8.7
MC 336	homog	0.6742	1	0.0832	0.47	0.24	515.3	4.6	523.2	8.4
MC 336	homog	0.6696	1.1	0.0835	0.5	0.23	517.1	5	520.5	8.6
MC 336	homog	0.6691	1	0.0836	0.41	0.21	517.4	4.1	520.1	8
MC 336	homog	0.6778	1.1	0.0836	0.37	0.17	517.5	3.7	525.4	9.3
MC 336	homog	0.672	1	0.0836	0.36	0.18	517.7	3.5	521.9	8
MC 336	homog	0.6715	1	0.0838	0.41	0.21	519.1	4.1	521.6	8.4
MC 336	homog	0.6654	0.9	0.0841	0.36	0.20	520.3	3.6	517.9	7.2
MC 336	homog	0.6687	0.8	0.0841	0.5	0.31	520.5	5	519.9	6.2
MC 353 Salahorn Fm. paragneiss (724335/151886/2900)										
MC 353	osc	0.6802	1.3	0.0838	0.51	0.20	518.7	5.1	526.9	10.3
MC 353	osc	0.6564	1.1	0.0831	0.81	0.37	514.8	8	512.4	8.7
MC 353	osc	0.6723	1.2	0.0833	0.46	0.19	516	4.5	522.1	9.9
MC 353	osc	0.6754	1.2	0.0843	0.67	0.28	521.9	6.7	524	9.9
MC 353	osc	0.6554	0.8	0.0837	0.44	0.28	518.4	4.3	511.8	6.4
MC 353	osc	0.6862	0.9	0.0847	0.43	0.24	524.2	4.3	530.5	7.6
MC 353	osc	0.695	1.1	0.084	0.49	0.22	520	4.9	535.8	8.9
MC 353	osc	0.686	0.9	0.0846	0.51	0.28	523.6	5.2	530.4	7.5
MC 353	osc	0.6666	0.8	0.0833	0.47	0.29	516.1	4.7	518.7	6.8
MC 353	osc	0.6773	1.4	0.0837	0.62	0.22	518.2	6.1	525.2	11.7
MC 353	osc	0.6784	1.1	0.083	0.46	0.21	513.7	4.5	525.8	9.3
MC 353	osc	0.6732	0.8	0.0847	0.83	0.52	524.2	8.4	522.7	6.7
MC 353	osc	0.6778	1.2	0.0844	0.85	0.35	522.3	8.5	525.4	9.8
MC 353	osc	0.6631	1.3	0.0834	1.54	0.59	516.1	15.3	516.5	10.3
MC 353	osc	0.6852	1.4	0.0828	1.02	0.36	512.8	10.1	529.9	11.9
MC 353	osc	0.6508	1.3	0.0826	0.85	0.33	511.8	8.3	509	10.7

Table 3 *Continued*

2.3.6. Heinisch Stafel Formation

Zircons were found in one sample of banded amphibolite (Fig. 5a, MC 253). These zircons are relatively small (30-150 µm) and mainly prismatic and usually have a central channel. They are often xenomorphic. The CL texture is generally homogenous or exhibits a broad patchy zoning (Fig. 14g). A few grains show oscillatory zoning. The calculated median age is 451.1 +4.9 -2.5 Ma (Table 3; Fig. 15f), interpreted as the magmatic age of the volcanic rocks.

2.3.7. Zervreila orthogneiss

The Zervreila orthogneiss is rich in zircons. Their size ranges from 50-300 μm, and they are colourless to pale pink in colour and generally idiomorphic (Fig. 14a). They do not show any traces of abrasion, resorption, or overgrowth. Morphologically, the Zervreila orthogneiss zircons are mainly P-type zircons (Fig. 14a) according to the Pupin classification (1980). The CL texture of Zervreila orthogneiss zircons usually shows a magmatic narrow oscillatory zoning (Fig. 14b and c). Some xenocrystic cores are present but not frequent (Fig. 14c). Zircons affected by metamictisation are very common in the Zervreila orthogneiss. The elevated uranium content in these zircons is reflected by high U intensities in LA-ICPMS spectra.

Six samples of Zervreila orthogneiss (MC 120, MC 133, MC 138, MC 142, MC 239, and MC 241) were analysed. They were distributed throughout the northern Adula nappe (sample location on Fig. 2). The median TuffZirc ages for the six samples are as follows: 289.4 ± 2.5, 296.6 +2.5 -2.2, 292.7 +3.1 -4.0, 290.7 +1.4 -1.2, 290.2 +1.6 -1.5, and 287.7 +3.5 -2.1 Ma (Table 3; Fig. 15a). The CL textures and the age reproducibility clearly point to a magmatic age interpretation. Xenocrystic cores in all samples yielded concordant ages of 423.1 ± 6.4, 451.9 ± 6.8, 521.4 ± 14, and 974.3 ± 18.5 Ma (Table 3).

2.4. Discussion

2.4.1. Cambrian sedimentation and magmatism

Two magmatic rocks of the Salahorn Fm. (amphibole-plagioclase gneiss) were calculated to have ages of 514.7 +2.6 -2.2 and 517.1 +2.0 -3.7 Ma. The Salahorn Fm. Mafics (magmatic rocks of type (a)) could not be dated, but their ages are interpreted as being approximately the same as that of the amphibole-plagioclase gneiss intrusion based on field relations. Mafic rocks (type a) are widespread and is interpreted as volcanic deposits that are tholeiitic in nature with a calc-alkaline signature. Amphibole-plagioclase gneiss (type b) is less common and has a continental active margin or a back-arc environment geochemical signature. Both magmatic rocks are consistent with a back-arc geotectonic context. A very similar rock association (but Ordovician in age) was interpreted as a result of a continental break-up unrelated to contemporaneous subduction by Pin and Marini (1993). Nevertheless, an interpretation based only on the geochemistry of the geotectonic setting of the emplacement of these magmas is questionable. The interpretation of their emplacement also has to consider the sedimentary context of the surrounding metasediments.

The protolith of the Salahorn Fm. paragneiss is a clastic sediment composed of felsic non-mature detrital material and a considerable amount of carbonates. The source rock is quartzofeldspathic with some carbonates. This detrital sedimentation can be related to high-energy epicontinental sedimentation. Zircons from a paragneiss of the same formation yielded an age of 518 +4.0 -3.5 Ma (Table 4). The detrital zircons contained in the clastic metasediments have nearly the same age as the magmatic bodies intruding upon these sediments. The homogeneous age of detrital zircons, its similar age with the magmatic ones, and the immature character of the sediments, points to a proximal deposition and to a short time period between erosion and emplacement of the source.

We compare the Salahorn Fm. with situation described in the southern Peruvian magmatic arc, where Jurassic magmatic rocks intrude a clastic formation containing detrital zircons less than 3 Ma younger than the intrusion (Boekhout et al. 2012). Boekhout et al. (2012) demonstrated the rapid subsidence of the arc slope (with clastic sedimentation) in which arc-related magma intrudes.

The carbonates are most likely also of detrital origin because continuous carbonate beds were never found. A correspondence for the source can be found in the carbonate platforms documented in the Early-Middle Cambrian time on the Gondwana

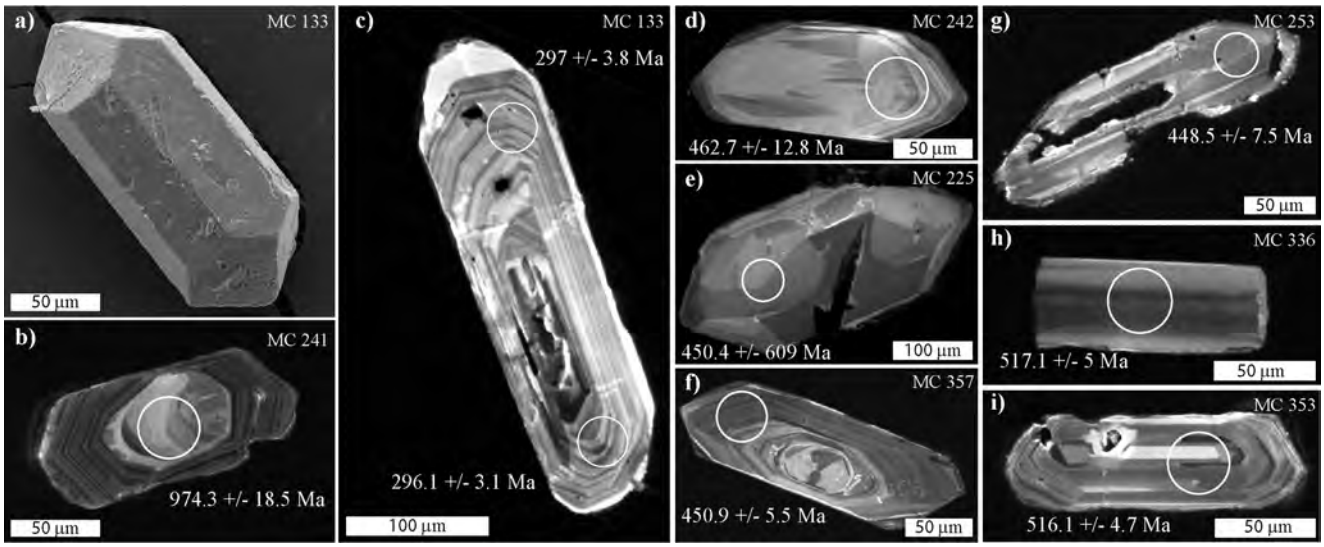

Fig. 14 *Selected zircon images from the analysed samples.* ***a*** *Zervreila Orthogneiss zircon, secondary electron (SE) image (Tescan Mira LMU, University of Lausanne).* ***b, c, d, e, f, g, h, i*** *Cathodoluminescence (CL) images of polished zircon sections (CamScan MV2300, University of Lausanne). Circles represent the LA-ICPMS analysis according to the respective* $^{206}Pb/^{238}U$ *age. All indicated ages are concordant. The sample numbers are indicated on each zircon.*

margin (Cocozza 1979; Liñán et al. 1993; Elicki 1994).

Large ultramafic bodies are also observed in the Salahorn Formation. In the Alpine basements, ultramafic-mafic bodies are classically interpreted as remnants of oceanic crust and Palaeozoic ophiolite series (Pfeifer et al. 1993). The occurrence of these ultramafic bodies proves the presence of an oceanic domain or a continental breakup process, concomitant to the Salahorn Formation deposit and magmatism. The mechanism by which to integrate these bodies in the clastic sediments can only be hypothetical; however, we suggest that mantle exhumation during rifting processes (Froitzheim and Manatschal 1996) is involved. Variscan and Alpine deformations are certainly responsible for the present-day geometry of the bodies enclosed within the basement.

Eclogites were found in the mafic rocks of the Salahorn Fm., but their age is unknown. Palaeozoic eclogitisation, in addition to the Alpine eclogitisation, can perhaps be considered equivalent to that of the Trescolmen Formation. Zircons from this formation do not retain clear metamorphic rims.

Several correspondences can be mentioned for a correlation of the Cambrian Salahorn Fm. An association of ultramafic and mafic rocks is also found at Loderio (near Biasca, Ticino) in the Lower Penninic under the Simano nappe. These rocks are also dated at 518 ± 11 Ma (U-Pb on zircon), and the mafic rocks show a MORB signature (Schaltegger et al. 2002). Cambrian magmatic rocks (528 ± 6 Ma) are also documented from the Cima di Gagnone area (Gebauer 1995) in the Cima Lunga Nappe. Bussien et al. (2011) noted a 540-Ma age for a banded mafic complex in the Sambuco-Maggia nappe. Cambrian clastic sediments, including intrusive and volcanic magmatic rocks, are noted in the External Crystalline Massifs (Guillot and Ménot 2009). Carbonates in the Early Palaeozoic Paragneisses are documented in these massifs as well (von Raumer and Bussy 2004). Signs of extensive normal faulting and of strong subsidence are widespread in the Early Middle Cambrian (Elicki 2006) and indicate a rifting process. Von Raumer et al. (2013) interpreted the Cambrian paleogeography of the Alpine basement rocks along the Gondwana margin in terms of an active margin followed by a complex pattern of back-arc rift opening.

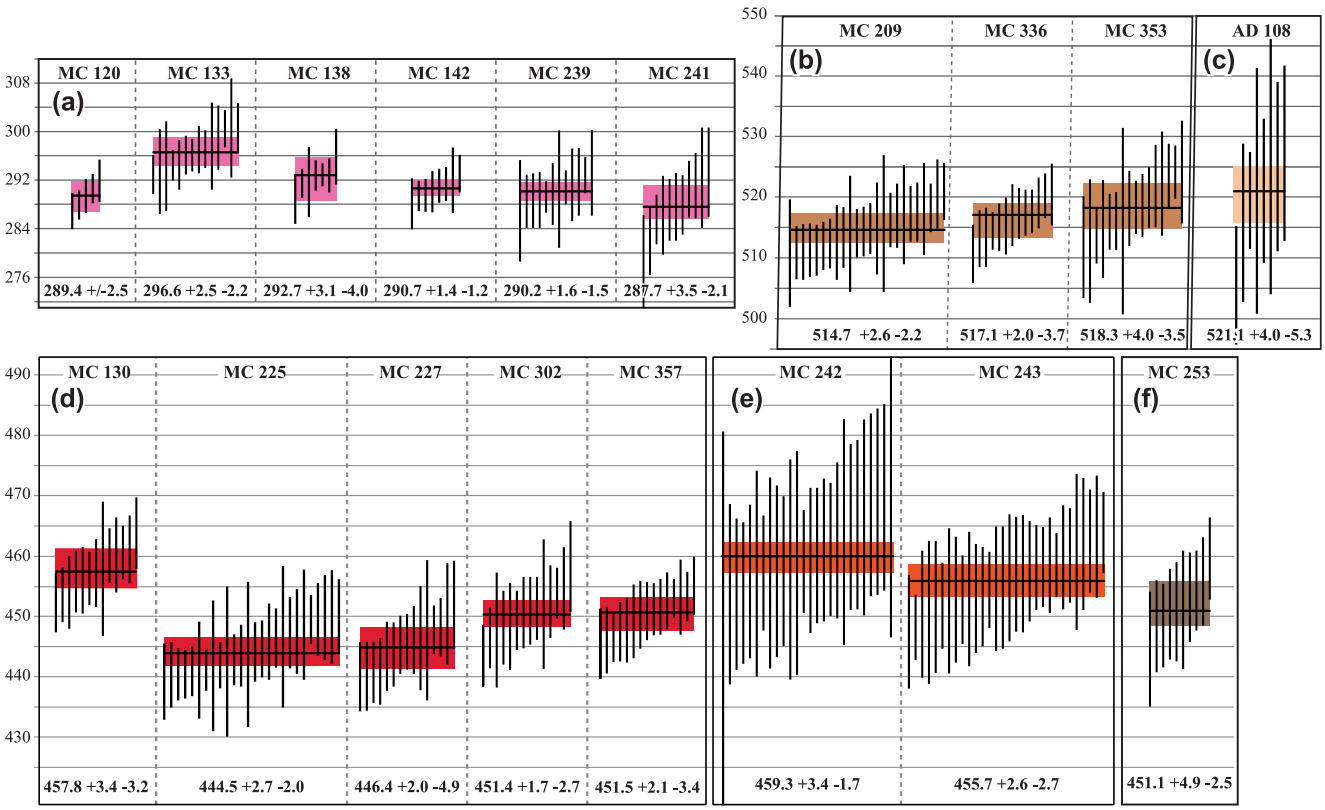

Fig. 15 *Calculated $^{206}Pb/^{238}U$ age of each sample. The age calculations were performed using Isoplot (Ludwig, 2003) and the TuffZirc equation (Ludwig and Mundil, 2002) based on the $^{206}Pb/^{238}U$ age. The median of the largest cluster is taken as the true age, with 95%-confidence errors. The uncertainty of each measurement is given as 2σ. Only concordant or sub-concordant analytical points were used. The same scale was used for all samples.* ***a.*** *Zervreila Orthogneiss.* ***b.*** *Salahorn Formation: one amphibole plagioclase gneiss and one paragneiss (MC 353).* ***c.*** *Trescolmen Formation mafic boudin (zircon extracted by Lucia Santini).* ***d.*** *Garenstock augengneiss metagranites and one mafic rock (MC 225).* ***e.*** *Rossa orthogneiss.* ***f.*** *Heinisch Stafel Formation meta-tuff layer.*

2.4.2. Trescolmen Formation: age and sedimentation environment

The Trescolmen Formation has the largest amount of geochronological data in the entire Adula nappe. However, the sedimentation age of this metapelitic formation and the age of the abundant mafic rock emplacement are difficult to determine. A kyanite-eclogite sample (AD 108) yielded an age of 521.1 +4.0 -5.3 Ma (Fig. 15c), the same age as that of the Salahorn Fm. magmatism (Chapter 4.1). Other zircon protolith ages were obtained for the mafic rocks of the Trescolmen Fm., such as 461 +4 -5 Ma (Santini 1992, concordant TIMS age). SHRIMP ages determined by Liati et al. (2009), sometimes obtained from a small number of analyses, are 587 ± 5 Ma (Pl Qtz Grt WM Am gneiss, sample CON 6), 595 ± 9 Ma (eclogite, sample CON 7), 561 ± 22 Ma (eclogite, sample TRE 5, based on 2 analyses), 655 ± 12 Ma (eclogite, sample TRE 6, based on one analysis), and 482 ± 8 Ma (eclogite, sample TRE 8, based on two analyses). The youngest magmatic core in zircons from the metapelites, interpreted as a minimum sedimentation age, is dated at approximately 460 Ma (Liati et al. 2009). The magmatic rocks included in the metapelites are all older than this minimal sedimentation age, except one sample of the same Ordovician age. The Palaeozoic HP metamorphic age is better constrained at ca. 370 and 340 Ma (Liati et al. 2009; Herwartz et al. 2011). The metapelites protolith is most likely a fine-grained, mature, carbonate-free, clastic sediment that can be categorised as shale. The bulk rock chemical composition of the lithology is in agreement with this interpretation (Cavargna-Sani 2008), and the sedimentation was most likely marine. The mafic boudins are mainly characterised as basalts due to their fine texture. The basic rocks of the Trescolmen Fm. have a MORB signature (Santini 1992) and are interpreted to be of oceanic origin. The nature of the contact between the mafic boudins and the metapelitic matrix in the Trescolmen Fm. cannot be clearly

determined: they always appear sharp in the field. The protolith ages of the mafic boudins are older than the youngest detrital zircon in the metapelitic matrix. This lithological association, and the scattered ages of the magmatic rocks, is typical for a detrital formation with blocs of older igneous rocks (Wildflysch-type deposit), or for a tectonic melange. Both interpretations imply that the Trescolmen Formation could represent a highly deformed zone, typical of a terrane accretion (also proposed by Liati et al. 2009) or an accretionary prism related to subduction.

The formation age of the Trescolmen Fm. protolith is very difficult to determine accurately. The maximum age is constrained by the youngest detrital zircon in the metapelitic matrix (~460 Ma; Liati et al. 2009). The minimum age is given by the age of the oldest high-pressure event at ~370 Ma (Table 4; Liati et al. 2009). The age and the sedimentation context of the protolith most likely correspond to a mélange formed during the subduction, producing the Variscan orogeny.

Analogies of the Trescolmen Formation can most likely be found in the Lac Cornu area in the Aiguilles-Rouges Massif (Liégeois and Duchesne 1981; von Raumer and Bussy 2004). In this area, mafic eclogites are included in various metasedimentary clastic rocks. Their age corresponds to the period between 463 Ma (Bussy et al. 2011; the basaltic protolith) and 321 Ma (Bussy et al. 2000; a high-temperature event that postdates the high-pressure events). The paleogeographic context of the Trescolmen Formation protolith emplacement and the high-pressure metamorphism must be assigned to the Variscan orogeny. This interpretation is consistent with the general evolution of the Pre-Mesozoic Alpine basements (von Raumer et al. 2013).

2.4.3. Ordovician evolution

Two analysed samples of the Rossa Orthogneiss yielded ages of 459.3 +3.4 -1.7 and 455.7 +2.6 -2.7 Ma (Fig. 15e); these two ages overlap within errors. Four ages of metagranites of the Garenstock Augengneiss are between 446.4 and 457.8 Ma (Fig. 15d, Table 4), and one amphibolite sample (interpreted as a metagabbro) from a boudin included in the metagranite has an age of 444.5 +2.7 -2.0 Ma (Fig. 15d, MC 225). Although these values overlap only partially within the errors, we assume that they are the expression of the same Ordovician magmatic episode. Field criteria suggest interpreting the Rossa and Garenstock granites and the associated mafic rocks as K-rich calc-alkaline granitoids within the Barbarin (1999) granite classification. Geochemical characteristics suggest interpreting the granites as K-feldspar-rich calc-alkaline granites and a concomitant calc-alkaline basaltic magma. They are emplaced in an active-margin geodynamic environment.

Ordovician granitoids are common in the Alpine basements. In the Lower Penninic nappes, Ordovician granitoids identified in the Sambuco-Maggia nappe (Bussien et al. 2011) and in the Monte Leone nappe (Bergomi et al. 2007). In the better known External Massifs, they are found in the Gotthard and Tavetsch Massifs (Oberli et al. 1994), the Aar Massif (Schaltegger et al. 2003), and the Aiguilles-Rouges and Mont-Blanc Massifs (von Raumer and Bussy, 2004; Bussy et al. 2011). For a more complete dataset, the reader is referred to the reviews by Schaltegger and Gebauer (1999), von Raumer et al. (2002), and Schulz et al. (2008).

The Heinisch Stafel Formation can be interpreted as a typical volcano-sedimentary basin deposit. One sample in the volcanic interlayer yielded zircons of 451.1 +4.9 -2.5 Ma (Fig. 15 f). This age is interpreted as the deposition age of the volcano-sedimentary series. Further volcano-sedimentary basins of this age are documented in the Alpine realm. Gansser and Pantic (1988) studied the metamorphosed volcanic-sedimentary series of the Edolo Schists (Southern Alps, bordering the Tonale Line) and dated it by palynomorphs. In the Middle Penninic Métailler nappe, volcanic-sedimentary deposits are also dated at ca. 460 Ma (Gauthiez et al. 2012). The Heinisch Stafel volcano-sedimentary formation is almost contemporaneous with the emplacement of the Ordovician Rossa and Garenstock granites.

The reviews by Stampfli et al. (2011) and von Raumer et al. (2013) suggest a subduction zone under the N-Gondwana continental margin (the future Alpine basements). This subduction zone involves the production of large amounts of Ordovician magmatic rocks. These reviews suggest a crustal extension for the pre-Alpine basements from the Middle Ordovician. This scenario can also be assumed for the emplacement of the formations described above.

2.4.4. Variscan metamorphism

The Variscan orogeny in the Adula nappe is evidenced by a few Variscan metamorphic ages. Liati et al. (2009) describe two generations of metamorphic rims in zircons (370 and 330-340 Ma) both interpreted as high-pressure events based on REE patterns. Herwartz et al (2011) report a minimum Lu-Hf garnet age of ~330 Ma. This age is not related to specific metamorphic conditions. Traces of granulitic metamorphism or migmatisation were never observed.

The 370 Ma, probably high-pressure, metamorphic event can be ascribed to the Devonian subduction phase (early Variscan; Stampfli et al. 2002; von Raumer et al. 2009; Guillot and Ménot 2009; von Raumer et al. 2013). The eclogite-facies rocks of the Lac Cornu area in the Aiguilles Rouges Massif have a possible age close to 345 Ma (Bussy et al. 2011). The successive high-temperature decompression melting after the eclogite-facies is better constrained and dated at ~320 Ma in the Aiguilles Rouges Massif (Bussy et al 2000).

The contact between the previously described formations (Salahorn Fm., Trescolmen Fm., Heinisch Stafel Fm., and the Garenstock and Rossa orthogneisses) is perhaps a result of the Variscan nappe stack. This nappe stack is proven in less deformed Alpine Palaeozoic terrain (Guillot and Ménot 2009).

2.4.5. Late Variscan granites emplacement

The six studied Zervreila Orthogneiss samples were found to have ages between 287.7 and 296.6 Ma (Fig. 15a, Table 4). Six ages overlap within errors. MC 133 is the oldest and overlaps only partially with the other samples. However, field criteria or geochemistry do not show evidence for a clearly different magmatic event. We therefore interpret the whole Zervreila Orthogneiss as having been formed during a single magmatic event, but most likely composed of different intrusion pulses at approximately 292 Ma. The mineralogical and geochemical characteristics of the Zervreila orthogneiss suggest a late- or post-orogenic geotectonic environment for their emplacement. Well-preserved magmatic contacts between the Zervreila Orthogneiss and the other formations have not been observed. The present geometry (Fig. 2) suggests that the Zervreila granite intruded the older polymetamorphic formations, forming a structured Variscan basement at this time (Fig. 16).

Molasse-type detrital sediments of Late Palaeozoic-Early Triassic (Verrucano) are not found in the Adula nappe. Alterations and paleosols under the Triassic sedimentary cover are clearly revealed on the Garenstock Augengneiss of the Plattenberg area, which suggests that the northern Adula nappe basement was exposed prior to the Triassic transgression and most likely formed a topographic high during the Permian basin-and-range tectonic environment. The Adula history contrasts with that of the nappes placed north of it in the Triassic paleogeographic environment (Luzzone-Terri nappe, Lucomagno nappe, and Gotthard nappe) because these nappes include Carboniferous-Permian clastic sediments (Baumer et al. 1961; Galster et al. 2012). The Adula nappe is a possible source of the sediments deposited in a north-laying basin currently located in the aforementioned nappes. A Mesozoic cover is not observed directly on the Zervreila orthogneiss.

Variscan post- (or late-) collisional granitoids are documented in several Alpine domains. They are particularly developed and documented in the External massifs (Bussy et al. 2000; von Raumer et al. 2009) and in the Lower Penninic basement, where this magmatism is also widely represented (Bussien et al. 2011). An age of 292 Ma for the Zervreila orthogneiss is

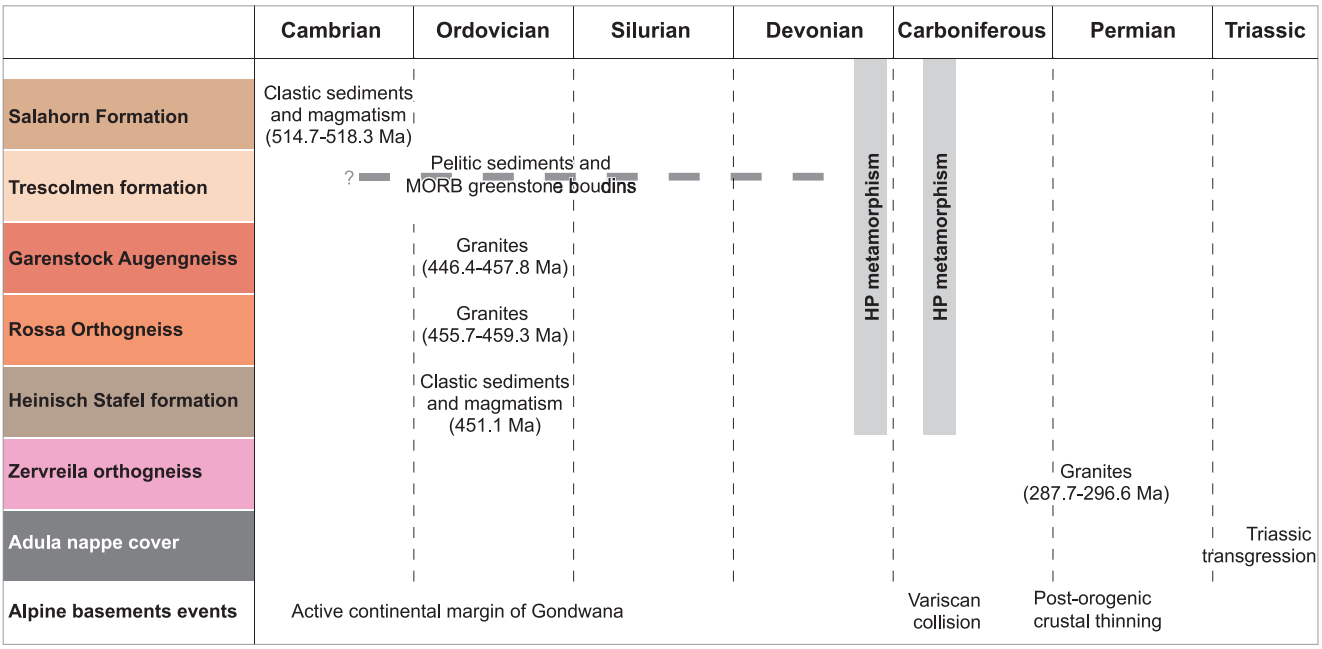

Table 4 *Sedimentation and magmatic ages of the northern Adula nappe basement formations. Alpine basement events were obtained from von Raumer et al. (2013).*

comparable with the ages of 291 ± 4 Ma (Bussy, unpublished data) and 289 ± 3 Ma (Bergomi et al. 2007) of the Verampio granite. The Antigorio granite yielded ages between 296 ± 2 and 289 ± 4 Ma (Bergomi et al. 2007). Both nappes are Lower Penninic and paleogeographically attached to the internal Helvetic domain (Matasci et al. 2011). Similar granites are also found in the western Tauern Window (Eichhorn et al. 2000; Vesela et al. 2010)

The Zervreila orthogneiss emplacement is probably part of the post-orogenic readjustment of the over-thickened crust (Ménard and Molnar 1988). The tectonic scenario could be controlled by uplift and exhumation, which produces basins and topographic highs caused by large-scale strike slips and associated with significant concomitant magmatic activity (see the review by von Raumer et al. 2013 and references therein).

2.4.6. Triassic transgression and Mesozoic stratigraphy

The Mesozoic autochthonous cover of the Adula nappe exists and is coherent throughout the different outcrops (Cavargna-Sani et al. 2010; Galster et al. 2012). The presence of a pre-Triassic Verrucano-type sediment, similar to what is described in the nearby Luzzone-Terri nappe (Galster et al. 2010), was not found. The Triassic transgression (Fig. 16) is found in the Garenstock Augengneiss, the Heinisch Stafel, and the Trescolmen Formations. The Zervreila Orthogneiss perhaps did not crop out during Triassic times because no direct contact between the Triassic deposits and the Zervreila Orthogneiss was noted. Triassic deposits of the Adula nappe are related to the North Penninic Triassic type (Galster et al. 2012) characterised by the typical “dolomie bicolori”. Jurassic stratigraphy shows an emersion followed by a marine transgression at the end of the Jurassic (Cavargna-Sani et al. 2010; Galster et al. 2012). These data show that the Adula nappe is part of a coherent paleogeographic domain that was strongly affected by extensional tectonics during Jurassic rifting.

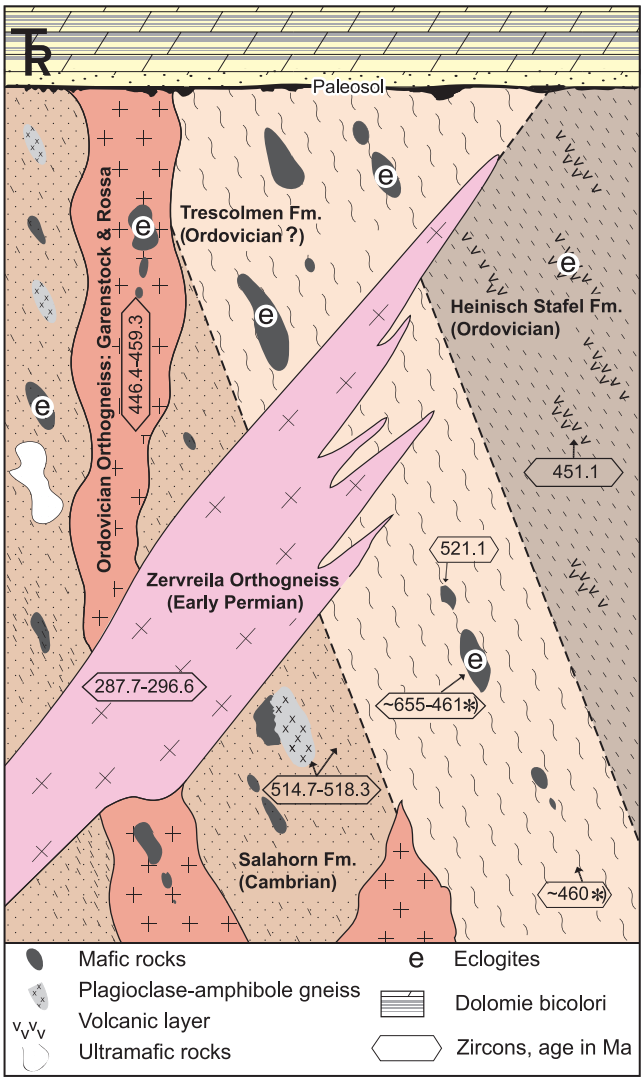

Fig. 16 *Adula nappe basement formations and age relations.(*) ages are based on the work of Liati et al. (2009).*

2.4.7. Implications for Alpine tectono-metamorphic evolution

The suggested Palaeozoic lithostratigraphy demonstrates the consistency of the geotectonic evolution of the northern Adula basement. This evolution implies that different pre-Mesozoic unconformities formed by pre-Alpine tectonics and stratigraphy are involved in the Alpine orogeny. The lithologic variety of the Adula basement originates clearly from the complexity of the Palaeozoic geotectonic evolution.

Supporting the consistency of the basement and cover, we do not ignore the extreme tectonic and metamorphic complexity of the Adula nappe. The geometry of the monometamorphic Zervreila orthogneiss (Fig. 2) make obvious the intensity of the Alpine deformation.

Tromsdorff (1990) interpreted the Adula nappe as a lithospheric mélange. Furthermore, Berger et al. (2005) proposed the Adula nappe as part of a “Paleogene Tectonic Accretion Channel” (TAC, Engi et al. 2001). These models suggest a tectonic mixing during the subduction and exhumation of pieces of different paleogeographic origins. However, the northern Adula nappe cannot be considered as having been formed by a lithospheric mélange with pieces of different tectonic plates because the Adula nappe retain an internally consistent pre-Alpine entity. Our results suggest using a different scale to determine the kinematics that produced such a complex structure and the close imbrication of different rock types. We consider the Adula nappe as an expression of a ductile shear zone involving the entire nappe. The imbricate structure is the consequence of several phases of folding and shearing of a coherent and pre-structured pre-Alpine Adula.

2.5. Conclusions

The northern Adula nappe displays a consistent Palaeozoic geological evolution, despite severe Alpine deformation and metamorphism. The oldest formation is a Cambrian paragneiss recording bimodal magmatism (Salahorn Fm.) in a back-arc geotectonic setting. The Trescolmen Fm. protolith is characterised by a chaotic formation composed of marine argillaceous sediments and oceanic crust formed in a subduction-related setting with a minimum age at 460 Ma and a metamorphic age at 370 Ma. Ordovician rocks constitute both metagranitoids and a paragneiss formation. Ordovician metagranites are associated with contemporaneous mafic rocks; both rock types are calc-alkaline and emplaced in an active margin geodynamic environment. The Ordovician Heinisch Stafel Fm. protolith is formed by volcanoclastic sediments. The above-mentioned formations were probably all involved in the Variscan orogeny and record a polyorogenic evolution. The Permian Zervreila granite intrudes these polyorogenic formations during the post-orogenic crustal readjustment of the Variscan crust (synthetic sketch of the basement lithology; see Fig. 16). The major Palaeozoic events recorded elsewhere in Alpine Palaeozoic nappes can also be traced in the northern Adula nappe.

The unconformity suggested by the entire lithostratigraphic record between pre-Variscan and younger rocks within the Adula nappe is evidence of the inheritance of pre-Alpine structures in the Adula nappe basement. The present-day structural complexity of the Adula nappe is the result of the intense Alpine ductile deformation of a pre-structured coherent entity. Mélange models for the tertiary emplacement of the Adula nappe involving an assemblage of lithological entities of different paleogeographic origins are not consistent and must be rejected.

ACKNOWLEDGEMENTS

This study is supported by the Swiss National Science Foundation, grant no. 200021_132460. We thank T. Nagel and F. Finger for their very useful comments on the manuscript. We would like to thank also L. Nicod for thin sections preparation and mounts polishing, P. Vonlanthen for support at SEM, J.-C. Lavanchy for XRF measurements and N. Hürlimann for support by glass discs LA-ICP-MS measurement. We thank F. Galster, F. Humair, H. Masson, A. Pantet, D. Schreich and A. Steck for field support and fruitful discussions. We are grateful to the Museo Cantonale di Storia Naturale for authorization to collect samples in Ticino.

3. Structure, geometry and kinematics of the northern Adula nappe (Central Alps) and its emplacement in the Lower Penninic nappe stack.

Mattia Cavargna-Sani, Jean-Luc Epard, Albrecht Steck

Submitted to: Swiss Journal of Geosciences

ABSTRACT

The Adula nappe is the highest basement nappe in the Lower Penninics of the Eastern Lepontine Dome in the Central Alps. Its paleogeographic position is at the distal European margin. The Adula nappe consists mostly of pre-Triassic basement rocks locally associated with outcrops of cover rocks enfolded within the basement. The nature of the deformation and the high-pressure metamorphism recorded in the nappe reveal a complex history with several deformation phases.

We provide a detailed structural analysis focused mainly on the Alpine nappe stack deformation phases in the northern part of the Adula nappe.

The early Ursprung ductile deformation phase is characterized by folds that are compatible with a top-to-south shearing. This phase occurs only in the upper part of the nappe. The Zapport phase is partially contemporaneous with the Ursprung phase. The Zapport phase produces the main structural features of the nappe by ductile northward-directed shear and forms two generations of isoclinal nappe-scale folds. These folds are revealed by detailed mapping in areas preserved by later deformation. The Zapport phase folds form complex synclines cored by the sedimentary cover at the front of the nappe.

The emplacement of the Adula nappe is essentially driven by the ductile deformation of a coherent preexisting domain. In contrast, the nappes derived from paleogeographic domains located south of the Adula domain are placed by detachment and basal accretion. This different emplacement mechanism led the Adula nappe to subduct more deeply than the surrounding units.

Two later deformation phases postdate the main nappe emplacement. The Leis and Carassino deformation phases are principally characterized by NW-vergent folds. These deformations affect the nappe front formed during the previous nappe emplacement phases.

3.1. Introduction

Eclogitic rocks in mountain belts are commonly associated with a suture zone corresponding to old subduction zones (Ernst 1971; Dal Piaz et al. 1972; Ernst 1973). Nappes containing eclogite relicts are found in the Alps in the following two structural positions: the Upper Penninic nappes, which represent the suture of the Alpine-Tethys Ocean, and the more enigmatic eclogitic zone of the Lower Penninic nappes, which represents the closure of the North Penninic paleogeographic domain (Oberhänsli 1994). One of the most important eclogitic nappes of the Lower Penninics is the Adula nappe. The present paper contributes to a better understanding of the present-day geometry of the Adula nappe and the different deformation phases that have affected it. The northern Adula nappe is crucial to deciphering the Lower Penninic nappe stack kinematics. The subduction-related high-pressure metamorphic conditions in the Adula nappe have been extensively studied (Heinrich 1986; Löw 1987; Meyre et al. 1999; Nimis and Trommsdorff 2001; Nagel et al. 2002a; Dale and Holland 2003; Hermann et al. 2006; Zulbati 2008; Zulbati 2010). However, currently, the structures related to the exhumation of the high-pressure rocks are not well understood (Nagel 2008).

Similarly, the overall geometry of the nappe produced by successive deformation phases has not been clearly described. The internal structure of the Adula nappe is extremely complex. Recent lithostratigraphic studies allow for a better understanding of map-scale structures and the stratigraphic significance of the infolded Mesozoic cover (Cavargna-Sani et al. 2010, Galster et al. 2012, Cavargna-Sani et al. submitted). The difficulty of studying the extremely complicated internal structure of the Adula nappe is balanced by the outstanding outcrop conditions in most of the nappe. The particular outcrop situation, the exceptional deformation, the presence of eclogitic facies rocks and the structural position at the top of the Lower Penninic crystalline nappe pile make the Adula nappe a natural laboratory for understanding the processes of nappe stacking and subsequent deformation in an Alpine-type suture zone. The comprehension of its kinematics and geometry has major consequences for the study of orogenic processes in the Central Alps.

The extreme structural complexity of this region requires detailed investigation on a small (meter to kilometer) scale. Furthermore, as some structures are visible only at a larger scale, investigation at the nappe scale is also necessary. This study is mainly based on detailed geologic and structural mapping of several representative key areas in the northern Adula nappe. This study has also been extended to a multi-scale structural analysis of the nappe on a broader scale. The research was mainly focused on the northern part of the nappe because its deformation and metamorphic grade are weaker, and the rock types are better known. The interferences between successive deformation phases are also much clearer in the frontal part of the nappe.

3.2. Geological setting

The Adula nappe is located in the eastern part of the Lepontine Dome and is one of the uppermost crystalline nappes of the Lower Penninics. This nappe is situated on the top of the Simano nappe (Fig. 1c), partially separated by a thin band of Mesozoic rocks.

North-west of the front of the Adula nappe and limited in the northwest by the Gotthard Crystalline basement fold, there are several nappes and tectonic slices composed mainly of Mesozoic sedimentary rocks (Fig. 1, 2 and 3; as described below). Galster et al. (2012) grouped these units into the Internal Klippen belt. These units are now placed under the Adula nappe, but according to their Triassic stratigraphy and structures, they must be rooted between the Adula and Tambo nappe. On the *Gotthard* basement fold and its autochthonous Triassic series, the *Scopi* zone and the *Peidener* slices have a Jurassic Helvetic-type stratigraphy (Baumer et al. 1961). The *Grava* nappe is composed mainly of “Bündnerschiefer”-type clastic sediments of North Penninic origin (Steinmann 1994). Voll (1976) demonstrated that the Grava nappe is continuous around the front

of the Adula nappe. So that, as typical in the Central Alps the present Adula nappe front represents a recumbent post-nappe fold (e.g. Milnes 1974). The *Güida* and *Alpettas* zones are connected by the Lunschania antiform hinge (Kupferschmid 1977). Its Jurassic and Triassic sedimentary series are deposited on the southern border of the Liassic Helvetic basin, south of the Luzzone-Terri domain (Galster et al. 2012). The *Luzzone-Terri* nappe outcrops in the core of the Lunschania antiform (Fig. 1 and 2). The stratigraphy of this nappe reveals a Briançonnais-type Triassic stratigraphy followed by a Helvetic-type Liassic sequence (Galster et al. 2010). This situation is unique in the Alps and demonstrates the continuity and proximity of the future Briançonnais and Helvetic domains during the Triassic and Liassic periods. The *Garzott* slices that can also be observed in the core of the Lunschania antiform contain a more internal Triassic stratigraphic sequence with respect to the Luzzone-Terri nappe but maintain a slight Briançonnais affinity. The Jurassic sediments are sedimented on an erosive surface and are composed of dolomitic breccias interpreted as syn-rift sediments (Galster et al. 2012). These breccias are overlaid by calcschist. The *Darlun* zone, close to the front of the Adula nappe, is mainly composed of shale that is similar to the Luzzone-Terri Liassic. This zone is also formed by various tectonic slice zones. The slice zone next to the Adula nappe is located in the same structural position as the Lower Valser slices (described later). North of the termination of the Simano nappe, the *Soja* nappe is a small nappe composed of basement rocks with a Triassic sedimentary cover (Egli 1966; Galster et al. 2010) of the North Penninic type (Galster et al. 2012).

The stratigraphy of the described nappes, including that of the Adula nappe, reveals continuity between the Helvetic and Briançonnais Triassic series and the emergence of an Adula rise between basins during the Middle Jurassic period (Cavargna-Sani et al. 2010; Galster et al. 2010; Galster et al. 2012). On the top of the Adula nappe, the Middle Penninic Tambo and Suretta nappes present a typical Briançonnais stratigraphy (Baudin et al. 1995; Rück 1995).

The Adula nappe is separated from the Middle Penninic nappes by the Mesolcina (Misox) zone. Several nappes and slices of metasedimentary clastic rocks comprise this zone and are described below (Fig. 1 and 2). Directly on top of the Adula nappe at the base of the Mesolcina zone are the *Lower and Upper Valser slices*. These two units are composed of slices of various rock types such as gneiss, greenstone and marble. Calcschists are observed only in the Upper Valser slices. The Triassic stratigraphy of the Valser slices differs from that of the Adula nappe (Galster et al. 2012). This demonstrates that the origin of the slices is not in the domain of the Adula nappe. The Aul, Tomül and Grava nappes are formed by sediments that are Jurassic to Cretaceous in age and were deposited in the North Penninic basin (Steinmann 1994). The *Aul* nappe was formed principally by Jurassic impure calcareous marble with some greenstone (Kupferschmid 1977; Steinmann 1994). The *Tomül* and the *Grava* nappes are mainly composed of "Bündnerschiefer"-type clastic sediments (calcschist) with a few Jurassic ophiolitic rocks (Gansser 1937; Steinmann 1994; Liati et al. 2005). The Aul, Tomül and Grava nappes are characterized by coherent sedimentary sequences together with slice zones. Several units in the area are composed of slices (e.g., Valser, Garzott and part of the Darlun and Aul units) with significant lateral continuity, and the coherent stratigraphic characteristics for each slice are within one unit. There is no recognizable matrix between the slices. These units are most likely not "chaotic mélanges", as can be found in other Alpine units (i.e., the Teggiolo zone and the Antigorio nappe) (Matasci et al. 2011), where they have been interpreted as Wildflysch formations. In our opinion, the observed slices in our area have a primarily tectonic origin.

The southern part of the Adula and Tambo nappes are separated by the Forcola normal fault (Meyre et al. 1998).

The units surrounding the Adula nappe experienced a subduction-related metamorphism of lower grade (blueschist) in comparison to the Adula nappe (Bousquet et al. 2002, Wiederkehr et al. 2008). The Mesolcina (Misox) zone between the Adula and Tambo nappes experienced a high-pressure metamorphic event of upper blueschist to eclogitic grade as determined by the presence of eclogite preserved within the basic rocks (e.g., "Neu Wahli" outcrop) (Gansser 1937; Santini

1992). The metasedimentary rocks NW of the Adula nappe experienced a high-pressure - low-temperature metamorphism of approximately 350-400°C and 1.2-1.4 GPa, evidenced by Mg-carpholite and chloritoid occurrences (Bousquet et al. 2002; Wiederkehr et al. 2008; Wiederkehr et al. 2011). This metamorphism was dated at approximately 42-40 Ma (Wiederkehr et al. 2009). The high-pressure event in the metasediments around the Adula nappe is characterized by a lower peak temperature in comparison to estimates for the northern part of the Adula nappe. The Tambo nappe experienced peak pressure conditions of ~1.0-1.3 GPa and temperatures ranging from approximately 400°C in the N to 550°C in the central part of the nappe (Baudin and Marquer 1993). The Simano nappe retains peak pressures of approximately 1.0-1.2 GPa (Rütti 2003).

The isograds of the subsequent Barrovian metamorphism crosscut the nappe boundaries (Todd and Engi 1997; Nagel 2008; Wiederkehr et al. 2011).

The Adula nappe is classically considered to be connected to the Gruf. However, (Galli et al. 2011) demonstrated that they are two independent tectonic units. Based on its lithological similarity and structural position, the high-pressure Cima Lunga unit is interpreted as being part of the Adula nappe, but Quaternary sediments filling the large Ticino Valley mask the connection between these two units.

For a description of the larger regional setting of the Lepontine Alps, the reader is referred to (Steck 2008, Steck et al. in press) and to the tectonic map of (Berger and Mercolli 2006) and its explanatory notes (Berger et al. 2005) with its exhaustive reference list.

The Adula nappe has a distinct Mesozoic sedimentary sequence. This sedimentary sequence is refolded within the basement (Heim 1891; Jenny et al. 1923), but stratigraphic contact between the basement and cover can be still observed. The Mesozoic cover enclosed within the basement is classically called Internal Mesozoic (Heim 1891; Heinrich 1983) and this name is also used in the present paper. The Triassic stratigraphic sequence of the Adula nappe is of the North Penninic type. The Jurassic is characterized by an emersion with subsequent Late-Jurassic marine drowning (Cavargna-Sani et al. 2010; Galster et al. 2012). The Mesozoic paleogeographic position of the Adula domain is situated at the distal Helvetic margin (Steinmann 1994; Cavargna-Sani et al. 2010; Galster et al. 2012).

The Adula basement is composed of several Paleozoic formations (undifferentiated paragneiss, shown in Fig. 2), as outlined by Cavargna-Sani et al. (submitted) and briefly described below. The Salahorn Fm. (Fig. 3) is composed of Cambrian sediments with a few magmatic bodies, and significant amounts of carbonates are frequently reported on the map of Jenny et al. (1923). The Trescolmen Fm. (Fig. 3) is composed of metapelites with oceanic magmatic blocs related to a subduction zone environment (the age of this chaotic formation span from 460 to 370 Ma). The Garenstock augengneiss and the Rossa orthogneiss are Ordovician granites (regrouped under Ordovician paragneiss in Fig. 2). The Heinisch Stafel Fm. (Fig. 3) is composed of Ordovician volcanoclastic sediments. The Permian Zervreila granite intrudes into the prestructured Variscan basement formed by the formations presented previously (Fig. 2). The complex pre-Mesozoic evolution of the Adula basement must be considered during the examination of Alpine structures. The mono-orogenic Permian granites and the Mesozoic sediments are the best markers for discriminating the Alpine deformation from older ones.

The overall structure of the Adula nappe is a classic recumbent north-vergent fold-nappe rooted in the south between the zone of Orselina-Mergoscia-Bellinzona and the Simano nappe (Fig. 2c; Jenny et al. 1923; Schmid et al. 1996). The Adula nappe is refolded by S-verging post-nappe folds in the southern region (Nagel et al. 2002a). However, the internal structure of the nappe is more complicated than a simple fold-nappe superimposed by back-folding in the south. The presence of Mesozoic rocks refolded within the Paleozoic basement known as the Internal Mesozoic is a distinctive feature of the internal structure of the Adula nappe. The internal structure and the nappe geometry are the result of several deformation

phases that are detailed below.

The Adula nappe is famous for its metamorphic rocks and the occurrence of well-preserved eclogites and high-pressure metapelites. The high-pressure peak conditions in the Adula nappe increase from north to south. In the northern region (Vals area), the pressure and temperature peak conditions are as follows: 1.0-1.3 GPa, 450-550°C (Heinrich 1986; Löw 1987); 1.7 GPa, 580-640°C (Dale and Holland 2003); and ~1.9 GPa, ~580°C (Zulbati 2010). In the central part of the nappe (Alp da Confin, Alp da Trescolmen), the peak conditions are at ~2.2 GPa, ~650°C (Heinrich 1986; Meyre et al. 1999; Dale and Holland 2003). In the southern part of the Adula nappe (Monte Duria garnet peridotites) and in the Cima Lunga nappe, the peak conditions reach ~3.0 GPa, ~800°C (Heinrich 1986; Nimis and Trommsdorff 2001, Hermann et al. 2006). Subsequent to these high-pressure metamorphic conditions, the Adula nappe underwent Barrovian metamorphism from greenschist facies in the north of the nappe, gradually increasing to amphibolite facies to the south. These conditions are reached through a continuous loop of high-pressure conditions (Löw 1987; Meyre et al. 1999; Nagel et al. 2002b; Dale and Holland 2003; Zulbati 2008). The Barrovian metamorphic isograds crosscuts the Adula and surrounding nappes. The different P-T path between the Adula and surrounding nappes suggests a post-nappe – emplacement thermal peak. Nagel (2008) discusses this aspect of the metamorphic conditions in the Adula nappe in detail.

The age of the high-pressure metamorphism in the Adula nappe has been the subject of recent debate (Liati et al. 2009; Zulbati 2010; Herwartz et al. 2011). In the northern part of the nappe, some P-T estimations are obtained from Mesozoic metapelites in the Hennasädel locality (Fig. 2) (Löw 1987; Zulbati 2008; Wiederkehr et al. 2011). The Alpine age for these data is unambiguous. However, the eclogites are part of the Paleozoic basement and exhibit a polymetamorphic history. Liati et al. (2009) dated the high-pressure metamorphism as Devonian to Mid-Carboniferous, based on the analysis of zircon metamorphic rims. They also determined an Alpine age of 30-32 Ma for the peak temperature conditions in zircons of the central part of the nappe. Herwartz et al. (2011) obtained Carboniferous and Eocene ages for eclogitic garnets in the central part of the nappe. This finding confirms the presence of Alpine eclogite facies metamorphism in the Paleozoic mafic rocks of the central Adula nappe.

3.3. Structures of the northern Adula nappe

3.3.1. Introduction

The overall geometry of the northern Adula nappe is presented in a general map (Fig. 2) and in several cross-sections (Fig. 3). Within this part of the Adula nappe, the following three areas are of primary importance to understanding the structure and geometry: the Zapport Valley, the Hennasädel area and the Plattenberg area. These areas have exceptional outcrop conditions and rock formation that well define the structures. Moreover, the general orientation of the outcrops is appropriate for a structural study. These key regions were carefully mapped at a 1:5’000 or 1:10’000 scale (see Chapter 3.2, 3.3 and 3.4). Simplified maps and the localization of the detailed maps are presented in Figure 1.

The Alpine deformation phases are presented below in advance of a more detailed description in the following chapters. The phases are then synthesized in chapter 3.6. The *Ursprung* phase (D_U) is the earliest phase that has been observed. A few E-verging folds (F_U) and a schistosity (S_U) are attributed to this deformation phase. The *Zapport* phase (D_Z) (Löw, 1987) corresponds to the main pervasive structure in the nappe. This phase can be divided into two folding phases using fold interferences. Locally, the phases are divided into two distinct schistosities, but they cannot be distinguished outside of the specific interference fold patterns, where they present the same characteristics. A stretching lineation (L_Z) associated with shear sense indicators seems to correspond to only one main phase; for this reason, the Zapport deformation phase (Dz) is

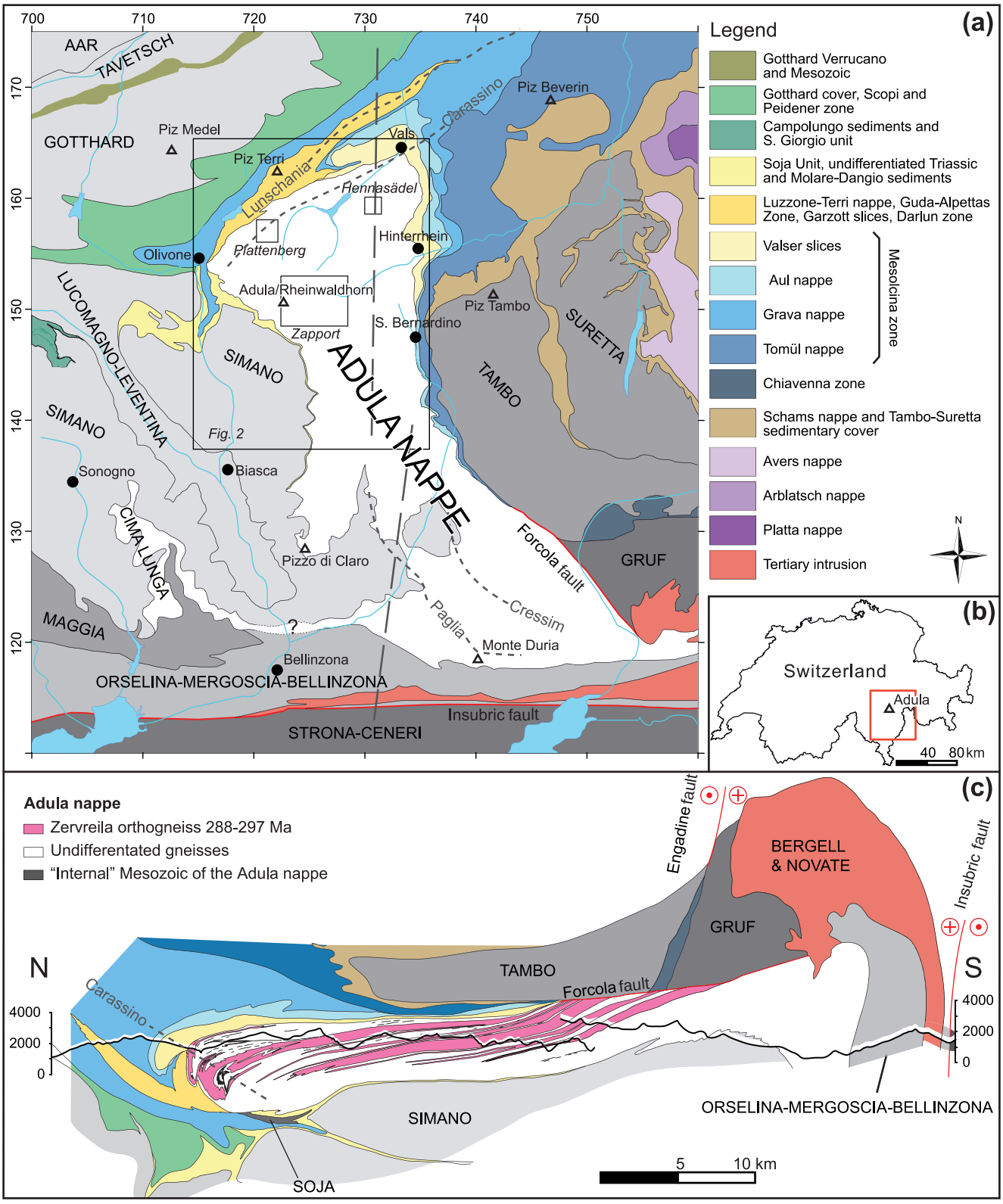

Fig. 1 *Regional setting of the northern Adula nappe.* ***a.*** *Tectonic map of the Eastern Lepontine Alps. Basement nappes are shown in grey or white; sediments are shown in color. Modified after Spicher (1980), Berger & Mercolli (2006), Steck (2008) and Galster et al. (2012) and updated. The large rectangle indicates the limit of Figure 2, and small rectangles with names in italics indicate the detailed map location (Fig. 5, 8 and 12). The indicated traces represent the principal antiform of different phases. The coordinate system is the kilometric Swiss grid (CH 1903).* ***b.*** *Location of the tectonic map (Fig. 1a)* ***c.*** *Cross-section of the Eastern Lepontine Alps. Data are acquired from this work for the northern Adula nappe (composite cross-section from Fig. 3) and from Schmid et al. 1996, Nagel et al. 2002a, Berger et al. 2005, Galli et al. 2012 and Galster et al. 2012. The legend is the same as in Fig. 1a for the tectonic units outside the Adula nappe. The traces of the cross-section are indicated on the map (Fig. 1a).*

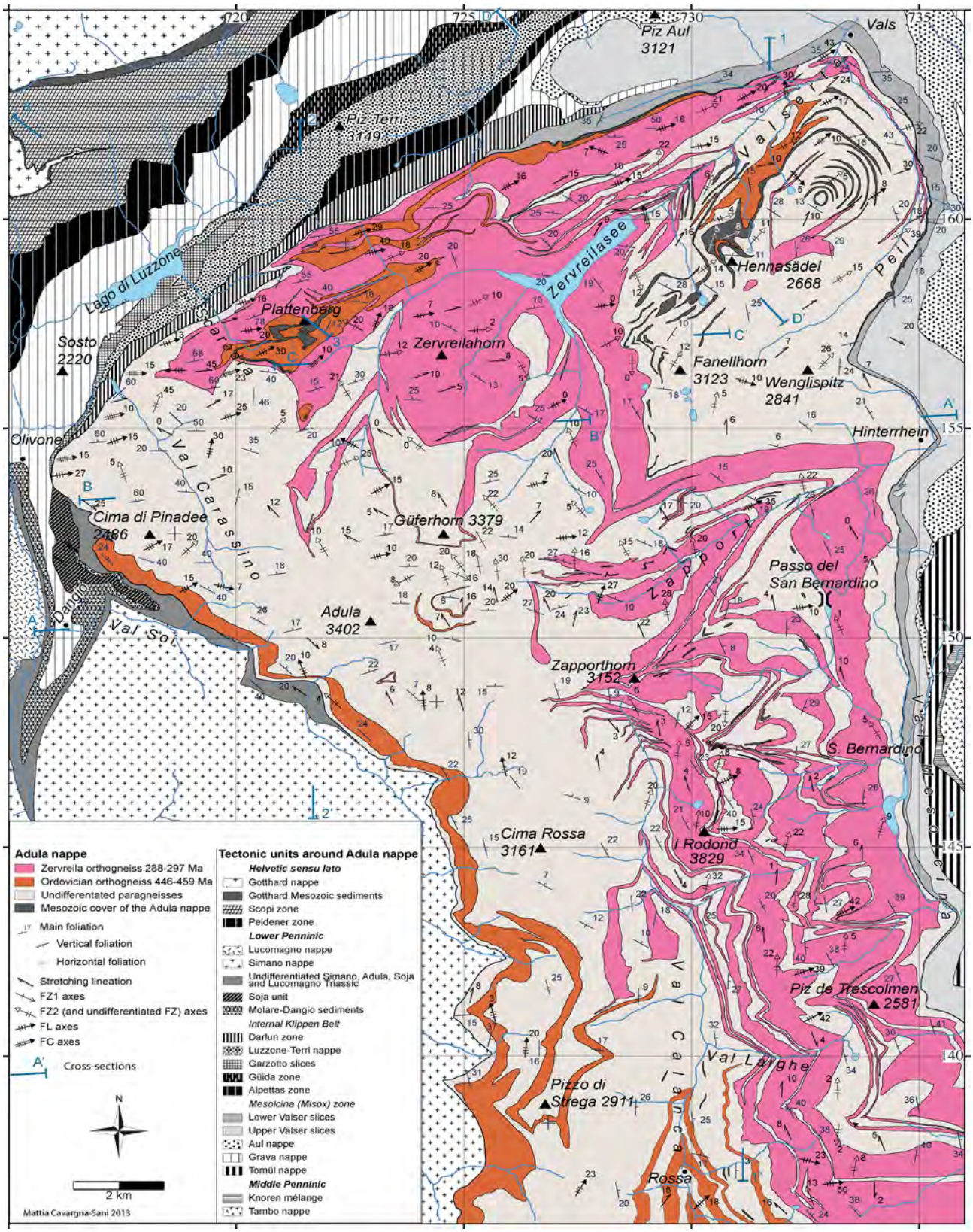

Fig. 2 *Geologic map of the northern Adula nappe. New area mapped by M. Cavargna-Sani (this work) and compilation of maps from Jenny et al. (1923), Künding (1926), Van der Plas (1959), Egli (1966), Frey (1967), Pleuger et al. (2003), Berger and Mercolli (2006), Arnold et al. (2007), Cavargna-Sani (2008), Galster (2010) and Swisstopo (2012). The coordinate system is the kilometric Swiss grid (CH 1903).*

Fig. 3 *Cross-sections through the northern and central Adula nappe. Section 3-3'partially after Galster et al. 2012.* ▶

Fig.3 Cross-sections through the northern and central Adula nappe

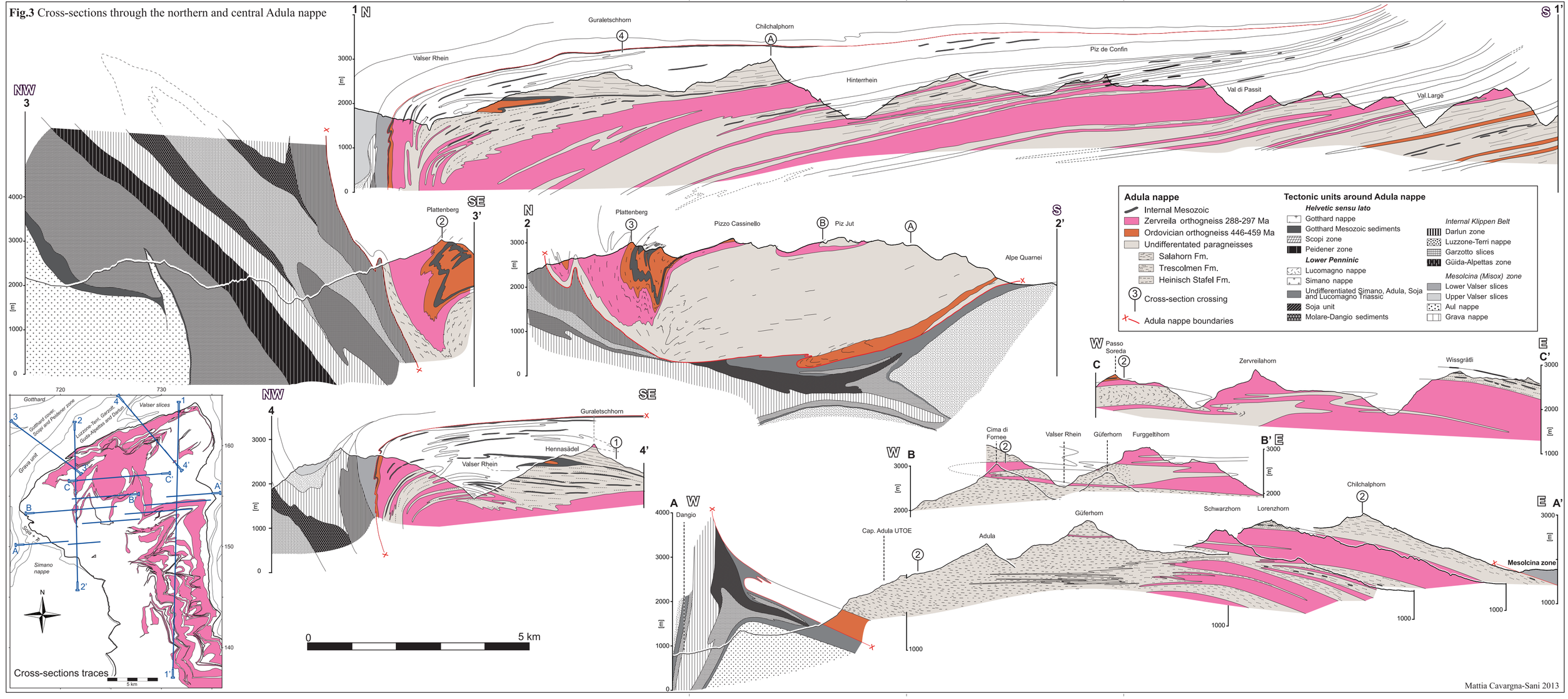

Mattia Cavargna-Sani 2013

divided into *Zapport 1* (D_{Z1}) and *Zapport 2* (D_{Z2}) where possible. The *Leis* phase (D_L) (Löw, 1987) is expressed by folds (F_L) and locally by a cleavage (S_L) associated with a stretching lineation (L_L). The last *Carassino* phase (D_C) (Löw, 1987) principally forms the NW-verging Carassino antiform in the front of the nappe. The Zapport, Leis and Carassino phases were first established by Löw (1987). The deformation phases described above are all recognized in the Paleozoic basement, the younger Permian granites and the Mesozoic sediments; they are unambiguously the product of the Alpine deformation.

3.3.2. Zapport Valley

The geological map of the Zapport Valley (Fig. 4) covers the left-hand side of the upper part of the valley. The whole area was mapped at a 1:10'000 scale. This area was previously mapped by G. Frischknecht at 1:50'000 (in Jenny et al. 1923), but at that time, some areas were covered by glaciers. Later, Löw (1987) investigated the structures. This part of the valley exhibits perfect outcrop conditions perpendicular to the F_Z fold axes and allows for an examination of the widest segment and the deepest structural level of the central part of the Adula nappe. The outcropping formations in this area are as follows: the Salahorn Fm., the Trescolmen Fm., the Zervreila Orthogneiss and a few boudins of the Internal Mesozoic cover (dolomitic and calcareous marble). This area is preserved from the latest deformation phases, which is most likely why the earliest phase (D_U) is so well preserved. The D_U, D_{Z1}, D_{Z2} and D_L deformation phases are visible at the outcrop scale. F_{Z1} and F_{Z2} are clearly visible at the map scale and form the principal features of the area (Fig. 4 and 5).

D_U structures are characterized by some folds and a relict schistosity. Folds FU are isoclinal and range from a few centimeters to decimeters in amplitude. The fold axes are approximately N-S (Fig. 5). These folds are E-vergent on the hectometric W-vergent F_Z fold limbs (Fig. 6a and b). They form type 3 (Ramsay, 1967) fold interference patterns. The opposite vergence of the D_U folds with respect to the F_Z is a key feature used to distinguish between these two deformation phases and to provide a kinematic interpretation of the D_U deformation. The folds of the D_U phase do not show any earlier schistosity refolded in their hinges. S_U is the axial surface schistosity of the previous described folds (Fig. 6a and b). It can also be considered a relict structure refolded in the hinge of the F_{Z1} (Fig. 6c and d).

Interferences between F_{Z1} and F_{Z2} folds are frequent. These interferences can be observed at the outcrop (Fig. 6c and d) and map scale (Fig. 4 and 5). The F_{Z1} are isoclinal recumbent folds (Fig. 6c and d). At the map scale and according to outcrop analysis, they indicate a general W vergence. An axial plane schistosity (S_{Z1}) is developed in the F_{Z1}. This schistosity is also refolded in the F_{Z2}.

F_{Z2} are isoclinal recumbent folds with a N-S fold axis and a general W vergence clearly visible on the cross-section (Fig. 5). These folds refold the earlier D_U and D_{Z1} features (Fig. 6c and d). S_{Z2} is the axial plane schistosity associated with F_{Z2}. The combination of S_{Z1} and S_{Z2} forms the main fabric of this area. The schistosity plane carries an N-S stretching mineral lineation associated with top-to-N shear criteria. The folds associated with D_{Z1} and D_{Z2} are the main folding structures visible in the Zapport Valley (Fig. 4 and 5). A few F_Z folds also deform the Internal Mesozoic bands.

In this area, D_L is expressed by centimeter- to decameter-scale, open to close, N- to NW-vergent folds (Fig. 6e). The fold axes plunge towards the E to NNE (see map, Fig. 2), and the axial planes dip towards the S to SE with a variable dip. No map-scale folds have been observed in the area. The S_L crenulation cleavage appears restricted in a few fold hinges. No stretching lineation associated with D_L is discernible.

In an E-W cross-section, the main structures are bent from an almost horizontal attitude to a gentle E-dip in the eastern part of the Zapport Valley. This flexure may be related to the eastern termination of the Lepontine dome.

The mountain slope is crosscut by W-dipping normal fault passing through the Clubhüttentälli and the Höberglücke (Fig.

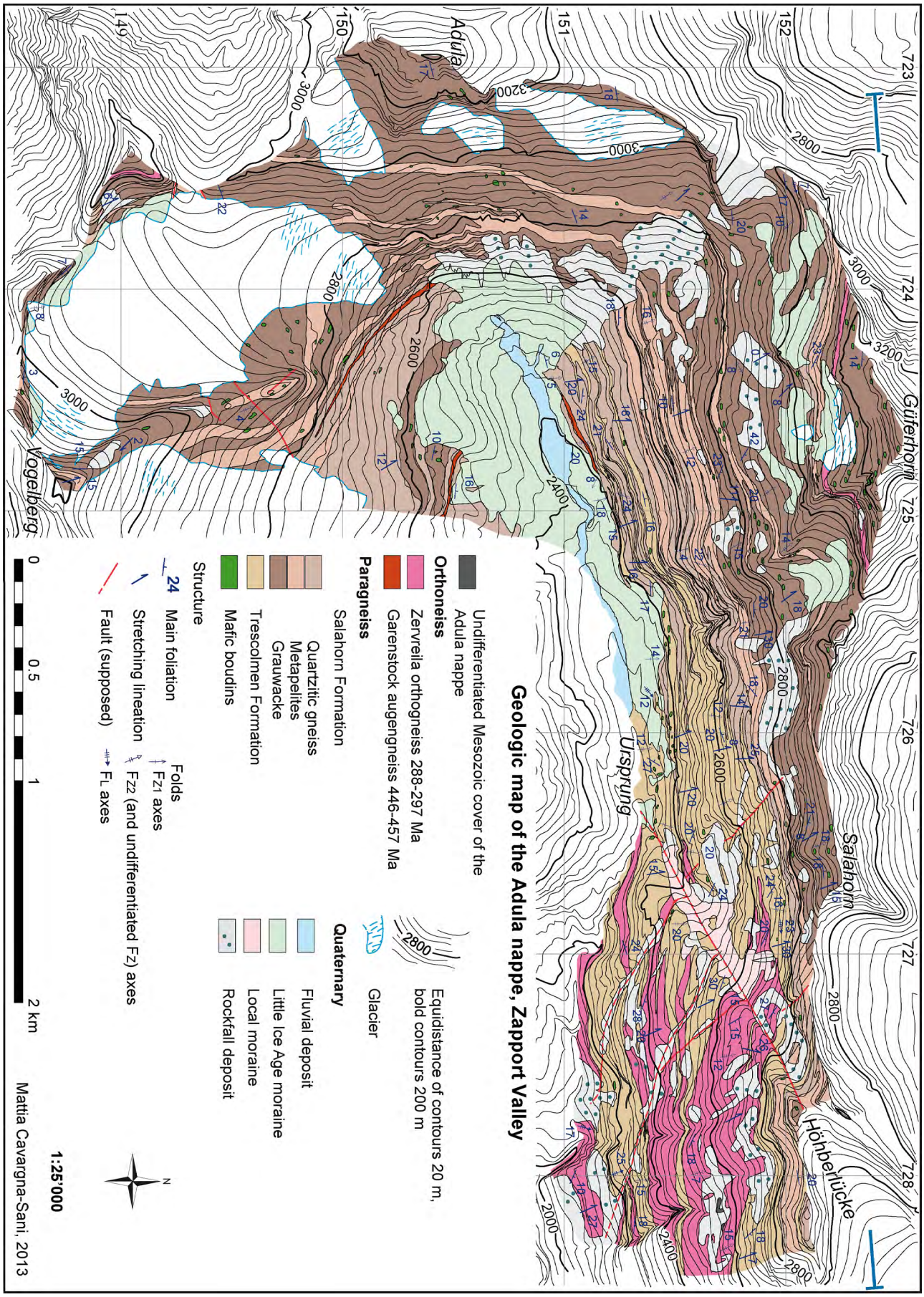

Fig. 4 *Geologic map of the Zapport Valley. The locality type of Ursprung (Ursprung deformation phase) is indicated. This locality is at the front of the glacier on the Jenny et al. (1923) map. The coordinate system is the kilometric Swiss grid (CH 1903).*

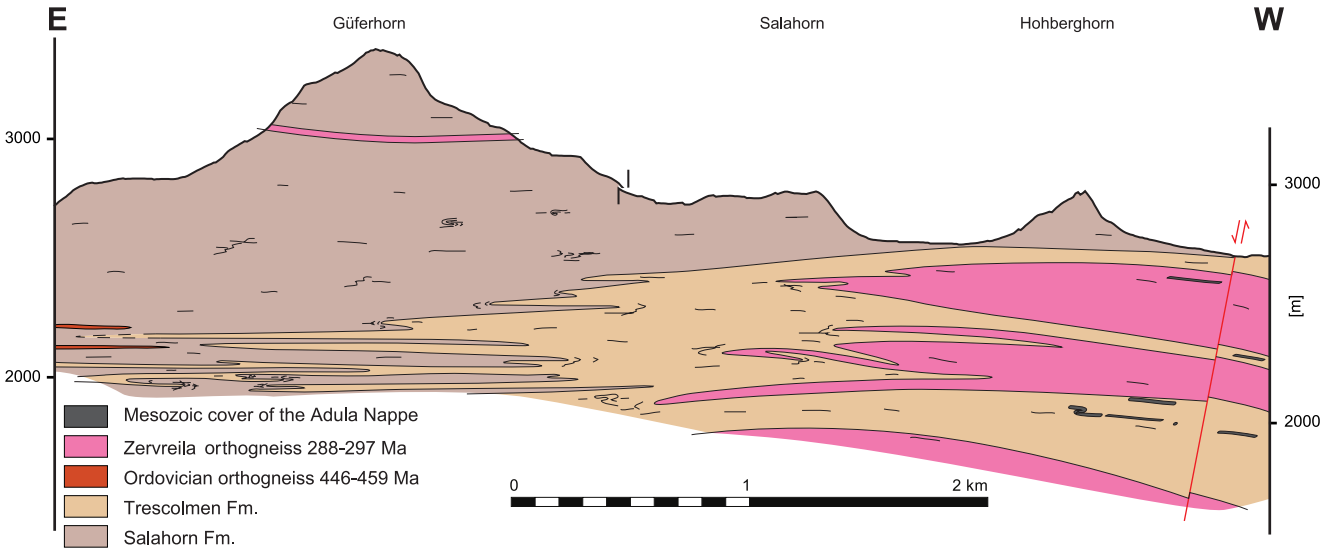

Fig. 5 *Cross-section of the Zapport Valley. The cross-section trace is indicated in Fig. 4.*

4 and 5). This fault may be very recent as suggested by the morphology of the Hinterrhein River, which includes sediment accumulation upstream towards the hanging wall of the normal fault and a strongly erosive gorge downstream towards the uplifted footwall.

3.3.3. Hennasädel

The Hennasädel hill is situated on the SE slope of the Upper Valsertal, above the Zervreila dam. The hill was mapped at a 1:5000 scale (Fig. 7). The cross-section (Fig. 8) is perpendicular to the F_{Z1} and F_{Z2} fold axes. This area was previously mapped by Kopp (in Jenny et al. 1923), Van der Plas (1959), Thüring (1990) and Zulbati (2008) and is represented on the 1:25'000 Swisstopo atlas map Vals (Arnold et al. 2007). However, these maps were not sufficiently focused on providing a lithostratigraphic and structural understanding.

The Hennasädel exposes one of the most interesting sequences of the Adula Internal Mesozoic. The basement is formed by the following three distinct Paleozoic formations briefly described in the introduction (Chapter 2): the Heinisch Stafel Fm., the Trescolmen Fm. and the Garenstock augengneiss. A sample of this orthogneiss from the Hennasädel outcrop was dated at ~451 Ma (Cavargna-Sani, in press). The Mesozoic series is composed of a well-identified Triassic and Jurassic sequence. The age of the younger segments of the series is uncertain, although they are most likely correlated with Cretaceous formations. The Triassic series starts with a transgressive quartzite and transitions into "dolomie bicolori" (Galster et al. 2012). The Lower and Middle Jurassic are absent, most likely due to an unconformity. The Upper Jurassic starts with a drowning phase marked by metasandstones and turns into a rather pure marble interpreted as the equivalent of the Helvetic Quinten-Fm. The younger series continues with a diverse sequence of calcschists, quartzites and metapelites.

This Mesozoic series has a stratigraphic contact on the Heinisch Stafel Fm. and the Garenstock augengneiss. The contact to the Trescolmen Fm., on the top of the outcrop, is an abnormal contact as there is no Triassic rocks on the contact with the Paleozoic Fm. (Fig. 7 and 8).

D_U is marked by a schistosity refolded in the younger F_{Z1} (Fig. 9a). Folds of the early D_U are not observed in this area.

D_Z are the most prominent structures of this outcrop (Fig. 8). F_{Z1} and F_{Z2} and their associated schistosity can be distinguished by outcrop- (Fig. 9c) and map-scale (Fig. 8) fold interference patterns. A map-scale F_{Z1} recumbent syncline outcrops in this

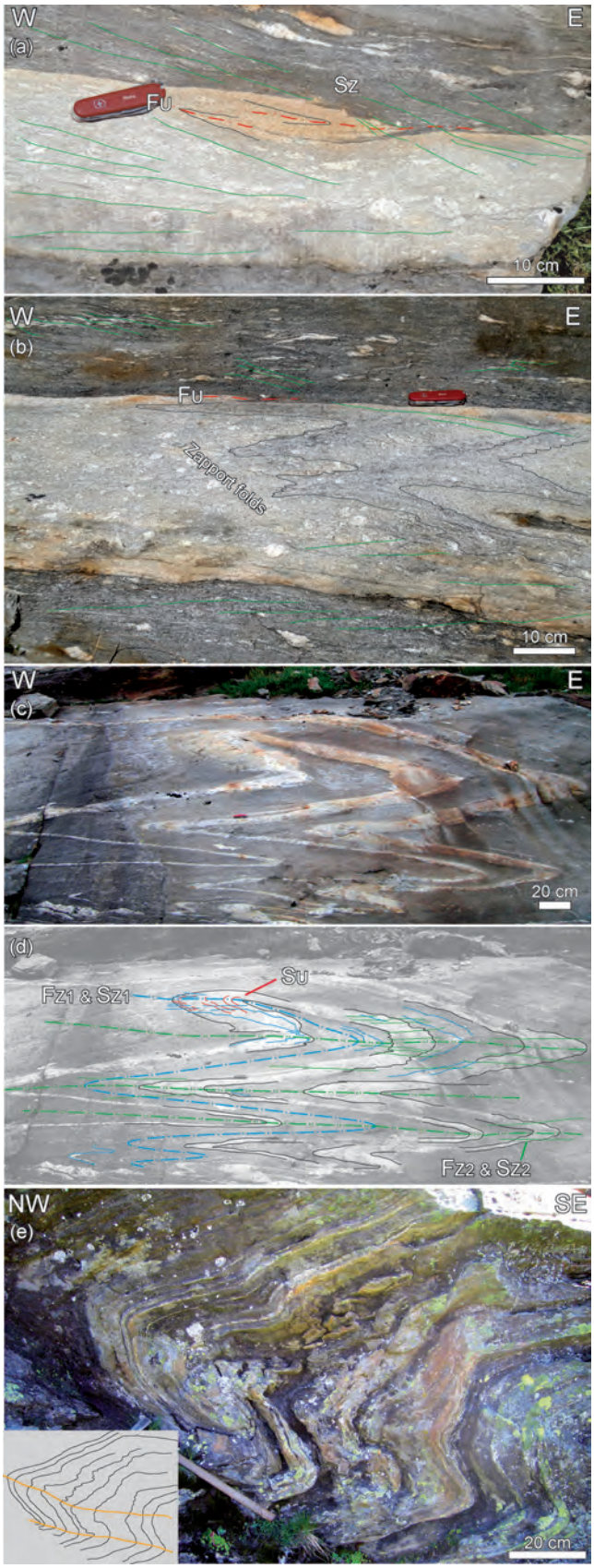

Fig. 6 *Outcrop-scale structures in the Zapport Valley* ***a.*** *E-vergent Ursprung phase folds at the limit between orthogneiss and paragneiss (724800/151150)* ***b.*** *E-vergent Ursprung phase fold on a fold limb of a hectometric Zapport phase W-vergent fold (724800/151150)* ***c.*** *and* ***d.*** *Interference between F_{Z1} and F_{Z2}. The Ursprung phase schistosity is folded in the first Zapport phase fold (725950/151470).* ***e.*** *Leis phase fold (727680/151150).*

area and is associated with numerous second-order folds at the meter to decameter scale (Fig. 9a). These second-order folds are asymmetric ("S" and "Z" criteria) and clearly underline the main Z_1 fold (Fig. 9b). Their vergence is locally incompatible with the evident second-order F_{Z2} fold (Fig. 9b). The F_{Z1} fold is also clearly confirmed by the stratigraphy (Fig. 8). This fold is a syncline compatible with the general NW vergence of F_{Z1}. F_{Z1} is associated with an S_{Z1} schistosity (Fig. 9a). The outcrop analyses show that the F_{Z1} syncline is refolded by an F_{Z2} recumbent fold; this finding is also confirmed by smaller-scale fold interferences (Fig. 9c).

The most obvious structure of the Hennasädel is an $F_{Z2,}$ NW-vergent recumbent fold with the Garenstock augengneiss in its core (Fig. 8). This structure folds the F_{Z1} syncline (Fig. 8) described above. Several second-order F_{Z2} folds (Fig. 8) are associated with the map-scale first-order fold and are visible in all formations. F_Z synclines evidenced by Triassic dolomites (often with a clear stratigraphic contact marked by Triassic quartzites) between Hennasädel and Wissgrätli are frequent and obvious (Fig. 3, cross-section 4). These outcrops are F_Z synclines that close to the SE in accordance with the general NW-vergence of these F_Z folds.

A clear stretching lineation, parallel to fold axis, plunging towards the NE is related to the D_Z deformations. The shear sense observed parallel to this lineation is top-to-NE. In addition to the usual kinematic indicators (i.e., sigma clasts in the Garenstock augengneiss), the snowball garnets observed in quartzites and micaschists of the cover series (Fig. 9d and e) are spectacular. Both limbs of the map-scale F_{Z2} fold present the same top-to-NE shear sense criteria.

D_L and D_C deformations are weakly discernible on the Hennasädel hill. This area is essentially devoid of these deformation phases; they are stronger to the north-west of the presented area.

The contact on the top of the Mesozoic cover with the Trescolmen Fm. is an interesting feature of this outcrop. This contact appears not to be folded by the prominent Z_2 fold. Near the contact, there is no sign of post-S_Z shear indicators or brittle fracturing as would be expected if the structure is a late, post-D_Z, thrust. An alternative interpretation is provided in the discussion (Chapter 4.5).

The whole right flank of the Valsertal is affected by gravitational faults. These faults are also evident on the Hennasädel (Fig. 7 and 8).

3.3.4. Plattenberg

The Plattenberg area outcrops very well at high altitude. A map of this region (Fig. 10) was made at a 1:5000 scale. Heim (1891) described the dolomites between Plattenberg and Passo Sorreda. Jenny (1923) described this area in detail and mapped it. Egli (1966) also mapped this area, and Löw (1987) provided a structural map and a detailed cross-section. The primary feature of interest in this area is the impressive Internal Mesozoic outcrop with multiple folding that are clear on a map scale (Fig. 10 and 11). The Mesozoic sequences lies systematically on top of the Garenstock augengneiss. This gneiss contains some mafic rocks with a few eclogite boudins. The gneiss under the Mesozoic cover shows a clear weathering alteration, and a paleosol is preserved locally (Cavargna-Sani et al. in press). The cover-basement contact is stratigraphic; the presence of transgressive quartzite at the basis and the cover coherence is confirmed by the basement pre-Triassic weathering. The cover starts at the base with a Triassic sequence (Fig. 12a). This Triassic sequence is distinctive and is characterized by quartzite at the basis, dolomitic micaschist, yellow dolomite and "dolomie bicolori" (Fig. 12a). This sequence is specific to the North Penninic Triassic type (Galster et al. 2012). The Triassic is overlain by Upper Jurassic breccia with crinoids (Plattenberg Fm.) and by younger (post-Jurassic) calcschists and graphitic micaschists (Cavargna-Sani et al. 2010).

The tectonics of the area are dominated by map-scale folds of the Mesozoic sequence within the gneisses. The first obvious structures visible in the Plattenberg area are Z_1 isoclinal folds (Fig. 12b). These folds are associated with an S_{Z1} schistosity. The rock types most suitable for observing these structures are the quartzite and dolomitic breccia of the Plattenberg Fm.; this formation has good markers and is less deformed by later D_L. No earlier schistosity (S_U) has been observed in this area. The F_{Z1} are clearly refolded by F_{Z2} isoclinal folds, which can be observed at the outcrop scale (Fig. 12b) and map scale (Fig. 10 and 11). Outside of the interference patterns, the main pervasive schistosity in most rock types must be attributed to S_Z. The F_{Z2} folds form clear interferences with the younger F_L at the outcrop scale (Fig. 12b) and map scale (Fig. 11). Leis phase folds are the main structural feature of this area and forms kilometer-scale close to tight folds (Fig. 11). The fold geometry is strongly influenced by the competence contrast between the different rock types (especially between the more competent dolomite and the Garenstock Augengneiss). An axial plane S_L cleavage is developed in the fold hinges, varying from a crenulation cleavage to a mineral foliation (Fig. 12c and 12d). A NE-plunging stretching L_L lineation is sometimes associated with S_L. The late D_C forms rather open folds locally associated with a crenulation cleavage. This phase refolds all of the previously described fold phases. Fold interferences can also be observed at the map scale (Fig. 10 and 11).

A cross-section (Fig. 11) was built on the basis of the new mapping and structural analysis. This cross-section is therefore somewhat different from the interpretation of Löw (1987), who published one of the first modern structural analyses of the area and defined the commonly used deformation phases. The main contribution of our study with respect to the foundation provided by Löw (1987) is achieved by demonstrating the autochthony of the cover series with respect to the basement (Fig. 12a; Cavargna-Sani et al. 2010). This result enables us to distinguish and interpret the earlier deformation phases. Löw (1987) defined the Sorreda phase as a tectonic inclusion of slices of Mesozoic in the basement rocks. However, this contact does not represent a deformation phase. The formation of the Internal Mesozoic in the frontal part of the nappe is primarily

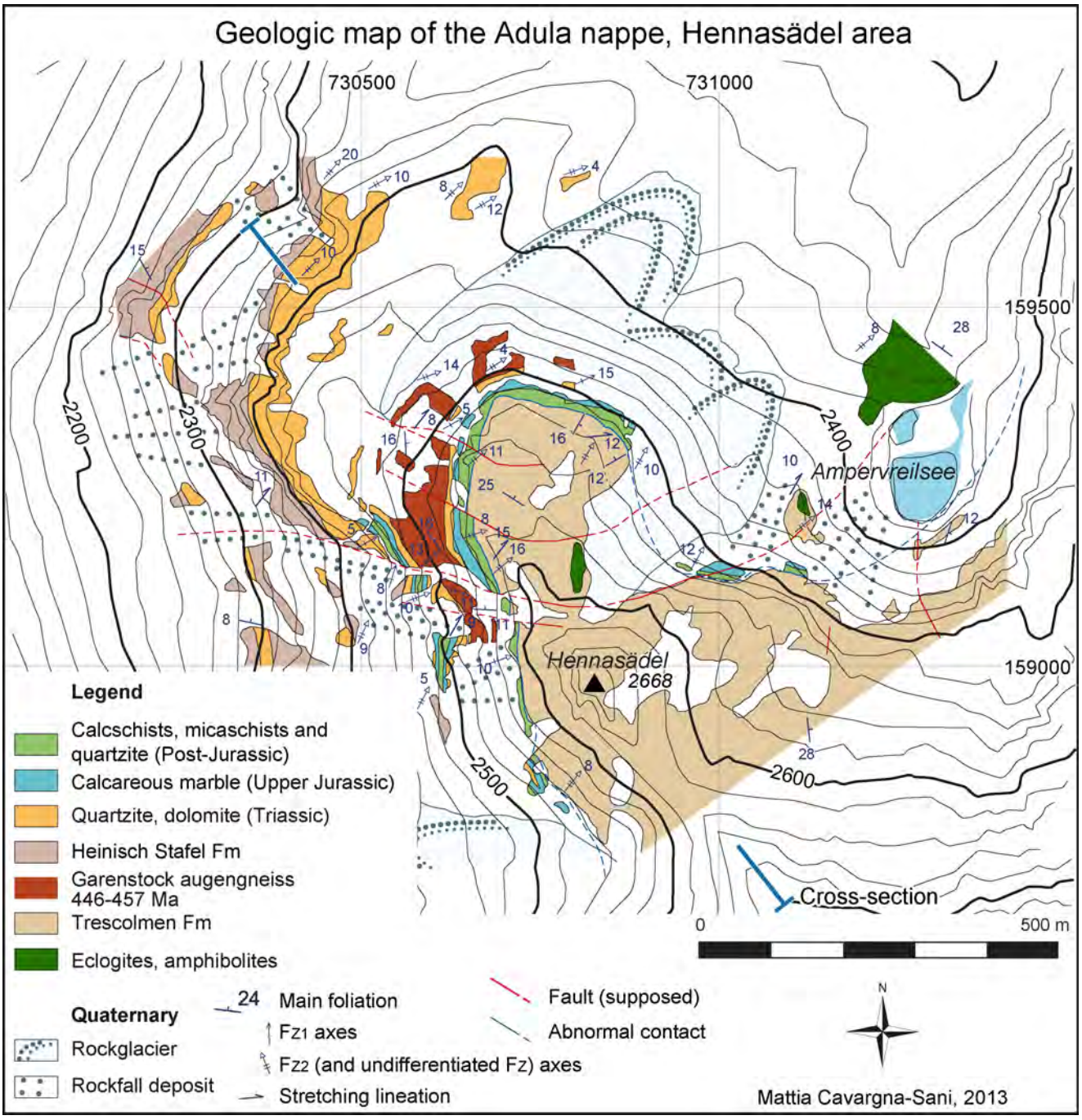

Fig. 7 *Geologic map of the Hennasädel area. The coordinate system is the metric Swiss grid (CH 1903).*

due to F_{Z1} and a subsidiary F_{Z2} syncline; the Mesozoic cover has a stratigraphic contact on the basement. The overall Plattenberg Internal Mesozoic outcrops can be simplified by an F_{Z1}syncline refolded by the following deformation phases. The original connection of this syncline to a hypothetical "external Mesozoic" is eroded. The geometry proposed by the axial trace interferences (Fig. 11) can also been observed at the outcrop scale (Fig. 12b). This finding confirms the consistency of our proposed cross-section.

3.3.5. Nappe-scale geometry and structure

The nappe-scale structure analysis is primarily based on the map of the northern Adula nappe shown in Figure 2 and in the cross-sections of Figure 3. The general map (Fig. 2) is a compilation and extension of the detailed mapping of key

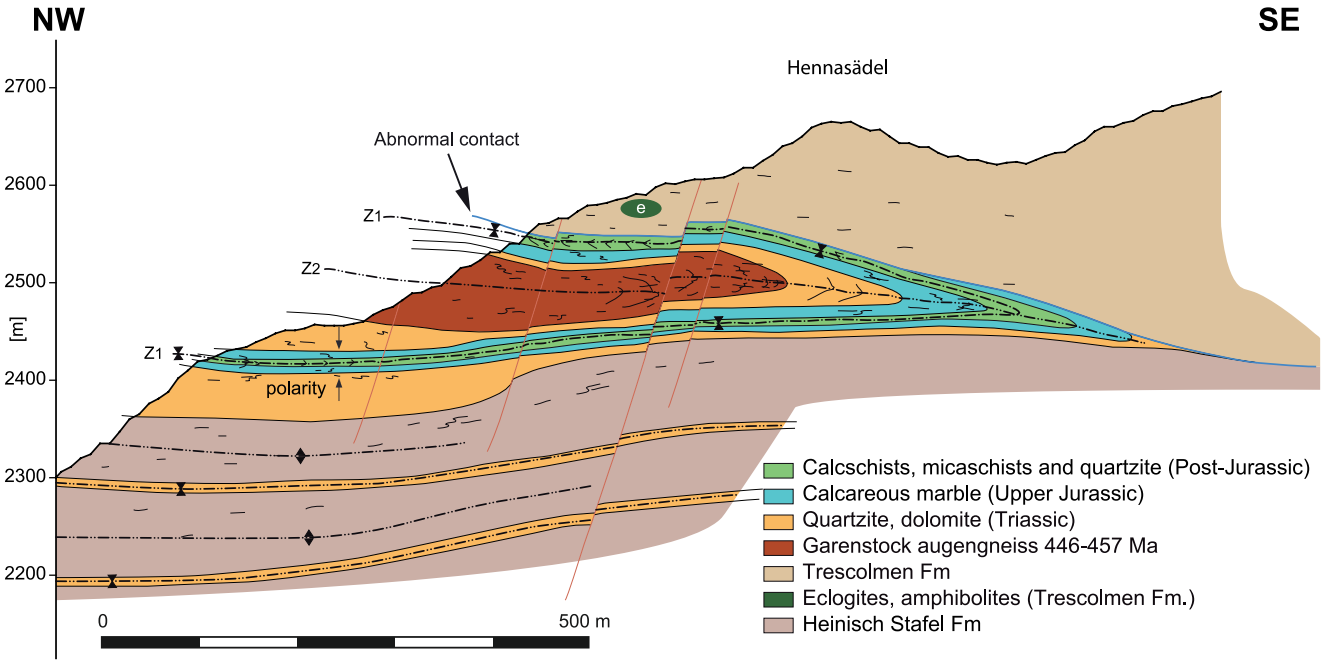

Fig. 8 *Cross-section of the Hennasädel area. The cross-section trace is indicated in Fig. 7.*

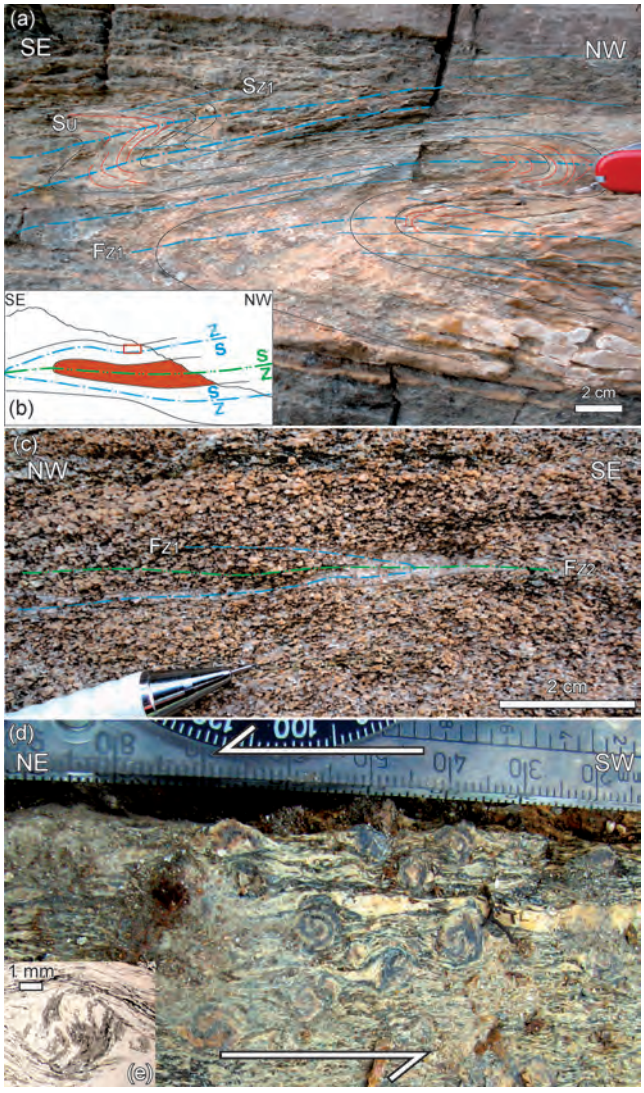

Fig. 9 *Outcrop-scale structures in the Hennasädel area.* ***a.*** *Zapport 1 folds (730840/159350)* ***b.*** *Position of 9a (red rectangle); schematic indication of the vergence of the F_{Z1} and F_{Z2} second-order folds; the cross-section has the same orientation as in (a).* ***c.*** *F_{Z1}- F_{Z2} fold interference pattern (730640/159200).* ***d.*** *Snowball garnet porphyroblasts in the quartzitic schists of the Mesozoic cover indicating the top-to- NE shear sense of the Zapport phase (730830/159340).* ***e.*** *Snowball garnet in a thin section.*

areas presented in Figures 4, 7 and 10. It is also based on the reinterpretation of previously published maps using the new lithostratigraphy proposed in Cavargna-Sani (submitted). The cross-sections of Figure 3 are based on the general map of Figure 2, on the more detailed cross-sections of Figures 5, 8 and 11 and on the additional new field observations. The cross-sections are presented here to illustrate the main structures and overall geometry of the nappe. The orientation of the main structural features (fold axes, lineations and schistosity) is indicated on the map in Figure 2 and is illustrated on stereographic projections (Fig. 13). The axial traces of the northern Adula nappe are summarized in Figure 14.

The E-W cross-sections (Fig. 3, sections A-C) are perpendicular to the F_Z fold axes. The N-S cross-sections (Fig. 3, sections 1 and 2) are parallel to the stretching lineations and also correspond to the classical sections

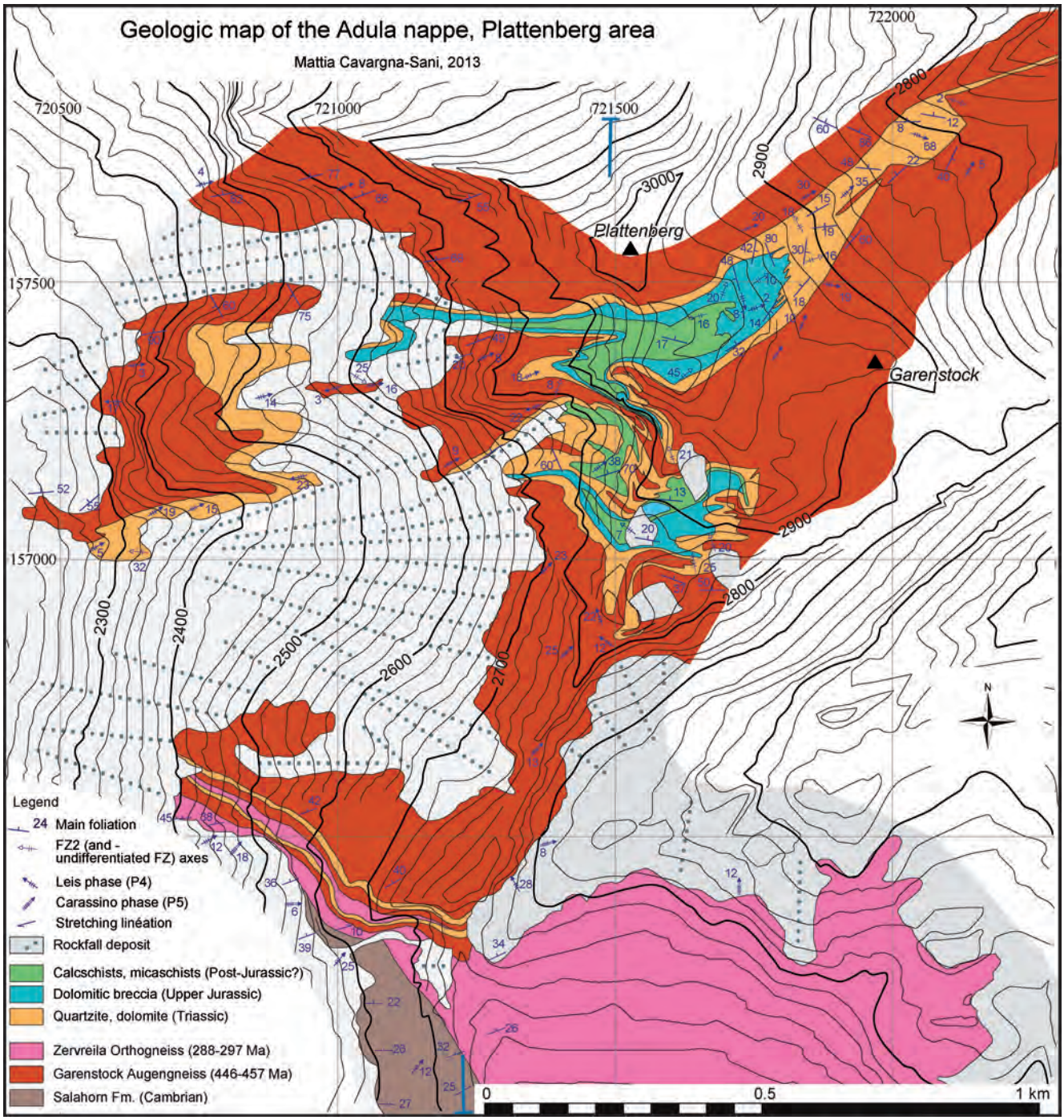

Fig. 10 *Geologic map of the Plattenberg area. The coordinate system is the metric Swiss grid (CH 1903).*

published by Jenny et al. (1923) that were later actualized and completed by Nagel (2008). In the frontal part of the nappe, the cross-sections (Fig. 3, sections 3 and 4) are perpendicular to the F_L and F_C fold axes. A 3D representation would be very difficult because of the type 2 (of Ramsay, 1967) folding interferences.

The occurrences of the Internal Mesozoic are not randomly distributed. These occurrences are grouped in specific areas of the Adula nappe. The upper part of the nappe exposes a concentration of small (metric) boudins in which the stratigraphy is difficult to precisely determine; the boudin trails are frequently aligned on the same structural plane. The most notable outcrops of the Internal Mesozoic are found in the frontal part of the nappe, where lithostratigraphic sequences several meters thick can be observed (e.g. Hennasädel and Plattenberg).

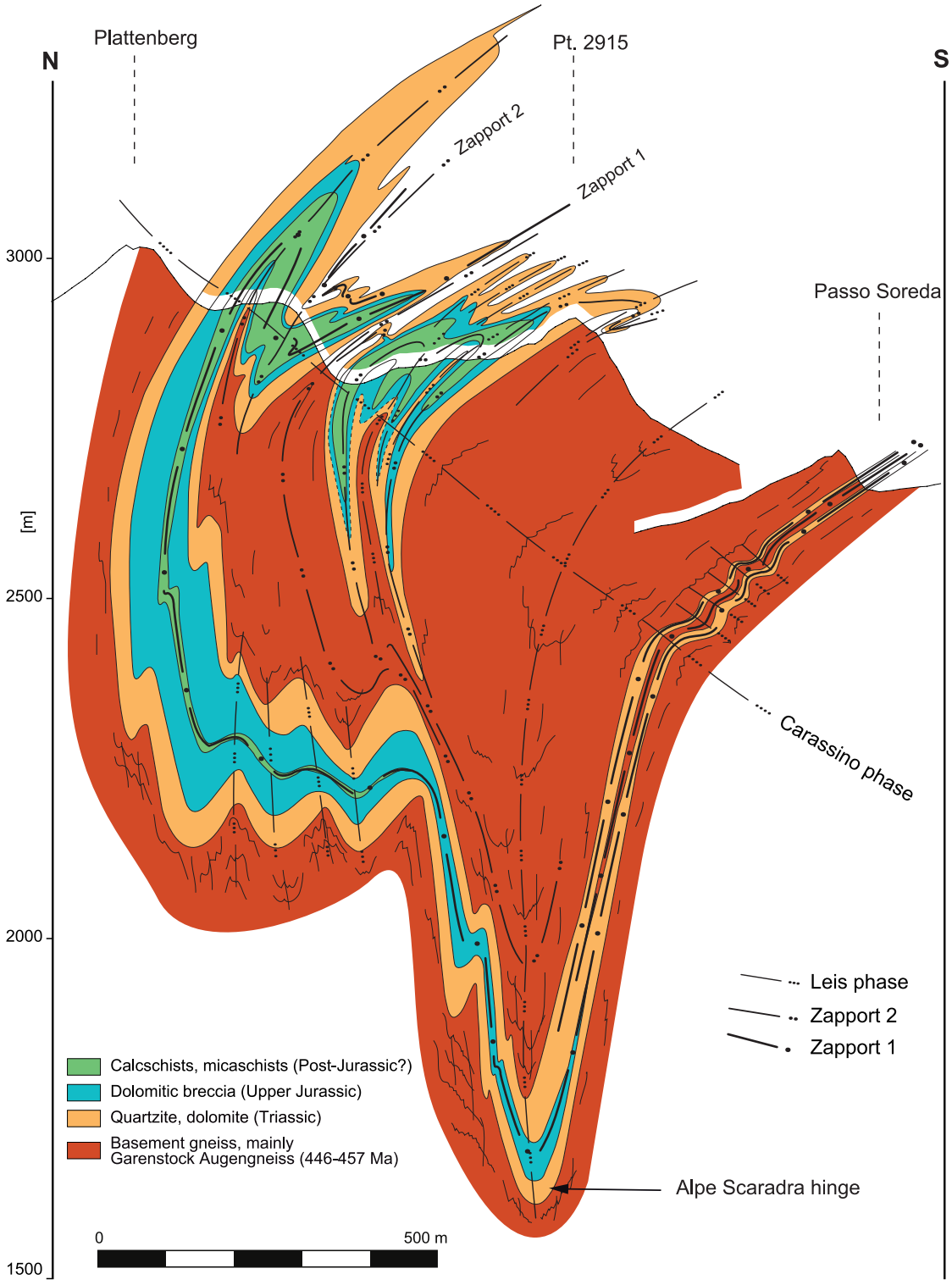

Fig. 11 *Cross-section of the Plattenberg area. The cross-section trace is indicated in Fig. 10.*

The upper part of the eastern N-S cross-section (Fig. 3, section 1 and Fig. 1c) displays a nappe-scale structure that requires further discussion. The Internal Mesozoic, the Zervreila orthogneiss bands and the lithological contacts dip to-the-N with respect of the top of the nappe. The bands of the different rock formations thin out towards the south. This structure forms an unconformity at the nappe-scale, but no clear triple points can be precisely distinguished. This structure has been represented on previously published cross-sections (Jenny et al. 1923; Nagel 2008). To the south, the Forcola fault (Fig. 1) also clearly marks a discordant structure on the top of the nappe, but we cannot consider this tectonic line as part of the structure described above because the Forcola fault is a much younger structure (Meyre et al. 1998; Ciancaleoni and

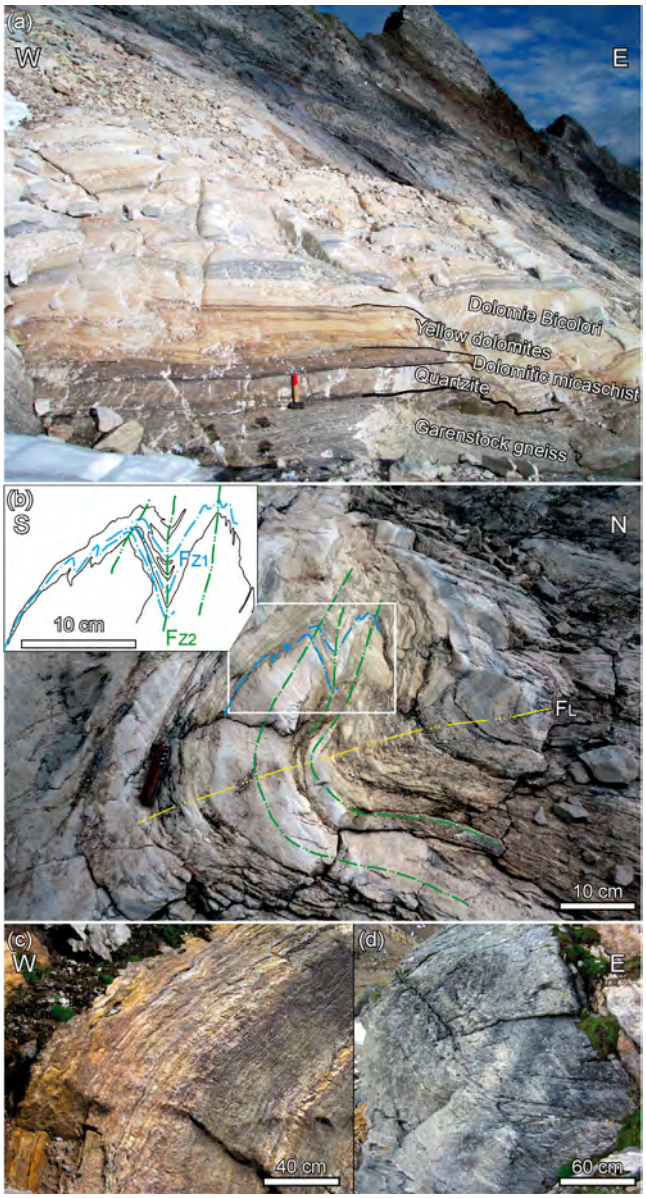

Fig. 12 *Outcrop-scale structures in the Plattenberg area* ***a.*** *Basement-cover contact (721870/157500)* ***b.*** *Fold interference for F_{Z1}, F_{Z2} and F_L (721790/157520).* ***c.*** *Leis fold and cleavage in dolomites (721510/156740).* ***d.*** *Leis fold and cleavage in the Garenstock Augengneiss (721550/157120).*

Marquer 2006). As illustrated in the above-described cross-section, the outcrops of the Internal Mesozoic are restricted to the upper and frontal parts. The upper part contains only metric boudins (the size is enlarged on the cross-section). The frontal part the Internal Mesozoic outcrops are larger and more complete (e.g. Hennasädel and Plattenberg).

In the Zapport valley, the tectonic phase responsible for the inclusion of boudins of Mesozoic rocks within the basement must be earlier than the D_Z, as the boudins trails are refolded by F_{Z1}. In the frontal part, this inclusion is related to the F_{Z1} synclines. A connection from the Internal Mesozoic to the nappe boundary is not observed.

F_Z and S_Z form the main structures in the Adula nappe. The effect of this deformation phase seems obvious at the outcrop to map scale. In the central Adula area (Fig. 3, section A), the effect of the later phases of deformation is not marked at the map scale, which explains why the fold interferences between the two W-vergent F_Z are locally very clear in the cross-section.

Large map-scale F_L are essentially developed in the NW Adula nappe (Fig. 3, sections 1-4). In contrast to the previous phases, the D_L is not restricted to the Adula nappe. This phase also affects the tectonic contact with the overthrust tectonic units and can be observed outside the Adula nappe.

The staurolite isograd (St_1/St_2 isograd of Nagel et al. 2002b) indicates the Barrowian metamorphic isograd cross-cut across the central Adula nappe. It is clearly placed post-nappe, as indicated by the straight crossing of the nappe boundaries.

F_C antiform is obvious at the frontal part of the nappe (Fig. 3, sections 1-4 and Fig. 11). This late folding affects the overthrust nappes, but it disappears downward and does not propagate in the nappes underlying the Adula nappe. In the eastern part of the central Adula, the main foliation dips E towards the Mesolcina Valley. This structure forms a large, gentle flexure (Fig. 3, section A) that marks the eastern termination of the Lepontine window.

The structures recognized in the northern Adula nappe are summarized in Table 1.

	Folds (F)	Schistosity	Lineation	Shear sense	
Carassino (D_C)	**NW-Adula:** - Open folds - N-vergent - Carassino antiform *Fold axis:*~ NE-SW	Localized crenulation cleavage			
Leis (D_L)	**NW-Adula:** - Close folds - Nappe scale - NW-vergent *Fold axis:* NE-SW **Central- an NE-Adula:** - Close to tight folds - Metric scale - N-vergent *Fold axis:* E-W	**NW-Adula:** Mineral cleavage in the folds hinges **Central- an NE-Adula:** locally crenulation cleavage in the folds hinges	**NW-Adula:** Mineral lineation *Orientation:* E-W to SW-NE	Top-to-the-North	
Zapport (D_{Z2})	- Isoclinal, similar folds - Nappe to mm scale - Recumbent - W-vergent *Fold axis:* NW Adula: variable NE Adula: SW-NE Central Adula : N-S	Main pervasive schistosity forming locally a mylonitic fabric	Main stretching lineation / mineral lineation *Orientation:* **Central-Adula**: N-S **NE-Adula**: NE-SW **NW-Adula:** mainly Leis phase	Top-to-the-North	
Zapport (D_{Z1})	- Isoclinal, similar folds - Map to mm scale - Recumbent - W-vergent *Fold axis:* Parallel to F_{Z2}				
Ursprung (D_U)	**Zapport valley:** - Isoclinal folds - E-vergent - Outcrop scale *Fold axis :* ~N-S	**Zapport and Hennasädel :** Relict schistosity in F_{Z1}		**Top of the nappe** top-to-the-South	

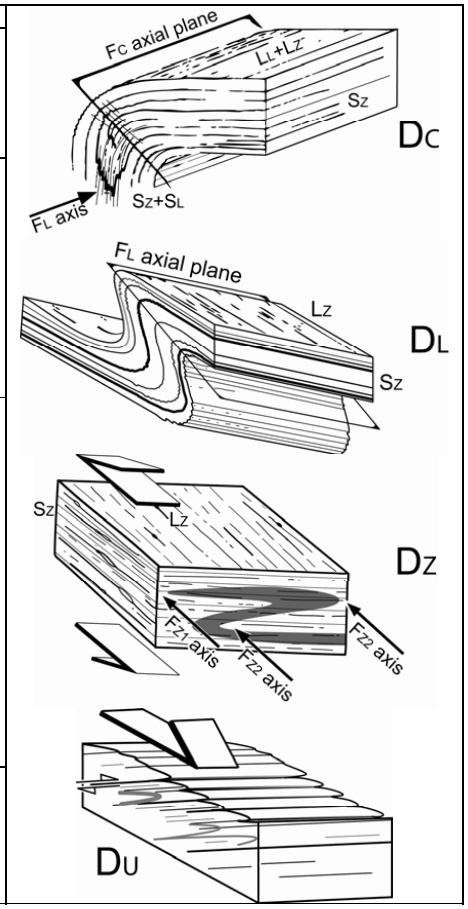

Table 1 *Summary of the Adula nappe structures. The orientations of the structures are indicated in Figures 2 and 14.*

3.4. Discussion

3.4.1. The pre-Alpine Adula

The Mesozoic sedimentary series was deposited on a strongly pre-structured Paleozoic Alpine basement that influences the current internal geometry of the nappe. The geological history of the basement is described in Cavargna-Sani (in press, Chapter 2). The basement shows several unconformities, some of which are most likely related to the Variscan orogeny. The late Variscan Permian granite intrudes in an already strongly structured basement. The Triassic cover is deposited on top of a clear unconformity.

The Adula nappe has a proper sedimentary cover with a characteristic and coherent Triassic series (Cavargna-Sani et al. 2010; Galster et al. 2012; Cavargna-Sani et al. submitted). This observation excludes the formation of the northern Adula nappe as an Alpine tectonic mélange, mixing different elements originating from several paleogeographic domains. This Triassic series is the most important marker in the study of the Alpine-derived structures of the Adula nappe. Studies of the stratigraphy of the Mesozoic cover of the Adula nappe reveal a complex Jurassic syn-rift sequence (Cavargna-Sani et al. 2010; Galster et al. 2012; Cavargna-Sani et al. submitted). The extensional structures inherited from this rifting period have strongly influenced the later Alpine structures.

3.4.2. The Ursprung phase – nappe exhumation

The Ursprung phase is characterized by a fold vergence opposite to the more obvious Zapport phase. This phase is also

underlined by nappe-scale N-dipping rock-type limits and by N-dipping Internal Mesozoic boudins trails at the top of the nappe.

The orientation of the stretching lineation associated with D_U was not precisely established, as no clearly identifiable mineral lineation has been assigned to this deformation phase. In the Zapport Valley, where this deformation phase has been established, the kinematic shear indicators are all consistent with a top-to-N movement. A few eclogitic boudins show a pre-Zapport E-W mineral lineation (Meyre and Puschnig 1993; Partzsch 1998). Kurz et al. (2004) studied the crystallographic preferred orientations of omphacite in the eclogite boudins of the Adula nappe. These structures generally have an L-type fabric and an E–W stretching lineation. However, this orientation, limited to a few competent boudins, cannot be interpreted as the original Alpine eclogite facies stretching orientation because it has certainly rotated during the strong overprinting of the subsequent Ursprung and Zapport deformation. The top-to-E Ursprung phase fold vergence observed in the Zapport Valley cannot be used as a direct indicator of material transport direction. However, it is significant that this vergence is clearly opposite to that of the Zapport folds. We assume that the displacement direction associated with the Ursprung phase in the Adula nappe corresponds to an N-S direction. This direction is coherent with the later deformations and the general early displacement direction in the Central Alps.

The nappe-scale discordance at the top of the nappe is formed by N-dipping structures with respect to the upper limit of the nappe. This unconformity is not inherited from the pre-Alpine structures because the Internal Mesozoic boudin trails follow the same type of structure. The unconformity must therefore be an Alpine structure. The Ursprung phase observed in the Zapport Valley is associated with a ductile schistosity, infolds the Mesozoic cover within the basement and shows a planar structure. We interpret the Internal Mesozoic structure of the area as marking the axial traces of deep multi-kilometric synclines. These synclines would be compatible with a top-to-S shear movement.

A simple kinematic model is proposed in Figure 15 to test the geometric effect of the superimposition of an N-vergent Zapport phase fold produced by a heterogeneous simple shear (e.g. Epard and Escher 1996; Bauville et al. 2013) onto a top-to-S Ursprung shearing phase. The Ursprung phase produces synclinal shear zones from pre-existing heterogeneity (e.g. Krayenbuhl and Steck 2009; Bellahsen et al. 2012). This simple kinematic model offers a mechanism for the inclusion of the Internal Mesozoic at the upper part of the nappe; it also explains the discordance observed at the upper part of the nappe and its preservation during an opposite-facing fold phase.

The Ursprung deformation phase locally forms the first schistosity in the Adula nappe as well as the first folds that also produce the Internal Mesozoic at the top of the nappe. The Ursprung phase is strongly overprinted by the later Zapport phases. This phase has been recognized only in the upper part of the Adula nappe but not outside the Adula nappe. We suggest that these top-to-S movements are partly coeval with the early top-to-N movements attributed to the Zapport phase at the bottom of the nappe.

The Ursprung phase can be related to the exhumation of the Adula nappe between units that suffered lower pressure (Chapter 2, Fig. 1c). This exhumation corresponds to the first decompression phase from the peak pressure. In the northern part of the nappe, the peak metamorphic conditions are 1.2-1.7 GPa and 500-600°C (Heinrich 1986; Löw 1987; Dale and Holland 2003; Zulbati 2008). In the central part (Trescolmen), the peak conditions are ~2.2 GPa and ~650°C (Heinrich 1986; Meyre et al. 1999; Dale and Holland 2003), and in the south, they are 2.8-3.0 GPa and ~800°C (Heinrich 1986; Nimis and Trommsdorff 2001; Hermann et al. 2006). Classically, kinematic modeling of the Adula nappe has assumed the conversion of pressures estimated with mineral assemblages to depth values using a lithostatic gradient (e.g., Schmid et al. 1996; Froitzheim et al. 2003; Herwartz et al. 2011). This conversion has recently been questioned, and the high-pressure values estimated in

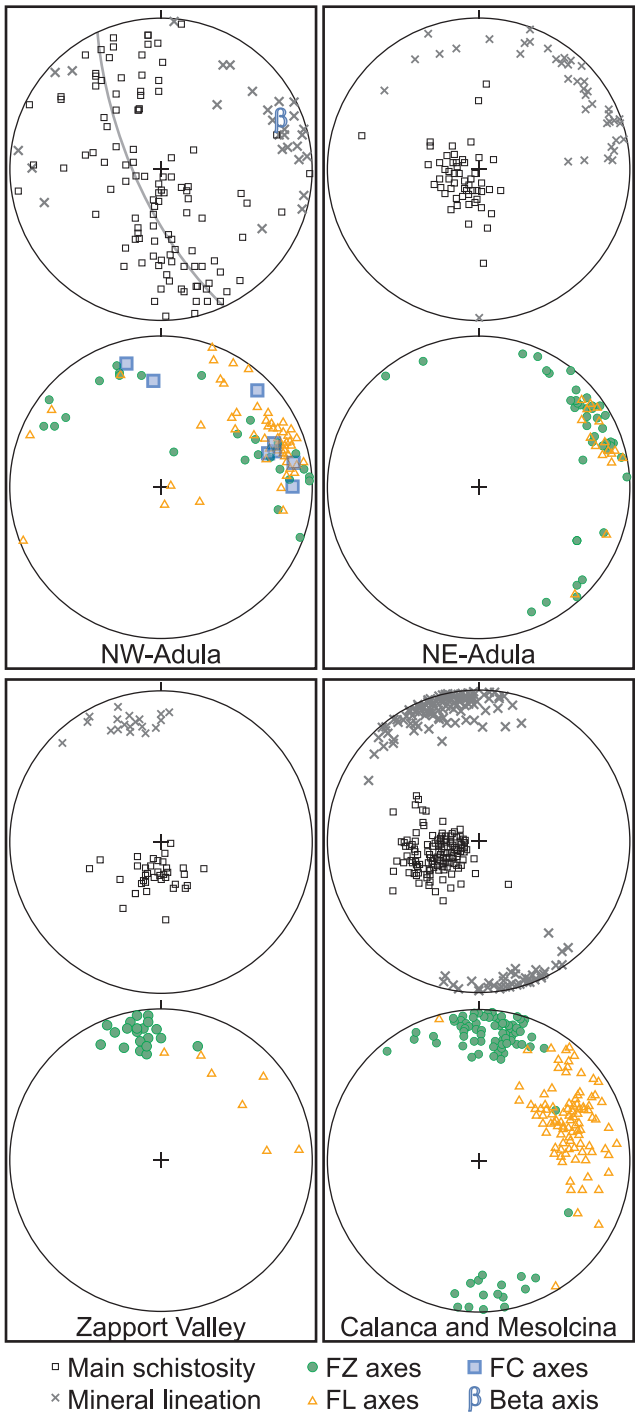

Fig. 13 *Stereographic projection of the main structures of the northern Adula nappe. The geographic subdivision of the measurements is outlined in Fig. 15 b. The lineations in the NW Adula are principally attributed to L_L; the lineations are not separated between different deformation phases because L_L is nearly indistinguishable from L_Z. The best-fit girdle and the beta axis indicating the fold axis of the Carassino-antiform (plunging 14° towards 066°) are shown. Lambert equal-area projection, lower hemisphere.*

the Adula nappe can also be partly explained by tectonic overpressure (Petrini and Podladchikov 2000; Mancktelow 2008; Vrijmoed et al. 2009; Pleuger and Podladchikov 2012; Schmalholz and Podladchikov 2013 and particularly Pleuger and Podladchikov; in prep.). It is beyond the purpose of the present paper to discuss in detail the effect of tectonic overpressure on the metamorphic conditions of the Adula nappe. However, for the proposed kinematic model (Fig. 16 and 17), depth values for the Adula nappe have been estimated using a lithostatic pressure gradient for the northern and central parts of the nappe. This approach is supported by the following arguments: 1) the metamorphic condition in the northern part of the Adula nappe is compatible with conditions estimated for the Simano nappe; 2) the measured metamorphic condition is the same in the competent eclogitic boudins and the less competent metapelitic matrix (e.g., Heinrich 1986; Meyre et al. 1999); 3) the P-T loop is consistent with subduction-related metamorphism and subsequent decompression to regional Barrovian metamorphism (Nagel 2008); 4) the increasing relative pressure estimates from N to S are compatible with the subduction of the Adula domain towards the S (Heinrich 1986; Dale and Holland 2003); and 5) the Ursprung phase suggests a first extrusion movement.

However, if depth values are simply estimated using a lithostatic gradient, the pressure estimates in the Adula imply an extremely thin and elongated initial geometry for the Adula nappe (see Nagel 2008). This leads to difficulties in the elaboration of a realistic model. In consequence, the high-pressure peak conditions for the northern and central part (e.g., Trescolmen) can correspond to the lithostatic pressure. The burial depth could have been ~45 km for the Vals area and ~80 km in Trescolmen (Fig. 16). The higher pressures established in the southern part of the Adula nappe could be influenced by tectonic overpressure as proposed by Schmalholz and Podladchikov (2013) and have been ignored in the model. An extrusion of less than 20 km accommodated by the first Ursprung phase has been assumed (estimation of the lithostatic pressure difference between peak pressure and the pressure of the onset of the Zapport phase).

A first stage of exhumation corresponding to rapid decompression has been demonstrated in the southern Adula (Hermann

et al. 2006). This exhumation occurred between a maximal age of ~38 Ma for the high-pressure event (Herwartz et al. 2011), ~35 Ma during the high temperature peak in Trescolmen (Liati et al. 2009) and ~ 1.0 GPa at 720°C in Monte Duria,

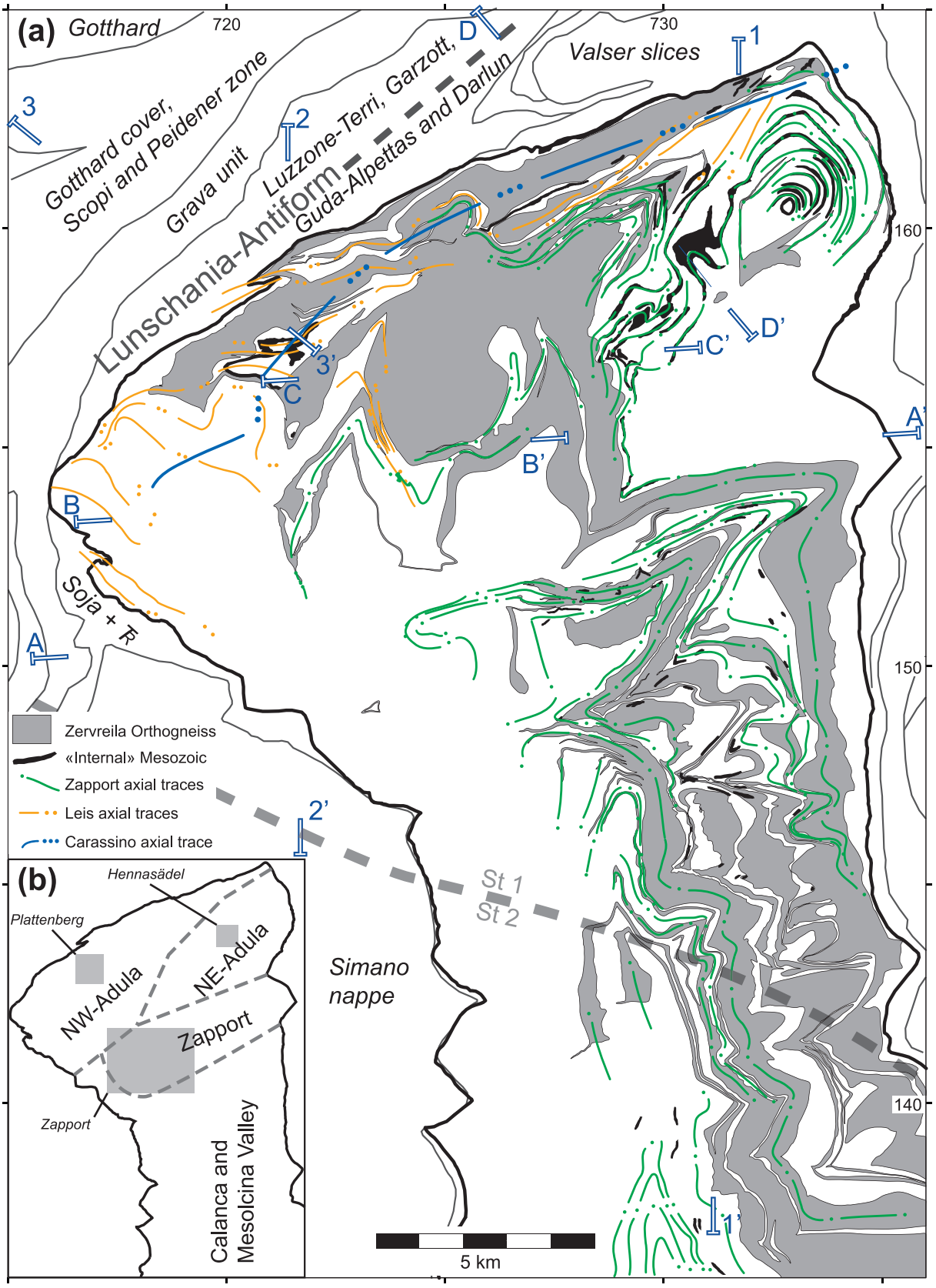

Fig. 14 a. *Axial traces of the principal folds. F_Z axial traces are not exhaustively represented. The coordinate system is the kilometric Swiss grid (CH 1903).* ***b.*** *Structural measurement subareas (Fig. 13). Grey rectangles indicate the position of the detail maps (Fig. 5, 8 and 12) with the respective names indicated in italics.*

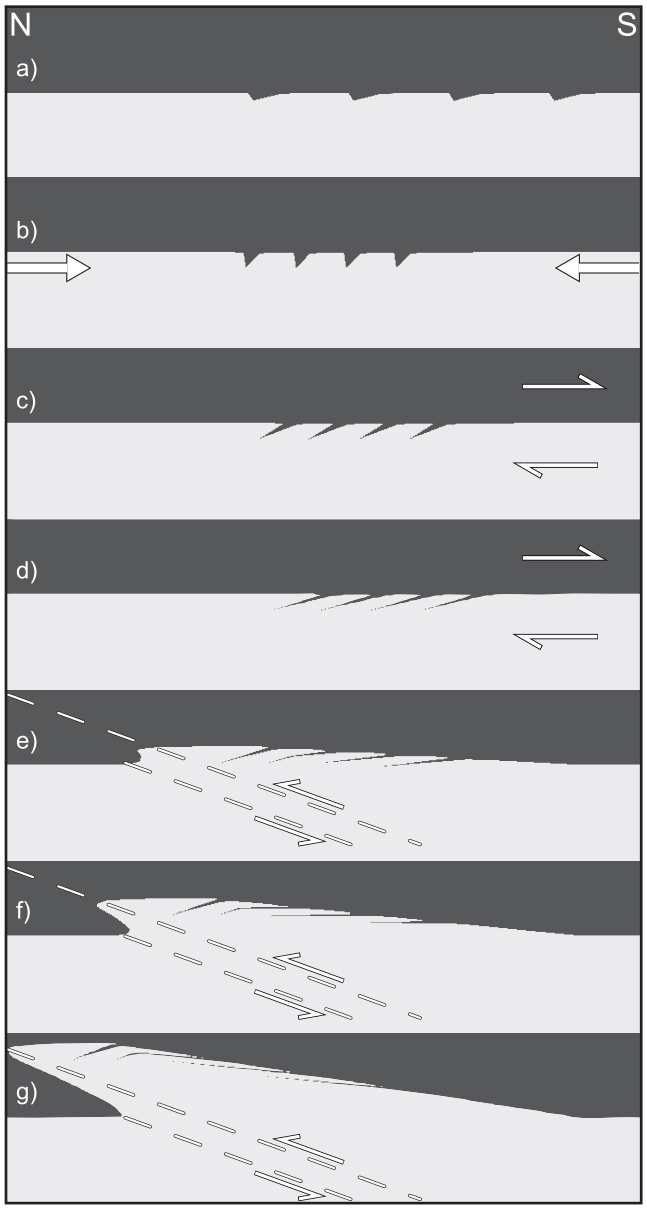

Fig. 15 *Kinematic 2D model developed with the Shear2F software (Rey 2002) to test the geometric and kinematic coherence of the suggested interpretations. The model highlights superimposed deformation of a domain consisting initially of two horizontal layers. The light grey layer represents basement and the dark grey domain sediments. The shear deformations represent the D_U (b, c and d) and D_Z (e, f and g) phases.* ***a.*** *Initial condition showing initial heterogeneities representing synsedimentary half-grabens.* ***b.*** *Horizontal pure-shear increases the relative depth of the half grabens (50% shortening).* ***c*** *and* ***d.*** *Top-to-the-south homogeneous simple shear generates oblique half-grabens (γ=3), .* ***e, f*** *and* ***g.*** *Top-to-the-north heterogeneous simple shear with 20° southwards dip generates a fold nappe.*

et al. 2006). This exhumation occurred between a maximal age of ~38 Ma for the high-pressure event (Herwartz et al. 2011), ~35 Ma during the high temperature peak in Trescolmen (Liati et al. 2009) and ~ 1.0 GPa at 720°C in Monte Duria, southern Adula (Hermann et al. 2006). In the Cima Lunga, zircon rims formed during decompression yielded ages of ~35 Ma (Gebauer 1995). Therefore, we suggest that the age of the extrusion recorded by the Ursprung phase postdate 38 Ma (Fig. 16a). Extrusion could be the result of a combination of pure and simple shear driven by buoyancy forces in a subduction channel (Fig. 16a and 17a), which is most likely caused by changes in the mechanism of the subduction zone because the light continental crust is subducted (beginning of the subduction of the European crust, Fig. 17a). The produced pure shear forces the Adula nappe extrusion (Fig. 17a). It would imply a channel flow-type extrusion, but precise mechanism is unknown and out of the scope of the present paper.

3.4.3. The Zapport phases – nappe placement

The Zapport deformation phase produces the most pervasive structures in the entire Adula nappe (see also Löw 1987; Nagel et al. 2002a; Nagel 2008). This phase represents the main schistosity that carries an N-S stretching lineation. The Zapport phase is associated with a top-to-N movement attested by widespread and clear shear sense indicators. The strong Zapport phase fabric obliterated practically all pre-existing structures (excepted locally where the Ursprung phase has been preserved).

Zapport phase folding is also widespread throughout the entire Adula nappe from the outcrop scale to the map scale. The axes of the folds of the Zapport phase are parallel to the stretching lineation (N-S to NE-SW), and the folds have a general W-NW vergence. The reorientation of the fold axes parallel to the stretching lineation is common in strongly deformed terrains (e.g., Escher and Watterson 1974). In the Central Alps, the vergence of these reoriented folds is always W-facing

(Steck 1989; Steck 2008). Detailed mapping in the Zapport Valley demonstrates the presence of large-scale W-vergent folds. The overall geometry exposed in the valley forms a fold-nappe. The frequent Zapport phase synclines cored by Mesozoic rocks at the northern part of the Adula nappe (e.g., Hennasädel and Plattenberg) suggest the closeness of a hypothetical Zapport nappe front. The Zapport deformation is less intense in this frontal part and is stronger in the upper part of the nappe. This deformation can be compared to a similar fold produced by heterogeneous simple shear (e.g., Fig. 15b). During the shearing of the upper part of the nappe, the relative position of the high-pressure metamorphic rocks is preserved. The front of the nappe with respect to the Zapport phase is masked by the superimposition of the Leis and Carassino phases.

The Zapport deformation phase is associated with retrograde metamorphic conditions; the peak condition of the Barrovian regional metamorphism (amphibolite facies in the south and greenschist facies in the northern part of the Adula nappe) postdates the Zapport phase (Meyre and Puschnig 1993; Partzsch 1998; Meyre et al. 1999; Nagel et al. 2002b; Cavargna-Sani 2008; Nagel 2008; Zulbati 2008). The Zapport phase postdates the high-pressure event of ~38 Ma (Herwartz et al. 2011) and most likely occurred during decompression approximately 35 Ma (Hermann et al. 2006; Gebauer 2005).

We interpret the Zapport deformation as the consequence of a simple shear-dominated N-directed displacement. This displacement is a continuation of the ductile N-directed exhumation revealed by the Ursprung phase without a kinematic break. The Zapport deformation kinematics are related to the general nappe emplacement in the Central Alps (Fig. 16c). The exceptionally strong Zapport phase shear fabric in the Adula nappe, with respect to the fabric in the adjacent nappes, is caused by its position in the Lepontine nappe stack, which is on top of the Lower Penninic basement nappes and under the North Penninic sediments. This deformation is stronger in the Zapport fold-nappe limbs, particularly in the upper part of the nappe. The Adula nappe acted as a major shear zone during the Penninic nappe emplacement.

3.4.4. Leis and Carassino – nappe front and post-nappe emplacement deformation

The younger Leis and Carassino deformation phases are mainly post-nappe emplacement deformations.

The Leis deformation phase is characterized by nappe-scale NW-vergent folds visible at the front of the nappe. In the central part of the nappe, the folds are smaller, restricted to the outcrop scale, N-vergent folds. This observation suggests an N-directed ductile shear in continuation with the Zapport phase. These folds are partially refolding the nappe limits, suggesting a post-nappe-stacking deformation, at least for the final steps of the Leis phase deformation.

The structure orientations (Fig. 2 and 13) clearly reveal a reorientation of the Zapport phase structural features in the northern part of the nappe. In the central part of the nappe, the stretching lineation directions and the fold axes related to the Zapport phase have a constant N-S orientation. The orientation of the structure becomes more variable going north, where they are scattered around an NE-SW orientation. This reorientation suggests a post-Zapport dextral ductile shear in the northern part of the nappe that turns the original Zapport features. This dextral shear is most likely related to the Leis deformation phase, given that the Leis phase fold axes are not reoriented.

The Carassino antiform is a NW-vergent nappe-scale fold in the frontal part of the Adula nappe and the nappes directly on top of it. This fold corresponds to the last N-directed ductile shear at the Adula nappe front. Deformations related to back-folding, such as the Claro and Cressim folds discussed later, are not observed in the northern Adula nappe.

The Claro and Cressim phases (Nagel et al. 2002a) are observed in the southern part of the Adula nappe and are also present in the Simano nappe. The Claro deformation phase is related to SW-facing folds with top-to-SE shearing. Nagel (2008) discusses the tectonic significance of this orogen-parallel shearing. The Claro phase is not directly related to any phase in the

northern Adula, but the Leis and Claro are most likely contemporaneous (Nagel et al. 2002a). These two folding phases are related to back-folding of the nappe pile in the Central Alps (Fig. 1c).

The Barrovian metamorphic conditions in the Adula nappe, the greenschist facies in the north and the amphibolite facies in the south (Fig. 14) were achieved by decompression from the high-pressure metamorphic peak without significant reheating (see the discussion of Nagel 2008). The Leis deformation phase predates the peak Barrovian event and is also associated with decompression (Löw 1987; Nagel et al. 2002a; Cavargna-Sani 2008; Nagel 2008). The Carassino deformation phase is not related to specific metamorphic conditions because no specific mineral growth is associated with it.

The age of the Leis deformation postdates the major decompression events at ~32 Ma (Hermann et al. 2006;Liati et al. 2009) and predate the backfolding event occurring in the southern Adula (the Novate granite postdates the backfolding at ~25 Ma, (Liati et al. 2000)). The Carassino antiform is younger than the Leis deformations; however, a more precise age cannot be suggested.

3.4.5. The Internal Mesozoic

The Internal Mesozoic is one of the major peculiarities of the Adula nappe. The kinematics interpretation proposed here provides an explanation for the occurrence of this feature.

The occurrence of the Internal Mesozoic is not randomly scattered within the nappe but is concentrated and aligned on specific planes as boudin trails in the upper part of the northern and central Adula nappe. These trails form the deformed core of the Ursprung phase syncline, strongly stretched by the later Zapport phases. They also exist in well-defined cover sequences preserved in synclinal F_Z fold hinges in the frontal part of the nappe (e.g., Hennasädel and Plattenberg). In this case, the Mesozoic cover forms the core of Zapport 1 synclines, which is well preserved in the hinges of the Zapport 2 fold. Outside the hinge areas, the Internal Mesozoic is strongly stretched and deformed.

The outcrop of the Hennasädel exposes a locally interesting tectonic basement-cover contact (see Chapter 3.3). This tectonic contact is not easily explained by a simple thrust on the top of a coherent stratigraphy and the hinge of the F_{Z1} fold. Therefore, we suggest that the position of the contact could be inherited from syn-rift structures. Other examples in the Alps have indicated that this type of syn-rift normal fault is not reactivated during the Alpine orogeny, and these pre-existing heterogeneities localize the Alpine deformation where the basement-cover contact is strongly pre-structured (Krayenbuhl and Steck 2009; Bellahsen et al. 2012). We therefore suggest that the tectonic contact on the top of the Hennasädel Mesozoic could represent a refolded pre-Alpine structure rather than a late Alpine thrust. Synsedimentary structures of this type have most likely also played a major role in the inclusion of pieces of the autochthonous cover series in the Adula basement.

3.4.6. The structures of the Adula nappe in a regional context

The paleotectonic setting and the tectono-metamorphic history of the nappes surrounding the Adula nappe are key elements that must be integrated into the kinematics of the Adula nappe in the context of the Central Alps.

We suggest that the Ursprung phase play a significant role on a regional scale because it accommodates an extrusion of the Adula nappe (Fig. 17). However, the extrusion is relative to the nappes located on the Adula nappe. With respect to the Simano nappe, the extrusion of the Adula nappe cannot be distinguished from a conventional nappe emplacement (Fig. 17). The stratigraphy of the Triassic rocks (Galster et al. 2012) confirms the vicinity of the Adula and Simano domains during the Mesozoic. Furthermore, the peak pressure metamorphic conditions of the northern Adula nappe are compatible with the peak

pressures estimated in the Simano nappe (1.0-1.2 GPa, Rütti 2003). There is no need to suggest a missing paleogeographic domain, subducted between Adula and Simano (as proposed in some kinematic models; Schmid et al. 1996; Scheiber et al. 2012). We therefore interpret the limit between the Adula and Simano nappes as formed by a narrow syncline produced during the Adula nappe emplacement on top of the Simano nappe. This emplacement requires relative top-to-N movement. Consequently, the top-to-S Ursprung deformation has significance only in the upper part of the Adula nappe (Fig. 17).

The Zapport deformation phase, relative to the nappe emplacement, can be correlated to phases with the same kinematics outside the Adula nappe (e.g., the D2 or Ferrera phase of Milnes and Schmutz 1978; Schmid et al. 1997; Wiederkehr et al. 2008), although there is no known Zapport structure crossing the nappe boundaries.

The units composing the Internal Klippen belt and the Valser slices are important for understanding the regional geology. These units are rooted south of the Adula, but due to the lower peak pressure of metamorphism, they were not subjected to deep subduction. The current position with respect to the Adula nappe is most likely pre-Zapport as these units can be found below the Adula nappe. We suggest that these units were detached from a substratum situated south of the Adula nappe, thereby allowing them to escape subduction. During the nappe emplacement, they would have been pushed by the massive Adula nappe and partially overridden by it.

The Leis phase can be correlated to the structure forming the Lunschiania antiform (D3 or Domleschg phase; Schmid et al. 1997). The significant Lunschania antiform is likely formed during the Adula N-directed movement. The Internal Klippen belt tectonic units are only partially refolded with the Adula nappe by the Leiss phase. This fact suggests that the relative movement between the Adula nappe and the Internal Klippen belt stops during this deformation phase. The Carassino fold also affects the units at the top of the Adula nappe. However, this fold cannot be correlated to other structures at a regional scale. In the southern Adula, the post-Zapport deformation is clearly post-nappe emplacement as it refolds the complete nappe stack (Nagel et al. 2002a).

3.4.7. Subduction of the Adula nappe

The regional context of the Adula nappe leads to one important question: why are higher metamorphic pressures found in the Adula nappe and not in units closer to the southern end of the European (s.l.) slab? In other words, the Briançonnais terrains and all of the other North Penninic units located south of the Adula paleogeographic domain would have been expected to be driven deeper in the subduction.

Some authors explain this contradiction through the presence of two subduction zones, one in the North Penninic domain and one in the Liguro-Piemont Ocean (Frisch 1979; Frisch 1981; Froitzheim et al. 2003; Berger and Bousquet 2008). The classic kinematic reconstruction proposed in the NFP-20-East cross-section (Schmid et al. 1996) and in numerous recent publications (e.g., Handy et al. 2010; Scheiber et al. 2012) postulate a single subduction zone. Nagel (2008) reports the controversy between one or two subduction zones as a major open question regarding the kinematics of the Central Alps.

The Middle Penninic and Mesolcina zone nappes (on the top of the Adula nappe) are affected by structures supporting an emplacement by narrow basal shear zones and accretion in the orogenic prism (Schmid et al. 1997; Schreurs 1993; Mayerat Demarne 1994; Scheiber et al. 2012). The deformation mechanism in the Lower Penninic basement nappes (included the Adula nappe) points to the formation of fold-nappes (Argand 1916; Steck 1990; Escher et al. 1993; Schmid et al. 1997; Rütti 2003; Steck 2008), which suggests that the Middle Penninic nappes (Suretta, Tambo and Schams), the North Penninic sediments and the units forming the Internal Klippen belt are detached from their substratum and accreted in the accretion prism due to narrow basal shear zones. This early detachment prevented deeper subduction. These observations illustrate

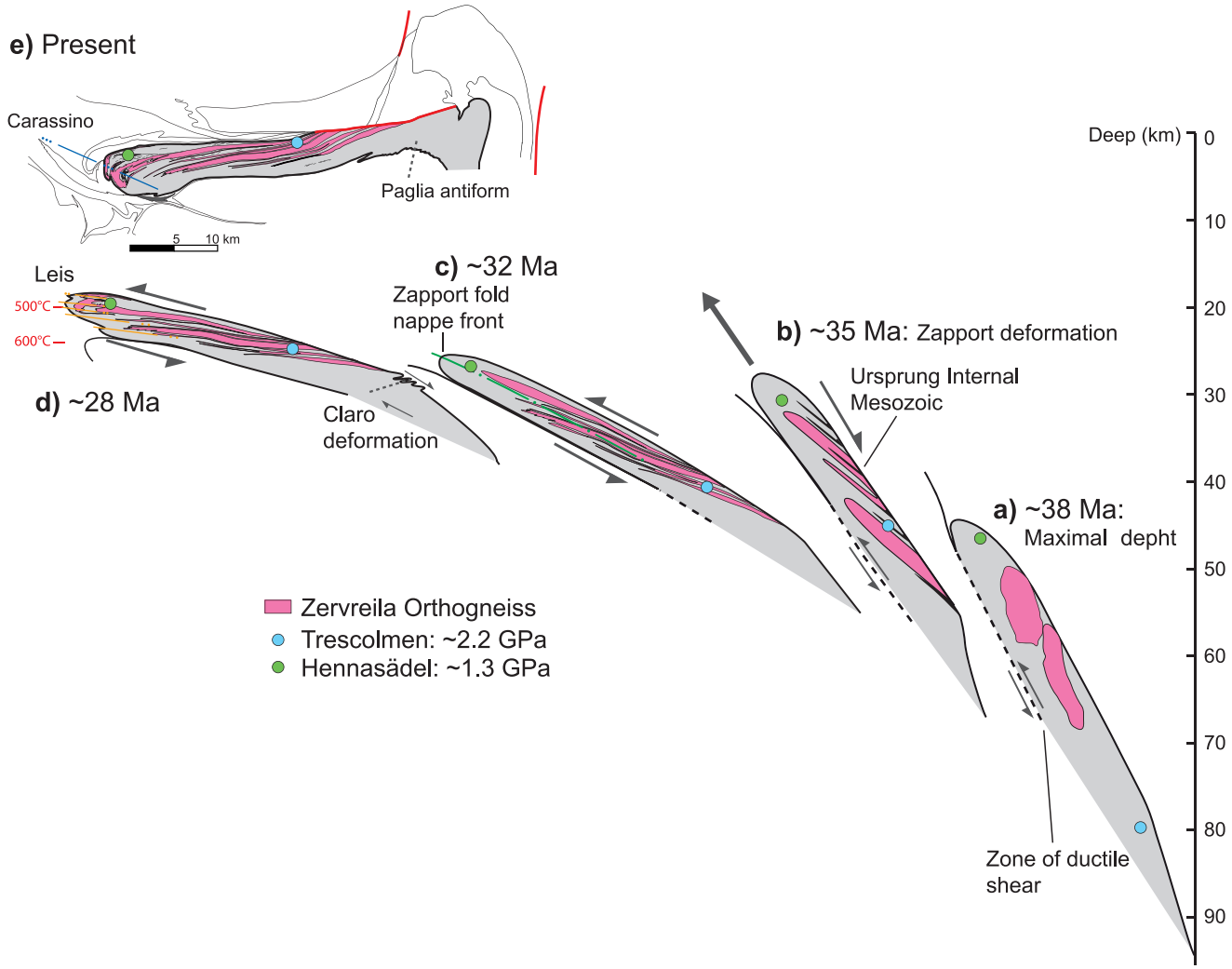

Fig. 16 *Kinematic model of the Adula nappe deformation phases.* ***a.*** *~38 Ma. Maximal burial depth of the Adula nappe based on the assumption that the peak pressure is the lithostatic pressure (~1.3 GPa in Hennasädel Dale and Holland 2003; Löw 1987), 2.0-2.5 GPa in Trescolmen (Dale and Holland 2003; Meyre et al. 1999).* ***b.*** *~35 Ma. Ursprung deformation phase: extrusion with top-to-S shearing at the top of the nappe.* ***c.*** *~32 Ma. Zapport deformation phase: intense folding (fontal part as a fold-nappe) and intense top-to-N shearing.* ***d.*** *~28 Ma. Post-nappe emplacement deformation. Leis deformation phase in the north and central Adula nappe: nappe-scale folds of the nappe front, N-vergent outcrop-scale folds in the northern and central nappe, N-directed shearing. The Claro deformation phase in the southern Adula and Simano nappes, roughly contemporaneous with the Leis phase corresponding to localized S-verging nappe-scale folds and S-directed shearing.* ***e.*** *Present day. See also Fig. 1c. Conditions after the last Carassino deformation phase in the front of the nappe and back-folding of the southern Adula nappe.*

the following two different types of Alpine nappes as suggested by Escher et al. (1993), which can also be applied to the classic Central Alps section (Schmid et al. 1996): 1) detachment and accretion in the subduction prism of the thrust-nappe; 2) ductile deformation at the nappe scale leading to fold-nappes. In a subduction zone, we can imagine the detachment of several “superficial” units while the rest of the slab continues its subduction until it is deep and warm enough to form a fold. In this scenario, a second subduction zone for the Lower Penninics is unnecessary. The first continental crust to undergo ductile deformation, without basal detachment, is the Adula nappe (Fig. 17). The detachment and subsequent basal accretion of the Briançonnais units would have been driven by inherited rift structures. Manatschal et al. (2006) suggested that at least a part of the Eastern Briançonnais domain was an extensional allochthon. For the units located south of the Adula domain, Galster et al. (2012) illustrated the strong inheritance of the Jurassic synsedimentary rift-related structures.

The paleogeographic position of the Adula nappe is certainly of prime importance. The Adula domain was at the leading

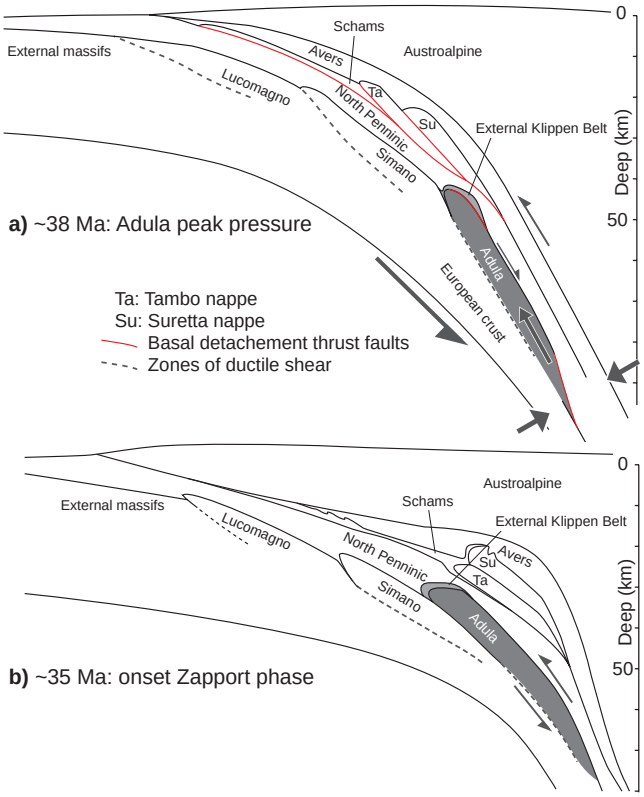

Fig. 17 *Kinematic evolution of the Eastern Central Alps representing the extrusion of the Adula nappe (modified after Schmid et al. 1996, Scheiber et al. 2012).*

edge of the European continental crust just before the hyper-extended margin and the North Penninic Ocean. It was also involved in the rift-related crustal thinning. The more "oceanic" units (sensu Manatschal 2006) detached and were incorporated in the nappe stack by basal accretion. The Adula nappe was driven more deeply into the subduction zone until it was warm enough to undergo ductile deformation. It was then extruded and continued its emplacement by forming a fold-nappe on top of the other European crust-derived nappes (Fig. 17).

3.5. Conclusions

The northern Adula nappe has experienced a complex deformation history with several deformation phases. Before the Alpine collision, the part of the continental crust that is now forming the Adula nappe was subject to extension structures during Jurassic rifting. This pre-structuring partially affected the Alpine structures. The coherency of the cover and basement stratigraphy excludes the formation of the nappe by a tectonic mélange. The early *Ursprung* ductile deformation phase is characterized by schistosity, folds compatible with a top-to-S shearing and is restricted to the upper part of the nappe. The first Internal Mesozoic formation in the upper part of the nappe is related to folding of the Ursprung phase. This deformation is related to N-directed exhumation from peak pressures at 38-35 Ma with less than 20 km of extrusion. The *Zapport* phase produces the main structural features of the nappe with isoclinal folding, the main schistosity and a N-directed shear. This phase forms folds at the front of the nappe, as revealed by complex synclines folding the sedimentary cover. This phase is also responsible for the nappe emplacement in the Lower Penninic nappe stack during decompression and before the peak temperature of the regional metamorphism in the Lepontine dome. During the nappe emplacement, the Adula nappe acts as a major shear zone for the emplacement of the Lower Penninic sediments and the Middle Penninic nappes on top of the other Lower Penninic basement nappes. This explains why it is so complexly and intensively deformed. The *Leis* phase produces nappe-scale folds in the frontal part of the Adula nappe and is associated with a general top-to-N shearing. The Leis phase can be regionally associated with one of the most important post nappe-fold structures north of the Adula nappe, the Lunschania antiform. The *Carassino* antiform is a late N-vergent post-nappe fold in the northern Adula nappe and in the units on top of it.

In the eastern transect of the Central Alps, the Adula nappe and the nappe derived from paleogeographic domains south of the Adula domain (hyper-extended margin) are mostly emplaced by detachment and basal accretion in the Alpine accretionary prism. In contrast, the Adula nappe and the other nappes located northward in the paleogeography are derived from a coherent European slab and form a fold nappe. The specific paleogeographic position of the Adula domain at the leading edge of a coherent European slab explains why this unit was subducted deeper than the others. This is the main reason for the presence of a high-pressure metamorphism in the Adula and the absence of such metamorphism in the Middle Penninic Tambo and Suretta nappes.

ACKNOWLEDGEMENTS

This study is supported by the Swiss National Science Foundation, grant no. 200021_132460 and the Société Académique Vaudoise. We would like to thank L. Nicod for thin sections preparation. We thank S. Schmalholz for discussions and comments and D. Schreich and A. Pantet for support in the field. We are grateful to the Museo Cantonale di Storia Naturale for authorization to collect samples in Ticino.

4. Stratigraphy of the Mesozoic sedimentary cover of the northern Adula nappe, Central Alps

Mattia Cavargna-Sani, Jean-Luc Epard, Federico Galster, Henri Masson

Submitted to: Swiss Journal of Geosciences

ABSTRACT

New stratigraphic data of the autochthonous metamorphic sedimentary cover of the Adula nappe (Central Alps) are presented. The Adula cover reveals an identifiable sedimentary sequence containing several stratigraphic groups. The Triassic stratigraphy is characterized by a North Penninic Triassic. It marks the transition between the Helvetic and the Briançonnais Triassic types. The Middle Jurassic is characterized by an emersion. This emersion, and the consequent erosion, is probably the cause of the absence of Lower and Middle Jurassic sediments. The late Middle Jurassic and the Upper Jurassic marks a transgression and a drowning phase. Following this drowning, the sedimentation in the Adula sedimentary cover consists of a pure limestone, comparable to the Upper Jurassic limestone of the Helvetic and Subbriançonnais domains. A detrital series overlies a pronounced unconformity. This detrital series can be compared to a flysch s.l. Its age is probably late Upper Cretaceous to Palaeogene.

The stratigraphic content of the Adula cover reveals a consistent and characteristic paleogeographic domain on the northern border of the North Penninic basin. This stratigraphic domain can be compared with those of the Monte Leone, Pizzo del Vallone and Teggiolo nappes.

The study of the cover also helps to decipher the Alpine structures of the Adula nappe. It points to the conclusion that the Adula is mainly a coherent nappe and that the sedimentary relicts preserved inside the nappe (Internal Mesozoic) represent the hinges of early synclines and not the trace of thrusts.

4.1. Introduction

The importance of stratigraphy to studying the geological history of mountain belts has been well established (Trümpy 1970). The stratigraphic investigation of the sedimentary cover series in the Lepontine Dome runs into major difficulties because of the strong deformation, metamorphism and the lack of fossils. However, as recently demonstrated, stratigraphic investigations are also possible in the Lepontine nappes and can lead to noteworthy results (e.g., Bianconi 1965; Bianconi 1971; Carrupt 2003; Cavargna-Sani et al. 2010; Galster et al. 2010; Matasci et al. 2011; Galster et al. 2012).

This contribution aims to give an overview of the stratigraphy of the Mesozoic (-Tertiary?) sedimentary cover of the northern Adula nappe. The Adula nappe mainly comprises Palaeozoic basement rocks, however, as previously noted by Heim (1891), this basement encloses many bodies of Mesozoic (-Tertiary?) rocks called "Internal Mesozoic," which are the topics of the present study.

The stratigraphic framework is established by classical lithological criteria. The stratigraphic sections are compared to well-known, less metamorphic sections from similar paleogeographic Alpine domains to propose an age and a tectonostratigraphic interpretation.

The stratigraphy of the Adula cover was the topic of a few recent papers (Cavargna-Sani et al. 2010; Galster et al. 2012 as Chapter 5 of this thesis). This contribution presents new data providing a sedimentologic and stratigraphic interpretation of the northern Adula Mesozoic (-Tertiary?) rocks.

4.2. Regional setting

The Adula nappe is located in the eastern part of the Lepontine Dome and is one of the uppermost crystalline nappes of the Lower Penninic (Fig. 1a). It overlies the Simano nappe. At the front of the Adula and confined to the north-west by the Gotthard crystalline massif, there are several nappes and slices composed mainly of Mesozoic sediments (Fig. 1a and b). These units are folded around the front of the Adula nappe and presently occupy a lower position, but their Triassic stratigraphy implies that they must be rooted between the Adula and Tambo nappes (Voll 1976; Probst 1980; Galster et al. 2012). Because of this peculiar tectonic position, Galster et al. (2012) named this group of units the "Internal Klippen Belt". On the top of the Adula nappe, a group of units mainly made of Mesozoic (and Tertiary) sediments is exposed in the Mesolcina (Misox) zone (Fig. 1a): the Valser slices, the Aul nappe, the Grava nappe and the Tomül nappe (Gansser 1937; Steinmann 1994). They belong to the Lower Penninics. The Mesolcina zone is overlain by the Middle Penninic Tambo and Suretta nappes.

The following paragraph summarises the stratigraphy of the units surrounding the Adula nappe (Fig. 1a and b).

On the Gotthard massif and its Triassic autochthonous cover, the Scopi zone and the Peidener slices comprise Lower and Middle Jurassic Helvetic type rocks (Baumer et al. 1961). The Lucomagno and the Simano nappes are characterised by the first appearance of the Dolomie Bicolori ("Dolomia grigia listata con bianca" containing Ladinian crinoids; Bianconi 1971). Galster et al. (2012) introduced the concept of "North Penninic Triassic". This Triassic facies represents the transition between the Helvetic and the Briançonnais Triassic domains. It is characterised by the Ladinian Dolomie Bicolori, white-grey banded dolomites. The Leventina and Lucomagno nappes are also part of the northern border of the North Penninic Triassic domain. The Adula Triassic stratigraphic sequence is also the North Penninic Triassic type facies (Cavargna-Sani et al. 2010; Galster et al. 2012) and will be described in detail in the present paper. The Triassic stratigraphy of the Soja nappe, with the typical Dolomie Bicolori, is similar to that of the Adula nappe (Galster et al. 2012). The Lower and the Upper Valser slices (Valser Mélange following Steinmann 1994) are comprised of various rock types: gneisses, dolomitic marbles,

calcareous marbles, metabasalts (Jurassic?) and calcschists (Wyss and Isler 2007). The Triassic stratigraphy of the Valser slices is different from the Adula nappe (Galster et al. 2012). This demonstrates that the Valser slices have an independent origin and are not in the décollement zone from the external part of the Adula nappe. The Garzott slices contain Triassic rocks of a more external domain with respect to the Luzzone-Terri nappe but still with Briançonnais characteristics. The Jurassic (and younger?) rocks are interpreted as supra-detachment basin sediments (Galster et al. 2012). The stratigraphy of the Luzzone-Terri nappe reveals a Briançonnais Triassic superposed by a Liassic sequence of Helvetic type (Galster et al. 2010). It is a unique case in the Alps and a demonstration of the continuity between the Briançonnais and Helvetic domains during Triassic and Liassic times. The Darlun zone contains several tectonic slices. Its stratigraphy is similar to that of the Luzzone-Terri Liassic. The Güida and Alpettas zones contain Jurassic series and lacunar Triassic sediments. Their homeland is at the southern border of the Liassic Helvetic basin, south of the Luzzone-Terri domain (Galster et al. 2012).

The stratigraphy of all these nappes and tectonic units demonstrates a continuous transition from the Helvetic to Briançonnais Triassic facies (Galster et al. 2010; Galster et al. 2012).

The units of the Mesolcina zone have their homeland in the Jurassic – Cretaceous North Penninic basin (Steinmann 1994). The Aul nappe is formed principally by Jurassic quartz-rich calci-turbidites (Kupferschmid 1977; Steinmann 1994). The Tomül and Grava nappes mainly comprise Cretaceous calcschists (Bündnerschiefer). Each of these nappes contains a basal zone of slices with dismembered Triassic carbonate rocks, Jurassic calcschists and metabasites (Gansser 1937; Steinmann 1994) dated at approximately 160 Ma (U/Pb zircon age; Liati et al. 2005).

The Middle Penninic Tambo and Suretta nappes and the Schams nappes have a classical Briançonnais stratigraphy (Baudin et al. 1995; Rück 1995).

The internal structure of the northern Adula nappe (Fig. 1b) results from several deformation phases (Löw 1987, Cavargna-Sani et al. submitted, Chapter 3). The first phases, the Ursprung and the Zapport deformation phases, are responsible for the extrusion and emplacement of the nappe. They generate the strong deformation observed in the entire Adula nappe (Cavargna-Sani et al. submitted, Chapter 3). The Internal Mesozoic outcrops are principally found in deep synclines within the basement formed during these two deformation phases. The younger Leis and the Carassino deformation phases form large scale folds in the front of the nappe (Löw 1987; Cavargna-Sani et al. submitted, Chapter 3) and are post-nappe emplacement structures.

The Adula basement is composed of several Paleozoic formations defined by Cavargna-Sani et al. (in press, Chapter 2). Cambrian sediments containing a few magmatic bodies and a significant amount of carbonates are defined as the Salahorn Fm. These carbonates are often indicated on the map of Jenny et al. (1923) and should not be mistaken for the Internal Mesozoic. The Trescolmen Fm. is composed by meta-argillite with oceanic magmatic blocks related to a subduction zone environment (the age of this chaotic formation has a minimal age given by its metamorphic age of 370 Ma). The Garenstock Augengneiss and the Rossa Orthogneiss are Ordovician granites (both dated at ~450 Ma). The Heinisch Stafel Fm. is comprised of Ordovician volcanoclastic sediments. The entire basement was structured by the Variscan orogeny before the intrusion of the Permian Zervreila granite (~292 Ma) (Fig. 1a).

The northern Adula nappe experienced eclogitic metamorphic conditions. It is important to note that remarkably fresh eclogites have been described at the top of the Hennasädel section described below. The Alpine high-pressure peak conditions in the northern Adula nappe (Vals region) are 1.2-1.9 GPa 450-600°C (Heinrich 1986; Löw 1987; Dale and Holland 2003; Zulbati 2008; Zulbati 2010). The subduction related metamorphic conditions increase towards the south of the nappe. Radiometric ages in the Central Adula nappe reveal two ages (Carboniferous and Eocene) of high-pressure related metamorphism in the basement (Liati et al. 2009; Herwartz et al. 2011).

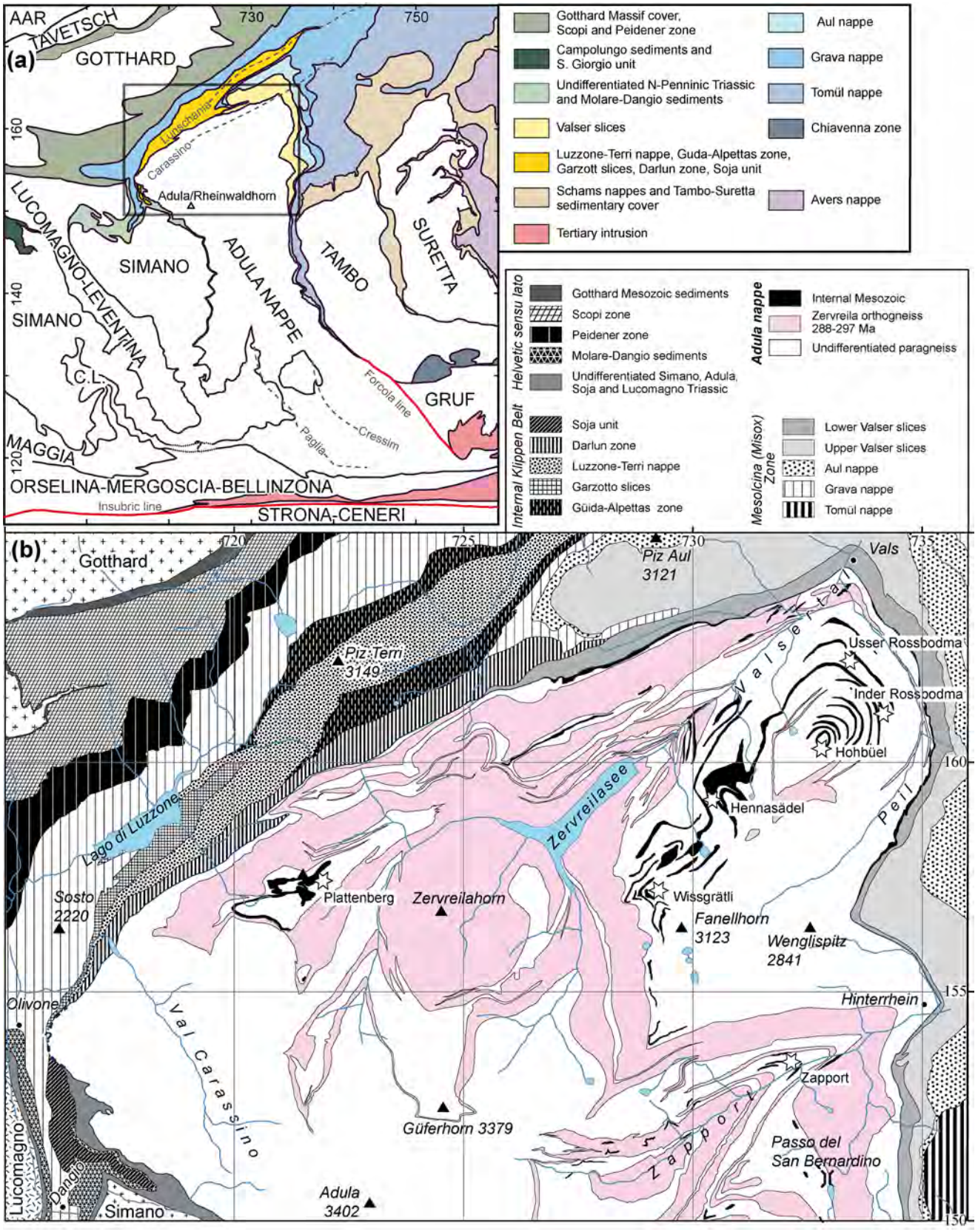

Fig. 1 a *Tectonic map of the eastern Lepontine Alps. Basement is left in white. Modified after Spicher (1980), Berger & Mercolli (2006), Steck (2008), and Galster et al. (2012). The limit of Figure 1b is indicated.* ***b.*** *The geologic map of the northern Adula nappe (studied area). Modified after Jenny et al. (1923), Künding (1926), Van der Plas (1959), Egli (1966), Frey (1967), Pleuger et al. (2003), Arnold et al. (2007), Galster (2010), and Cavargna-Sani et al. (submitted). The coordinates correspond to the kilometric Swiss grid (CH 1903).*

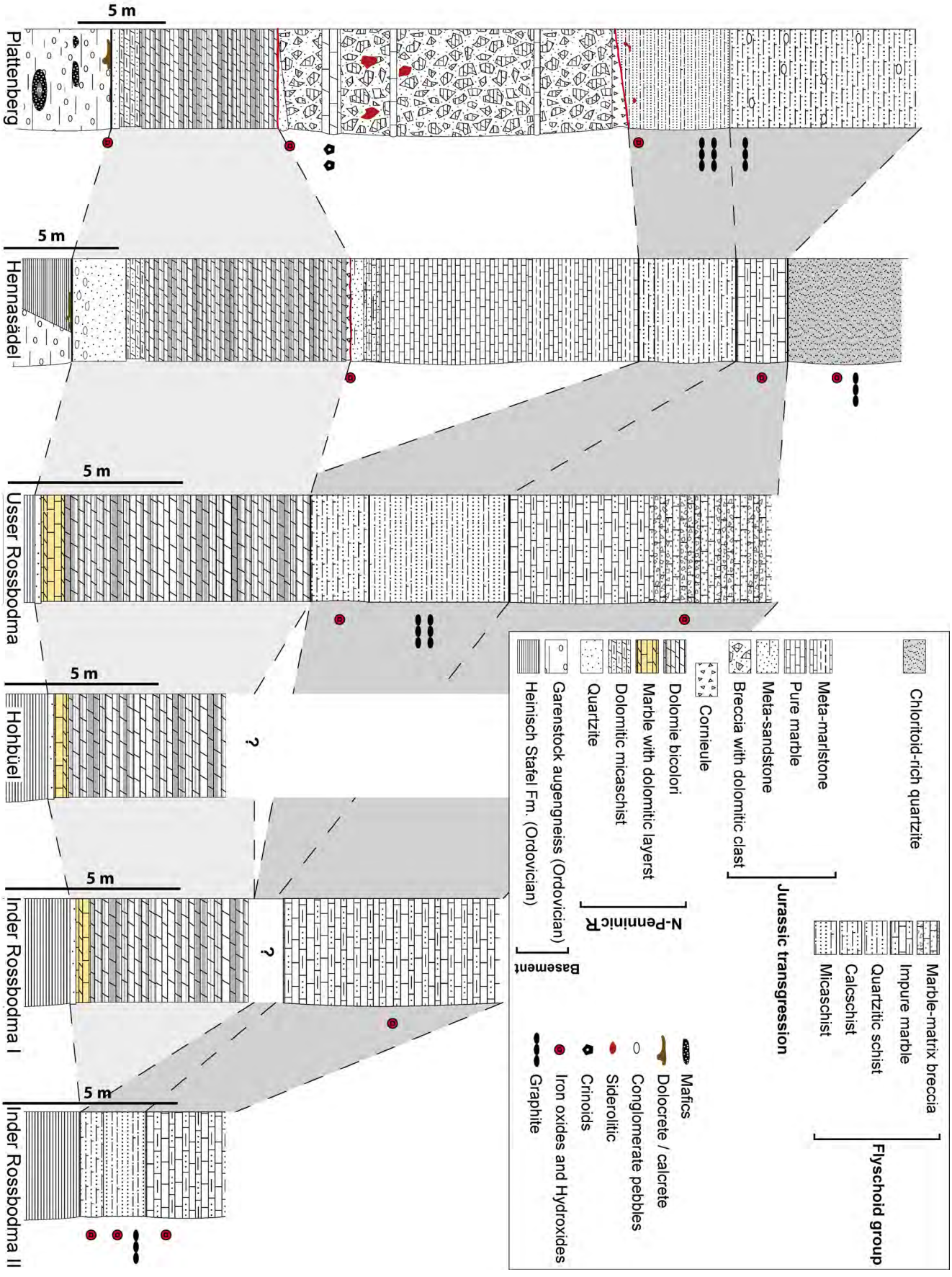

Fig. 2 *Synthetic stratigraphic sections of the studied localities. The position of the localities are given in Figure 1.*

4.3. Sedimentary cover outcrops of the northern Adula nappe

4.3.1. Introduction

In the following chapters, each different outcrop that was used for the stratigraphic correlations is described in detail. It is necessary because of the structural complexity preventing cartographic connections between outcrops of the sedimentary series. Additionally, the stratigraphic content of the described sections are significantly different and cannot be summarised in one synthetic stratigraphic column.

In each section we recognise lithological groups that reveal distinct sedimentary cycles separated by stratigraphic gaps (Fig. 2). We use the names and ages introduced by Cavargna-Sani et al. (2010) and Galster et al. (2012), and we will complete them with new names when necessary.

The strong deformation in the Adula nappe requires a precise structural analysis for each section (see Cavargna-Sani et al. submitted; Chapter 3). Stratigraphic correlations are proposed only if the structure is reasonably well understood, if the series are coherent and if the contact on the basement is stratigraphic. The strong strain in the Adula nappe tends to parallelise the contacts between formations, but this parallelisation is not an obstacle to identifying stratigraphic contacts. Reliable criteria are the pre-Triassic weathering of the basement, transgressive facies of the basal sediments and the coherence of the succession. The original thickness of the bedding is obviously not preserved and cannot be used for correlations.

4.3.2. Plattenberg

The Plattenberg (Fig. 1b; Fig. 2) Internal Mesozoic has previously been described by Cavargna-Sani et al. (2010); the main results are summarised and new observations are added. The entire outcrop is a complex interference pattern of a Zapport phase syncline refolded by Leis phase folds (Cavargna-Sani et al. submitted, Chapter 3). The basement is formed by the Ordovician Garenstock augengneiss. This gneiss is locally weathered below the contact with the cover, and locally, lenses of paleosol can be observed as calcrete and dolocrete. A white-grey quartzite of 30 cm maximum thickness (Fig. 3a) is in sharp contact with the gneiss. The base of the quartzite is essentially a pure quartzite with a few feldspars, white mica and oxide grains. The quartzite is followed by yellow dolo-schist that passes into a pure yellow dolomite. The dolomite turns into Dolomie Bicolori after a few meters. This sequence represents the first sedimentary cycle of Triassic age (Cavargna-Sani et al. 2010; Galster et al. 2012).

The Plattenberg Breccia overlies the dolomites with a sharp contact (beginning of the second sedimentary cycle). At its base, a dm-thick quartzite is often present. The composition of this quartzite is variable and spans from pure quartzite to dolo-quartzite with abundant oxides. The Plattenberg Breccia mainly comprises dolomitic fragments, locally in a quartzitic matrix. The dolomitic breccia can easily be confused with a true Triassic dolomite. The breccia also contains some dolarenitic or calcarenitic intercalations locally with well-preserved crinoid fossils (Fig. 3d and 4b). A few pebbles in the breccia are composed principally of spheroidal hematite concretions and also contain some magnetite, limonite and porphyroblasts of white mica and kyanite (Fig. 4b). We interpret these pebbles as fragments of siderolitic deposits formed in sub-aerial weathering processes. These siderolitic pebbles indicate the erosion and later sedimentation in the breccia of rocks formed during an emersion phase. This second sedimentary cycle is transgressive on an eroded paleo-surface. The sedimentation of the breccia follows a drowning phase in marine conditions as shown by the presence of crinoids in the sediments. The age of the breccia age is supposed to be (late?) Middle Jurassic (Cavargna-Sani et al. 2010; Galster et al. 2012).

The breccias are always overlain by a layer of cornieule. Cornieule results from hydraulic fracturing of dolomite and can

also be injected into discontinuities (Masson 1972; Milovsky et al. 2003). In this case the cornieule may result from a transformation of the underlying dolomitic breccia or by injection of cornieules formed at the expense of Triassic dolomites. These cornieules contain many metamorphic micas suggesting a pre-metamorphic formation of this rock. The cornieule also may be interpreted as indicating a thrust plane prior to the main deformation phases and metamorphism.

On the top of the cornieule is a formation of micaschist and calcschist (third sedimentary cycle). The micaschist contains a significant amount of porphyroblasts of garnet, chloritoid and kyanite that are typical of Al-rich metapelites. The base of the micaschist is enriched in Fe-oxides and hydroxides (such as hematite, ilmenite, and limonite) and brown carbonate forming brown-reddish nodules. With the exception of the brown carbonates in the nodules, the micaschist is generally poor in carbonates. The Fe-oxides and hydroxides are no longer present above a few meters from the base where the micaschist becomes rich in graphite. The graphite-rich micaschists develop upwards into layered calcshist and pelitic marbles. The calcschist also contains graphite at the base. The presence of pebbles of pure limestone scattered in the calcschist has to be noted.

4.3.3. Hennasädel

The lower part of the section of the Hennasädel (Swiss coordinates: 730700/159299; Fig. 1 b and 2) Internal Mesozoic outcrop is partially described in Galster et al. (2012). The Hennasädel Internal Mesozoic outcrop is preserved in the core of Zapport phase syncline hinges, forming an interference pattern (Cavargna-Sani et al. in press; Chapter 3). The Heinisch Stafel Fm. and the Garenstock Augengneiss form the basement under the Mesozoic cover. Lenses and nodules of calcrete and dolocrete can be locally observed at the contact between the basement and the cover.

The Mesozoic cover starts with a white-grey quartzite. Its base has a sharp contact with the basement and is locally conglomeratic. The quartzite is rather impure, and the content in phyllosilicates, feldspars, and carbonates increases upwards. The overlaying rock is a yellow-brown dolomitic micaschist. This dolomitic micaschist passes into a yellow impure dolomite. It is overlain by a thick series of Dolomie Bicolori. The top of the dolomites is sometimes brecciated into a cornieule that displays strong axial plane schistosity. This sequence represents the first sedimentary cycle; its age is clearly Triassic.

The Triassic series is directly followed with a sharp contact by a ~50 cm meta-sandstone bed (Fig. 3b). This bed marks the onset of the second sedimentary cycle. The base of the meta-sandstone bed comprises mainly quartz with a variable amount of white mica, spheroidal hematite, pyrite and detrital carbonates. A few pluri-millimetric chloritoid and kyanite porphyroblasts can be observed. The bed shows a gradual enrichment in carbonates and disappearance of Fe-oxides and pyrites. This meta-sandstone corresponds to a sedimentary transgression and the start of the second sedimentary cycle. The meta-sandstone bed turns into quartzitic banded marble (Fig. 3b). This impure marble transitions into a pure marble (Fig. 3b) in which the weathered surface appears slightly banded. A banded formation comprising an alternation of calcschist and marble overlay the pure marble formation (Fig. 3b). The calcschist layers contain calcite, quartz with micas, a few coarse crystals of apatite and porphyroblasts of garnet, chloritoid and plagioclase.

The third sedimentary cycle starts with ~50 cm of calcschist above a sharp contact (Fig. 3b). This calcschist is overlain by a ~1.5 m thick massive bed of quartzitic micaschist. It principally comprises quartz, white mica, and plagioclase, with less than 5% carbonate. The top of the bed is richer in carbonate nodules and transitions into a micaschist. A sharp contact marks the start of ~4 m of impure banded marble. The detrital horizons principally comprise grains of quartz and white mica.

On the top of the banded marble there is a massive level comprising a peculiar dark chloritoid-rich quartzite formation. This formation looks heterogeneous but is characterised by the abundance of quartz and aluminium-rich silicate porphyroblasts

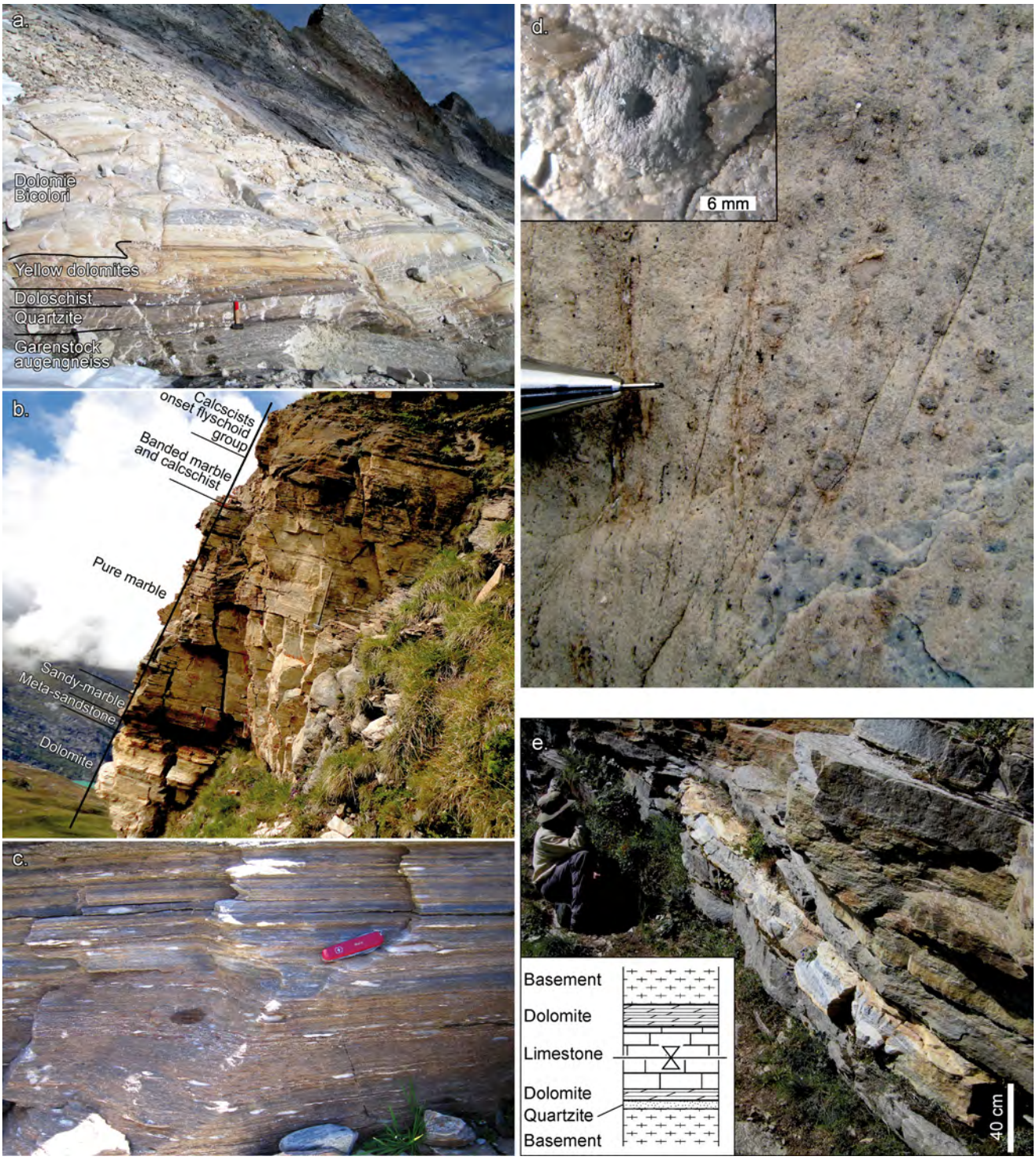

Fig. 3 *Pictures of the sedimentary cover of the Adula nappe.* ***a.*** *Triassic stratigraphic section of the Plattenberg on the Garenstock augengneiss.* ***b.*** *Triassic and Jurassic cycle of the Hennasädel.* ***c.*** *Metamorphic calcareous matrix-supported breccia, flyschoid group, Usser Rossbodma.* ***d.*** *Crinoids calco-dolarenite intercalation in the Plattenberg breccia. Upper left enlargement of crinoid detail (modified after Cavargna-Sani et al. 2010)* ***e.*** *Internal Mesozoic outcrop composed by a narrow syncline with pure limestone in his core and dolomites on the rims. Hinterrhein (729900/151900).*

included in rock that is poor in phyllosilicates. The observed porphyroblasts are garnets, chloritoids and kyanites (Fig. 4c and d). White mica, graphite and brown-reddish carbonates are locally present in variable proportions. Hematite, illmenite and limonite are common and sometimes abundant. Chemical analysis of these rocks shows an abundance of Si, Fe and Al and a very low content of alkaline elements (Table 1).

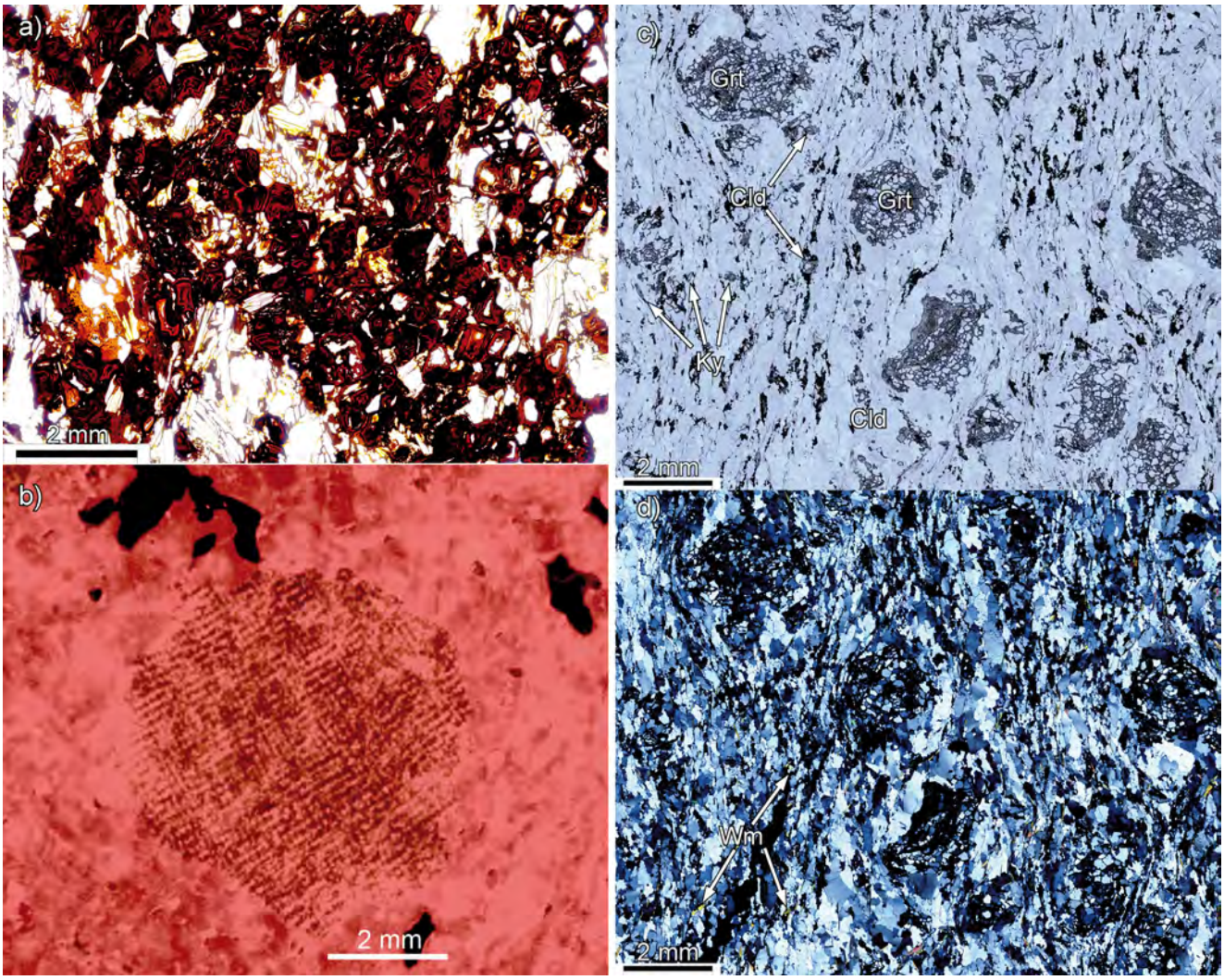

Fig. 4 *Photomicrographs.* ***a.*** *Siderolithic pebble of the Plattenberg breccia.* ***b.*** *Optical cathodoluminescence image of a crinoid fossil found in a calco-dolarenite intercalation in the Plattenberg breccia.* ***c.*** *and* ***d.*** *Sample MC 309, chloritoid-rich quartzite of the Hennasädel. Note the quartz aboundance and the extreme scarcity of micas. Cld: chloritoid; Grt: garnet; Ky: kyanite; Wm: white mica.*

4.3.4. Usser Rossbodma

The Usser Rossbodma (733430/161900; Fig. 1b and 2) Internal Mesozoic section crop out in the core of a Leis phase antiformal syncline. The basement corresponds to the Ordovician Heinisch Stafel Fm. Near the cover series, the basement rocks contain a large amount of dolocrete nodules.

The first Mesozoic sedimentary cycle starts with a few centimetres of thick white-grey quartzite followed by ~50 cm thick calcareous marble. The marble contains some phyllosilicates at the base and numerous thin dolomitic layers. This marble is overlain by a ~7 m thick sequence of the Dolomie Bicolori formation that becomes homogeneously white at the top. This first sedimentary cycle typically corresponds to a North Penninic Triassic.

In sharp contact with the dolomite, ~1.5 m of calcschist can be observed. The calcschist passes gradually to a carbonate poor, graphite rich, white mica-garnet-chlorite schist, with a few kyanites and a variable amount of hematite and limonite. It is followed and in sharp contact with a ~4 m thick impure marble. The impure marble comprises an alternation of white pure marble levels with horizons that are rich in quartz, feldspars, micas, and a few opaque minerals. The detrital marble transitions to a matrix-supported breccia (Fig. 3d). The matrix is mainly calcite with variable quartz content and white

Sample	MC292	MC309	MC321
SiO2	55.69	84.66	79.63
TiO2	0.76	0.31	0.42
Al2O3	14.40	3.50	5.10
Fe2O3	5.83	4.64	3.94
MnO	0.08	0.05	0.06
MgO	1.50	0.24	0.23
CaO	9.97	3.71	5.33
Na2O	0.36	0.00	0.00
K2O	1.83	0.18	0.76
P2O5	0.16	0.10	0.09
LOI	8.91	2.64	4.54
Total	99.52	100.03	100.09

Table 1 *Chemical analysis of some samples of chloritoid-rich quartzite of the Hennasädel. Major elements (wt.%) were measured by XRF (Philips PW2400 spectrometer, Université de Lausanne).*

mica. Some layers are rich in hematite, limonite and opaque minerals. The pebbles are quartzite and pure marble. Only two sedimentary cycles can be described from this series

4.3.5. Hohbüel

The Hohbüel Hill (732830/160600; Fig. 1b and 2) is formed by an overturned series of the Internal Mesozoic. The top of the hill is formed by the paragneisses of the Heinisch Stafel Fm. The series will be described following the stratigraphic order, opposite to the topographic position.

The stratigraphic basis of the Mesozoic cover series is marked by several centimetres of grey quartzite followed by a calcschist that gradually turns into a white marble with thin dolomitic layers. Then, an ~1 m thick limestone formation is followed by an ~1.5 m pale yellow dolomite. These dolomites turn transitionally into the Dolomie Bicolori. This sedimentary series is interpreted to be Triassic in age. The rest of the series is covered by Quaternary deposits comprising Quaternary dolomitic breccia.

4.3.6. Inder Rossbodma

Near the Inder Rossbodma high-mountain pasture (Fig. 1b), numerous Internal Mesozoic outcrops can be observed. The most noteworthy outcrop is described here and is located on a little cliff south of the mountain hut (733900/160940). Herein, we describe two distinct sections that are connected by a SW verging Leis phase fold.

The basement under *section I* (Fig. 2) comprises the Heinisch Stafel Fm. A few centimetres of white-grey quartzite are on top of the basement and are followed by ~15 cm thick white marble with a few thin dolomitic layers and by ~4 m of Dolomie Bicolori. This first sedimentary cycle corresponds to a North Penninic Triassic series.

After an ~1 m outcrop gap, a few meters of impure marble with thin layers of detrital sediments can be observed. The layer with the higher content of detrital grains contains quartz, micas (greenish mica), and a few grains of brown carbonate. This marble contains a few green amphibole and epidote porphyroblasts. This impure marble is progressively enriched upwards with its detrital constituents. The rest of the series does not outcrop.

Section II (Fig. 2) is underlain by the gneiss and schist of the Heinisch Stafel Fm.

The base of the sequence is erosive and starts with ~15 cm of detrital regenerated basement rock with abundant opaque minerals (principally hematite and limonite) and some brown carbonates. This first deposit is evidence of a transgression on the basement. The characteristic Triassic sediments are absent and were most likely eroded away down to the basement level before the transgression.

The next rock type develops transitionally into quartz-rich garnet chloritoid micaschist containing graphite, hematite, limonite and brownish carbonates. This layer is ~1.2 m thick. In sharp contact with the top of the micaschist is a 1.5 m thick black quartzitic marble containing some white mica and garnet. The protolith is almost certainly a quartz-rich calcarenite. The metamorphic calcarenite grades transitionally to a marble with thin detrital layers made of quartz, micas and brownish oxides (limonite principally). Metamorphic aluminium rich silicates (garnet, kyanite and chloritoid) and plagioclase porphyroblasts also can be observed. The series is truncated upwards by a tectonic contact.

4.3.7. Scattered outcrops

Some Internal Mesozoic outcrops with complex structures that prevent a stratigraphic reconstruction are briefly described here. These outcrops are significant for the general overview of Adula nappe cover rocks .

The *Wissgrätli Mountain* (729000/157200; Fig. 1b) and the neighbouring ridges expose a large amount of Internal Mesozoic cover rocks. The structure of these outcrops is much too complicated to reconstruct a coherent stratigraphy. However, individual formations can be observed. They can be compared with those of the Hennasädel sequence. For instance, the Dolomie Bicolori can be easily recognised in this area. This outcrop is described by Van der Plas (1959).

The *Peiltal Valley* (Fig. 1b), SE of the village of Vals, exposes the contact between the NE border of the Adula nappe and the Valser slices. This contact is refolded by the Leis phase folds. In previously published studies, a tectonic contact between the two units is placed at the base of the Mesozoic series. However, our new observations clearly identified the systematic presence of a Triassic thin cover attached to the Adula basement with a clear stratigraphic contact and in a normal position. This Triassic thin cover is limited to the Triassic base of the quartzite and to the transition of the Dolomie Bicolori to dolomite. Nearby, the Triassic of the Valser slices is characterised by a ~5 m thick limestone that is probably equivalent to the St. Triphon Formation, which is overlain by the Dolomie Bicolori (Galster et al. 2012). A few large outcrops of the Triassic at the base of the Aul slices can be observed on top of the Valser slices in the Peiltal Valley. They show a limestone series with possible remnants of vermiculated limestone.

Metric Internal Mesozoic boudins also occur in the *Zapport Valley* (Fig. 1b). Some interesting outcrops are situated directly on the mountain trail to the Zapport hut upstream of the army training ground. The Mesozoic cover is strongly strained and reduced to a band that is ~40 cm thick (Fig. 3e). Nevertheless, the stratigraphic formations can be identified. Usually the Internal Mesozoic appears as a symmetrical syncline with the Triassic formation on each side in contact with the basement, with pure marble preserved in the core (most likely Upper Jurassic marble).

The upper *Val Soi* (directly south of the map border in Figure 1b) is located in the overturned limb of the Adula nappe. It is also marked by the sedimentary zone between the Simano and the Adula nappes. This sedimentary zone is principally composed of Dolomie Bicolori. At the upper end of the Val Soi, a few outcrops of the Adula nappe cover are in an overturned position and described by Galster (2010).

4.4. Stratigraphic correlation

4.4.1. Correlation base

Some settled stratigraphic sections are used for the stratigraphic correlations. Data published in Galster et al. (2012) are the starting point to interpret the Triassic and the Jurassic stratigraphy of the units from the Adula to the Gotthard. The sedimentary section of the Teggiolo zone (Antigorio nappe cover; Matasci et al. 2011) is also a key reference for our

correlations. The Teggiolo zone is the unique complete well-established stratigraphic sequence described in the Lower Penninics. Its inferred paleogeographic position is also one of the closest to the Adula nappe. The stratigraphy of the Monte Leone nappe cover (Carrupt 2003) is also useful for correlations.

4.4.2. Pre-Triassic

The detailed analysis of the basement and the cover of the Adula nappe reveal the absence of Permian Verrucano-type detrital rocks (Cavargna-Sani et al. submitted; Chapter 3). This absence of "Verrucano" contrasts with the neighbouring Luzzone-Terri and Soja nappes. Remnants of paleosols in the form of dolocrete and calcrete lenses and nodules are found on and immediately below the surface of the polymetamorphic basement. These dolocrete and calcrete formations are equivalent to the well-known paleosols in less metamorphic domains (Aiguilles rouges (Demathieu and Weidmann 1982); Mont Blanc (Epard 1989); Aar (Gisler et al. 2007)). We ascribe this paleosol to an emersion before the Triassic transgression. The Adula domain, with its pre-Triassic emersion and erosion, is perhaps the source for detrital sediments transported in the neighbouring domains (e.g., Luzzone-Terri nappe Verrucano; Galster et al. 2010).

4.4.3. The Triassic sedimentary cycle

The Triassic sedimentary cycle is the most obvious and easy to interpret. It is also the most constant sedimentary group within the Adula nappe cover.

The quartzite, ubiquitous at the basis of the Mesozoic sections, represents the transgression and the start of the sedimentary cycle (Fig. 3a). The quartzite is also the most precious marker to display the autochthony of the described series. It presents definite similarities with the Lower Triassic quartzite of the Briançonnais domain.

On the quartzite, meter-thick limestone with thin dolomitic beds is observed in the sections of Usser Rossbodma, Hohbüel, and the Inder Rossbodma (Fig. 2) is interpreted as a reduced equivalent of the St. Triphon Fm. (Baud 1976; Baud 1987). This interpretation is supported by the recent discovery of a nearly continuous transitional chain from the classical Briançonnais sequence to the extremely reduced sections of the Adula (Galster et al. 2012). In this chain, a key link is provided by the Luzzone Triassic, in which the typical Briançonnais characteristics are well preserved despite a strong trend towards thinning and increasing of dolomitisation (Galster et al. 2010). With the metre-thick limestone between quartzite and Dolomie Bicolori, we reach the limit of the St. Triphon Anisian basin. This limestone is absent at Plattenberg (Cavargna-Sani et al. 2010). Thus, the shoreline of this basin passed through the Adula nappe (Fig. 5). The Dolomie Bicolori Fm. is constant and typical in every section. This formation has an Upper Anisian to Lower Ladinian age (Bianconi 1965; Galster et al. 2012) and can be interpreted as a lateral equivalent of the Briançonnais Champcella Fm. (Megard-Galli and Baud 1977) (Fig. 5). The Luzzone section provides a crucial transition (Galster et al. 2010).

In conclusion, the Triassic stratigraphy of the Adula nappe is characteristic of the North Penninic Triassic paleogeographic domain (Fig. 5). This domain was located between the Helvetic and the Briançonnais Triassic paleogeographic domains (Fig. 5) (Galster et al. 2012).

4.4.4. The Lower and Middle Jurassic

Lower and early Middle Jurassic sediments were not apparent in the Adula. These sediments are, on the contrary, developed in the adjacent paleogeographic domains (both in an external and internal position with respect to the Adula). The

continuity from the Gotthard domain (Helvetic) stratigraphy (Baumer et al. 1961) to the more internal Luzzone-Terri series (Kupferschmid 1977; Galster et al. 2010; Galster et al. 2012) proves that they were part of the same sedimentary basin during the Lower and Early Middle Jurassic. The dynamics of the Helvetic Lower Jurassic Gotthard – Luzzone-Terri basin reveals a migration of the basin axis (Galster et al. 2012). The Stgir and Inferno Formation (Hettangian – Toarcian) show a deeper sedimentation in the more internal Luzzone-Terri nappe. However, the Coroi Formation (Aalenian) facies suggest a deeper sedimentation on the more external Gotthard territory than the equivalent formation in the Luzzone-Terri domain. It is interpreted as the onset of the uplift in a more internal territory. The homeland of the Adula nappe is located between these two sedimentary domains. The presence of similar Lower Jurassic formations surrounding the Adula domain suggests that these formations were deposited onto the Adula domain but must have been eroded later.

The Plattenberg breccia presents evidence for a post-Triassic emersion. Emersions in the Alpine context are generally observed during the Middle Jurassic and are linked to the uplift of horst-like blocks in an extensional regime, e.g., in the Briançonnais domain (Baud and Masson 1975), the Teggiolo zone (Matasci et al. 2011) and the nearby Garzott slices (Galster et al. 2012). The age of the emersion cannot be dated directly in the Adula nappe. The sedimentary record in the nearby basins also contains the possible trace of this emersion as coarser detrital sedimentation. The sedimentation in the Scopi zone and the Luzzone-Terri nappe demonstrates that the emersion was after the Toarcian – Aalenian age (Galster et al. 2012). We suggest, therefore, that the age of the emersion in the Adula nappe is Middle Jurassic (Fig. 6).

4.4.5. The Jurassic transgression and onset of carbonate sedimentation

The Plattenberg breccia and the Hennasädel post-Triassic sandstone clearly show a transgressive sedimentation on an eroded surface over the Triassic Dolomie Bicolori (Fig. 3b).

The Plattenberg breccia is most likely a sedimentary formation related to a local sedimentary context, as suggested by the abundance of angular elements. These sediments reveal the existence of a paleorelief. The pebbles made of siderolitic material (Fig. 4b) give a clear indication of the pre-Plattenberg breccia emersion. The Hennasädel sandstone is also the sedimentary expression of a transgression.

The sedimentation of these detrital rocks occurred during a drowning phase under marine conditions as shown by the discovery of crinoids in the Plattenberg breccia. The age of this transgression and the beginning of the drowning phase are constrained by the Upper Jurassic limestone (see below). It most likely corresponds to the late Middle Jurassic.

The Hennasädel is the only section that displays a thick pure calcitic marble formation in the post-Triassic sequence. A thinly bedded sandy marble occurs at its base and records a transition from the sandstone to the pure massive marble. A similar transition is observed in the Helvetics (Oxfordian e.g., Anatra 1986). Above the pure marble, we observe an alternation of beds of yellowish impure marble and calcschist. The age of the pure marble can without difficulty be ascribed to the Upper Jurassic. It is comparable to the Quinten Formation in the Helvetics, the Sevinera marble in the Teggiolo zone (Matasci et al. 2011), or the massive Malm limestone of the Subbriançonnais domain. The overlaying alternation with calcschist is similar to the Vanis Formation of the Teggiolo zone and can be compared with the marly alternations of Lower Cretaceous age in the Southhelvetic basin (Anatra 1986).

This second sedimentary cycle can be compared to the Antabia group of the Teggiolo zone (Matasci et al. 2011). In the Adula nappe, the pure limestone is observed only in the Hennasädel section. Its absence in the other described sections is most likely the consequence of subsequent erosion. This observation contrasts with the situation in the Teggiolo zone where the Sevinera limestone is always present (Matasci et al. 2011). The presence of pure limestone pebbles in the overlaying detrital

formations (see next chapter) is interpreted as the effect of the erosion of the Upper Jurassic limestone in the Adula nappe.

4.4.6. Flyschoid sediments group

The third sedimentary cycle is dominated by detrital rocks and is grouped under the loose term of "flysch" s.l. (flyschoid), although real turbidites were never described. They most likely, rather, result from more complex mechanism of sedimentation that can combine the effects of both downslope and bottom currents.

The rocks of this group are less characteristic than the previous ones, and the potential correlations with well-established formations are more difficult.

This stratigraphic group is deposited over a discordant surface. At the Hennasädel, the group is deposited on the Lower Cretaceous limestone and calcschist. At Usser- and Inner Rossbodma, it cuts down to the Triassic Dolomie Bicolori, and even at Inner Rossbodma, it is directly transgressive on the basement. The nature of contact with the Plattenberg Fm. is more dubious because of the presence of the cornieule and could be tectonic. However, the overlying sequence is comparable to the flyschoid group of the other sections. We suggest that this significant unconformity observed in every section marks an important stratigraphic gap. No traces of emersion have been observed in relation to this stratigraphic gap.

This unconformity is comparable with those occurring below the North Penninic Flysch (e.g., Niesen nappe (Badoux and Homewood 1978), Valais s.s. of the Tarentaise (Antoine 1971), in the Teggiolo zone (Matasci et al. 2011), in the Monte Leone cover (Carrupt 2003) and in the Helvetic Wildhorn nappe (Stacher 1980).

The flyschoid group is essentially formed from detrital sediments. The first formation consists of quartz-rich-micaschists, which contain variable amounts of carbonates and graphite. It is followed by an impure marble, which varies from a white marble with some impure layers to carbonate rich schists. The marble contains a variable amount of detrital components and is most likely formed mainly by the erosion and re-sedimentation of limestone. It turns upward to a conglomerate containing pure limestone (similar to the pure marble of the Hennasädel section) pebbles or quartz-rich pebbles in a sandy-marble matrix. The presence of the pebbles suggests the erosion and re-sedimentation of the Upper Jurassic limestone and indicates a post-Upper Jurassic age for these formations.

The sedimentation of the flyschoid group of the Adula nappe cannot be correlated directly to the typical North Penninic Flysch. The Niesen Flysch (Ackermann 1986), the Gurnigel-Schlieren Flysch (Caron et al. 1989; Trümpy 2006) and the Arbalatsch Flysch (Ziegler 1956) are thick and rather monotonous stacks of typical turbidites. The sediments of the Adula Flyschoid are most likely to be compared with the Valais s.s. detrital sediments (Trümpy 1954; Jeanbourquin and Burri 1991) or the lower part of the Teggiolo calcschists (Matasci et al. 2011).

The age of this sedimentary group is certainly post-Jurassic. In the Alps, late Cretaceous flyschoid are commonly deposited on a discordant and erosive surface. The sedimentation of the flysch or flyschoid in the North Penninic basins usually starts at the end of Upper Cretaceous (Campanian-Maastrichian; see discussion in Matasci et al. 2011). In the Helvetic domain the Wang Fm. (Maastrichian) is clearly deposited on a deeply discordant surface (Stacher 1980). Consequently we suggest a Late Cretaceous to Paleogene age for the Adula flyschoid sediments.

4.4.7. Chloritoid-rich quartzite of the Hennasädel

The recurrence of chloritoid– garnet rich quartzite that is restricted to the Hennasädel merits a special discussion. This rock,

suitable for metamorphic investigations (Zulbati 2008), has such an unusual composition that it poses a sharp problem of protolith and source of the sediment. We are unable to correlate it with any stratigraphic formation of large extent in the neighbouring parts of the Alps. Consequently, our attempt of a stratigraphic interpretation will be based on a discussion of the extraordinary composition of this rock-type. Its mineralogy, characterised by the abundance of quartz, consists of Al-rich silicates and opaques (Fig. 4c and d) and is consistent with its chemical composition that is marked by variable but often high Al, relatively abundant Fe, low K and Mg and a nearly complete absence of Na (Table 1). The protolith of the chloritoid-rich quartzite must have been a very mature detrital sediment. A rock weathered in sub-aerial conditions is a good candidate for this type of source. Kaolinite might be an important mineral. Our chemical analyses (Table 1) are remarkably similar to those found for the Eocene Siderolitic deposits in the Helvetic (Wieland 1976). Emerged land is required to provide this specific source rock. However, the continental source could have been reworked into a detrital marine deposit. As emerged land seems improbable the Late Cretaceous, we suggest a Paleogene age. In any case, this could be the youngest rock found in the Adula nappe, consistent with its position in the core of a first phase syncline (Cavargna-Sani et al. submitted; Chapter 3).

4.5. Discussion

4.5.1. Significance of the Triassic stratigraphy of the Adula nappe

Triassic stratigraphy has a noteworthy significance in the geology of the Western-Central Alps: it marks the onset of a new tectonic cycle and represents the territory assemblage preceding the major tectonic changes starting during the Jurassic. Triassic stratigraphy is uniformly characterised by shallow water sedimentation without any major tectonic disturbance (Trümpy 1982).

Galster at al. (2012) define the North Penninic Triassic and interpret it as a transition between the Helvetic Triassic and the Briançonnais Triassic. This North Penninic type of sedimentation is characterised by the scarcity of limestones (abundant in the Briançonnais Triassic) and the occurrence of the Dolomie Bicolori. Anisian St. Triphon limestone (Calcaire vermiculé) is typical of the Briançonnais series (Megard-Galli and Baud 1977; Baud 1987) Anisian St. Triphon limestone is gradually reduced from the south to north and thinned out. The Adula nappe is characterised by the North Penninic Triassic type of sedimentation. Of utmost importance is the fact that the St. Triphon limestone vanishes between the Rossbodma – Hohbühl and the Hennasädel – Plattenberg sections. The northern shoreline of the St Triphon basin is cutting through the Adula nappe (Fig. 2 and 4).

The Triassic of the Adula nappe provides some evidence for the paleogeographic position of the Adula domain before the Alpine rifting phase. The Triassic Adula domain is situated south of the southern limit of the Helvetic Triassic territory but in connection with it. The Triassic series of the Adula cover can be correlated with those of the Monte Leone cover (M. Eichenberger oral communication).

4.5.2. The role of the Adula block in Alpine rifting

The stratigraphic record in the Adula cover and the surrounding units justifies special attention in this key tectono-stratigraphic cycle. Detailed discussions on the rifting activity in the territories surrounding the Adula homeland can be found in Galster et al. (2012). The topic of the present paper is more focused of the Adula nappe cover sedimentary record.

The image of the “Adula Schwelle” (Adula rise) of Kupferschmid (1977) is confirmed by our stratigraphic analysis. The sections of the Plattenberg and of the Hennasädel confirm the post-Triassic erosion and the consequent stratigraphic gap

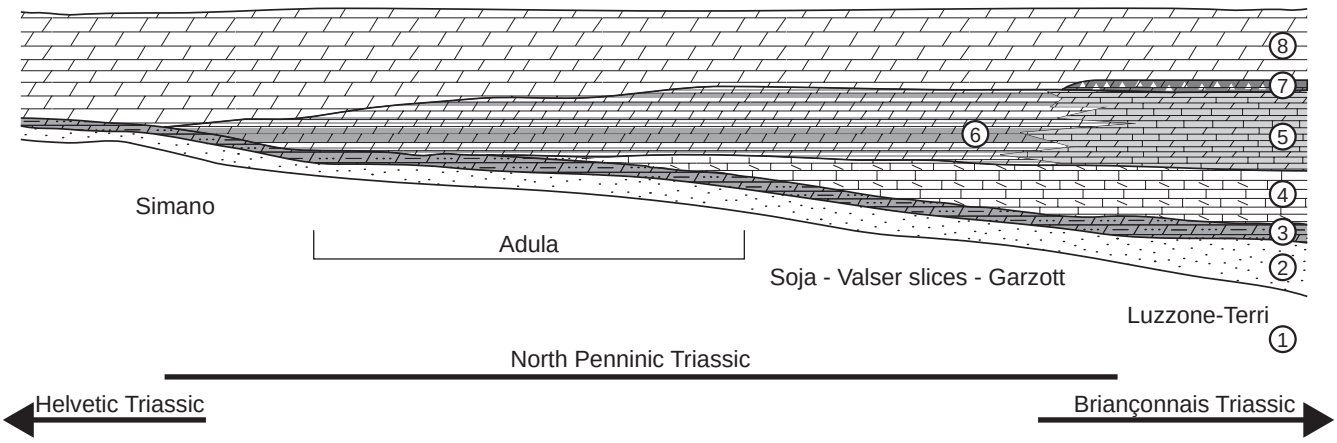

Fig. 5 *Palinspastic section for the Triassic formations. 1) Undifferentiated basement; 2) Lower Triassic quartzites; 3) Anisian doloschist; 4) dolomitic limestone and vermiculated limestone (reduced Briançonnais St. Triphon Fm.); 5) ash-grey laminated calcareous dolomite (reduced Briançonnais Champcella Fm.); 6) Dolomie Bicolori; 7) intraformational dolomitic breccia (Briançonnais Clot-la-Cime Fm.); and 8) yellow dolomites.*

during Lower and early Middle Jurassic. The reworked continental deposits of the Plattenberg breccia testify to the emergence of the Adula during mid-Jurassic times. The Adula domain is part of a larger system of rises in the North Penninic – distal Helveric domain (e.g., Monte Leone nappe and the Teggiolo zone; as confirmed by several detrital sediments of the same age in the North Penninic series; see discussion in Galster et al. 2012). Classically these rises are viewed as uplift counterparts of the deepening basins. Galster et al. (2012) suggested that this mechanism was coupled with a general uplift of the entire domain between the Helvetic margin and the Briançonnais land during the Middle Jurassic, resulting in increased buoyancy consequent to lithospheric thinning and mineral phase transitions. The resulting stratigraphic gap marks a turning point in the tectono-sedimentary history of the Alps and is a direct consequence of the onset of the Jurassic rifting.

The sedimentary record shows the persistent preservation of the Triassic series under the post-Triassic erosion. This preservation of the pre-rift sediments is important to understand the rifting mechanism in the Adula nappe. The base of the Upper Jurassic post-rift sequence is never observed transgressing directly on the basement (different from the Teggiolo zone).

The transgressive deposit on the Triassic dolomites in the Plattenberg and the Hennasädel sections records the drowning phase subsequent to the emergence. This drowning phase is associated to tectonic activity. The Plattenberg breccia is most likely the result of a sedimentary setting because of normal faulting. Therefore, we interpret this breccia as a syn-rift sediment. The presence of crinoids indicates a high-energy submarine formation of the breccia. The Plattenberg breccia deposited on pre-rift dolomites is the only breccia observed in the Adula nappe. Breccias directly overlaying the basement, as in more central rift systems (Masini et al. 2011), are absent from the Adula nappe. Hints of detachment are exposed in the nearby Garzott slices (Galster et al. 2012).

The transgression culminates in the onset of the Upper Jurassic carbonate sedimentation. The late Middle Jurassic transgressive detritals and the Upper Jurassic limestone – Berriasian marls of the Adula nappe are more reminiscent of the stratigraphy of the Helvetic domain than of a North Penninic basin. The North Penninic basins have the post-rift onset of basin-type Bündnerschiefer sedimentation, with some late Middle Jurassic basaltic manifestations (Steinmann 1994; Liati et al. 2005). These basaltic rocks are also clearly observed in the nearby Valser slices (Steinmann 1994; Steinmann and Stille 1999). The rift related detachment of the Garzott slice suggests a structure of a hyper-extended margin. The inherited rift structures of the tectonic units now grouped in the Internal Klippen Belt and in the Mesolcina zone may have helped the

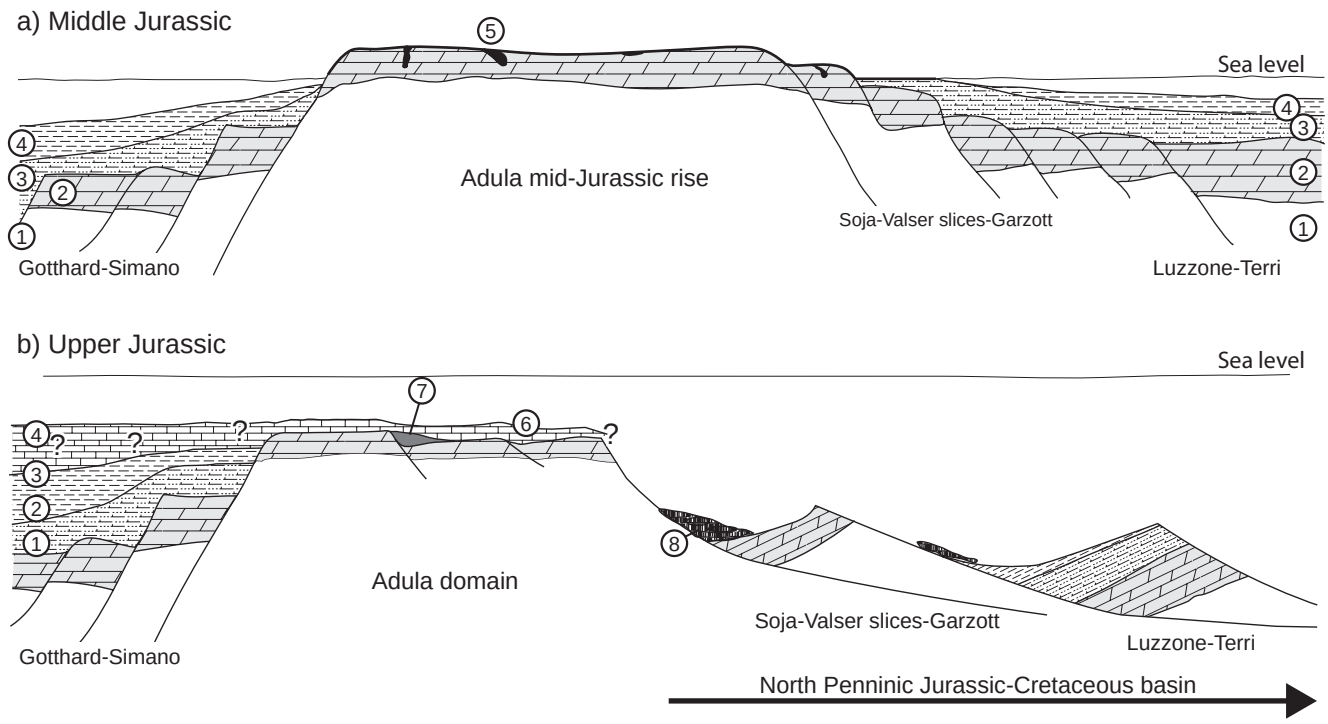

Fig. 6 *Palinspastic sections during* ***a.*** *Middle Jurassic and* ***b.*** *Upper Jurassic. 1) Undifferentiated basement; 2) undifferentiated Triassic; 3) Lower Jurassic Stgir and Inferno Fm.; 4) Aalenian Coroi Fm.; 5) sub-aerial weathering deposits; 6) Upper Jurassic limestone; 7) Plattenberg breccia; and 8) North Penninic basaltic formations (late Middle Jurassic?).*

formation of numerous slices during Alpine orogeny (as previously suggested by Steinmann 1994).

The Adula domain seems to escape to this general basin opening and to the rift-related basaltic manifestations. Evidence of a hyper-extended margin are observable in the more internal units, but in the Adula, the only visible hint of tectonic activity is limited to the Plattenberg breccia. We suggest, therefore, that the Adula nappe was situated near the external margin of the Upper Jurassic – Cretaceous North Penninic basin. The paleogeographic position of the Adula within the Alpine rift system is the southern limit of the European crust and directly north of the hyper-extended distal domain, and it indicates that it is not directly a part of the detachment system observed in the Alpine rift (e.g., Manatschal et al. 2006; Masini et al. 2013).

4.5.3. The Adula domain during the Cretaceous and Tertiary

The nearby Bündnerschiefer of the Mesolcina zone are also of North Penninic origin. They form a thick, relatively homogeneous detrital sedimentary group. This sedimentation most likely started during the Jurassic and developed to more distal deposits during the Cretaceous (Steinmann 1994). These types of sediments are not comparable to those observed in the flyschoid group of the Adula cover. We suggest, therefore, that the Adula domain was at the margin of the main Cretaceous North Penninic basin (homeland of the Bündnerschiefer of Aul, Grava and Tomül nappe). This position is also supported by the pronounced angular unconformity at the base of the flyschoid group. We interpret the Adula domain as a submarine topographic high. This higher position is most likely responsible for the Cretaceous non-deposition or erosion. Our observations are consistent with the stratigraphic observations in the Teggiolo zone (Matasci et al. 2011), Monte Leone cover and Pizzo del Vallone nappe (Carrupt 2003), suggesting a similar domain at the North Penninic border.

The youngest sediments in the North Penninic stratigraphy are typically a wildflysch (Trümpy 2006; Matasci et al. 2011). This is never observed in the Adula nappe. We suppose that the sedimentary record is not complete and that the flysch and

wildflysch formations could have been lost because of tectonic offscraping.

4.5.4. Variation in time of the limits of the paleogeographic domains

Unravelling the original paleogeographic position of Alpine nappes depends on the correlations of sedimentary and stratigraphic domains. The term domain must be understood as the spatial extension of a given, distinctive, sedimentary environment. These sedimentary domains are defined only during a specific time interval and vary in space and time. Correlation of the stratigraphic domains is independent from the future nappe structure.

The Triassic of the Adula nappe displays a North Penninic Triassic. The Jurassic – Lower Cretaceous sedimentary cycle can be compared to the interbasinal rise of the Helvetic domain (e.g., Aiguilles-Rouges, Gastern, Internal Mt. Blanc sedimentary cover, and the Antabia group of the Teggiolo zone). The flyschoid sediments can be linked to the similar Valaisan s.s. sediments. The nearby Luzzone-Terri cover also shows this domain fluctuation. In this tectonic unit, Briançonnais Triassic sediment is overlain by a Helvetic type Lower Jurassic sediment (Galster et al. 2012).

4.5.5. Orogenic connotation of the Adula nappe cover

The northern Adula nappe can definitively not be considered a lithospheric mélange unlike what is suggested by Trommsdorff (1990) and Berger and Mercolli (2006). The sedimentary record of the northern Adula nappe is consistent throughout the different outcrops. This record consists of uniform and specific sedimentary domains that can be correlated with neighbouring nappes (e.g., units of the Internal Klippen Belt; Galster et al. 2012) or with similar sedimentary domains (e.g., Monte Leone, Carrupt 2003; Teggiolo zone, Matasci et al. 2011). The structural complexity is not questioned by this assertion, but we conclude that this complexity is the consequence of the Alpine deformation on an initially coherent homeland.

The complex sedimentary structure of the Adula nappe homeland has certainly influenced the deformation geometry. The sedimentary series record the presence of synsedimentary structures (normal fault). The mechanical heterogeneity with respect to the Alpine deformation of these pre-existing structures has certainly played a major role in the creation of the Internal Mesozoic. Basin inversion through ductile shearing and folding are clearly demonstrated in less deformed environments (Krayenbuhl and Steck 2009; Bellahsen et al. 2012).

The Internal Mesozoic is a very useful marker to decipher the internal geometry of the Adula nappe. Nevertheless, meticulous study of the Adula nappe Internal Mesozoic demonstrates, yet again, that the bands of cover metasediments have not been interpreted systematically as the trace of thrusts and nappe or sub-nappe division. Detailed investigation of the Adula nappe shows that stratigraphic contact of the cover (even if it is a thin sedimentary cover) upon the basement is more the rule than the exception. It has also strong consequences on the Adula structure and kinematics interpretation.

Unfortunately, the results presented here cannot be compared to the sedimentary series in the Central- or Southern-Adula nappe. The deformation in these regions is even stronger, and only some Internal Mesozoic boudins without a clear stratigraphic signature are preserved. Nonetheless, the northern and the southern Adula nappe represent a coherent unit, as demonstrated by the detailed study of the basement lithostratigraphy (Cavargna-Sani et al. in press).

The preservation of the cover sequences in the Adula nappe depends on their specific structure and position. These outcrops are mainly synclinal hinges (Chapter 3) of isoclinal folds where the deformation is less intense (Ramsay 1968).

4.6. Conclusions

Several important conclusions can be drawn from this study:

- Detailed stratigraphic analyses are possible in the highly metamorphic and deformed Adula nappe. The detail of this stratigraphic study has major consequences for the pre-orogenic history of the Adula nappe and for the kinematic interpretation of its Alpine deformation history.
- The proper autochthonous cover of the Adula nappe is characterised by several definite sedimentary formations.
- The Adula domain cannot be considered the homeland of detached units of the Mesolcina (Misox), zone because it retains its autochthonous sedimentary cover.
- The thinness of the Adula sedimentary cover is not only the expression of a high strain, but rather the consequence of two important sedimentary gaps.
- The Triassic of the Adula nappe has to be assigned to North Penninic Triassic facies. The Adula nappe homeland, consequently, must be placed between the Helvetic and the Briançonnais Triassic domains. More precisely, the position of the Adula nappe homeland is between the Simano and the Luzzone-Terri nappe homelands.
- The Adula domain represents a mid-Jurassic rise at the southern limits of the more or less normal European crust, immediately north of the hyper-extended margin.
- The second rifting cycle caused the marine drowning of the Adula block, which remains at the margin of the main delamination and creation of the North Penninic basin.
- The flyschoid series assigned to the North-Penninic is deposited with an unconformity on the post-rift sediments. This reflects a major stratigraphic gap. The possible age is Maastrichian and younger.

ACKNOWLEDGEMENTS

This study is supported by the Swiss National Science Foundation, grant no. 200021_132460 and the Société Académique Vaudoise. We would like to thank L. Nicod for thin sections preparation. We thank D. Schreich, A. Pantet and A. Steck for support in the field. We are grateful to the Museo Cantonale di Storia Naturale for authorization to collect samples in Ticino.

5. New stratigraphic data from the Lower Penninic between the Adula nappe and the Gotthard massif and consequences for the tectonics and the paleogeography of the Central Alps

Federico Galster, Mattia Cavargna-Sani, Jean-Luc Epard and Henri Masson

Published in: Tectonophysics 579 (2012) 37-55

ABSTRACT

New stratigraphic data along a profile from the Helvetic Gotthard Massif to the remnants of the North Penninic Basin in eastern Ticino and Graubunden are presented. The stratigraphic record together with existing geochemical and structural data, motivate a new interpretation of the fossil European distal margin.

We introduce a new group of Triassic facies, the North-Penninic-Triassic (NPT), which is characterised by the Ladinian "dolomie bicolori". The NPT was located in-between the Briançonnais carbonate platform and the Helvetic lands. The observed horizontal transition, coupled with the stratigraphic superposition of an Helvetic Liassic on a Briaçonnais Triassic in the Luzzone-Terri nappe, links, prior to Jurassic rifting, the Briançonnais paleogeographic domain at the Helvetic Margin, south of the Gotthard. Our observations suggest that the Jurassic rifting separated the Briançonnais domain from the Helvetic margin by complex and protracted extension.

The syn-rift stratigraphic record in the Adula nappe and surroundings suggests the presence of a diffuse rising area with only moderately subsiding basins above a thinned continental and proto-oceanic crust. Strong subsidence occurred in a second phase following protracted extension and the resulting delamination of the rising area.

The stratigraphic coherency in the Adula's Mesozoic questions the idea of a lithospheric mélange in the eclogitic Adula nappe, which is more likely to be a coherent alpine tectonic unit. The structural and stratigraphic observations in the Piz Terri-Lunschania zone suggest the activity of syn-rift detachments. During the Alpine collision these faults are reactivated (and inverted) and played a major role in allowing the Adula subduction, the «Penninic Thrust» above it and in creating the structural complexity of the Central Alps.

5.1. Introduction

The Alps, as a mountain belt, are the result of Cretaceous convergence and Tertiary collision between European and African derived plates following the closure of oceanic domains (Dewey et al., 1989). Their history, however, starts long time before Cretaceous convergence and experienced periods of extension (Trümpy, 1958).

The pre-orogenic evolution of the Alpine realm leads to the creation and differentiation of several paleogeographic domains whose remnants have subsequently been stacked in the orogenic belt during tertiary collision (Schmid et al., 1996; Steck, 2008). From an internal (Upper) toward an external (Lower) position the following domains are generally distinguished: the Adriatic plate *sensu lato* in South Alpine and Austroalpine position; the remnants of the Liguro-Piemontese ocean in Upper Penninic level; the nappes and klippes issued from the Briançonnais paleogeographic domain stacked in the Middle Penninic; the remnants of the North Penninic Basin and its North margin assembled in the Lower Penninic nappes together with the series originated from the Valais Through; finally the Helvetic *sensu lato* domain that is distributed in the Ultrahelvetic and Helvetic nappes and in the external Massifs.

This repartition and its paleogeographic significance are not devoid of discussions. Of particular interest and matter of passionate debates is the role played by the units currently stacked in a Lower Penninic position.

A portion of the Lower Penninic of the Western Alps (the "zone de sion-courmayeur-Tarentaise", Valais *s. str.*) is characterised by a typical lithological association: the "Trilogie Valaisanne" of Cretaceous or younger age (Trümpy, 1951, 1955). This group of facies, that belong to the core of the definition of the Valais s.str., has never been found in the eastern Alps, where in a Lower Penninic position, there is a monotonous package of calcschists, the so called Bündnerschiefer, that during Jurassic and Cretaceous filled the North Penninic basin *s.l.* (Probst, 1980; Steinmann, 1994).

Based on the presence of MORB-type metamafics, several workers (e.g. Dürr et al., 1993; Steinmann & Stille, 1999) proposed the presence of oceanic crust in the internal North Penninic. Where radiochronologically dated the supposed oceanic rocks are of late Middle-early Upper Jurassic time (~61 Ma, Liati et al., 2005). Concerning the Valais Trough, the birth of an early Cretaceous Ocean has been proposed (Frisch, 1979; Stampfli, 1993) but has not yet been proven convincingly by the dating of Cretaceous oceanic crust. Where dated, metabasites in the Valais domain *s.str.* (i.e. zones characterised by the "Trilogie Valaisanne") are Paleozoic (Masson et al., 2008). Moreover a Cretaceous age for the supposed Mesozoic Ocean is at odds with the Jurassic age reported for the Oceanic crust in the North Penninic.

Currently two hypotheses are the most widely accepted to explain the significance of Lower Penninic units and the connection Valais-North Penninic.

The first one considers the North Penninic and the Valais as one domain, located between the Helvetic margin and the Briançonnais domain, that experienced hyper extension during the Jurassic rifting, at the same time that the Liguro-Piemontese Ocean opened to the south (Manatschal et al., 2006). The second hypothesis, on the other hand, regards the Valais domain as a Cretaceous transcurrent Ocean which opened oblique into the older Liguro-Piemontese Ocean to the east and into the European margin to the west, where it separated and isolated the Briançonnais domains from the Continent (Stampfli, 1993). In this last scenario the Briançonnais domain is regarded as a far travelled exotic Terrane that during the Cretaceous Time migrated eastward and duplicated the European Margin in the Western and Central Alps (Stampfli et al., 2002).

In this contribution we will investigate the aspect and the distribution of pre- syn- and post-rift facies on the distal European margin in the Central Alps in order to shed light on the tectonostratigraphic evolution of the North Penninic rifting and to understand the Helvetic-Briançonnais relationship. The refinement of the stratigraphic record coupled with structural and

metamorphic information is used as a tool to extricate the extremely complex tectonic around the eclogitic Adula nappe.

5.2. Geological setting and background

The study area is located at the northeastern edge of the Lepontine dome, SW of the Gotthard Massif, astride northeastern Ticino and western Graubünden (fig 1a and 2a). The tectonic map of the Central Lepontine Alps (Berger & Mercolli, 2006) and its explanatory note (Berger et al., 2007) give a good overview of the geological setting. The Lepontine dome consists in a highly deformed pile of nappes mainly made of Paleozoic or older gneissic basement with remnants of sedimentary cover (Preiswerk et al., 1934). The contrasted tectonic syntheses of Maxelon & Mancktelow (2005) and of Steck (2008) give a measure of the uncertainties that still characterize our present-day understanding of its tectonic structure. During Alpine collision the Lepontine dome suffered severe metamorphic conditions increasing from upper greenschist facies in the north to upper amphibolite in the south (e.g. Trommsdorf, 1966; Frey, 1969, 1978; Niggli, 1970; Wenk, 1970; Fox, 1975). This Barrowian metamorphism is preceded by a subduction related high-pressure event, ranging from blueschist to eclogite conditions (e.g. Heinrich, 1982, 1986; Nagel, 2008, Wiederkehr et al., 2008). The metamorphic evolution of the metasediments in the Northern part of the Lepontine dome has been recently reviewed and improved by Wiederkehr et al. (2008, 2009, 2011). Despite deep subduction and strong deformation the nappes usually still preserve more or less complete remnants of their original Mesozoic-Tertiary sedimentary cover (e.g. Matasci et al., 2011). Moreover between the main nappes it is possible to find thinner zones of allochtonous metasediments, detached from more internal homelands (Bianconi, 1971; Etter, 1987; Galster et al., 2010; Probst, 1980) . The remnants of the former Jurassic distal European margin are now distributed among these different tectonic units, i.e.: the Gotthard massif, the Lucomagno-leventina nappe, the Simano nappe, the Soja unit, the Piz-Terri Lunschania zone, the Adula nappe and the Misox zone. (fig. 1).

The Gotthard massif is the lowest tectonic element in the study area. It consists in Paleozoic and older gneisses covered by Permian “Verrucano” and Triassic dolomites (Baumer et al., 1961; Brunnschweller, 1948; Fehr, 1956). The Jurassic to Tertiary cover has been detached and transported further North into the Helvetic nappes (Etter, 1987). The Gotthard massif is overthrusted by the Scopi and the Peidener zones (the so-called “Gotthard Massivischer Mesozoikum” GMM; Spicher, 1980) consisting of Mesozoic sediments of Triassic and Jurassic age. The Scopi zone lays partly overturned but its stratigraphic content is coherent and perfectly recognizable. It is of Helvetic type: above a thin Helvetic Triassic, three thicker subdivisions of Jurassic age are distinguished: the Stgir, the Inferno and the Coroi Formations (Baumer et al., 1961; Jung, 1963; Baumer, 1964; Frey, 1967; Etter, 1987). The Stgir and the Inferno Formations have also been recognized in the imbricated Peidener zone (Baumer et al., 1961), where the stratigraphic record is slightly different but still of Helvetic type. These series provide an important tool of correlation and are a precious link between the classical Helvetic Liassic of the Glarus nappe (further North; Trümpy, 1949) and the Liassic cover of several Penninic units (e.g. Galster et al. 2010). We briefly summarize them here: 1) The Stgir Formation: above a quartzite layer (“Lias Basis Quarzite”), it is composed by the Basal Stgir (shales), the Lower Stgir (marls, marly limestones and shales) and the Upper Stgir series (richer in sandstones and quartzites).

2) The Inferno Formation: rich in belemnites, it is divided into a Lower (alternation of marls and marly limestones), a Middle (marls) and an Upper member (marls and marly limestones). The second half of the Formation is richer in detrital content. Locally the homogeneity of the Formation prevents the distinction of the three subdivisions.

3) The Coroi Formation is a homogeneous thick series of calcite-free black shales.

The Lucomagno-Leventina nappe is the next higher gneissic-body. Its thin Triassic cover, formed of arkosic sandstones and

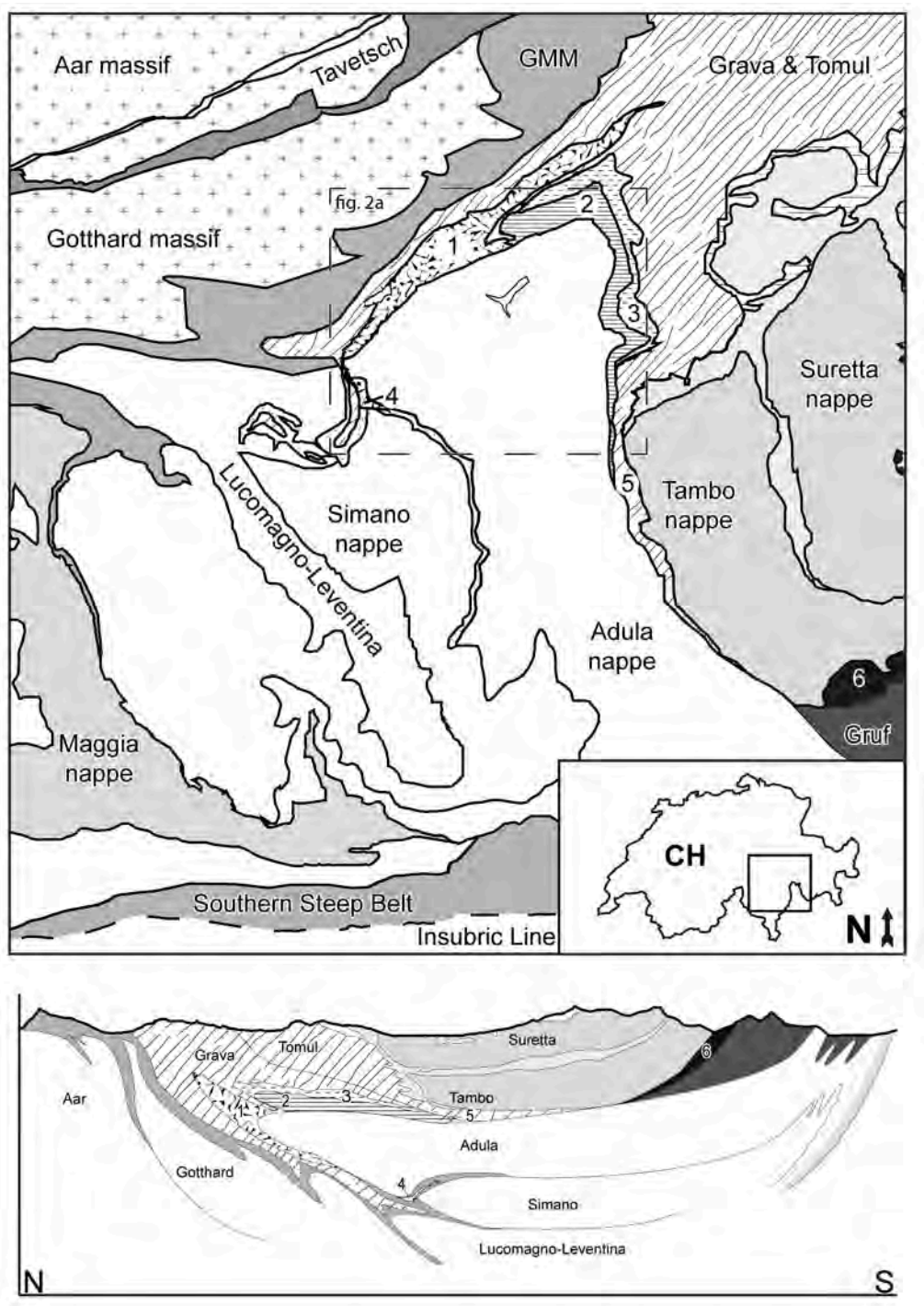

Fig. 1 a) *Tectonic map of the Central Alps. Modified from Spicher (1980).* ***b)*** *Simplified tectonic profile trough the Central Alps, modified after Schmid et al. (1996) and Galli et al. (2011). 1) Piz Terri-Lunschania zone. 2) Lower and upper Valser slices. 3) Aul unit 4) Soja unit. 5) Misox zone 6) Chiavenna peridotite. GMM) "Gotthard-Massivisher-Mesozoikum".*

dolomites, is of Helvetic type (Amman, 1973; Baumer, 1964).

The Molare synform (Amman, 1973) separates the Lucomagno nappe from the overlaying Simano nappe, a thick and complex recumbent gneissic-body that preserves a sole of Triassic cover. The sediments of the upper normal limb of this nappe form the lower limb of the north Claro syncline (Figure 1 and 2a), a structure interpreted as a nappe separator between the Simano and the overlaying Adula nappe (Maxelon & Mancktelow, 2005).

Apparently in the core of the Claro syncline, there is the thinner Soja unit, whose precise tectonic position is still an open

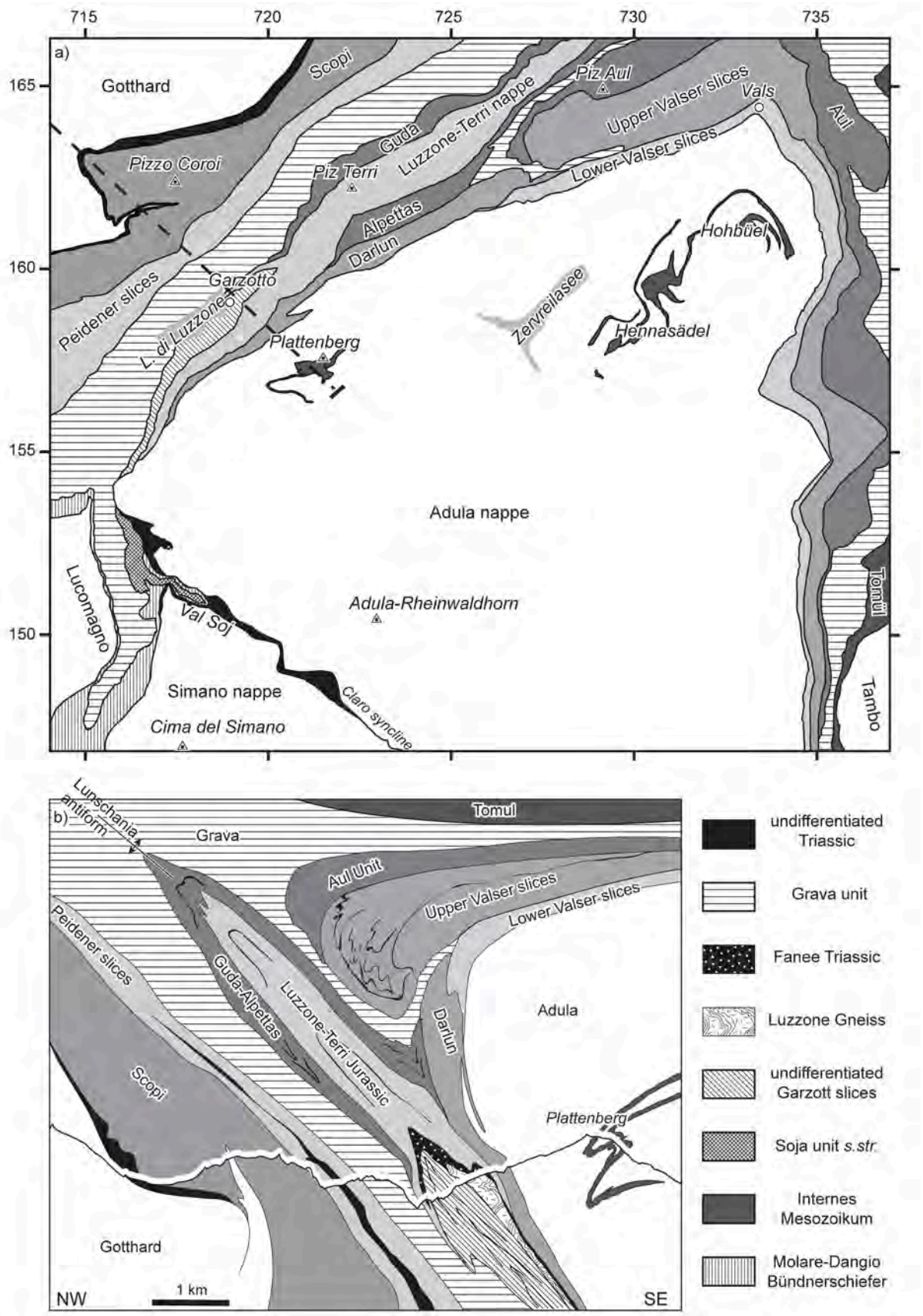

Fig. 2 a) *Tectonic map of the Study area, modified from Berger & Mercolli (2006); Jenny et al. (1923); Wiederkehr et al. (2008) and personal observations.* ***b)*** *Simplified tectonic profile through the study area, trace of profile in figure 2a.*

question (Argand, 1918; Jenny et al., 1923; Egli, 1966; Galster et al., 2010). The unit is enclosed tectonically into allochtonous metasediments (Molare-Dangio Bündnerschiefer after Probst, 1980).

The Adula nappe is a large tectonic unit that overlies the Simano and Soja units. Its internal structure is extremely complicated (e.g. Jenny et al., 1923; Löw, 1987; Berger et al., 2007; Nagel, 2008). It mainly consists in a basement made of Paleozoic and older para- and orthogneisses with associated metabasites and a few ultramafic lenses, assembled during the Variscan (and older?) orogen and intruded by late Variscan granitoids, such as the Zervreila orthogneiss (~293 Ma; Cavargna-Sani et al., 2010). Near the front of the nappe (figure 2) the basement is at several places coated by a thin, highly deformed metasedimentary cover that also forms isoclinal folds of multi-kilometric amplitude penetrating deep into the basement (the so-called "Internes Mesozoikum" of the classical literature; Jenny et al., 1923; Löw, 1987). The lithological heterogeneity, the presence of intercalated Mesozoic bands and the relatively frequent existence of eclogite boudins (of both Alpine and Variscan age; Liati et al. 2009; Herwatz et al., 2011) suggested to some authors that the Adula nappe was a lithospheric mélange rather than a coherent unit (e.g. Trommsdorf, 1990; Engi et al., 2001).

Above the Adula nappe and below the Middle Penninic (Briançonnais) Tambo nappe, there is the Misox zone (Gansser, 1937), characterized by thick sequences of mostly Cretaceous calcschists (the so-called Bündnerschiefer) with few basement slices and intercalated Jurassic MORB-type metamafics and rare serpentinites (Dürr et al., 1993; Gansser, 1937; Kupferschmid, 1977; Liati et al., 2005; Nabholz, 1945; Steinmann, 1994; Steinmann & Stille, 1999). The Misox zone consists of two nappes and three imbricated zones, respectively and from top to bottom these are: the Tomul and the Grava nappes (with their basal mélanges), the Aul unit, the Upper Valser and the Lower Valser slices ("Valser Schuppen") (Wyss & Isler, 2007).

To the north the Grava nappe is folded by the Lunschania antiform (a fold formed during a post-nappe folding phase) below the Adula nappe (figures 1b and 2b). Between these two nappes and in the core of the Lunschania antiform there is the Piz Terri-Lunschania zone consistsing of imbricated slices of metasediments (figure 2). At the bottom of the zone, near the Luzzone lake, the gneissic substratum of the lowest slice is exposed. The gneiss, mainly derived from Verrucano, was classically considered as the northern continuation of the Soja unit (Egli, 1966; Jenny et al., 1923; Kupferschmid, 1977; Probst, 1980, Wiederkehr et al., 2008). Recently Galster et al. (2010), based on stratigraphic arguments, separated the Verrucano in the Piz Terri-Lunschania zone from the Soja nappe and proposed an Ultra-Adula origin (i.e.: the homeland was located in a more internal position relative to the Adula) for the zone. Currently the Piz Terri-Lunschania zone is divided in 3 different groups of tectonic elements, from bottom to top: the Luzzone-Terri nappe, the Darlun zone and the Guda-Alpettas zone (Galster et al., 2010; Kupferschmid, 1977; Probst, 1980). In this contribution we will add a fourth group of tectonic elements that is located at the bottom of the zone: the Garzott slices (figure 2, see section 3.5.2).

5.3. Stratigraphic data

We present 10 synthetic stratigraphic sections from 7 units located in the Lower Penninic of the Central Alps (table 1). Some of these sections have already been presented in the literature, but new structural observations permit to reinterpret their stratigraphic content and to integrate it in the frame of modern Alpine Stratigraphy. Others sections have recently been investigated and are presented here for the first time.

In this section we introduce a new group of Triassic facies that we name "dolomie bicolori". This group consists in a characteristic alternation of cm to metric yellow and grey dolomitic beds. The colour of the yellow beds is a pale pastel yellow or locally a more accentuated lemon yellow. The grey in itself is an ash grey, sometimes darker with a drift towards a grey-violet tint. Careful observations in the "dolomie bicolori" reveal that the chromatic alternation is partly enhanced by

folding, but it is also an original sedimentary feature. A first dark-grey, locally marly, dolomitic bed marks the beginning of the bichromatic alternation.

The "dolomie bicolori" are also exposed in the Campo Lungo area (Western Simano nappe), where they are described in detail by Bianconi (1971).

5.3.1. The Simano nappe

Two different groups of facies characterise the sedimentary cover of the Simano nappe: one is observed along the upper and normal flank in the SE of Val Soj (lower limb of the Claro syncline, Figure 1 and 2), the other outcrops especially around the front in the NW of Val Soj and in the lower limb of the eastern Simano. The most striking difference is the presence (respectively absence) of the "dolomie bicolori" in one limb (upper) compared to the other (lower).

5.3.2. Soja unit s.str.

The stratigraphic column described for the Soja unit *s.str.* can be extended to the entire pile of sediments that separates it from the overlaying Adula nappe.

The unit is complexly folded and shows a core of old polycyclic gneiss. Cover sediments are best developed in the upper part of the unit, above the polycyclic basement, but the presence of arkosic sandstones and conglomerates (Soja Verrucano) on both sides of the polycyclic gneiss suggests the existence of an anticline folding the Soja unit.

The "dolomie bicolori" characterise the Triassic Formations (figure 3a)

5.3.3. Adula nappe

Among the several occurrences of the Mesozoic cover of the Adula, we describe the most significant and best-exposed outcrops. These are: 1) the area around the Plattenberg summit (3041m). The area is characterised by complex folding (Egli, 1966; Jenny et al., 1923; Löw, 1987), but thanks to the high altitude the outcrops are of excellent quality (figure 3b). A detailed stratigraphic description of this area is given in Cavargna-Sani et al. (2010a). 2) the Hennasädel cliff (2466 m), where the stratigraphic column is complexly folded (Zulbati, 2008) but still recognizable (e.g. Van der Plas, 1959). 3) the Hohbüel hill (2426m), where the stratigraphic section lies in an overturned position below the flat hill.

See figure 2a for outcrops locations.

Noteworthy are the stratigraphic nature of the contact between basement and cover and the presence of the "dolomie bicolori" in the three sections. At the Plattenberg and at the Hennasädel, where the stratigraphic column is more complete, there are several lines of evidences suggesting important sedimentary gap and the presence of syn-sedimentary faults.

5.3.4. Valser slices

The stratigraphic content of the Lower Valser Slice differs from that of the Upper Slice. Triassic lithologies and well-known marker horizons are missing in the Upper Valser Slice, thus we focus especially on the Lower Valser Slice, where the "dolomie bicolori" are well developed. Table 1 reports the uppermost Triassic occurrence in the lower Valser slice, directly below the thrust of the Upper slice (Wissflue cliff, 1km SE of Vals)..

	Simano nappe		Soja unit	Adula nappe		
	Lower limb	Upper limb	Soja unit s.*str.*	Plattenberg (fig. 3b)	Hennasädel (fig. 3c)	Hohbüel
younger than Triassic	Unknown	Unknown	Unknown	- Plattenberg Formation: dolomitic breccia with quartzitic to dolarenitic matrix. The Breccia contains siderolithic pebbles and presents several dolarenitic to calcarenitic intercalations. One of this intercalations is studded with crinoidal plates. The uppermost part of the breccias contains some intercalations of pure limestone bed. - Coarse-grained micaceous quartzite, only locally present.	- Alternating series of calcschists and impure marbles. - Pure marble (>10m), the fresh rock is banded, especially at the basis (cm alternation of white and light-blue marble). - Sandy marble, the marble lost rapidly (<50cm) all the impurities upsection. - Metasandstone (<1m), it is mainly composed of quartz-feldspar and minor amount of micas, brown calcite and dolomite.	Unknown
Triassic	- Tabular and yellow dusty dolomite with intercalations of a granular dolomite (Zellen Dolomite) - Coarse-grained arkose with few intercalations of a grey quartzite. The arkose is richer in dolomite and calcite upsection.	- "Dolomie bicolori". - Grey and massif quartzite.	- The series is cut by the thrust of the Molare-Dangio Bündnerschiefer (Section 2, fig 1 and 2). - Sugary white massif dolomite, whose bright and massif aspect vanishes upwards. - "Dolomie bicolori". - Dark yellow dolomite (5-8m), impure at its base. - Alternation (1m) of quartzite, impure marble, calcareous micaschists and impure dolomite. - Grey and massif quartzite, it becomes rich in micas upsection.	- "Dolomie bicolori". - Dark yellow dolomite. - Carbonate-rich micaschists. - Thin white grey quartzite, in sharp contact with the basement.	- "dolomie bicolori". - Pale yellow or off-white dolomite. - Carbonate-rich micaschists with few thin intercalations of a sandy and micaceous dolomite. - Grey quartzite, partly conglomeratic at its basis. It becomes rich in impurities upsection.	- "Dolomie bicolori". It starts with a first dark-grey bed. - Homogeneous dark-yellow dolomite (2m). - Marble (1m), it can be white or blue and it is intimately intercalated with several centimetric dolomitic beds. - Quartzitic and calcareous micaschists (<1m). - Grey quartzite (<1m), in sharp contact (reversed) with the basement.
older than Triassic	- Old polycyclic para- and orthogneiss.		- Arkosic sandstones, few conglomeratic intercalations (the so-called Soja Verrucano) are present between the arkosic sandstones and the overlying quartzite. - Old polycyclic gneiss, locally with lenses of amphibolites.	- Garenstock Augengneiss with eclogitic boudins (Cavargna-Sani et al., 2010a; Jenny et al., 1923).	- Heterogeneous pre-variscan basement.	- Old paragneiss.

Table 1. *Descriptions of the stratigraphic content of the differnet units discussed in section 3. See section 4 and figure 8 for more precise stratigraphic correlations. The "Lias Basis Quartzite" and the "Basale Stgir" are probably Rethian (Triassic), but since its lithological character is even Liassic (Infralias) they are classed in the "Younger than Triassic" row. We limit to the Triassic row only the typical Triassic lithologies (e.g. Melser, Roti, Quartenschiefer).*

Valser slices		Piz Terri-Lunschania zone		
Lower Valser slices	Garzott slices	Luzzone-Terri nappe		Güda-Alpettas zone
younger than Triassic				
Unknown	Above an erosive surface the sequence is sealed by a coarse and monomicte dolomitic breccia with a quartzitic matrix. Locally the breccias are deposited even directly above the gneissic basement (figure 4), in which case it is always an altered phyllite or a green chlorito-schists (rubefied and iron-rich in its uppermost part). Laterally and upward the breccias can evolve towards a polymictic breccia intercalated with calcareous sandstones and quartzites. Coarse-grained reconstituted basement is also present and intercalated with monogenic dolomitic breccias in the lowest part of the series. Upwards and laterally the series evolve towards a more fine-grained calcschist rich in quartzitic beds, sandstones and shaly intercalations. Locally these lay directly on Triassic dolomites or on the gneiss.	**Terri schists:** - *Corai Formation*: Thin sole of black non-calcareous shales. - *Inferno Formation*: thick sequence of non-calcareous shales in the most internal part of the nappe. The calcareous content increases downsection and towards the front of the nappe (marls to marly limestones). The upper part contains intercalations of carbonate-rich and sandy schists. - *Stgir Formation*: thick (50-100m) sequence of marls, shales and few thin beds of sandstone, limestones or dark quartzites. The alternating series is sealed by a white, weakly calcareous and very fine-grained quartzite (coarser in the frontal part of the nappe, it disappears backwards). Associated at the most internal occurrence of the quartzite there is an encrusted surface (condensation surface) - *Lias basis Quartzite and basal Stgir series*: the Quartenschiefer contains few thicker dolomitic beds (max 1m) in the upper part and is covered by a coarse-grained dolomite-rich sandstone (1-2m). The Dolomite content of the sanstone decreases upwards and is progressively replaced by a shaly matrix. A black, non-calcareous, level of shale (1m) is omnipresent above the sandy shales. the non-calcareous shales become progressively calcareous upsection.	- Alternating series of marls and shales. - sandstones (10m). - Alternating series (10-20m) of marls, marly limestones and brown weakly calcareous shales. - *Gneissquartzite*: thick (5 to 100m) and heterogeneous detritic level with a weakly calcareous matrix. Several decimetric to metric microconglomeratic beds (rich in quartz and feldspars) alternate with more fine-grained sandstones, quartzites or sandy limestones. Few shaly intercalations appear upwards. At the basis the Gneissquartzite is conglomeratic and sporadically overlays a dolomitic breccia. - *Corai Formation*: black, partly sandy, non-calcareous shales (1m or less). - *Inferno Formation*: homogeneous sequence of marls and marly limesto ne. The calcareous content decreases upwards. - *Upper Stgir Series*: Sandstones and quartzites. - *Lower Stgir Series*: alternating sequence of marls, marly limestones and weakly calcareous shales. It is covered by an ammonite bearing marble (Arnioceras sp.). - *Basal Stgir*: Black non-calcareous shales.
Triassic				
- Dark-brown dolomite (cornieule). - "Dolomie bicolori" (30-40m), the series starts with a first dark-grey and marly dolomite (8m). Upwards the colour in the grey levels is lighter. In few levels is possible to observe an intense and fine lamination of sedimentary origin. - Brown dolomite (1-2m) - Blue sandy (10%) marble (2-4m) rich in micas and dolomitic impurities, with hints of bioturbation. It is a reduced and metamorphosed vermiculated limestone. - Dark-brown and sandy dolomite. - Micaceous and dolomitic quartzite. - 10-20 cm gap. - White and fine grained quartzite.	The dolomitic formation ends with an erosion surface that can cut at any level. - Monotonous pale yellow dolomite. - Sequence of off-white dolomites alterna ting with light grey marly dolomites. Locally the alternating dolomites are more pigmented and it is thus possible to recognize the "dolomie bicolori". - Brown dolomite (1m). - Marble with hints of bioturbation (2-4m). - Brown dolomite. - Fine-grained quartzite with a grey or reddish arkose at the basis.	**Fanee Triassic:** - Pale yellow dolomites rich in green phyllitic intercalations (Quartenschiefer). - Banal pale yellow dolomites (30-40m, dolomies blondes). - Intraformational dolomitic breccias (1-2m, Clot-lacime Formation). - Banded and finely laminated ash-grey dolomites, weakly calcareous. (20m, Champcella Formation). - Vermiculated limestone enclosed in two dolomitic beds (15-20m, St-Triphon Formation, fig 4). - At the basis there is an alternating series of quartzites, micaschistes and brown dolomite (5m, Dorchaux member, fig 4a). - white and fine-grained pure quartzite, partly conglomeratic at its basis.		
older than Triassic				
- Coarse-grained conglomerate, laterally it is substituted by a green schist. - well-bedded arkosic sandstone rich in ankeritic spots and conglomerates.		**Luzzone gneiss:** - coarse-grained conglomerate (>5m) composed of cm quartz pebbles in a quartzitic matrix. - Arkosic sandstones (20-100m) scattered with abundant ankeritic spots and rich in conglomeratic intercalations and green micaschists.		Unknown

Table 1.*Continued*

5.3.5. The Piz Terri-Lunschania zone and its tectonic substratum

The Luzzone-Terri nappe

The stratigraphy of the Luzzone-Terri nappe has recently been discussed by Galster et al., (2010). These authors highlighted the Briançonnais affinity of the gneissic "basement" (Luzzone gneiss) and the Triassic cover (Fanee Triassic, figure 4). On the other hand the Liassic cover, in stratigraphic contact (figure 5) with the Briançonnais Triassic, is of clear Helvetic affinity.

The arkosic sandstones in the Luzzone gneiss displays clear analogies with the Moosalp Formation (Permian) in the external part of the Briançonnais paleogeographic domain (Thélin, 1982; Genier et al., 2008). The overlying conglomerate with its quartz pebbles is similar to the Embd Member (upper Permian) of the external Briançonnais (Genier et al., 2008) or more generally to the Verrucano Briançonnais (Trümpy, 1966). The Fanee Triassic displays definite analogies with the Triassic Formations that characterise alpine units classically assigned to the Briançonnais Paleogeographic domain elsewhere in the Alps (St-Triphon, Champcella and Clot-la-Cime Formations)

In the Liassic cover we recognise the Helvetic Stgir, Inferno and Coroi Formations that characterise the so-called Gotthard-Massivisher-Mesozoikum in the Lukmanier-Pass area (Baumer et al., 1961) or the cover of the Gotthard Massif near the Nufenen-Pass further to the West (Liszkay, 1965).

The Garzott slices

Detailed fieldwork and mapping in the core of the Lunschania antiform around the Luzzone Lake reveal the existence of several tectonic objects below the thrust plane of the Luzzone-Terri nappe (figures 2 and 11). These objects, that we call Garzott slices, are the best candidates to represent the original tectonic substratum of the Luzzone-Terri nappe. The stratigraphic content of these slices is fundamental to link the Luzzone-Terri nappe, together with its Briançonnais content, to the Helvetic margin.

Our mapping suggests that the Verrucano of the Luzzone-Terri nappe that on its back transport the whole Piz Terri-Lunschania zone, is only partly folded by the Lunschania antiform and does not constitutes its core at all (fig 2b).

Moreover the Verrucano body of the Luzzone-Terri nappe (the former northern Soja nappe, Galster et al., 2010) which was considered by previous workers as folded in a tight anticline does not show any reversed flank and is simply thrusted above several slices of gneiss and dolomites that have previously been erroneously attributed to its original inverse limb (compare our figure 2 with figure 25 in Probst (1980) and figure 3 in Wiederkehr et al. (2008)). Only the originally more advanced part of the nappe developed an inversed limb by fold ramps and has been subsequently refolded by the Lunschania antiform.

An independent confirmation to our new interpretation arises from the stratigraphy, which is different from that established in the Luzzone-Terri nappe (absence of the Embd member as well as the Champcella and Clot-la-Cime Formations, the latters are replaced by an analogue of the "dolomie bicolori").

The small river east of "Alp Garzott" is filled with blocks of breccias and conglomerates fallen down from the Garzott slices exposed in the cliff south of the river. Some megaclasts embedded in a pelitic or sandy matrix show a strong hydraulic fracturation or even a cataclastic fabric, features not observed in the surrounding matrix (perfectly preserved). Fracturation, comminution and fluids precipitation occurred prior to the incorporation of the block into the matrix. Moreover in the uppermost part of the Triassic series (which is cut by an erosion surface) it is possible to observe a deformed tectonic breccia preserving former "jigsaw puzzle" structures (tarasewicz et al., 2005).

These observations strongly suggest the presence of a paleofault that controlled the sedimentation in the Garzott slices.

Guda-Alpettas zone

The Guda-Alpettas zone is divided in two parts. These are the Alpettas zone in the upper limb of the Lunschania antiform and the Guda zone in the lower flank. The two zones are interpreted to merge in only one zone at the hinge of the fold (Kupferschmid, 1977; Probst, 1980).

The Güda zone is characterised by two m to hm quartzitic beds, the so-called Gneissquarzite (Kupferschmid, 1977; Probst; 1980; Uhr, unpublished; Wyss & Isler, 2007). The thickness of the two beds decreases more or less simultaneously towards the SW and both disappear before reaching the Luzzone Lake. Our observations reveal that their disappearance is a consequence of folding: the two quartzitic beds are the same stratigraphic level folded around a tight synform which folds the whole Güda zone and ends near the banks of the Luzzone Lake. The fold is an anticline reversed by the Lunschania antiform (figure 7).

If looked under this perspective, the stratigraphic content of the Güda zone is straightforward; above a remnant of Triassic rocks it is possible to recognise the Stgir (with its Sinemurian ammonites occurring in a limestone bed at the top of the Formation), the inferno and the Coroi Formations.

The described sequence is folded in-between the Gneissquarzite (see above). The contact between the detrital formations and the underlying shales (Coroi) is always sharp (in the original upper limb of the "Güda anticline" the basis of the Gneissquarzite can be erosive below the Coroi formation). In contrast the upper part of the Gneissquarzite it pass in a transitional way into an alternating series of marls and marly limestones.

On the other side of the Lunschania antiform, in the more internal Alpettas zone the stratigraphic content is similar (Kupferschmid, 1977; Probst, 1980), but a reef limestone (Geyer, 1977) replaces the Ammonite bearing limestone and in general all the facies suggest shallower conditions. The Gneissquarzite can be erosive even below the inferno formation and is in general coarser (quartz grains up to 5mm).

5.4. Stratigraphic correlations

For the stratigraphic correlation only few paleontological data are available. However some correlations can be proposed based on a highly variable vertical record, several marker beds and the possibility to compare our sections with similar well-dated stratigraphic sections located elsewhere in the Alps. Therefore we are able to trace some lines of correlation among the different sections (figure 8).

The restoration of the different units to their original relative positions in the Mesozoic is a combination of both stratigraphic and structural criteria. With the exception of the Piz Terri-Lunschania zone and Soja unit positions it does not differ substantially from already published restorations (e.g. Probst, 1980; Schmid et al., 1996; Wiederkehr et al., 2008 and 2009).

5.4.1. Permian and lower Triassic

The "eotriassic quartzites" are the first well distributed marker bed. Some sections show a thick sedimentary formation already below this level. These sediments can be seen as a "Verrucano" and considered late Paleozoic-early lower Triassic in age (Dössegger & Trümpy, 1972; Trümpy, 1966;).

In the Briançonnais basin the Quartzites are lower Triassic. For the Helvetic realm, in the Mont Blanc area the arkoses are

Fig. 3 a) *The "Dolomie bicolori" with the characteristic metric, decimetric and centimetric chromatic banding. Soja unit at Ri della Foppa, 1km NNE of Aquila.* ***b)*** *The Plattenberg outcrop, "Internes Mesozoikum" in the eclogitic Adula nappe. GS=Garenstock ; TrQ=Triassic Quartzite ; MS=Micaschists lDol= Impure Dolomite ; DolBi= Dolomie Bicolori ; Breccia= Plattenberg Breccia.****c)*** *The Hennasädel: outcrop of "internes Mesozoikum" in the Adula nappe. The partly eroded pre-rift "dolomie bicolori" (North-Penninic-Triassic) are stratigraphically overlain by the post-rift Upper Jurassic pure marble (Quinten Formation). It is noteworthy the lacking of syn-rift sediments. 1) Dolomie Bicolori 2) microconglomeratic sandstone 3) pure marble 4) impure marble and calcschists. The white zig-zag line indicate the erosion surface at the top of the "Dolomie Bicolori". See text for further details.*

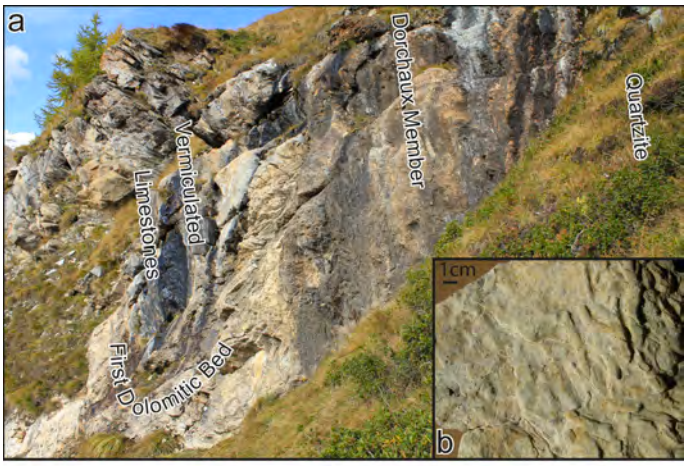

Fig. 4 a) *The Dorchaux member at the Basis of the St-Triphon Formation (Fanee Triassic) folded in a syncline. Further to the NW, at the opening of the fold it is possible to observe a second dolomitic bed, the Champcella and the Clot-la-Cime Formation.* ***b)*** *exemple of a Vermiculated Limestone from the Fanee Triassic in the Luzzone-Terri nappe. Modified after Galster et al. (2010).*

Fig. 5 a) *stratigraphic transition from the Briançonnais Fanee Triassic to the Helvetic Terri Schists in the Luzzone-Terri nappe. This contact is unique in the Alps and has important paleogeographic consequences (Galster et al., 2010, see text for details).* ***b)*** *Detail of figure 5a showing the perfect transition from the quartzites and the dolomitic sandstones at the top of the yellowish Triassic lithologies to the shales at the basis of the black Liassic formations (see text for details).*

lower to early middle Triassic (Avanzini & Cavin, 2009) and in the Aar massif they are Anisian (Gisler et al., 2007).

5.4.2. Middle-Upper Triassic

In some sections, there is a clear transition from silicoclastic to carbonate sedimentation, which spans from few centimetres to some meters testifying ephemeral conditions (Dorchaux member, figure 4a) prior to the definitive drift towards carbonate sedimentation.

The progress of the carbonate front can be followed from the Luzzone-Terri nappe, where the Dorchaux member spans 5m, to the Adula nappe, where the same horizon is progressively reduced to a few centimetres (we interpret the carbonat-rich micaschists as a reduced Dorchaux member). The Dorchaux member in the Briançonnais basin is early Anisian (Baud, 1976, 1987).

The St-Triphon Formation is clearly present in the Luzzone-Terri nappe but it can be followed only in the Garzott slices

till the Valser slice, then it is progressively reduced, first to few limestone beds almost intercalated into a more dolomitic formation and finally to dark yellow or brown dolomitic beds located directly above the calcareous micaschists (Dorchaux). The St-Triphon Formation is completely absent in the Simano and Lucomagno nappes.

The St-Triphon Formation in the Middle Penninic is dated as Lower to Middle Anisian (Baud, 1976, 1987).

The Champcella Formation, present in an already reduced form in the Luzzone-Terri nappe is only a far kin of the "Dolomie Bicolori" of the Garzott slices. Some of its characteristics can still be observed in the Lower Valser slice but then they vanish in the "Dolomie bicolori" of the Adula nappe. The age of the Champcella formation is Upper Anisian to Lower Ladinian (Mégard-Galli & Baud, 1977), we extend this age to the Dolomie bicolori. This extrapolation seems to be confirmed by ladinian crinoids in the Campolungo "bicolored dolomites" of the western Simano nappe (Bianconi, 1965 pag. 574).

Fig. 6 *A detail of the contact between the altered iron-rich Garzott gneiss and the fresh Garzott breccias. Dol = dolomite ; Phyl=Phyllite.*

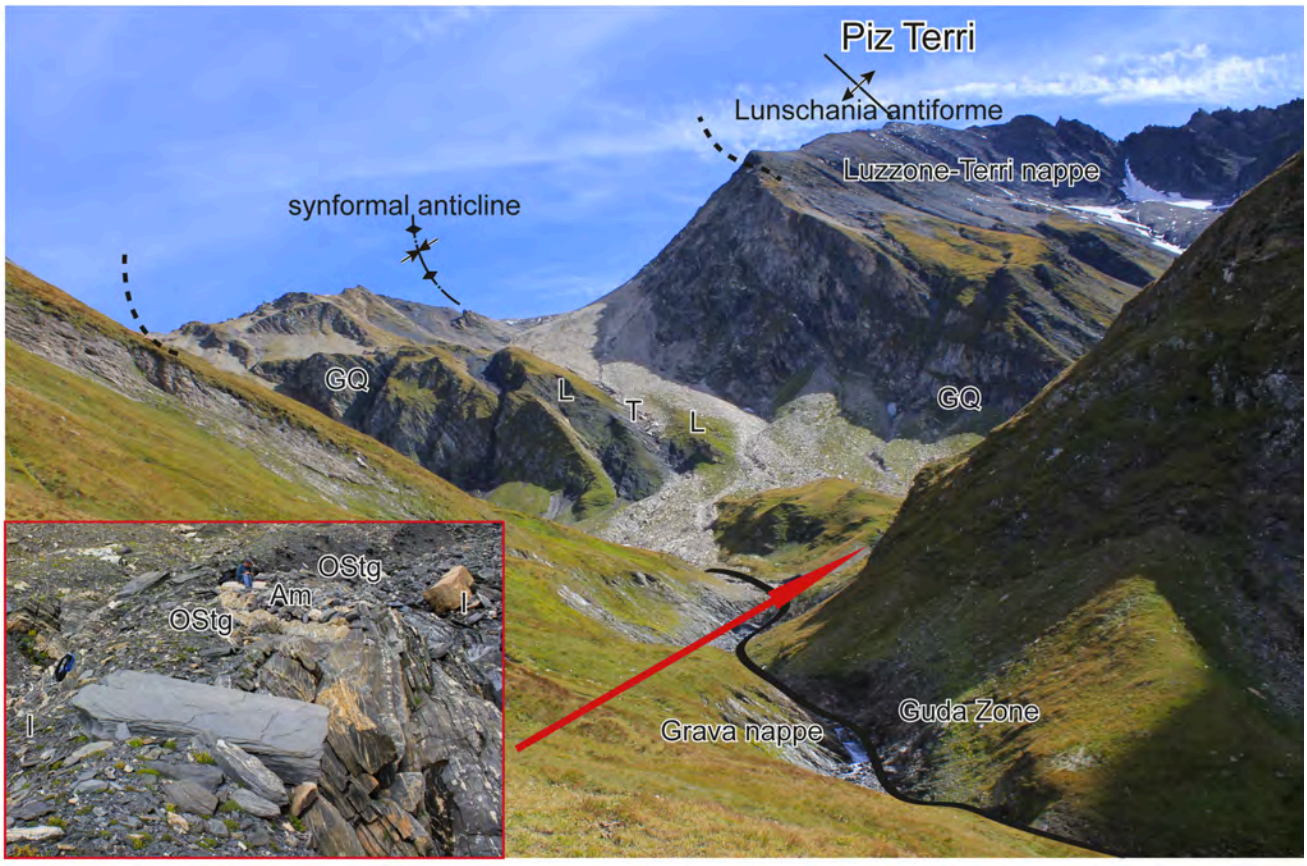

Fig. 7 *View on the Piz Terri and the Upper Guda Valley from the SW (point 2276m). The Grava nappe and the Guda zone are refolded by the Lunschania antiform below the Luzzone-Terri nappe (see figure 2b). The stratigraphic record in the Guda zone is enclosed in a synformal anticline. The fold's hinge is showed in the small box. The man is sitting on the Sinemurian ammonite limestone in the core of the fold. T=Triassic; L=Liassic; GQ=Gneissquarzite; Am=ammonite limestone (Sinemurian); Ostg=upper Stgir Serie; I=Inferno Serie.*

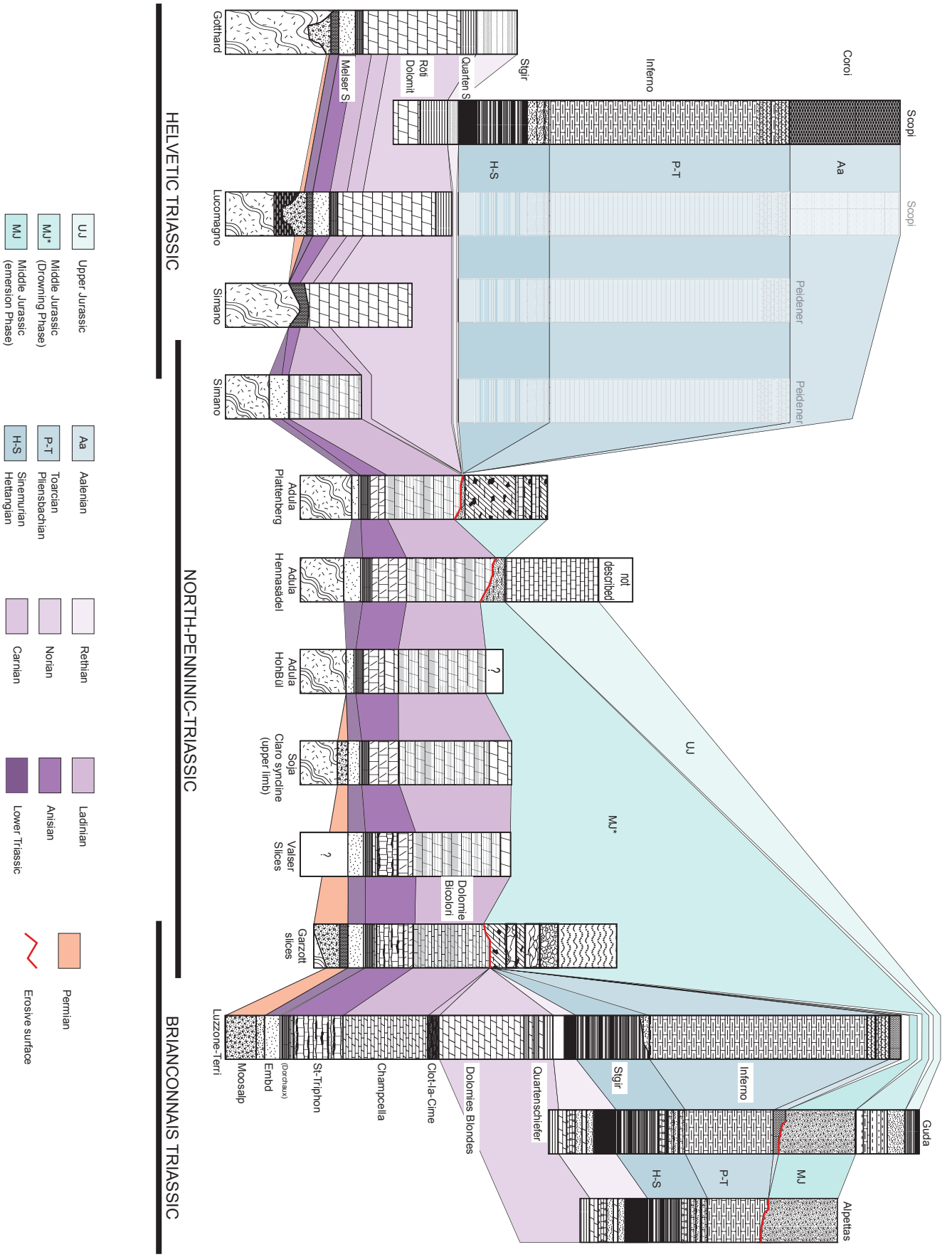
HELVETIC TRIASSIC
NORTH-PENNINIC-TRIASSIC
BRIANCONNAIS TRIASSIC
Gotthard
Stgir
Quarten S
Röti Dolomit
Melser S
Lucomagno
Simano
Simano
Coroi
Inferno
Scopi
Aa
Scopi
P-T
Peidener
H-S
Peidener
Adula Plattenberg
Adula Hennasädel
Adula HohBül
Soja Claro syncline (upper limb)
Valser Slices
Garzott slices
Dolomie Bicolori
not described
?
?
UU
MJ*
Luzzone-Terri
Moosalp
Embd
(Dorchaux)
St-Triphon
Champcella
Clot-la-Cime
Dolomies Blondes
Quartenschiefer
Stgir
Inferno
Guda
Alpettas
MJ
P-T
H-S
UU
Upper Jurassic
MJ*
Middle Jurassic (Drowning Phase)
MJ
Middle Jurassic (emersion Phase)
Aa
Aalenian
P-T
Toarcian Pliensbachian
H-S
Sinemurian Hettangian
Rethian
Norian
Carnian
Ladinian
Anisian
Lower Triassic
Permian
Erosive surface

Fig. 8 *Graphical summary of the Stratigraphic content of the studied units. The different sections are arranged following Galster et al. (2010) and new stratigraphic and structural observations (see sections 2, 3, 6 and 7). The stratigraphic sections of the Gotthard Massif, the Scopi and the Peidener zones are showed as a tool of correlation (modified after Baumer et al., 1961). The Lucomagno stratigraphy is modified after Amman (1973). The Jurassic series of the Scopi and the Peidener zones are extrapolated above the Lucomagno and the Simano Triassic (light colours). Note the stratigraphic superposition of an Helvetic Liassic above a Briançonnais Triassic in the Luzzone-Terri nappe as well as the presence of a new group of Triassic facies (North-Penninic-Triassic) between the sections with typical Briançonnais and Helvetic Triassic. See text for details and discussion on age assignments.*

The Clot-la-Cime formation has been recognised only in the Luzzone Terri nappe, In the Middle Penninic its age spans from the upper Ladinian to the Carnian (Megard-Galli, 1972; Baud & Megard-Galli, 1975). After the Carnian crisis the stratigraphic differences between the Briançonnais basin (especially its external part) and the Helvetic one are attenuated. The thick Briançonnais "dolomies blondes" cannot be distinguished from the Helvetic dolomitic formation in the absence of the middle Triassic part of the sequence, especially in metamorphic terranes.

The arkoses at the base of the external Simano Triassic are partly dolomitic, especially in their upper part and they are directly followed by a thick pale yellow dolomitic formation.

Considered the massif encroachement of the dolomies blondes (mor or less the Briançonnais equivalent of the Haupt Dolomit, Norian) we suggest that most of the dolomitic deposition in the external Simano and northward is a direct consequence of this phenomenon.

A confirmation to this scenario is suggested by few thin and extremely rare ash-grey marly dolomites (already reported by Ammann, 1973) intercalated at the basis of the Lucomagno Dolomitic sequence (the most external occurrences of an extremely reduced Dolomia Bicolore).

5.4.3. Rethian

The close association of quartzite, sandstones, dolomites, shelly-limestones, micaschists and black, non calcareous, shales is typical for the "Infralias" of the ancient authors, dated as Rethian-early Hettangian in the Glarner Alps (Trümpy, 1949).

5.4.4. Hettangian-Sinemurian

The attribution to the Hettangian and Sinemurian is based on the recognition of the Stgir Formation, which is dated by Gryphea *arcuata* and Arnioceras *sp.* directly below and inside the detrital input (Upper Stgir) (Baumer, 1964; Jung, 1963). The Stgir formation in the Güda zone, can be dated directly by the Sinemurian Arnioceras *sp.* found by A. Uhr (Unpublished, courtesy of A. Isler). The reef limestone in the Alpettas zone is dated as Sinemurian (Geyer, 1977; Kupferschmid, 1977; Uhr, unpublished). The paleontological findings allow a good correlation with the most typical Helvetic sections where similar facies are present. A good marker is the Lotharingian (upper Sinemurian) detrital input (e.g. Loup, 1992).

5.4.5. Pliensbachien-Toarcian

The inferno series is Post-Sinemurian and correlated with the Pliensbachian-Toarcian Sexmore series in the Glarner Alpen (Baumer et al., 1961). At this regard a Pliensbachian age fit well with the presence of a second detrital input that can be correlated with the Domerian detrital event in the Helvetic basins (Loup, 1992).

5.4.6. Aalenian

The Aalenian Dugny Formation in the French Alps (Epard, 1990) finds a perfect equivalent in the Coroi shales. The same equivalence can be done with the Aalenian in the Glarner Alps (Trümpy, 1949) as highlighted by Baumer et al. (1961). Locally in the basin the shaly non-calcareous formation starts already in Toarcian (Epard, 1990; Aubert de la Rue & Weidmann, 1966) and partly replaces the marly formation, it seems to be the same in the internal part of the Luzzone-Terri nappe (table 1).

5.4.7. Middle Jurassic

The Gneissquarzite is deposited directly above the Coroi Formation of probable Aalenian age and its detrital content (Qtz+Fsp) suggests the presence of an emerged land subjected to erosion. Since the Inferno and the Coroi formations in the Güda Zone are only weakly detritic we assume that this land emerged during or after the early middle Jurassic or that this period coincide with a major current reorganisation in the basin.

The Plattenberg formation and the breccias in the Garzott slices includes dolomitic and calcareous pebbles of different type, none of these displays a facies different from Triassic or Lower Jurassic rocks, thus they can be considered Lower Jurassic or younger with a great probability of a middle Jurassic age (absence of pebbles from the Upper Jurassic limestone).

Moreover the Plattenberg Breccia reworks siderolithic pebbles, contains crinoids and follows a quartzitic microconglomerate above an eroded Triassic dolomite. From this we deduce that its formation is subsequent to an emersion phase and happened during a drowning phase.

The most suitable period for these formations is the Middle Jurassic, a period during which generalised emersion is observed in several domains (e.g. Badoux & Mercanton, 1962; Baud & Masson, 1975; Trümpy, 1945). The Gneissquarzite is considered as deposited during the emersion phase (Aalenian to Bathonian?), the Garzott slices, the Plattenberg breccias and the formations above the Gneissquarzite during the drowning phase (Bathonian to Oxfordian?).

5.4.8. Upper Jurassic

The thick and extremely pure marble at the Hennasädel recalls the Kimmeridgian-Thitonian marbles in the Quinten Formation (e.g. Anatra, 1986; Kugler, 1987). It is deposited above an eroded surface and lies directly above a sandstone bed locally microconglomeratic at its basis.

This situation is identical to the stratigraphy of the Antabia group, recently established in the lower Penninic Antigorio nappe (Matasci et al., 2011). We therefore correlate the stratigraphy at the Hennasädel with the Antabia group for which an upper Jurassic age has been proposed (Matasci et al., 2011).

The sandstones below the “Upper Jurassic” marble can be considered as late Middle Jurassic or even early Upper Jurassic (drowning phase, see above).

5.5. The Stratigraphic signature in the local context

Prior to discuss the integrated interpretation of the tectonostratigraphic record and its eventual contribution towards a better understanding of both preorogenic and orogenic history of the Central Alps we need to highlight some important aspect of some sections.

5.5.1. The Garzott slices

The discovery of the Garzott slices is important for the regional tectonics of the Piz Terri-Lunschania zone and adds important information even on the pre-orogenic significance of the zone.

The Stratigraphic record around the Luzzone Lake indicates the presence of paleo-faults.

In rifted margin the existence of high angle normal faults related to extension is known since the beginning of modern basins analysis (e.g. Vening-Meinesz, 1950). More recently several studies highlighted the existence of low angle normal faults in distal rifted margin (e.g. Froitzheim & Eberli, 1990; Witmarsch et al., 2001), these faults that act as detachments, are an efficient mechanism to thin the continental crust (Lavier & Manatachal, 2006).

Masini et al. (2011) described in detail the evolution of the Samedan basin (Lower Austroalpine, Graubunden), which is convincingly interpreted as a supra-detachment basin. The signature for supradetachment basins as indicated by Masini et al. (loc cit.) corresponds with the tectonosedimentary record observed in the Garzott slices (section 3.5.2). The analogies are: 1) the evolution from monomictic (dolomitic) breccias towards coarse-grained reconstituted basement and 2) the interbedding of these two deposits, testifying the simultaneous availability of two completely differents sources (Hangingwall vs Footwall); 3) the upwards evolution to polymictic breccias and sandstones (reddish litharenites) reworking pre- and early syn-rift sediments (Triassic and Liassic) and 4) the sealing with a more fine-grained sequence of shales and more mature arkosic beds. The distal turbidites reported by Masini et al. (2011) in the Samedan Basin are not actually recognised in the Garzott slices.

On the light of these analogies we propose that the Garzott fault and the associated sediments testify the presence of a "supradetachement" basin bordered by allochtones (the Garzott slices and maybe even the biggest Luzzone-Terri nappe).

The Ultra-Adula origin of the Piz Terri-Lunschania zone (Galster et al., 2010; see sections 2 and 7.1), its rootless character and its close relationship with "ophiolitic" units (Valser slices and Aul unit) is in agreement with this proposed scenario.

5.5.2. The Guda-Alpettas zone

The Gneissquarzite in the Guda-Alpettas zone has previously been interpreted as derived from the erosion of a southerly located emerged land. Since the proximity to the Adula front, the different authors proposed the Adula as a potential source (Kupferschmid, 1977; Probst, 1980; Wyss & Isler, 2007). The homeland of the Guda-Alpettas zone was probably located south of the Adula, being the zone thrusted on top of the Luzzone-Terri nappe, which in turn has an Ultra-Adula origin (sections 2 and 7.1). Thus the southerly-located emerged land is probably not the Adula rise. But the interpretation of an existing emerged land is still valid and even reinforced by some coal finding associated with the Gneissquarzite (Galster, 2010).

5.5.3. The Adula nappe

Curiously the interpretation of an emerged Adula is still valid. In fact the stratigraphic record in the "Internes Mesozoikum" strongly supports the activity of distributed normal faults allowing the emersion of at least part of the Adula. Emersion is in particular proved by the siderolithic near the Plattenberg and suggested by Triassic erosion followed by drowning under high-energy conditions (crinoids).

Another interesting point outlined by the new stratigraphic results is the coherency of the stratigraphic record in the northern

Adula nappe. This coherency speaks against a lithospheric mélange created in a subduction channel (e.g. Engi et al., 2001; Trommsdorf 1990) and suggests that the northern Adula is a coherent nappe. A possible scenario is that the presence of Paleo-faults, systematically associated with the "Internes Mesozoikum", has played a major role in creating the "Internes Mesozoikum". During an early phase of subduction the reactivation and inversion of the faults preserved the basement-cover contact by a mechanism where the sediments onto the hanging block are trapped by its inversion above the footwall. A similar scenario has been proposed by Krayenbuhl & Steck (2009) in order to explain the complex basement-cover relationship in the Jungfrau syncline (external massifs).

The proposed mechanism could prevent sediments off scraping and allows the preservation of the cover even in highly deformed nappes submitted to eclogitic conditions.

5.6. Discussion on the Preorogenic history

5.6.1. The North Penninic Triassic: The missing link between the Briançonnais and the Helvetic?

The Briançonnais character of the Permo-Triassic in the Luzzone Terri nappe has been demonstrated recently by Galster et al. (2010). The Helvetic character of the Triassic formations in the Gotthard massif and Lucomagno nappe is obvious and already evoked by several workers (Baumer et al., 1961; Brunschweiler 1948; Fehr, 1956; Probst, 1980). Which of the two categories of facies represents at best the Triassic characterised by the "dolomie bicolori" that is located in-between? For the further discussion we will call the Triassic characterised by the "dolomie bicolori" the North-Penninic-Triassic.

The scarcity of limestones and the abundance of dolomites in the North-Penninic-Triassic argue in favour of an Helvetic character. On the other hand, thanks to its sedimentological characteristics, the "dolomie bicolori" evoke the Champcella Formation at Fanee, which in turn is an external equivalent of the Champcella Formation typical for the Briançonnais Triassic.

The Valser and the Garzott slices are instructive in this regard. With the vermiculated limestones, they share the same basis with the Luzzone (Briançonnais) Triassic but continued upward with the "Dolomie Bicolori". Then, toward the more external units (Adula and Simano), the St-Triphon Formation is progressively reduced, but the "Dolomie bicolori" are still present.

The age of the "Dolomie bicolori" is probably Ladinian, as testified by the exceptional fossils founding of Bianconi (1965, pag 574) in the Campolungo area where the "Dolomie bicolori" are well expressed in the Simano Triassic (see Bianconi, 1971). Thus the progressive facies transformation and the chronological equivalence support the idea that the "Dolomie bicolori" are an external equivalent of the Champcella Formation.

Moreover the following aspects are noteworthy: a) the adjacency of the North-Penninic-Triassic to the Fanee (Briançonnais) Triassic, b) the extremely reduced St-Triphon (Briançonnais) Formation at the basis of the most internal (Valser Slices) North-Penninic-Triassic and c) the fact that this reduced (or disappeared) equivalent is stratigraphically followed by a family of Ladinian facies that mimic a reduced Champcella (Briançonnais) formation. Therefor several line of evidences suggest that the North-Penninic-Triassic was deposited on the banks of the great Briançonnais basin. We propose that the units bearing this kind of Triassic represent the external limit of the Briançonnais Triassic Paleogeographic domain.

In its most external part, the Simano nappe (which is characterised by the "dolomie bicolori" in its internal part) shares the same Triassic that is normally ascribed to the Helvetic domain. A clear Helvetic Triassic is omnipresent over the immediately adjacent Lucomagno nappe and just to the north in the Gotthard massif (see section 2).

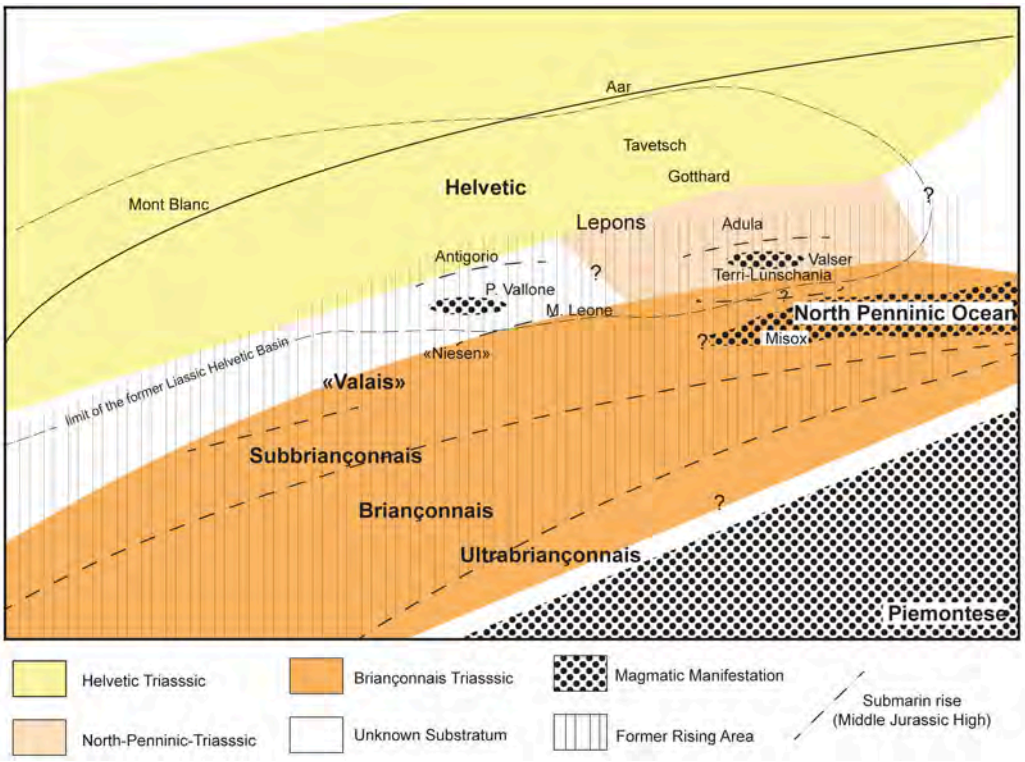

Fig. 9 *Upper Jurassic distribution of the Paleogeographic domains (bold script) and of the tectonic units (regular script) distinguished in the Central Alps. The former Antigorio (Matasci et al., 2011) and Adula high are now submarine rises that separate Helvetic basins from the North Penninic Basin. The former Briançonnais high is now a submarine rise that separates the North Penninc from the Liguro-Piementese Ocean. The term Lepons indicates the area that originated the future lepontine dome. The term "Valais" indicates the future location of the Valais Trough (see section 1). The Triassic Substratum is also represented, with large incertitude.*

These observations indicate that, during the Triassic, the Briançonnais Paleogeographic domain was located southwards from the Helvetic domain. It has probably been separated from the European plate sensu stricto by Jurassic rifting (see section 6.3). Therefore, the apparent exotic character of the Briançonnais Jurassic facies (Schardt, 1898) could be explained under this perspective rather than evoking a far travelled origin (e.g. Stampfli, 1993).

5.6.2. The Jurassic rifting and the associated subsidence: when and where?

An apparent astonishing situation that results from the stratigraphic record in the distal European margin, south of the Gotthard, is the absence of strong subsidence during the middle Jurassic, a period that correspond with the onset of magmatic activity in the penninic oceans (e.g. Hauser & Müntener, 2011; Manatschal et al., 2006). This situation is similar to that already documented for the Briançonnais domain and in the Middle Penninic units (e.g. Badoux & Marcanton, 1962).

In this section first we focus on the timing of rifting and subsidence evolution in the internal Helvetic and Lower Penninic nappes and then we propose some working-hypothesies in order to explain our observations (keeping in mind that, as highlighted by Trümpy (1976, pag. 262), "le role des hypothèses de travail n'est pas celui de fournir des solutions, mais avant tout de poser des questions").

The Jurassic stratigraphic column of the Scopi and Peidener zones in the "Gotthard Massivischer Mesozoikum" finds a natural continuation in that of the Luzzone-Terri nappe (Table 1 and figure 8) suggesting that the differents units originated from the same Liassic basin. But Helvetic conditions, that during Liassic time extended from the Tavetsch south of the Adula, into the Piz Terri-Lunschania zone, gently disappeared south of the Güda zone, where shallower conditions indicate

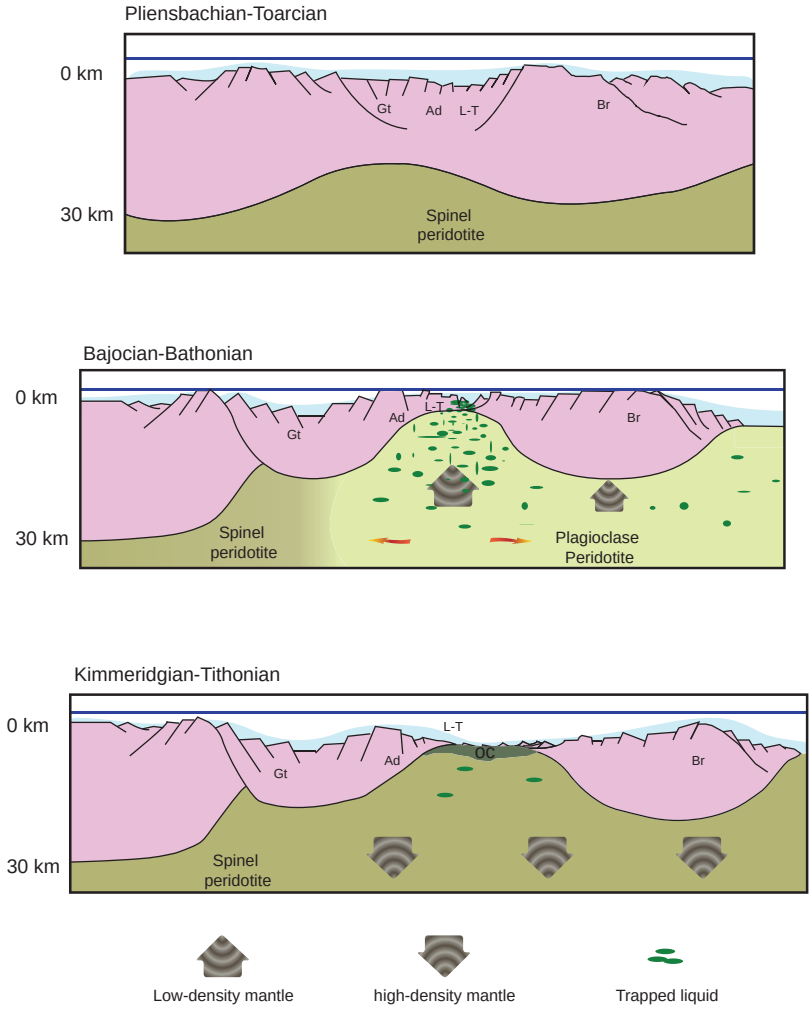

Fig. 10 *Schematic representation of a hypothetical evolution of the European lithosphere during the Jurassic Rifting.* ***Liassic:*** *The stretching phase leads to delocalized deformation on vast areas and the instauration of neritic to emi-pelagic sedimentation in several basins and subbasins that are bounded by high angle normal faults.* ***Middle Jurassic:*** *further extension allows asthenospheric upwelling and the beginning of magmatic activity in the future Liguro-Piemontese Ocean and partly even in the North Penninc. The Briançonnais ribbon is partly isolated from the Continental Europe by the formation of the North Penninic system of rises and basins. Heating by asthenospheric upwelling and decompression allow mineral phase transition (e.g. Spinel → plagioclase) in the lithospheric mantle leading to a decrease in density. Magmatic fluids trapped in the lithospheric mantle enhance the decrease in density.* ***Late Midle Jurassic-Upper Jurassic:*** *Protracted extension leads to extreme crustal thinning, mantle exhumation and important magmatic activity (pillow lavas) in the North Penninc Basin and spreading in the Liguro-Piemontese Ocean. Thermal relaxation near the continental margin leads to the lost of the buoyant lithosphere (Plagioclase → Spinel). The Briançonnais Microcontinent is definitively separated from the continental Europe by the North Penninic.*

Ad= Adula; Br= Briançonnais; Gt= Gotthard ; L-T= Luzzone-Terri; oc= oceanic crust.

the presence of the southern border of the Liassic Helvetic basin (figure 9).

At the beginning of Middle Jurassic, the area south of the Aar massif was being filled by the Aalenian shales, whose thickness is still remarkable in the Scopi zone (500m) but then is reduced drastically in the Peidener and the Piz Terri-Lunschania zone. In many sections the reduction is in part an artefact of tectonic off scraping, but not in the Güda zone, where the Coroi shales never exceed a few meters. If during Sinemurian and Pliensbachian time the deepest part of the basin was located in the Luzzone-Terri nappe (cf the Upper Stgir and the Inferno Formations), during the Toarcian it seems to migrate toward the external part of the basin (Gotthard and Tavetsch). The Middle Jurassic of the internal part instead suffered an inversion and emerged, as testified by the Adula and the Guda-Alpettas stratigraphy (Table 1 and figure 8).

This wide zone of emerged land is intimately associated with oceanic crust: the Misox zone and the Valser slices are rich in MORB-type metamafic (Dürr et al., 1993, Steinmann & Stille, 1999). For the Misox zone a Jurassic age is testified by U-Pb dating on zircon (~161 Ma, Liati et al., 2005), for the Valser slices it is supported by facies analysis (Steinmann, 1994). It is noteworthy that part of the magmatic activity is recorded in tuffites and others volcanoclastic manifestations (Kupferschmid, 1977).

The combination of our tectonostratigraphic data with existing geochemical data suggests that, in the North Penninic basin, in the most distal part of the European margin, crustal thinning, break-off and magmatic activity were coupled with uplift and only moderate localised subsidence.

Classical rifting models (McKenzie, 1978; Wernicke, 1985) fail to explain our observations since they predict strong and rapid subsidence in response of crustal thinning in the most internal part of rifting.

A first hypothesis to account for the observed paleobathymetric evolution is that in the distal European margin the crust was not homogeneously thinned. Several unthinned high (preserved) separated several fault-bounded "deep" basins (mostly subducted) characterised by stretched crust

A second hypothesis is that progressive lithospheric thinning could be compensated by increasing buoyancy, it results in a delayed subsidence even in the most internal part of rifting.

Some recent developments in understanding rifting dynamics seems to support our second hypothesis: Muntener et al. (2010) proposed the creation of a "lithospheric sponge " by trapping in the mantle part of the liquid produced during rift-induced decompression melting in a non-optimal extraction system. The resulting lithospheric mantle is compositionally buoyant and able to inhibit the subsidence of thinned continental crust. Additionally Kaus et al. (2005) and Simon & Podladchikov (2008) highlighted the effect of subsolidus phase transition (e.g. spinel → plagioclase) on mantle density during thinning and asthenospheric upwelling and calculated some consequences for the uplift vs subsidence of the overlaying crust and sedimentary basins.

5.6.3. The rising area between the Helvetic distal margin and the Briançonnais

The above-mentioned effects on the evolution of distal margins could explain the generalised presence of emerged lands (or islets) during the Middle Jurassic in the Distal European Margin of the Alps and in the Briançonnais domain. In fact there is evidence for several highs in the distal part of the margin even further to the west of our study area (figure 9), where on the same transect we find again the Briançonnais rise, in a Middle Penninic Position (Badoux & Marcanton, 1962), the Monte Leone (Carrupt, 2003) and the Antigorio (Matasci et al., 2011) Highs in a Lower Penninic Position. In this case "middle Jurassic" metamafics are present in the Lower Penninic Pizzo del Vallone nappe (Carrupt, 2003). Even more to the west, the Subbriançonnais domain got a bathonian detrital input ("Quarzporphyr-Geröllen") from the North (Furrer, 1977, 1979), from a potential Valaisan high (Septfontaine, 1983).

The "rising area" in the middle of the Alpine rifting and extending from the distal Helvetic margin to the Briançonnais (already splendidly illustrated by Trümpy (1965, pag. 577), see also Sengor & Bernoulli, 2011 fig. 6) is the best exposed field example of inhibited or delayed subsidence in future deep-water margins.

In the distal European margin the end of the subsidence inhibition and the beginning of generalised subsidence started probably just before the upper Jurassic. The omnipresent Malm limestone on the proximal and distal Helvetic margin testifies

the accomplishment of this event. The recently reported hydrothermal activity at ~162Ma in the proximal margin and Jura Plateau (Efimenko, 2011) is in agreement and reinforces our scenario.

5.6.4. The Plattenberg and Garzott breccias: a second rifting or a protracted history?

At the Hennasädal the Adula shows post-Triassic erosion, drowning and subsequent sealing with Upper Jurassic post rift sediments of Ultra-Helvetic type (Quinten formation or even better the Antabia group, see section 4.8). At Plattenberg it is possible to deduce that the beginning of the drowning phase is followed by the activity of scarp faults. Probably this phase lasted until late Jurassic as the breccia follows in time the generalised emersion and since upwards it bears some intercalations of pure marble suggesting synchronism with the Hennasädel Upper Jurassic marble.

The Garzott slices show an analogue scenario. The two units were probably separated by the Valser slices (see later), which contain "ophiolitic" material originated from a depleted mantle source (Dürr et al., 1993; Steinmann, 1994; Steinmann & Stille, 1999).

Even if located further to the south the Guda-Alpettas zone shares some analogies with the Adula-Garzott problem. There the post-Alenian clastic sequence is separated in two part by several meters of marls and marly limestones (see section 3.5.3 and Table 1), in other words a first period of important tectonic activity and emersion is separated by a phase of quiescence from a second period of erosion and resedimentation.

The Basaltic manifestation in the North Penninic domain is followed by thousand of meters of mostly Cretaceous calcschists whose base is Late Jurassic or younger (Pantic & Gansser, 1977; Pantic & Isler, 1978, 1981; Steinmann, 1994 p. 92). It results that in the Central Alps transect, the first evidences of strong subsidence in the most distal European margin and adjacent oceanic domain is not older than the Late Jurassic.

The Middle Jurassic uplift and the late Jurassic generalised subsidence are separated by a spasmodic distensive phase during which submarine breccia (Plattenberg and Garzott), MORB (Misox) and allochtones (Garzott and maybe Luzzone and Guda-Alpettas) were created.

This particular protracted history is not unique to the studied transect. Noteworthy are the analogies existing between the Niesen Middle Jurassic substratum in the Prealps (Badoux & Homewood, 1978; Ringgenberg et al., 2001) and the Guda-Alpettas "Middle Jurassic" (in both there are two detrital inputs separated by a more fine grained and less detrital level). Moreover, several enigmatic late Middle Jurassic-early Upper Jurassic clastic series and Breccias characterise the Lower and Middle Penninic domains, but these are missing in the more external domains, where breccias are older (Trümpy, 1975). As example of enigmatic Penninc breccias we can quote the Bréches du Télégraphes and the Nielard Breccias (Barbier, 1948), the Schamser breccias (Schmid, 1990), the Falknis and the Tasna breccias (Gruner, 1981) and the most famous "Brèche Supérieur" in the Breccia Nappe (Schroeder, 1939), which is separated from the middle Jurassic "Brèche Inférieur" by the "Schistes Ardoisiers". The domains interested by these latecomer breccias are also affected by a later tectonic activity as reported by Felber (1984) in the Klippen of Central Switzerland, by Septfontaine (1983) in the Préalpes Médianes and more recently by Bertok et al. (2011) in the ligurian Briançonnais.

Thus since the scale involved is larger than the local or regional context, the explanation should be of first order (figure 10). We explain this protracted history as follows (partly inspired by Manatschal et al. (2006, 2007), Mohn et al. (2010) and Peron-Pinvidic et al. (2007, 2009 and 2010):

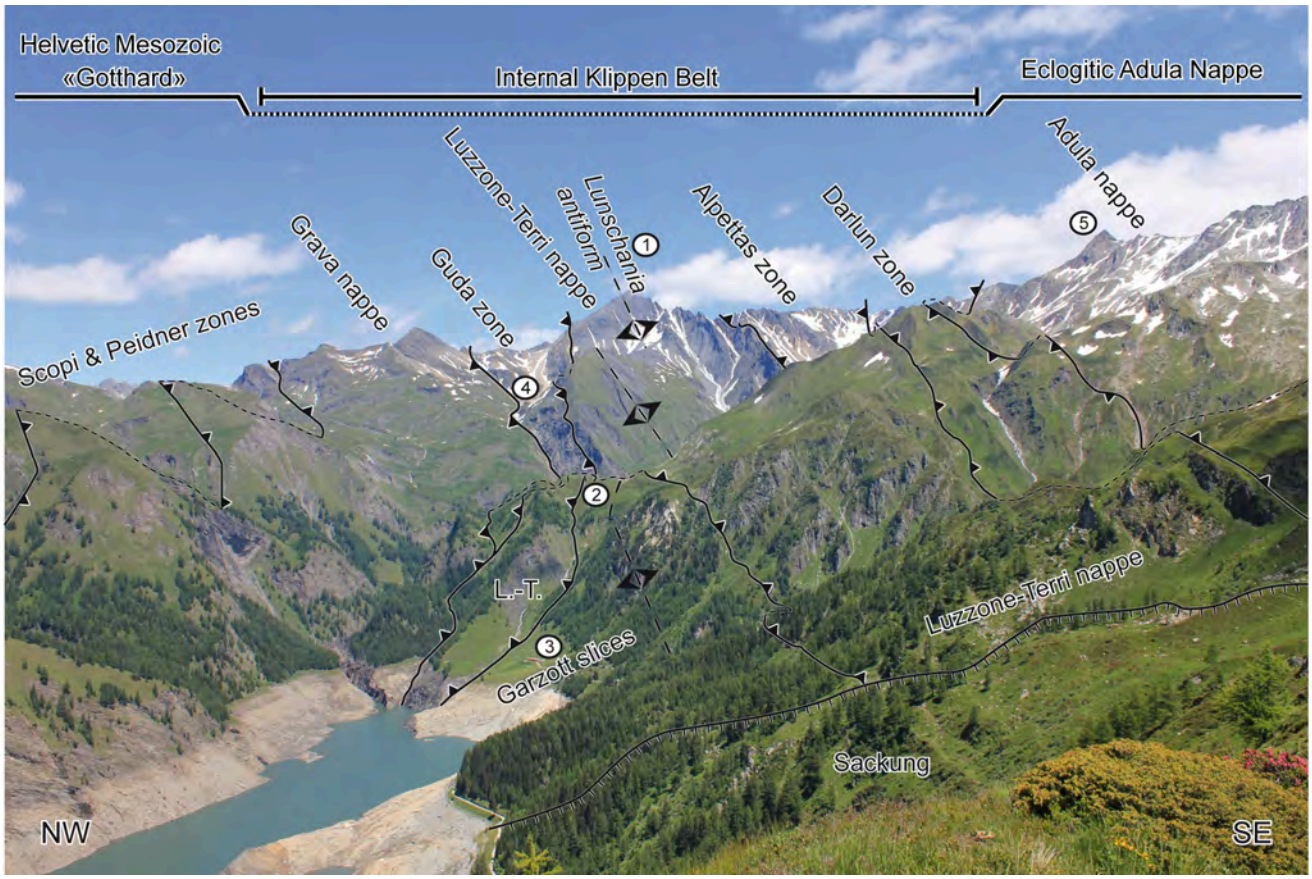

Fig. 11 *Views on the Piz Terri from Forcadona (From SW) showing the tectonic relationships among the different tectonic elements in the complex area E of the Luzzone Lake. In the left down corner a kilometric sackung hide the geological record. 1) Piz Terri summit (3179 m) 2) Fanee 3) Alpe di Garzott 4) Valle di Guda 5) Torrone di Garzora (317 m). See text for further explanation. The geometric relationships among the different units are illustrated in the section of figure 2b.*

The early phase of rifting is responsible for delocalised crustal thinning and the formation of the Helvetic basins.

The Lower and Middle Jurassic lithospheric thinning is responsible for the creation of the rising area between the internal South Helvetic and the Briançonnais domains by the mechanism evocated in section 6.2 (heating, phase's transition and "lithospheric sponge"), the opening of the Liguro-Piemontese Ocean and localised magmatic activity in the North Penninc. The next advanced phase of rifting abandoned proximal areas and prograded in the most internal part (a scenario predicted by Peron-Pinvidic et al., 2007, 2009), the consequence of this is the late Middle-Jurassic and early-Upper Jurassic spasmodic extension, which culminated with stronger magmatic activity (pillow lavas, e.g. Tomul). This phase leads to the delamination of the previously existing rises (e.g. Adula and Briançonnais) and is associated with the loss of the "Buoyant sponge" and "phase's transition" positive buoyancy effects (see above). The direct consequences of the resulting subsidence in this previously mistreated area are the thick and monotonous North Penninic Bündnerschiefer series, which were deposited over different pre- to syn-rift sequences and that are now stacked in many nappes and melanges zones within the Lower Penninic (Lucomagno and Molare-Dangio of Probst, the Garzott calcschists of this contribution, The Bündnerschiefer in the Valser, Aul and Grava Mélanges, The Grava and Tomul Bündnerschiefer).

5.7. Discussion on the orogenic history

Given the complex tectonic situation around the Adula front (figure 2), the precise position of the Piz Terri-Lunschania zone in the tectonostratigraphy of the Central Alps is controversial (cf. Baumer, 1964; Cavargna-Sani et al., 2010a; Egli, 1966; Galster et al., 2010; Jenny et al., 1923; Kupferschmid, 1977; Probst, 1980; Schmid et al., 1996, Wiederkehr et al., 2008).

The Ultra-Adula origin of the zone, suggested by Cavargna-Sani et al. (2010a) and Galster et al. (2010) is confirmed by our results. The discovery of the Garzott slices and the understanding of the original mechanical behaviour of the Piz Terri-Lunschania zone (fold ramps) clarify the complexity of the zone and give coherency even at the apparently complex tectonic situation.

5.7.1. The Piz Terri-Lunschania zone: an internal klippen-belt

The Grava unit is thrusted above the Piz Terri-Lunschania zone and is rooted in the Misox zone, above the Aul unit, the Valser slices and the Adula nappe. However it is folded below the Adula front for several kilometers. To the north, the Grava unit is thrusted above the external massifs and the Infra-Helvetic nappes. The part of the unit folded below the Adula nappe is a portion of the thrusting plane and it is probably not the original front. The rootless units located below this plane could be part of the same tectonic system: an "overriding-complex" that, originated from the North Penninic basin, has been thrusted above the distal and the proximal Helvetic margin. The Piz-Terri-Lunschania zone could be part of the "overriding-complex". In fact the "root-zone" of the Piz Terri-Lunschania zone is apparently sandwitched and smashed between the Adula nappe above and the overturned Grava unit below, a situation that gives to the piz Terri-Lunschania zone a rootless character.

The pre-rift stratigraphy from the Briançonnais carbonate platform to the Helvetic lands is extremely coherent if an Ultra-Adula origin of the Piz Terri-Lunschania zone is considered but become too complex and partitioned for the quiet Triassic period if the zone is regarded as rooted below the Adula nappe. For paleogeographic coherency the Luzzone-Terri nappe should be rooted between the Aul unit (where the Triassic comprises several tens of meters of (vermiculated?) limestones and where there is no sign of Helvetic Lias) and the Garzott slices, the Garzott slices on their side should be rooted between the Luzzone-Terri nappe and the Valser slices. The Valser slices are rooted between the Aul unit and the Adula nappe. Thus the tectonic order from below to above is: Adula nappe, Valser slices, Garzott slices, Luzzone-Terri nappe, Aul unit and Grava unit. The Guda-Alpettas zone is tectonically intercalated between the Luzzone-Terri nappe and the Grava unit. Its precise position, relative to the Aul unit is still unknown.

The Darlun zone consists of several imbricated slices thrusted above the Luzzone-Terri nappe. Northeastward it's flexured around the Adula front above the overturned internal Alpettas zone (fig 2 and 11). The flexuration around the overlaying nappe is unusual for an originally underlying body and suggests that the Darlun zone is located above the Adula nappe and that it represents the virtual connection between the Piz Terri-Lunschania zone and its homeland. The former connection has been dismembered and hidden by the advancing Adula nappe.

In Summary, the Piz Terri-Lunschania zone is considered as a klippe of Ultra-Adula origin that, together with the Grava unit, "climbed over" the Adula nappe during early subduction and then has finally been overtaken by the Adula front during the final uplift of the eclogitic nappe. The Piz Terri-Lunschania zone is thus part of an "internal Klippen Belt" (figure 11) pinched between the external massif (Gotthard) and the eclogitic unit (Adula nappe) by the uplift of the latter.

5.7.2. The Garzott fault: the escape from deep subduction

The existence of the Luzzone-Terri fold ramps suggests us the manner in which the Luzzone-Terri nappe achieves the difference in displacement with the Adula nappe. Fold ramps obviously need a ramp. The latter is in direct contact with the deepest part of the developing thrusting complex. In the case of the Penninic nappes of Ultra-Adula origin, the deepest portion of the complex is represented by the Garzott slices, in an advanced position, and by the lower Valser slice in a recessed position. Both are slices (Schuppenzones or mélanges) and both share the same typology of North-Penninic-Triassic facies (which evolve quickly from internal to external area), thus they can be seen as adjacent during their preorogenic history (Triassic) and then genetically linked during the orogenesis (Schuppenzonen). We have suggested a supradetachment affinity for the Jurassic stratigraphic record in the Garzott slices (section 5.1), close relationships between oceanic (Jurassic) and continental rocks characterise the Valser slices (Dürr et al., 1993; Kupferschmid, 1977; Steinmann & Stille, 1999; Wyss & Isler, 2007), suggesting a transition from the Continent to the Ocean (OCT). Thus proximity and a genetic link between the Garzott "supradetachment" and the Valser "OCT" seem to exist even during the Jurassic.

Considered the evolution of the Piz Terri-Lunschania zone and that of the Grava unit (see above) the most suitable scenario is that the Garzott slices together with the Valser slices are part of the ramp that allowed the overriding (from an Ultra-Adula to the current position); they have been "sampled" by the advancing penninic mass.

During the preorogenic history the Garzott slices are part of a supradetachment system, thus they are separated from an underlying exhumed basement by a detachment system (of which the Garzott fault is part). Since this basement is not currently present (the peculiarity of the Misox zone, compared to the South penninic ocean, is the scarcity of preserved exhumed mantle rocks) we speculate that it has been subducted with the Adula nappe below the ramp (the Rodingite of Alpe Duria and Cima di Gagnone are good candidates, as the Alpe Arami or Chiavenna peridotite and the mafic and ultramafic in the Southern Steep Belt). Thus a logical conclusion is that the Jurassic detachment, which allowed crustal thinning during rifting, acted as a ramp for the "detached" units during the tertiary collision.

5.8. Conclusion

In this contribution we reported new tectonostratigraphic information from the Central Alps, along a profile located between the Helvetic external massifs and the Briançonnais middle penninic units. Our results suggest that the Jurassic rifting separated the Briançonnais Paleogeographic domains from the Helvetic margin by complex and protracted extension. The future deep-water rifted margin stayed at shallower conditions during rifting paroxysm and the first magmatic activity. The most distal margin was characterised by a diffuse rising area with only moderately subsiding basins above a thinned continental and proto-oceanic crust. This apparent contradiction is explained by the isostatic response of the lithosphere to density changes in the mantle by heating, mineral phase transition and liquid trapping and by the fact that extreme thinning occurred in a second protracted step. The resulting system is isostatically buoyant. The lost of the buoyancy forces and the protracted extension are responsible for the delamination of the rising area followed by strong subsidence. The hints of this second phase are recorded in the enigmatic "Callovo-oxfordian" breccias distributed in the Penninic domain all along the chain. The Northern border of the rising area was characterised by a Triassic substratum different from the typical Briançonnais Triassic and even from the Helvetic one. This new group of Triassic facies is defined here for the first time and is called the North-Penninic-Triassic. This particular Triassic, characterised by the Ladinian "Dolomie bicolori" was deposited on the banks of the Briançonnais basin directly south of the Helvetic domain, thus is likely to had acted as connection between the Briançonnais carbonate platform and the Helvetic lands. The eclogitic Adula nappe is characterised by this particular stratigraphic association, this, together with the coherency of the stratigraphic record in the northern Adula

nappe and surrounding areas, questions the idea of a lithospheric mélange in the Adula nappe. The great and famous eclogitic nappe is more likely to be a coherent Alpine nappe that during Mesozoic time experienced a peculiar geodynamic history in the frame of Alpine paleogeography. During Tertiary collision the Adula nappe acted as a single tectonic object in a coherent tectonic context. In this scenario the reactivation of Mesozoic extensional structures played a major role in allowing Adula subduction, the Penninic overriding above it and in creating the structural complexity of the Central Alps.

ACKNOWLEDGMENTS

We thank Alfred Isler for having provided us with a copy of the unpublished manuscript of A. Uhr. Fruitfull discussions with Aymon Baud, Jean Guex, Geoffroy Mohn, Othmar Müntener, Phil Picuri, Caroline Wilhelm and the comments of Marco Beltrando and one anonymous reviewer helped us to improve considerably our work. We are grateful to the Museo Cantonale di Storia Naturale at Lugano for authorization to collect samples in Ticino.

6. General conclusions

The main results of the present dissertation are principally based on a classical approach including geological mapping, lithostratigraphy, structural analysis and dating. This multidisciplinary fieldwork approach complemented by specific analytical data provides a regional framework to the detailed geological and petrological data published in the literature. The new data of this thesis joined to the large amount of detailed geological and petrological investigations on the Adula nappe offer the necessary basis for a better understanding of high-pressure nappe formation and exhumation.

In the introduction, several scientific questions were pointed out as the main objectives for this thesis. Synthetic answers including the main results of the thesis will be presented below.

- *What is the pre-Triassic evolution of the Adula basement, the age of the magmatic rocks and is it possible to define and date the formations in the basement?*

The investigations on the basement of Adula nappe reveal its intricate pre-Triassic evolution. It is composed by a polycyclic basement including Cambrian paragneiss (Salahorn Fm.), a chaotic detrital formation build up in a subduction-related setting (Trescolmen Fm., Ordovician?), an Ordovician Paragneiss (Heinisch Stafel Fm.) and Ordovician (~450 Ma) orthogneiss. These formations experienced the Variscan and Alpine orogenesies, and it is therefore difficult to precisely reconstruct the geometry and the nature of the original contacts. The Permian Zervreila orthogneiss intrudes this polycyclic basement. It is dated at about 290 Ma. The Alpine basement is formed of a consistent pre-Alpine lithological group assemblage, coherent with the pre-Triassic basement evolution as known in less-deformed and well-studied areas. The Zervreila orthogneiss is a good marker for the Alpine deformation owing to its Permian age.

- *Is it possible to decipher the stratigraphic content of the Adula cover and to propose a Mesozoic – Tertiary stratigraphic evolution? What is the pre-orogenic significance of the Adula nappe in the regional tectono-sedimentary context?*

The Adula cover reveals an identifiable sedimentary sequence containing several stratigraphic groups. It is characterized by a North Penninic Triassic. It marks the transition between the Helvetic and the Briançonnais Triassic type. The Middle Jurassic is characterized by an emersion. This emersion, and the consequent erosion, is probably the cause of the absence of Lower and Middle Jurassic sediments. The Adula nappe is part of a generalised occurrence of rises of the distal European margin during the first rifting phase. The late Middle Jurassic and the Upper Jurassic mark a transgression followed by a drowning phase. This drowning corresponds to strong subsidence and extension in the domain located directly south of the Adula. Following the drowning, the sedimentation in the Adula sedimentary cover consists of a pure limestone, similar to the Upper Jurassic limestone of the Helvetic and Subbriançonnais domain. A detrital series overlies a pronounced unconformity. This detrital series can be compared to a flysch s.l. Its age is probably late Upper Cretaceous to Palaeogene. The stratigraphic content of the Adula cover reflects the presence of a consistent and characteristic paleogeographic domain on the northern border of the North Penninic basin. This stratigraphic domain can be compared with those of the Monte Leone, Pizzo del Vallone and Teggiolo nappes.

- *What is the internal geometry of the northern Adula nappe, and what is the kinematic evolution necessary to produce it?*

The northern Adula nappe has experienced a complex deformation history with several deformation phases during the Alpine orogeny. The early Ursprung ductile deformation phase is characterized by a schistosity, folds and top-to-S shearing restricted to the upper part of the nappe. This deformation is related to the N-driven exhumation from peak pressures at 38-35 Ma. The Zapport phase produces the main structural features of the nappe as isoclinal folding, the main schistosity associated to N-directed shear. This phase forms folds at the front of the nappe, as revealed by complex synclines of the sedimentary cover in the basement. This phase is also responsible for the nappe emplacement in the Lower Penninic nappe stack concomitant with decompression and before the peak temperature of the regional metamorphism in the Lepontine dome. During the nappe emplacement, the Adula nappe acts as a major shear zone for the emplacement of the Lower Penninic sediments and the Middle Penninic nappes on top of the other Lower Penninic basement nappes. The Leis phase produces nappe-scale folds in the frontal part of the Adula nappe and is associated with a general top-to-N shearing. The Carassino antiform is a late N-vergent post-nappe fold marked in the northern Adula nappe and in the units on top of it.

- *The role of the Adula nappe in the Lower Penninics.*

Our results suggest that the Adula nappe is the uppermost Lower Penninic basement nappe of the eastern transect of the Lepontine Dome stacked as an "Argandian" style fold-nappe. This feature is almost certainly related to its paleogeographic position and its pre-orogenic feature. Its Jurassic and Cretaceous position is the southern limit of the European plate. The nappe is composed by the last consistent continental-crust block in front of the hyper-extended margin. The Adula nappe can in fact be ascribed to a specific paleogeographic position and to a coherent pre-Alpine block of continental crust. Its kinematic interpretation as a Lower Penninic suture represented by a lithospheric mélange is not consistent.

- *The significance of the Adula nappe to unravel subduction and exhumation processes.*

The Adula nappe emplacement represents the first consistent continental block in the collision. We suggest that the nappe emplacement of the overlying nappes by basal detachment and accretion make the deeper subduction of the Adula nappe easier. Therefore we associate the high-pressure event of the Adula nappe with a collision-related process. The formation of the Adula nappe is more related to nappe emplacement rather than an extrusion. The case of the Adula nappe is therefore different from high-pressure bearing nappes formed from of a strongly pre-structured ocean-continent-transition (e.g., Beltrando et al. 2010) where the actual complexity is mainly due to inherited structures and the HP metamorphism in close relation with a subducting oceanic crust. The Adula nappe however can be used as a model for high-pressure nappe formation and exhumation of a coherent piece of continental crust in a collisional context.

REFERENCES CITED

Ackermann, A. (1986). Le flysch de la nappe du Niesen. Eclogae Geologicae Helvetiae, 79, 641-684.

Alonso-Perez, R., Müntener, O., Ulmer, P. (2009). Igneous garnet and amphibole fractionation in the roots of island arcs: experimental constraints on andesitic liquids. Contributions to Mineralogy and Petrology, 157, 541-558.

Ammann, P. (1973). Geologia e petrografia della regione del Pizzo Molare. PhD thesis, ETH Zürich.

Anatra, S. (1986). Les faciès pélagiques de l'Ultrahelvétique entre Arve et Simme. PhD thesis, Université de Fribourg.

Antoine, P. (1971). La zone des bréches de Tarentaise entre Bourg-Saint-Maurice (vallée de l'Isère) et la frontière italo-suisse. Travaux du Laboratoire de Géologie de l'Université de Grenoble, Mémoires, 9.

Argand, E. (1916). Sur l'arc des Alpes occidentales. Eclogae Geologicae Helvetiae, 14, 145-191.

Argand, E. (1918). Zur Tektonic des Val Blegno. Eclogae Geologicae Helvetiae, 14, 685-686.

Arnold, A., Fehr, A., Jung, W., Kopp, J., Kupferschmid, Ch., Leu, W., Liszkay, M., Nabholz, W., Van der Plas, L., Probst, Ph., Wyss, R. (2007). Blatt 121Vals. Geologischer Atlas der Schweiz 1:25'000, Swisstopo, Bern

Aubert de la Rue, E., Weidmann, M. (1966). Découverte nouvelles d'ammonites dans la couverture sédimentaire du massif du Gotthard. Eclogae Geologicae Helvetiae, 59.

Avanzini, M., Cavin, L. (2009). A new Isochirotherium trackway from the Triassic of Vieux Emosson, SW Switzerland: stratigraphic implications. Swiss Journal of Geosciences, 102, 353-361.

Badoux, H., Homewood, P. (1978). Le soubassement de la nappe du Niesen dans la région du Sépey (Alpes vaudoises). Bulletin de géologie, Lausanne, 228.

Badoux, H., Homewood, P. (1978). Le soubassement de la nappe du Niesen dans la région du Sépey (Alpes vaudoises). Bulletin de la Societé Vaudoise des Sciences Naturelles, 15, 15-23.

Badoux, H., Mercanton, C.H. (1962). Essai sur l'évolution tectonique des Préalpes médianes du Chablais. Eclogae Geologicae Helvetiae, 55, 135-188.

Barbarin, B. (1999). A review of the relationships between granitoid types, their origins and their geodynamic environments. Lithos, 46, 605-626.

Barbier, R. (1948). Les Zones Ultradauphinoise et Subbriançonnaise entre l'Arc et l'Isère. Mémoires Carte Géologique de France, 291.

Barboni. M., Bussy. F., Chiaradia, M. (2011). Origin of Early Carboniferous pseudoa-dakites in northern Brittany (France) through massive amphibole fractionation from hydrous basalt. Terra Nova, 23, 1-10.

Baud, A. (1976). Les terriers de Crustacés décapodes et l'origine de certains faciès du Trias carbonaté. Eclogae Geologicae Helvetiae, 69, 415-424.

Baud, A. (1987). Stratigraphie et sédimentologie des calcaires de Saint-Triphon (Trias, Préalpes, Suisse et France). Mémoire de géologie, Lausanne, 1, 322.

Baud, A., Masson, H. (1975). Preuves d'une tectonique liasique dans le domaine briançonnais: faillées conjuguées et paleokarst à Saint-Triphon (Préalpes Médianes, Suisse). Eclogae Geologicae Helvetiae, 68, 131-145.

Baud, A., Mégard-Galli, J. (1975). Evolution d'un bassin carbonaté du domaine alpin durant la phase pré-océanique: cycles et séquences dans le Trias de la zone briançonnaise des Alpes occidentales et des Préalpes. 9e Congr. intern. Sédiment, Nice, 5, 45-50.

Baudin, T., Marquer, D. (1993). Métamorphisme et déformation dans la nappe de Tambo (Alpes centrales suisses): évolution de la substitution phengitique au cours de la déformation alpine. Bulletin Suisse de Minéralogie et Pétrographie, 73, 285-299.

Baudin, T., Marquer, D., Barfety, J. C., Kerckhove, C., Persoz, F. (1995). Nouvelle interprétation stratigraphique de la couverture mesozoique des nappes de Tambo et de Suretta; mise en évidence d'une nappe de décollement précoce (Alpes centrales suisses). Comptes Rendus de l'Academie des Sciences Serie II, Sciences de la Terre et des Planètes, 321.

Baumer, A. (1964). Geologie der gotthardmassivisch-penninischen Grenzregion im oberen Bleniotal. Geologie der Blenio-Kraftwerke. Beiträge zur Geologie der Schweiz Geotechnische serie, 39.

Baumer, A., Frey, J. D., Jung, W., Uhr, A. (1961). Die Sedimentbedeckung des Gotthard-Massivs zwischen oberen Bleniotal und Lugnez). Eclogae Geologicae Helvetiae, 54, 478-491.

Bauville, A., Epard, J. L., Schmalholz, S. M. (2013). A simple thermomechanical shear model applied to the Morcles fold nappe (Western Alps). Tectonophysics, 583, 76-87.

Bellahsen, N., Jolivet, L., Lacombe, O., Bellanger, M., Boutoux, A., Garcia, S., Mouthereau, F., Le Pourhiet, L., Gumiaux, C. (2012). Mechanisms of margin inversion in the external Western Alps: Implications for crustal rheology. Tectonophysics, 560-561, 62-83.

Beltrando, M., Rubatto, D., Manatschal, G. (2010). From passive margins to orogens: The link between ocean-continent transition zones and (ultra) high-pressure metamorphism. Geology, 38, 559-562.

Beltrando, M., Frasca, G., Compagnoni, R., Vitale-Brovarone, A. (2012). The Valaisan controversy revisited: Multi-stage folding of a Mesozoic hyper-extended margin in the Petit St. Bernard pass area (Western Alps). Tectonophysics, 579, 17-36.

Berger, A., Bousquet, R. (2008). Subduction-related metamorphism in the Alps: review of isotopic ages based on petrology and their geodynamic consequences. Geological Society, London, Special Publications, 298, 117-144.

Berger, A., Mercolli, I. (2006). Tectonic and Petrographic map of the Central Lepontine Alps 1:100'000 (Map sheet 43 Sopra Ceneri). Carta Geologica Speciale, 127, Swisstopo, Bern.

Berger, A., Mercolli, I., Engi, M. (2005). The central Lepontine Alps: Notes accompanying the tectonic and petrographic 1:100'000 (Map sheet 43 Sopra Ceneri). Schweizerische Mineralogische und Petrographische Mitteilungen, 85, 109-146.

Bergomi, M. A., Tunesi, A., Shi, Y. R., Colombo, A., Liu, D. Y. (2007). SHRIMP II U/Pb geochronological constraints of pre-Alpine magmatism in the Lower Penninic Units of the Ossola Valley (Western Alps, Italy). Geophysical Research Abstract, 9.

Bertok, C., Martire, L., Perotti, E., d'Atri, A., Piana, F. (2011). Middle-Late Jurassic syndepositional tectonics recorded in the Ligurian Briançonnais succession (Marguareis–Mongioie area, Ligurian Alps, NW Italy). Swiss Journal of Geosciences, 104, 237-255.

Bianconi, F. (1965). Resti fossili in rocce mesometamorfiche della regione del Campolungo. Schweizerische Mineralogische und Petrographische Mitteilungen, 45, 571-596.

Bianconi, F. (1971). Geologia e petrografia della regione del Campolungo. Materiali Carta Geolgeologica Svizzera [N.S.], 142.

Boekhout, F., Spikings, R., Sempere, T., Chiaradia, M., Ulianov, A., Schaltegger, U. (2012). Mesozoic arc magmatism along the southern Peruvian margin during Gondwana breakup and dispersal. Lithos, 146-147, 48-64.

Bonin, B., Azzouni-Sekkal, A., Bussy, F., Ferrag, S. (1998). Alkali-calcic to alkaline post-collision granite magmatism: petrologic constraints and geodynamic settings. Lithos, 45, 45-70.

Bousquet, R. (2008). Metamorphic heterogeneities within a single HP unit: Overprint effect or metamorphic mix? Lithos, 103, 46-69.

Bousquet, R., Goffé, B., Vidal, O., Oberhaensli, R., Patriat, M. (2002). The tectono-metamorphic history of the Valaisan domain from the Western to the Central Alps: New constraints on the evolution of the Alps. Geological Society of America Bulletin, 114, 207-225.

Brunnschweiler, R.O. (1948). Beitrage zur Kenntnis der Helvetischen Trias östlich des Klausespasses. PhD Thesis, Universität Zürich.

Bussien, D., Bussy, F., Magna, T., Masson, H. (2011). Timing of Palaeozoic magmatism in the Maggia and Sambuco nappes and paleogeographic implications (Central Lepontine Alps). Swiss Journal of Geosciences, 104, 1-29.

Bussy, F., Hernandez, J., Von Raumer, J. F. (2000). Bimodal magmatism as a consequence of the post-collisional readjustment of the thickened Variscan continental lithosphere (Aiguilles Rouges-Mont Blanc massifs, Western Alps). In: Barbarin, B., Stephens, W. E., Bonin, B., Bouchez, J., Clarke, D. B., Cuney, M., Martin, H. (ed) Fourth Hutton symposium, The origin of granites and related rocks, 221-233.

Bussy, F., Péronnet, V., Ulianov, A., Epard, J. L., Von Raumer, J. (2011). Ordovician magmatism in the external French Alps: witness of a peri-gondwanan active continental margin. In: Gutiérrez-Marco, J. C., Rábano, I., García-Bellido, D. (ed) Ordovician of the World. Cuadernos del Museo Geominero, 14. Instituto Geológico y Minero de España, Madrid, 75-82.

Caron, C., Homewood, P., Wildi,W. (1989). The original Swiss flysch: a reappraisal of the type deposits in the Swiss Prealps. Earth-Science Reviews, 26, 1-45.

Carrupt, E. (2003). New stratigraphic, structural and geochemical data from the Val Formazza - Binntal area (Central Alps). Mémoires de Géologie (Lausanne), 41, 118.

Cavargna-Sani, M. (2008). Etude géologique et métamorphique du haut Val Calanca (GR), Nappe de l'Adula. MSc Thesis, Université de Lausanne.

Cavargna-Sani, M., Epard, J. L., Bussy, F., Ulianov, A. (2010). Zircon U/Pb dating of the Late Carboniferous Zervreila Orthogneiss, Adula Nappe. Abstract Swiss Geosciences Meeting Fribourg.

Cavargna-Sani, M., Epard. J. L., Masson, H. (2010). Discovery of fossils in the Adula nappe, new stratigraphic data and tectonic consequences (Central Alps). Bulletin de la Société vaudoise des Sciences naturelles, 92, 77-84 and Bulletin de géologie, Lausanne, 368.

Cavargna-Sani, M., Epard, J. L., Bussy, F., Ulianov, A. (in press). Basement lithostratigraphy of the Adula nappe: implications for Palaeozoic evolution and Alpine kinematics. International Journal of Earth Science, doi: 10.1007/s00531-013-0941-1

Ciancaleoni, L., Marquer, D. (2006). Syn-extension leucogranite deformation during convergence in the Eastern Central Alps: example of the Novate intrusion. Terra Nova, 18, 170-180.

Cocozza, T. (1979). The Cambrian of Sardinia. Memorie della Società Geologica Italiana, 20, 163-187.

Dal Piaz, G. V., Martinotti, G., Hunziker, J. C. (1972). La Zona Sesia-Lanzo e l'evoluzione tettonico-metamorfica delle Alpi nordoccidentali interne. Memorie della Societá Geologica Italiana, 11, 433-460.

Dale, J., Holland, T. J. B. (2003). Geothermobarometry, P-T paths and metamorphic field gradients of high-pressure rocks from the Adula Nappe, Central Alps. Journal of Metamorphic Geology, 21, 813-829.

Davidson, J., Turner, S., Handley, H., Macpherson, C., Dosseto, A. (2007). Amphibole sponge in arc crust? Geology, 35, 787-790.

De La Roche, H., Leterrier, J., Grandclaude, P., Marchal, M. (1980). A classification of volcanic and plutonic rocks using R1R2-diagram and major-element analyses - its relationships with current nomenclature. Chemical Geology, 29, 183-210.

Demathieu, G., Weidmann, M. (1982). Les empreintes de pas de reptiles dans le Trias du Vieux Emosson (Finhaut, Valais, Suisse). Eclogae Geologicae Helvetiae, 75, 721-757.

Deutsch, A. (1979). Serpentinite und Rodingite der Cima Sgiu (NW Aduladecke, Ticino). Bulletin suisse de minéralogie et pétrographie, 59, 319-347.

Dewey, J. F., Helman, M. L., Turco, E., Hutton, D. H., Knott, S. D. (1989). Kinematics of the western Mediterranean, in: Coward et al. (ed.). Alpine Tectonics, Geological Society Special Publication 45, 265-283.

Dössegger, R., Trümpy, R. (1972). Permian of Switzerland. In: Falke, H. (ed.). Rotliegend, Essays on European Lower Permian. Brill, Leiden, 189-213.

Dürr, S. B., Ring, U., Frisch, W. (1993). Geochemistry and geodynamic significance of North Penninic ophiolites from the Central Alps. Bulletin suisse de minéralogie et pétrographie,73, 407–409.

Efimenko, N. (2011). Origin of cadmium enrichments in carbonate rocks deposited in the Alpine Tethys area during the Middle-Late Jurassic. PhD thesis, Université de Lausanne.

Egli, W. (1966). Geologische-perographische Untersuchungen in der NW-Aduladecke und in der Sojaschuppe (Bleniotal, Kanton Tessin). PhD Thesis, ETH Zürich.

Elicki, O. (2006). Microbiofacies analysis of Cambrian offshore carbonates from Sardinia (Italy): environment reconstruction and development of a drowning carbonate platform. Carnets de Géologie / Notebooks on Geology - Article 2006/01.

Engi, M., Berger, A., Roselle, G. T. (2001). Role of the tectonic accretion channel in collisional orogeny. Geology, 29, 1143-1146.

Epard, J. L. (1989). Stratigraphie du Trias et du Lias dauphinois entre Belledonne, Aiguilles-Rouges et Mont-Blanc. Bulletin de la Societe Vaudoise des Sciences Naturelles, 79, 301-338.

Epard, J. L., Escher, A. (1996). Transition from basement to cover: a geometric model. Journal of Structural Geology 18, 533–548.

Ernst, W. G. (1971). Metamorphic zonations on presumably subducted lithospheric plates from Japan, California and the Alps. Contributions to Mineralogy and Petrology, 34, 43-59.

Ernst, W. G. (1973). Interpretative synthesis of metamorphism in the Alps. Geological Society of America Bulletin, 84, 2053-2078.

Escher, A., Masson, H., Steck, A. (1993). Nappe geometry in the Western Swiss Alps. Journal of Structural Geology, 15, 501-509.

Escher, A., Watterson, J. (1974). Stretching fabrics, folds and crustal shortening. Tectonophysics, 22, 223-231.

Etter, U. (1987). Stratigraphische und strukturgeologische Untersuchungen im Gotthardmassivischen Mesozoikum zwischen dem Lukmanierpass und der Gegend von Ilanz. PhD thesis, Universität Berne.

Fehr, A. (1956). Petrographie und Geologie des Gebietes zwischen val Zavragia – Piz Cavel und Obersaxen – Lumbrein (Gotthard-Massiv-Ostende). Bulletin suisse de minéralogie et pétrographie, 36, 351-452.

Florineth, D., Froitzheim, N. (1994). Transition from continental to oceanic basement in the Tasna Nappe: evidence for Early Cretaceous opening of the Valais Ocean. Schweizerische Mineralogische und Petrographische Mitteilungen, 74, 437-448.

Fox, J. S. (1975). Three-dimensional isograds from the Lukmanier-Pass, Switzerland, and their tectonic significance. Geological Magazine, 112, 547–564.

Frey, J. D. (1967). Geologie des Greinagebiets (Val Camadra, Val Cavalasca, Val Lariciolo, Passo della Greina). Beitrage zur Geologische Karte der Schweiz, 131, 113.

Frey, M. (1969). Die Metamorphose des Keupers vom Tafeljura bis zum Lukanier Gebiet. Beiträge zur Geologischen Karte der Schweiz, 137, 160.

Frey, M. (1978). Progressive low-grade metamorphism of a black shale formation, Central Swiss Alps, with special reference to Pyrophyllite and Margarite bearing assemblages. Journal of Petrology 19, 95-135.

Frisch, W. (1979). Tectonic progradation and plate tectonic evolution of the Alps. Tectonophysics, 60, 121-139.

Frisch, W. (1981). Plate motions in the Alpine region and their correlation to the opening of the Atlantic ocean. Geologische Rundschau, 70, 402-411.

Froitzheim, N., Eberli, G. P. (1990). Extensional detachment faulting in the evolution of a Tethys passive continental margin, Eastern Alps, Switzerland. Geological Society of America Bulletin, 102(9), 1297-1308.

Froitzheim, N., Manatschal, G. (1996). Kinematics of Jurassic rifting, mantle exhumation, and passive-margin formation in the Austroalpine and Penninic nappes (eastern Switzerland). Geological Society of America Bulletin, 108, 1120-1133.

Froitzheim, N., Pleuger, J., Roller, S., Nagel, T. (2003). Exhumation of high- and ultrahigh-pressure metamorphic rocks by slab extraction. Geology, 31, 925-928.

Furrer, U. (1977). Stratigraphie des Doggers der Östlichen Préalpes médianes. PhD thesis, Universität Bern.

Furrer, U. (1979). Stratigraphie des Doggers der Östlichen Préalpes médianes. Eclogae Geologicae Helvetiae, 72, 623-672.

Galli, A., Le Bayon, B., Schmidt, M. W., Burg, J. P., Caddick, M .J., Reusser, E. (2011). Granulites and charnockites of the Gruf Complex: Evidence for Permian ultra-high temperature metamorphism in the Central Alps. Lithos, 124, 17-45.

Galli, A., Le Bayon, B., Schmidt, M. W., Burg, J. P., Reusser, E., Sergeev, E. A., Larionov, A. (2012). U–Pb zircon dating of the Gruf Complex: disclosing the late Variscan granulitic lower crust of Europe stranded in the Central Alps. Contribution to Mineralogy and Petrology, 163, 353–378.

Galster, F. (2010). Stratigraphie des zones du Piz Terri-Lunschania et de Soja, Alpes Centrales (Suisse). Unpublished MSc Thesis, Université de Lausanne.

Galster, F., Epard, J. L., Masson, H. (2010). The Soja and Luzzone-Terri nappes: discovery of a Briançonnais element below the front of the Adula nappe (NE Ticino, Central Alps). Bulletin de la Société vaudoise des Sciences naturelles, 92, 61-75 and Bulletin de géologie, Lausanne, 368.

Galster. F., Cavargna-Sani. M., Epard. J. L., Masson, H. (2012). New stratigraphic data from the Lower Penninic between the Adula nappe and the Gotthard massif and consequences for the tectonics and the paleogeography of the Central Alps. Tectonophysics, 579, 37-55.

Gansser, A. (1937). Der Nordrand der Tambodecke. Schweizerische Mineralogische und Petrographische Mitteilungen, 17, 291-523.

Gansser, A., Pantic, N. (1988). Prealpine events along the eastern Insubric line (Tonale line, northern Italy). Eclogae Geologicae Helvetiae, 81, 567-577.

Gauthiez, L., Bussy, F., Ulianov, A., Guffon, Y., Sartori, M. (2012). Ordovician mafic magmatism in the Métailler Formation of the Mont-Fortnappe (Middle Penninic domain, western Alps) - geodynamic implications. Abstract, 9th Swiss Geoscience Meeting, Zürich, 110-111.

Gebauer, D. (1996). A P-T-t Path for some high-pressure uItramafic/mafic rock-association and their felsic fountry-rocks based on SHRIMP-dating of magmatic and metamorphic zircon domains. Example: Central Swiss Alps. In Basu, A., Hart, S. (Eds.), Earth processes:reading the isotopic code. Geophysical Monograph, 95. American Geophysical Union, Washington, 307-329.

Genier, F., Epard, J. L., Bussy, F., Magna, T. (2008). Lithostratigraphy and U-Pb zircon dating in the overturned limb of the Siviez-Mischabel nappe: a new key for Middle Penninic nappe geometry. Swiss Journal of Geosciences. 101, 431-452.

Geyer, O.F. (1977). Die “Lithiotis-Kalke” im Bereich der unterjurassischen Tethys: Neues Jahrbuch fur Geologie und Palaontologie, Abhandlungen, 153, 304-340.

Gisler, C., Hochuli, P. A., Ramseyer, K., Bläsi, H., Schlunegger, F. (2007). Sedimentological and palynological constraints on the basal Triassic sequence in Central Switzerland. Swiss Journal of Geosciences, 100, 263-272.

Gruner, U. (1981). Die jurassischen Breccien der Falknis-Decke und altersaequivalente Einheiten in Graubünden. Beitrage Geologische Karte der Schweiz, 154, 136.

Guillot, S., Ménot, R. P. (2009). Palaeozoic evolution of the external crystalline massifs of the Western Alps. Comptes Rendus Geosciences, 341, 253-265.

Handy, M. R., Schmid, M., Bousquet, R., Kissling,E., Bernoulli, D. (2010). Reconciling plate-tectonic reconstructions of Alpine Tethys with the geological-geophysical record of spreading and subduction in the Alps. Earth-Science Reviews, 102, 121-158.

Hauser, A. C., Müntener, O. (2011). New age constraints on the opening of the Piemont-Ligurian Ocean (Tasna-Nauders area, CH-A). Abstract Swiss Geosciences Meeting, Zürich.

Heim, A. (1891). Geologie der Hochalpen zwischen Reuss und Rhein. Beitrage Geologische Karte der Schweiz, 25.

Heinrich, C. A. (1982). Kyanite-eclogite to amphibolite facies evolution of hydrous mafic and pelitic rocks, Adula-nappe, Central Alps. Contributions to Mineralogy and Petrology, 81, 30-38.

Heinrich, C. A. (1983). Die reionale Hochdruckmetamorphose der Aduladecke, Zentralalpen, Schweiz. PhD Thesis, ETH Zürich.

Heinrich, C. A. (1986). Eclogite Facies Regional Metamorphism of Hydrous Mafic Rocks in the Central Alpine Adula Nappe. Journal of Petrology, 27, 123-154.

Hermann, J., Rubatto, D., Trommsdorff, V. (2006). Sub-solidus Oligocene zircon formation in garnet peridotite during fast decompression and fluid infiltration (Duria, Central Alps). Mineralogy and Petrology, 88, 181-206.

Herwartz, D., Nagel, T. J., Münker, C., Scherer, E. E., Froitzheim, N. (2011). Tracing two orogenic cycles in one eclogite sample by Lu-Hf garnet chronometry. Nature Geoscience, 4, 178-183.

Heydweiler, E. (1918). Geologische und Morphologische Untersuchungen in der Gegend des St. Bernardinpasses. Eclogae Geologica Helvetica 15, 149-296.

Jackson, S. (2008). LAMTRACE data reduction software for LA-ICP-MS. Laser Ablation ICP-MS in the Earth Sciences: Current Practices and Outstanding Issues. Mineralogical Association of Canada, Short Course Series, 40, 305-307.

Jeanbourquin, P., Burri, M. (1991). Les metasediments du Pennique inferieur dans la region de Brigue-Simplon; lithostratigraphie, structure et contexte geodynamique dans le bassin Valaisan. Eclogae Geologicae Helvetiae, 84, 463-481.

Jenny, H., Frischknecht, G., Kopp, J. (1923). Geologie der Adula. Beitrage Geologische Karte der Schweiz, [N.F.], 51.

Jung, W. (1963). Die mesozoischen Sedimente am Südostrand des Gotthard-Massivs (zwischen Plaun la Greina und Versam). Eclogae Geologicae Helvetiae, 56, 653-754.

Kaus, B. J. P., Connolly, J. A. D., Podladchikov, Y. Y., Schmalholz, S. M. (2005). Effect of mineral phase transitions on sedimentary basin subsidence and uplift. Earth and Planetary Science Letters, 233, 213-228.

Koch, E. (1982). Mineralogie und plurifazielle Metamorphose der Pelite in der Adula-Decke (Zentralalpen). Dissertation, Universität Basel.

Krayenbuhl, T., Steck, A. (2009). Structure and kinematics of the Jungfrau syncline, Faflertal (Valais, Alps), and its regional significance. Swiss Journal of Geosciences, 102, 441-456.

Kugler, C. (1987). Die Wildegg-Formation im Ostjura und die Schilt-Formation im östlichen Helvetikum; ein Vergleich. Mitteilungen aus dem Geologischen Institut der ETH und der Universität Zürich, 159, 209.

Kündig, E. (1926). Beiträge zur Geologie und Petrographie der Gebirgskette zwischen Val Calanca und Misox. Schweizerische Mineralogische und Petrographische Mitteilungen, 6, 3-110.

Kupferschmid, C. (1977). Geologie auf der Lugnezer Seite der Piz Aul-Gruppe. Eclogae Geologicae Helvetiae, 70, 1-58.

Kurz, W., Jansen, E., Hundenborn, R., Pleuger, J., Schäfer, W., Unzog, W. (2004). Microstructures and crystallographic preferred orientations of omphacite in Alpine eclogites: implications for the exhumation of (ultra-) high-pressure units. Journal of Geodynamics, 37, 1-55.

Lavier, L., Manatschal, G. (2006). Mechanism to thin continental lithosphere at magma poor margins. Nature 440, 324-328.

Leuthold, J., Müntener, O., Baumgartner, L. P., Putlitz, B., Chiaradia, M. (2013). A Detailed Geochemical Study of a Shallow Arc-related Laccolith; the Torres del Paine Mafic Complex (Patagonia). Journal of Petrology, 54, 273-303.

Liati, A., Froitzheim, N., Fanning, C. M. (2005). Jurassic ophiolites within the Valais domain of the Western and Central Alps: geochronological evidence for re-rifting of oceanic crust. Contributions to Mineralogy and Petrology, 149, 446-461.

Liati, A., Gebauer, D., Fanning, C. M. (2009). Geochronological evolution of HP metamorphic rocks of the Adula nappe, Central Alps, in pre-Alpine and Alpine subduction cycles. Journal of the Geological Society, 166, 797-810.

Liati, A., Gebauer, D., Fanning, M. (2000). U-Pb SHRIMP-dating of zircon from the Novate granite (Bergell, Central Alps): evidence for Oligocene˜Miocene magmatism, Jurassic-Cretaceous continental rifting and opening of the Valais trough. Schweizerische Mineralogische und Petrographische Mitteilungen, 80, 305-316.

Liégeois, J. P., Duchesne, J. C. (1981). The Lac Cornu retrograded eclogites (Aiguilles Rouges massif, Western Alps, France): evidence of crustal origin and metasomatic alteration. Lithos 14, 35-48.

Liñán, E., Perejón, A., Sdzuy, K. (1993). The Lower-Middle Cambrian stages and stratotypes from the Iberian Peninsula: a revision. Geological Magazine,130, 817-833.

Liskay, M. (1965). Geologie der Sedimentbedeckung des Südwestlichen Gotthard-Massivs in Oberwallis. Eclogae Geologicae Helvetiae, 58.

Loup, B. (1992). Evolution de la partie septentrionale du domaine helvétique en Suisse occidentale au Trias et au Lias: contrôle par subsidence thermique et variations du niveau marin. Publ. Dépt. Géol. Pal. Univ. Genève 12, 247.

Löw, S. (1987). Die tektono-metamorphe Entwicklung der Noerdlichen Adula-Decke (Zentralalpen, Schweiz). Beitrage Geologische Karte der Schweiz, 161, 1-84.

Ludwig, K. R. (2003). User's Manual for Isoplot/Ex version 3.00–A Geochronology Toolkit for Microsoft Excel, No. 4. Berkeley Geochronological Center, Special Publication.

Ludwig, K. R., Mundil, R. (2002). Extracting reliable U-Pb ages and errors from complex populations of zircons from Phanerozoic tuffs. Goldschmidt Conference Abstracts, 2002, 463.

Manatschal, G., Engström, A., Desmurs, L., Schaltegger, U., Cosca, M., Müntener, O., Bernoulli, D. (2006). What is the tectono-metamorphic evolution of continental break-up: the example of the Tasna Ocean˜Continent Transition. Journal of Structural Geology, 28, 1849-1869.

Manatschal, G., Müntener, O., Lavier, L.L., Minshull, T.A., Péron-Pinvidic, G. (2007). Observations from the Alpine Tethys and Iberia-Newfoudland margins pertinent to the interpretation of continental breakup. In G.D. Karner, G. Manatschal & L.M. Pinhero (Eds.), Imaging, mapping and modelling continental lithosphere extension and breakup. Geological Society of London Special Publications, 282, 291-324.

Mancktelow, N. S. (2008). Tectonic pressure; theoretical concepts and modelled examples. Lithos, 103, 149-177.

Maniar, P. D., Piccoli, P. M. (1989). Tectonic discrimination of granitoids. Geological Society of America Bulletin, 101, 635-643.

Masini, E., Manatschal, G., Mohn, G. (2013). The Alpine Tethys rifted margins: Reconciling old and new ideas to understand the stratigraphic architecture of magma-poor rifted margins. Sedimentology, 60, 174-196.

Masini, E., Manatschal, G., Mohn, G., Ghienne, J. F., Lafont, F. (2011). The tectono-sedimentary evolution of a supra-detachment rift basin at a deep-water magma-poor rifted margin: the example of the Samedan Basin preserved in the Err nappe in SE Switzerland. Basin research, 23, 652-677.

Masson, H. (1972). Sur l'origine de la cornieule par fracturation hydraulique. Eclogae Geologicae Helvetiae, 65.

Masson, H. (2002). Ophiolites and other (ultra)basic rocks from the West-Central Alps: New data for a puzzle. Bulletin de la Société vaudoise des Sciences naturelles, 88, 263-276.

Masson, H., Bussy, F., Eichenberger, M., Giroud, N., Meilhac, C., Presniakov, S. (2008). Early Carboniferous age of the Versoyen ophiolites and consequences: Non-existence of a «Valais ocean» (Lower Penninic, western Alps). Bulletin de la Société géologique de France 179, 337-355.

Matasci, B., Epard, J. L., Masson, H. (2011). The Teggiolo zone: a key to the Helvetic–Penninic connection (stratigraphy and tectonics in the Val Bavona, Ticino, Central Alps). Swiss Journal of Geosciences, 104, 257-283.

Mattinson, J. M. (2005). Zircon U-Pb chemical abrasion (CA-TIMS) method: Combined annealing and multi-step partial dissolution analysis for improved precision and accuracy of zircon ages. Chemical Geology, 220, 47-66.

Maxelon, M., Mancktelow, N. S. (2005). Three-dimensional geometry and tectonostratigraphy of the Pennine zone, Central Alps, Switzerland and Northern Italy. Earth Science Reviews, 71, 171-227.

Mayerat Demarne, A. M. (1994). Analyse structurale de la zone frontale de la nappe du Tambo. Materiaux pour la Carte Geologique de la Suisse, 165.

McDonough, W. F., Sun, S. S. (1995). The composition of the Earth. Chemical Geology, 120, 223-253.

McKenzie, D. (1978). Some remarks on the development of sedimentary basins. Earth and Planetary Science Letters 40, 25-32.

Mégard-Galli, J. (1972). Données nouvelles sur le Carnien dans la zone briançonnaise entre Briançon et la vallée du Guil: conséquences tectoniques et paléogéographiques. Géol. Alpine, 48, 131-142.

Mégard-Galli, J., Baud, A. (1977). Le Trias moyen et supérieur des Alpes nord-occidentales et occidentales: données nouvelles et corrélations stratigraphiques. Bulletin du BRGM, IV/3, 233-250.

Ménard, G., Molnar, P. (1988). Collapse of a Hercynian Tibetan plateau into a late Palaeozoic European Basin and Range province. Nature, 334, 235-237.

Meyre, C., De Capitani, C., Zack, T., Frey, M. (1999). Petrology of High-Pressure Metapelites from the Adula Nappe (Central Alps, Switzerland). Journal of Petrology, 40, 199-213.

Meyre, C., Marquer, D., Schmid, S. M., Ciancaleoni, L. (1998). Syn-orogenic extension along the Forcola Fault; correlation of Alpine deformations in the Tambo and Adula nappes (eastern Penninic Alps). Eclogae Geologicae Helvetiae, 91.

Meyre, C., Puschnig, A. R. (1993). High-pressure metamorphism and deformation at Trescolmen, Adula nappe, Central Alps. Schweizerische Mineralogische und Petrographische Mitteilungen, 73, 277-283.

Milnes, A. G. (1974). Post-nappe folding in the western Lepontine Alps. Eclogae Geologicae Helvetiae, 67, 333-348.

Milnes, A. G., Schmutz, H. U. (1978). Structure and history of the Suretta nappe (Pennine zone, Central Alps) - a field study. Eclogae Geologicae Helvetiae, 71, 19-33.

Milovsky, R., Hurai, V., Plasienka, D., Biron, A. (2003). Hydrotectonic regime at soles of overthrust sheets: textural and fluid inclusion evidence from basal cataclasites of the Murán nappe (Western Carpathians, Slovakia). Geodinamica Acta, 16, 1-20.

Mohn, G., Manatschal, G., Masini, E., Müntener, O. (2011). Rift-related inheritance in orogens: a case study from the Austroalpine nappes in Central Alps (SE-Switzerland and N-Italy). International Journal of Earth Sciences, 100, 937-961.

Mohn, G., Manatschal, G., Müntener, O., Beltrando, M., Masini, E. (2010). Unravelling the interaction between tectonic and sedimentary processes during lithospheric thinning in the Alpine tethys margins. International Journal of Earth Sciences, 99 (Suppl. 1), 75-101.

Müntener, O., Manatschal, G., Desmurs, L., Pettke. T. (2010). Formation of refertilized peridotite: geochemisty, spatial variability and the importance of a ‘lithospheric sponge’ during rifting and thinning of the continental crust. J Petrol, 51(1-2), 255-294.

Nabholz, W. K. (1945). Geologie der Bündnerschiefergebirge zwischen Rheinwald, Valser- und Safiental. Eclogae Geologicae Helvetiae, 38, 1-119.

Nagel, T. J. (2008). Subduction, collision and exhumation recorded in the Adula nappe, central Alps. In: Siegesmund S, Fügenschuh B, Froitzheim N (ed.) Tectonic Aspects of the Alpine-Dinaride-Carpathian System: Geological Society, London, Special Publications, 298, 365-392.

Nagel, T., Capitani, C., Frey, M., Froitzheim, N., Stcnitz, H., Schmid, S. M. (2002a). Structural and metamorphic evolution during rapid exhumation in the Lepontine dome (southern Simano and Adula nappes, Central Alps, Switzerland). Eclogae Geologicae Helvetiae, 95, 301-322.

Nagel, T., Capitani, C., Frey, M., Froitzheim, N., Stcnitz, H., Schmid, S.M. (2002a). Structural and metamorphic evolution during rapid exhumation in the Lepontine dome (southern Simano and Adula nappes, Central Alps, Switzerland). Eclogae Geologicae Helvetiae, 95, 301-322.

Nagel, T., De Capitani, C., Frey, M. (2002b). Isograds and PT evolution in the eastern Lepontine Alps (Graubunden, Switzerland). Journal of Metamorphic Geology, 20, 309-324.

Niggli, E. (1970). Alpine Metamorphose und alpine Gebirgsbildung. Fortschritte der Mineralogie, 47, 16-26.

Niggli, E and Niggli C.R. (1965). Karten der Verbreitung einiger Mineralien der alpidischen Metamorphose in der Schweizr Alpen (Stilpnomelan, Alkali-Amphibol, Chloritoid, Staurolit, Disten, Sillimanit). Eclogae Geologicae Helvetiae, 58, 335-368.

Nimis, P., Trommsdorff, V. (2001). Revised Thermobarometry of Alpe Arami and other Garnet Peridotites from the Central Alps. Journal of Petrology, 42, 103-115.

Oberhänsli, R. (1994). Subducted and obducted ophiolites of the Central Alps: paleotectonic implications deduced by their distribution and metamorphic overprint. Lithos, 33, 109-118.

Oberli, F., Meier, M., Biino, G. G. (1994). Time constraints on the pre-Variscan magmatic/metamorphic evolution of the Gotthard and Tavetsch units derived from single-zircon U-Pb results. Bulletin suisse de minéralogie et pétrographie, 74, 483-488

Pantic, N., Isler, A. (1978). Palynologische Untersuchungen in Bündnerschiefern (II). Eclogae Geologicae Helvetiae, 71, 447-465.

Pantic, N., Isler, A. (1981). Palynologische Untersuchungen in Bündnerschiefern (III). Eclogae Geologicae Helvetiae, 74, 1063-1072.

Partzsch, J. H. (1998). The tectono-metamorphic evolution of the middle Adula nappe, Central Alps, Switzerland. PhD thesis, Universität Basel.

Peacock, M. A. (1931). Classification of igneous rock series. The Journal of Geology, 39, 54-67.

Pearce, J. A. (1996). A users guide to basalt discrimination diagrams. Trace element Geochemistry of volcanic rocks: applications for massive sulphide exploration.Geological Association of Canada, Short Course Notes, 12, 79-113.

Pearce, J. A., Cann, J. R. (1973). Tectonic setting of basic volcanic rocks determined using trace element analyses. Earth and Planetary Science Letters, 19, 290-300.

Pearce, J. A., Stern, R. J. (2006). Origin of back-arc basin magmas: trace element and isotope perspectives. Geophysical Monograph Series, 166, 63-86.

Péron-Pinvidic, G., Manatschal, G. (2009). The final rifting evolution at deep magma-poor passive margins from Iberia-Newfoundland: a new point of view. International Journal of Earth Sciences 98, 1581-1597.

Péron-Pinvidic, G., Manatschal, G., Gernigon, L., Gaina, C. (2010). The formation and evolution of crustal blocks at rifted margins: new insights from the interpretation of the Jan Mayen microcontinent. Central and North Atlantic Conjugate Margins Conference, LISBON 2010.

Péron-Pinvidic, G., Manatschal, G., Minshull, T. A., Sawyer, D. S. (2007). Tectonosedimentary evolution of the deep Iberia-Newfoundland margins: evidence for a complex breakup history. Tectonics, 26, TC2011, 19.

Petrini, K., Podladchikov, Y. (2000). Lithospheric pressure-depth relationship in compressive regions of thickned crust. Journal of Metamorphic Geology, 18, 67-78.

Pfeifer, H. R., Biino, G., Ménot, R. P., Stille, P. (1993). Ultramafic rocks in the Pre-Mesozoic basement of the Central and External Western Alps. The Pre-Mesozoic geology in the Alps. Springer, Berlin Heidelberg, New York, 119-143.

Pin, C., Marini, F. (1993). Early Ordovician continental break-up in Variscan Europe: Nd-Sr isotope and trace element evidence from bimodal igneous associations of the Southern Massif Central, France. Lithos, 29, 177-196.

Pleuger, J., Hundenborn, R., Kremer, K., Babinka, S., Kurz, W., Jansen, E., Froitzheim, N. (2003). Structural evolution of Adula nappe, Misox zone, and Tambo nappe in the San Bernardino area: Constraints for the exhumation of the Adula eclogites. Mitteilungen der Österreichischen Geologischen Gesellschaft, 94, 99-122.

Pleuger, J., Podladchikov, Y. (2012). A new restoration of the NFP20-East cross section and possible tectonic overpressure in the Penninic Adula Nappe (Central Alps). EGU General Assembly Conference Abstract.

Preiswerk, H., Bossard, L., Grütter, O., Niggl, P., Kündig, E., Ambühl, E. (1934). Carta geologica delle Alpi Ticinesi fra Valle Maggia e Val Bleno 1:50'000. Commissione Geologica Elvetica delle Scienze naturali.

Probst, P. (1980). Die Bündnerschiefer des nördlichen Penninikums zwischen Valser Tal und Passo di San Giacomo. Materiaux pour la Carte Geologique de la Suisse, 153.

Pupin, J. P. (1980). Zircon and granite petrology. Contributions to Mineralogy and Petrology, 73, 207-220.

Ramsey, J. G. (1968). Folding and fracturing of rock. Mc-Graw-Hill, New York.

Rey, D. (2002). Shear2F: un logiciel de modélisation tectonique. Mémoires de Géologie (Lausanne), 37.

Ringgerberg, Y., Tommasi, A., Stampfli, G. M., (2001). The Jurassic sequence of the Niesen nappe in the region of Le Sépey-La Forclaz (Switzerland): witness of the Piemont rifting in the Helvetic paleogeographic domain. Bulletin de géologie, Lausanne, 348.

Rück, P. (1995). Stratigraphisch-sedimentologische Untersuchung der Schamser Decken. Beiträge zur geologischen Karte der Schweiz, 167, 1-78.

Rütti, R. (2003). The Tectono-metamorphic Evolution of the Northwestern Simano Nappe: Central Alps, Switzerland. PhD Thesis, ETH Zürich.

Santini, L. (1992). Geochemistry and geochronology of the basic rocks of the Penninic Nappes of East-Central Alps (Switzerland). PhD Thesis, Université de Lausanne.

Schaltegger, U., Abrecht, J., Corfu, F. (2003). The Ordovician orogeny in the Alpine basement: constraints from geochronology and geochemistry in the Aar Massif (Central Alps). Bulletin suisse de minéralogie et petrography, 83, 183-239.

Schaltegger, U., Gebauer, D. (1999). Pre-Alpine geochronology of the Central, Western and southern Alps. Bulletin suisse de minéralogie et pétrographie, 79, 79-87.

Schaltegger, U., Gebauer, D., Von Quadt, A. (2002). The mafic-ultramafic rock association of Loderio-Biasca (lower Pennine nappes, Ticino, Switzerland): Cambrian oceanic magmatism and its bearing on early Palaeozoic paleogeography. Chemical Geology, 186, 265-279.

Schardt, H. (1898). Les régions exotiques du versant Nord des Alpes Suisse. Préalpes du Chablais et du Stockhorn et les Klippes. Bulletin de la société vaudoise des sciences naturelles, 34, 113-219.

Scheiber, T., Pfiffner, O. A., Schreurs, G. (2012). Strain accumulation during basal accretion in continental collision-case study from the Suretta nappe (eastern Swiss Alps). Tectonophysics, 579, 56-73.

Schmalholz, S. M., Podladchikov, Y. Y. (2013). Tectonic overpressure in weak crustal-scale shear zones and implications for the exhumation of high pressure rocks. Geophysical Research Letters, 40, 1984-1988.

Schmid, S. M., Pfiffner, O .A., Schreurs, G. (1997). Rifting and collision in the Penninic zone of eastern Switzerland. In: Pfiffner, O.A., Lehner, P., Heitzmann, P., Mueller, S., Steck, A. (Eds). Deep structure of the Swiss Alps-Results from NFP/PNR 20: Birkhäuser Verlag, 160-185.

Schmid, S. M., Pfiffner, O. A., Froitzheim, N., Schönborn, G., Kissling, E. (1996). Geophysical-geological transect and tectonic evolution of the Swiss-Italian Alps. Tectonics, 15, 1036-1064.

Schmid, S. M., Rück, P., Schreurs, G. (1990). The significance of the Schams nappes for the reconstruction of the paleotectonic and orogenic evolution of the Penninic zone along the NFP-20 East traverse (Grisons, eastern Switzerland). In: Roure, et al. (Eds.): Deep structure of the Alps, Mémoire de la Société de France, Paris, 156, 263-287.

Schmid, S. M., Fügenschuh, B., Kissling, E., Schuster, R. (2004). Tectonic map and overall architecture of the Alpine orogen. Eclogae Geologicae Helvetiae, 97, 93-117.

Schreurs, G. (1993). Structural analysis of the Schams nappes and adjacent tectonic units; implications for the orogenic evolution of the Penninic Zone in eastern Switzerland. Bulletin de la Societe Geologique de France, 164, 415-435.

Schroeder, W. J. (1939). La brèche du Chablais entre Giffre et Drance et les roches éruptives des Gets. Thèse N°1004, Faculté des Sciences de l'Université de Genève, 138.

Schulz, B., Steenken, A., Siegesmund, S. (2008). Geodynamic evolution of an Alpine terrane - the Austroalpine basement to the south of the Tauern Window as a part of the Adriatic Plate (eastern Alps). Geological Society, London, Special Publications, 298, 5-44.

Sengör, C. A. M., Bernoulli, D. (2011). How to stir a revolution as a reluctant rebel: Rudolf Trümpy in the Alps. International Journal of Earth Sciences 100, 899-936.

Septfontaine, M. (1983). Le Dogger des Préalpes médianes suisses et françaises (Stratigraphie, évolution paléogéographique et paléotectonique). Mém. Soc. Helv. Sci. Nat. 97, 1-121.

Simon, N. S. C., Podladchikov, Y. Y. (2008). The effect of mantle composition on density in the extending lithosphere. Earth and Planetary Science Letters, 272, 148-157.

Spear, F. S. (1995). Metamorphic phase equilibria and pressure-temperature-time paths. Mineralogical Society of America, Washington.

Spicher, A. (1980). Carte tectonique de la Suisse, 1:500'000. Commission géologique Suisse, Swisstopo, Bern.

Stacher, P. (1980), Stratigraphie, Mikrofazies und Mikropaläontologie der Wang-Formation (Helvetische Oberkreide der Schweizer Alpen). Beitrage Geologische Karte der Schweiz,152.

Stampfli, G. M., Borel, G. D., Marchant, R., Mosar, J. (2002).Western Alps geological constraints on western Tethyan reconstructions. J. Virtual Explor. 8, 77-106.

Stampfli, G. M., Von Raumer, J., Wilhem, C. (2011). The distribution of Gondwana-derived terranes in the Early Palaeozoic. In: Gutiérrez-Marco JC, Rábano I, García-Bellido D (ed) Ordovician of the World. Cuadernos del Museo Geominero, 14. Instituto Geológico y Minero de España, Madrid, 567-574.

Stampfli, G.M. (1993). Le Briançonnais: terrain exotique dans les Alpes? Eclogae Geologicae Helvetiae, 86, 1-45.

Steck, A. (1989). Structures des déformations alpines dans la région de Zermatt. Bulletin Suisse de Minéralogie et Pétrographie, 69, 205-209.

Steck, A. (1990). Une carte des zones de cisaillement ductile des Alpes Centrales. Eclogae Geologicae Helvetiae, 83, 603-627.

Steck, A. (2008). Tectonics of the Simplon massif and Lepontine gneiss dome: deformation structures due to collision between the underthrusting European plate and the Adriatic indenter. Swiss Journal of Geosciences, 101, 515-546.

Steinmann, M. (1994). Die nordpenninischen Bündnerschiefer der Zentralalpen Graubündens: Tektonik, Stratigraphie und Beckenentwicklung. PhD Thesis, ETH Zürich.

Steinmann,M., Stille, P. (1999). Geochemical evidence for the nature of the crust beneath the eastern North Penninic basin of the Mesozoic Tethys ocean. Geologische Rundschau, 87, 633-643.

Sun, S. S., McDonough, W. F. (1989). Chemical and isotopic systematics of oceanic basalts: implications for mantle composition and processes. Geological Society, London, Special Publication, 42, 313-345.

Swisstopo, (2012) Sheet 1254 Hinterrhein; vector dataset (used maps see http://www.swisstopo.admin.ch/internet/swisstopo/fr/home/products/maps/geology/geocover.html). Swisstopo, Bern.

Tarasewicz, J. P. T., Woodcock, N. H., Dickson, J. A .D. (2005). Carbonate dilation breccias: examples from the damage zone to the Dent Fault, northwest England. Geological Society of America Bulletin, 117, 736-745.

Thélin, P. (1982). Les gneiss oeillés de la nappe du Grand-St-Bernard. PhD Thesis, Université de Lausanne, 484.

Thüring, M. (1990). Geologie um den Hennensädel im hintern Valsertal (GR). MSc Thesis, Universität Basel.

Todd, C. S., Engi, M. (1997). Metamorphic field gradients in the Central Alps. Journal of Metamorphic Geology, 15, 513-530.

Trommsdorff, V. (1966). Progressive Metamorphose kieseliger Karbonatgesteine in den Zentralalpen zwischen Bernina und Simplon. Schweizerische Mineralogische und Petrographische Mitteilungen, 46, 431-460.

Trommsdorff, V. (1990). Metamorphism and tectonics in the Central Alps: The Alpine lithospheric mélange of Cima Lunga and Adula. Memorie della Societa Geologica Italiana, 45, 39-49.

Trümpy, R. (1945). Le Lias autochtone d'Arbignon (Groupe de la Dent de Morcles). Eclogae Geologicae Helvetiae, 38, 421-429.

Trümpy, R. (1949). Der Lias der Glarner Alpen. Denkschr. Schweiz Natf. Ges. 79, 1-192.

Trümpy, R. (1951). Sur les racines helvétiques et les «schistes lustrés» entre le Rhône et la vallée de Bagnes (région de la Pierre Avoi). Eclogae Geologicae Helvetiae, 42, 338-347.

Trümpy, R. (1954). La zone de Sion-Courmayeur dans le haut Val Ferret valaisan. Eclogae Geologicae Helvetiae, 47, 315-359.

Trümpy, R. (1955). Remarques sur la corrélation des unités penniques externes entre la Savoie et le Valais et sur l'origine des nappes préalpines. Bulletin de la Societé Geologique de France, 5, 217-231.

Trümpy, R. (1958). Remarks on the pre-orogenic history of the Alps. Geologie en Mijnbouw, 10, 340-352.

Trümpy, R. (1965). Zur geosynklinalen Vorgeschichte der Schweizer Alpen. Umschau. Wiss. Techn. 65, 573-577.

Trümpy, R. (1966). Considérations générales sur le "Verrucano" de Alpes Suisses. In: Symposium sul Verrucano. Società Toscana di Scienze Naturali, Pisa, 212-232.

Trümpy, R. (1970). Stratigraphy in mountain belts. Quarterly Journal of the Geological Society, 126, 293-318.

Trümpy, R. (1975). Age and location of Mesozoic scarp breccias in the Alps. 9ème Congrès International de Sédimentologie, Nice, Thème 4, 313-318.

Trümpy, R. (1976). Du Pèlerin aux Pyrénées. Eclogae Geologicae Helvetiae, 69, 249-264.

Trümpy, R. (2006). Geologie der Iberger Klippen und ihrer Flysch-Unterlage. Eclogae Geologicae Helvetiae, 99, 79-121.

Trümpy, R. (1982). Das Phänomen Trias. Geologische Rundschau, 71, 711-723.

Uhr, A., unpublished. Geologische Untersuchungen im Gebiet des Piz Terri. Unpubl. report ETHZ, 73 p.

Ulianov, A., Muntener, O., Schaltegger, U., Bussy, F. (2012). The data treatment dependent variability of U-Pb zircon ages obtained using mono-collector, sector field, laser ablation ICPMS. Journal of Analytical Atomic Spectrometry, 27, 663-676.

Van der Plas, L. (1959). Petrology of the Northern Adula Region, Switzerland, (with particular reference to glaucophane-bearing rocks). Leidse Geol. Mededel, 24, 415-602.

Vaselá P., Söllner F., Finger F., Gerdes A. (2011). Magmato-sedimentary Carboniferous to Jurassic evolution of the western Tauern window, Eastern Alps (constraints from U–Pb zircon dating and geochemistry). International Journal of Earth Sciences, 100, 993–1027.

Vening Meinesz, F. A. (1950). Les "grabens" africains, résultat de compression ou de tension dans la croute terrestre? Bull. Royal Colon. Int. Belg. 21, 539-552.

Voll, G. (1976). Structural Studies of the Valser Rhine Valley and the Lukmanier Region and their Importance for the nappe Structure of the Central Swiss Alps. Schweizerische Mineralogische und Petrographische Mitteilungen, 56, 619-626.

Von Raumer, J. F., Bussy, F., Stampfli, G. M. (2009). The Variscan evolution in the External massifs of the Alps and place in their Variscan framework. Comptes Rendus Géosciences, 341, 239-252.

Von Raumer, J. F., Bussy, F. (2004). Mont Blanc and Aiguilles Rouges geology of their polymetamorphic basement (external massifs, Westerns Alps, France-Switzerland). Mémoires de Géologie, Lausanne, 42, 203.

Von Raumer, J. F., Bussy, F., Schaltegger, U., Schulz, B., Stampfli, G. M. (2013). Pre-Mesozoic Alpine basements - Their place in the European Palaeozoic framework. Geological Society of America Bulletin, 125, 89-108.

Von Raumer, J. F., Stampfli, G. M., Borel, G., Bussy, F. (2002). Organization of pre-Variscan basement areas at the North-Gondwanan margin. International Journal of Earth Sciences, 91, 35-52.

Vrijmoed, J.C., Podladchikov, Y. Y., Andersen, T. B., Hartz, E. H. (2009). An alternative model for ultra-high pressure in the Svartberget Fe-Ti garnet-peridotite, Western Gneiss region, Norway. European Journal of Mineralogy, 21, 1119-1133.

Wenk, E. (1970). Zur Regionalmetamorphose und Ultrametamorphose im Lepontin. Fortschritte der Mineralogie, 47, 34-51.

Wernicke, B. (1985). Uniform-sense normal simple shear of the continental lithosphere. Can. J. Earth Sci. 22,108-125.

Whalen, J. B., Currie, K. L., Chappell, B. W. (1987). A-type granites: geochemical characteristics, discrimination and petrogenesis. Contributions to Mineralogy and Petrology, 95, 407-419.

Whitmarsh, R.B., Manatschal, G., Minshull, T. A. (2001). Evolution of magma-poor continental margins from rifting to seafloor spreading. Nature, 413, 150-154.

Wiedenbeck, M., Alle, P., Corfu, F., Griffin, W. L., Meier, M., Oberli, F., Quadt, A., Roddick, J. C., Spiegel, W. (1995). Three natural zircon standards for U Th Pb, Lu Hf, trace element and REE analyses. Geostandards and Geoanalytical Research, 19, 1-23.

Wiederkehr, M., Bousquet, R., Schmid, S., Berger, A. (2008). From subduction to collision: Thermal overprint of HP/LT meta-sediments in the north-eastern Lepontine Dome (Swiss Alps) and consequences regarding the tectono-metamorphic evolution of the Alpine orogenic wedge. Swiss Journal of Geosciences, 101, 127-155.

Wiederkehr, M., Bousquet, R., Ziemann, M. A., Berger, A., Schmid, S. M. (2011). 3-D assessment of peak-metamorphic conditions by Raman spectroscopy of carbonaceous material: an example from the margin of the Lepontine dome (Swiss Central Alps). International Journal of Earth Sciences, 100, 1029-1063.

Wiederkehr, M., Sudo, M., Bousquet, R., Berger, A., Schmid, S.M. (2009). Alpine orogenic evolution from subduction to collisional thermal overprint: The 40Ar/39Ar age constraints from the Valaisan Ocean, central Alps. Tectonics, 28.

Wieland, B. (1976). Petrographie eozäner siderolithischer Gesteine des Helvetikums der Schweiz: ihre Diagenese und schwache Metamorphose, PhD Thesis, Universität Bern.

Winchester, J. A., Floyd, P. A. (1977). Geochemical discrimination of different magma series and their differentiation products using immobile elements. Chemical Geology, 20, 325-343.

Wyss, R., Isler, A. (2007). Blatt 1234 Vals.-Geologische Atlas der Schweitz 1:25‘000, Erläuterung.121. Geologischer Atlas der Schweiz, 127, Swisstopo.

Ziegler, W. H. (1956). Geologische Studien in den Flyschgebieten des Oberhalbsteins (Graubünden). Eclogae Geologicae Helvetiae, 49, 3-74.

Zulbati, F. (2008). Structural and metamorphic evolution of the phengite-bearing schists of the northern Adula Nappe (Central Alps, Switzerland). Geological Journal, 43, 33-57.

Zulbati, F. (2010). Multistage metamorphism and deformation in high-pressure metabasites of the northern Adula Nappe Complex (Central Alps, Switzerland). Geological Journal, 46, 82-103.